Strategies to overcome interferences during biomass monitoring with dielectric spectroscopy

by

Manuel Alberto Garcia Albornoz

Submitted for the degree of Doctor of Philosophy

Heriot-Watt University

School of Engineering and Physical Sciences

March 2013

ABSTRACT

Dielectric spectroscopy is extensively used to measure the level of viable biomass during fermentations but can suffer from interference by a variety of factors including the presence of dead cells, bubbles, electric and magnetic fields, changes in the medium composition, conductivity changes and the presence of non-cellular particles. Three different approaches were used to overcome these problems. The first involved the separate measurement of the spectra of the interferent and the cells. If the spectra were significantly different then spectra containing the signals of both cells and the interferent could be deconvoluted to separately determine the relative contribution of the cells and the interferent to the spectra. This deconvolution approach was successfully used to estimate the biomass levels of yeast in the presence of spent grains of barley and hardwood in the medium. A similar approach allowed the interference of electrode polarisation on spectra of yeast and microalgae to be compensated for. An attempt to determine the concentration of non-viable cells in a mixture of dead and live cells was less successful because the signal of the non-viable cells was quite small compared to that of viable cells. A second approach involved the use of a filter to keep the interferent away from the probe surface. This was used successfully in the measurement of the yeast concentration in the presence of spent barley grains. A third approach involved the use of a second sensor in addition to the biomass sensor. This allows the signal of the biomass sensor to be compensated for the interferent. In one set of experiments microelectrodes were developed which were able to confine the electric field to a small volume near the electrode surface. Covering the electrode surface with a gel or a membrane stopped cells from entering this volume whilst allowing medium to diffuse through. This allowed the measurement of changes in the electrical properties of the medium without a contribution by the cells. Whilst this approach worked, the response time was too long for practical use. More successful was the simultaneous measurement of the biomass with an infrared optical probe and a dielectric probe. It was found that the signal of the optical probe was independent of the cell viability, whilst the dielectric probe was quite insensitive to non-viable cells. The combined use of the dielectric probe and the optical probe allowed the culture viability to be determined in a straightforward manner.

DEDICATION

This thesis is dedicated to all my family, thank you all for your support and thank God for blessing me with the best family I could ever ask for. Chaac and Huera always in my heart.

DECLARATION STATEMENT

ACADEMIC REGISTRY
Research Thesis Submission

Name*:*	Manuel Alberto Garcia Albornoz		
School/PGI:	School of Engineering and Physical Sciences		
Version: *(i.e. First, Resubmission, Final)*	Final	Degree Sought (Award **and** Subject area)	PhD in Chemical Engineering (Bioprocessing)

Declaration

In accordance with the appropriate regulations I hereby submit my thesis and I declare that:

1) the thesis embodies the results of my own work and has been composed by myself
2) where appropriate, I have made acknowledgement of the work of others and have made reference to work carried out in collaboration with other persons
3) the thesis is the correct version of the thesis for submission and is the same version as any electronic versions submitted*.
4) my thesis for the award referred to, deposited in the Heriot-Watt University Library, should be made available for loan or photocopying and be available via the Institutional Repository, subject to such conditions as the Librarian may require
5) I understand that as a student of the University I am required to abide by the Regulations of the University and to conform to its discipline.

* *Please note that it is the responsibility of the candidate to ensure that the correct version of the thesis is submitted.*

Signature of Candidate*:*		Date:	21 March 2013

Submission

Submitted By *(name in capitals):*	MANUEL ALBERTO GARCIA ALBORNOZ
Signature of Individual Submitting:	
Date Submitted:	21 March 2013

For Completion in the Student Service Centre (SSC)

Received in the SSC by *(name in capitals):*	
1.1 Method of Submission *(Handed in to SSC; posted through internal/external mail):*	
1.2 E-thesis Submitted **(mandatory for final theses)**	
Signature:		Date:	

AKNOWLEDGMENTS

TABLE OF CONTENTS

LISTS OF TABLES AND FIGURES

LIST OF ABBREVIATIONS AND NOMENCLATURES

α	Cole-Cole parameter
$\Delta\varepsilon$	Dielectric increment
ε	Permittivity (F/m)
ε_∞	Permittivity at higher frequency
ε^*	Complex permittivity
ε'	Real part of complex permittivity
ε''	Imaginary part of complex permittivity
ε_L	Permittivity at lower frequency
ε_r	Relative permittivity
ε_o	Permittivity of free space (with a value of 8.854×10^{-14} F/cm)
ε_m	Permittivity of the medium
ε_s	Permittivity of the suspension
ε_p	Permittivity of the particle
μ	Permeability or Dipole moment
μF	Microfarads
μm	Micrometre
σ	Conductivity (S/m)
σ'	conductivity (S cm^{-1})
σ_0	conductivity at lower frequency (S cm^{-1})
σ_∞	conductivity at higher frequency (S cm^{-1})
σ_i	cell interior conductivity (S cm^{-1})
σ_m	conductivity of suspending medium (S cm^{-1})
ω	angular frequency of the (sinusoidal) electric field (rad s^{-1})
τ	characteristic response time or relaxation time (s)
A	Area of parallel plates (cm^2)
AC	Alternating current
ATP	Adenosine triphosphate
C	Capacitance (F)
cfu	Colony forming unit
cm	Centimetre

C_m	membrane capacitance (F)
CO_2	Carbon dioxide
conc.	Concentration
C_p	Parallel capacitance
d	distance between the plates (cm)
D	Displacement
d/A	cell constant (cm^{-1}).
DC	Direct current
E	Electromotive force
EMI	Electromagnetic Interference
F	Farads
f_c	characteristic frequency (sec^{-1})
FCM	Flow cytometry
g	grams
G	conductance (S)
G_m	membrane conductance per unit area $(S\ cm^{-2})$
h	hours
ITO	Indium tin oxide
J	Joules
j	$\sqrt{-1}$
K	Dielectric constant, Kelvin
kHz	kiloHertz
L	Litre
m	metre
M	Molar
ME	Microelectrode
MHz	Mega Hertz
min	minutes
ml	millilitre
mm	millimeter
MTT	3-(4,5-Dimethylthiazol-2-yl)-2,5-diphenyltetrazolium bromide
mS	milliSiemens
NMR	Nuclear Magnetic Resonance
O_2	Oxygen
OD	Optical density

p	Electric tension
P	Biomass volume fraction
PC	Personal computer
PEF	Pulsed electric field
pF	picoFarads
R or *r*	cell radius
rpm	Revolutions per minute
sec	Seconds
S	Siemens
UV	Ultraviolet
V	Voltage
WWII	World War II
XTT	2,3-bis-(2-methoxy-4-nitro-5-sulfophenyl)-2H-tetrazolium-5-carboxanilide

CHAPTER 1

GENERAL INTRODUCTION

Dielectric spectroscopy, also referred to as impedance or admittance spectroscopy, is an effective technique for the characterization and enumeration of cells. The technique can be used online, and there is no need for labels or any other pre-treatment of the cells before a measurement. Measurements of biomass levels using dielectric spectroscopy are based on the fact that in the frequency range between 0.1 and 100 MHz interfacial polarisation occurs at the cell membrane interfaces, causing large dipoles to be induced in the cells (Markx *et al*., 1999). As shown by Schwan (Schwan, 1957), the resulting increase in the capacitance at low frequencies is directly related to the volume fraction of membrane–enclosed material. Dielectric spectroscopy has been used extensively for the measurement of cell concentration in cell suspensions, and also to obtain information about cellular properties such as the conductivity of the cytoplasm, cell morphology and cell size.

When employing dielectric spectroscopy the overall electrical properties (capacitance and conductance) of the suspension are measured as a function of frequency, and the resulting dielectric spectra analysed to obtain the required information about the cells. When permittivity is measured at different frequencies some steps can be observed in the shape of the spectra. These steps are called dispersion and are due to a particular polarisation process as frequency increases. The β-dispersion occurs inside the cell and is due to the build up of charge at the cell membrane. This polarisation can only occur when the cell membrane is complete. When a cell dies, the membranes are often damaged. When a membrane becomes permeable charges cannot accumulate at the interface, and interfacial polarisation will be reduced. The accompanying reduction in the capacitance can be used to monitor cell death online and in real-time (Markx *et al*., 1999, Yang *et al*., 2008).

During biomass monitoring the signal that we get preferably is dependent on the concentration of viable cells only. In practice, unfortunately, this is not the case. Non-viable cells can show a significant amount of residual polarisation, and their presence

often leads to a measurable increase in the permittivity. The cells are suspended in medium. The medium has its own permittivity and conductivity. Medium permittivity and conductivity are dependent on the temperature; their values also depend on the composition of the medium. The presence of large amount of salts in particular affects the conductivity, which in turn can affect the permittivity baseline (crosstalk), and cause a significant increase in the permittivity at low frequencies through electrode polarisation. There may be particles (e.g. starch, cellulose, protein flocs, gels) in the medium which have their own dispersions; there may be oil droplets; bubbles. The fermenter wall may disturb the electric field; external magnetic or electric fields may disturb the signal. Clearly a lot of factors can and do interfere in biomass measurement with dielectric spectroscopy.

1.1 Aims and objectives

The general aim of the present work is the development of strategies to overcome the influence of external factors which interfere in attempts to obtain valuable data about cell suspensions using dielectric spectroscopy.

To achieve this aim, the work has the following objectives:

1. To analyze and develop strategies to overcome interference produced by the presence of non-cellular particles.

2. To explore the use of microelectrodes made by photolithography to improve dielectric measurements on cell suspensions. As part of this a reference microelectrode should be developed to sense changes in the electrical properties of the medium.

3. To evaluate of the impact of changes in the conductivity of the medium on biomass monitoring.

4. To evaluate and compare the differences between dielectric and optical technologies when in the presence of bubbles, change in temperature, colour and different cell types.

5. To analyse the effect of the presence of non-viable cells on the measurement of the level of viable biomass and develop strategies to compensate a dielectric signal for their presence.

CHAPTER 2

LITERATURE REVIEW

_____

2.1 Introduction

2.1.1 Biomass

The subject of this thesis is the measurement of biomass. Unfortunately, no satisfactory definition of biomass currently exists (Harris *et al*., 1987). Biomass can be defined or classified depending on the process, use or measuring methodology.
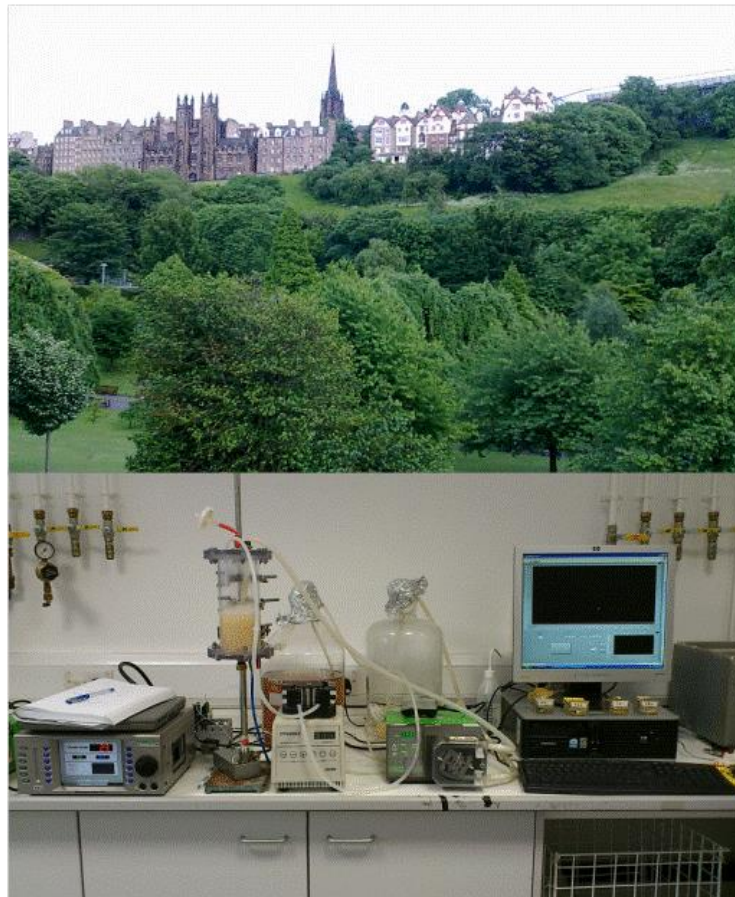
Figure 2.1 Biomass refers to material that is derived from biological organisms; this can be from macroscopic or microscopic organisms for a specific purpose.

2.1.2 Biomass as an energy source

Biomass is often mentioned as an energy source. From this point of view, biomass could be any kind of material that comes from living or dead organisms. Depending of the size of the organism, it could be macroscopic biomass (bulk) with the whole organism or some parts of it (feedstock, woodlands, branches, crop fields, yard clippings) or, in the case of unicellular or microscopic organisms, a suspension with microscopic organism in it (microalgae, fungi, bacteria) (See Figure 2.1).

Biomass can be used directly or indirectly for the production of energy. Directly, as plant matter for the generation of heat by direct combustion of the raw material, in gasifiers, or for the generation of electricity by moving turbines. Examples include forest residues such as trees and branches, solid wastes from crops, yard clippings and general waste. Indirectly use involves converting the biomass into other useful chemicals such as biofuels. Examples include first and second generation biofuels. First generation biofuels are biofuels such as bioethanol and biodiesel made from sugars, starch and vegetable oil. Bioethanol is produced by fermentation of sugars and starch from different crops such as barley, wheat, corn, sugar beets, sugar cane, potato or fruits (Nigam and Singh, 2011). Second generation biofuels are biofuels produced from sustainable feedstocks and not from food crops or edible products such as cellulosic ethanol from straw, wood or grass (Figure 2.2). In both, first and second generation biofuels, fermentation is an important part of the process (Wyman *et al*., 1992; Krishna *et al*., 2001; Sun and Cheng, 2002; Nigam *et al*., 2011).

Figure 2.2 Grass and other plant material are used for biofuel production.

A third generation of biofuels from microorganisms has also been proposed; these biofuels do no compete with crops for land use; often they are derived from microalgae. The third generation of biofuels involves growing genera such as *Chlorella*, *Dunaliella* and *Spirulina* for biofuel production. Other diverse applications for algae include the production of food and as animal feed, and the production of high value chemicals, bioactive compounds, fertiliser, aquaculture feed, antioxidants and colorants (Chisti, 2007; Converti *et al*., 2009; Demirbas, 2010; Harun *et al*., 2010; Griffiths *et al*., 2011; Day *et al*., 2012).

2.1.3 Biomass as a product of cell culture

Another way of viewing biomass is as the cellular material or cell derived material produced during cell culture. This definition of biomass is closely linked to the problem of monitoring biomass during cell culture (Harris *et al*., 1987). It would be desirable to have a general biomass monitoring technique that could meet the needs of industrial and research applications. However, despite the vast number of available techniques for measuring biomass, no single satisfactory method exists for all the applications and one of the causes is the lack of a general definition of biomass.

Biomass from macroscopic resources (bulk) can simply be weighed. For remote sensing of biomass, including the mapping of vegetation and other resources specific techniques are available such as multispectral imaging, discrete detectors, linear arrays, imaging spectrometry, digital frame cameras and astronaut photographic systems (Ahamed *et al*., 2011).

When we refer to biomass from microscopic organisms we are typically talking about a suspension of cells of microorganisms such as yeast, algae, fungi or bacteria. Several biomass monitoring techniques have been developed over the years, but all of them give different measures of biomass. One of the reasons for this is that it is difficult to obtain reliable measurements in the variety of environments in which the microorganisms exist, the diversity of the populations and the characteristics of the microorganisms themselves. The need for improvements in classical procedures for quantitative microbiological determinations has been urged (Harris and Kell, 1985).

A proposed classification of biomass monitoring techniques based on different definitions of biomass can be seen in Figure (2.3).
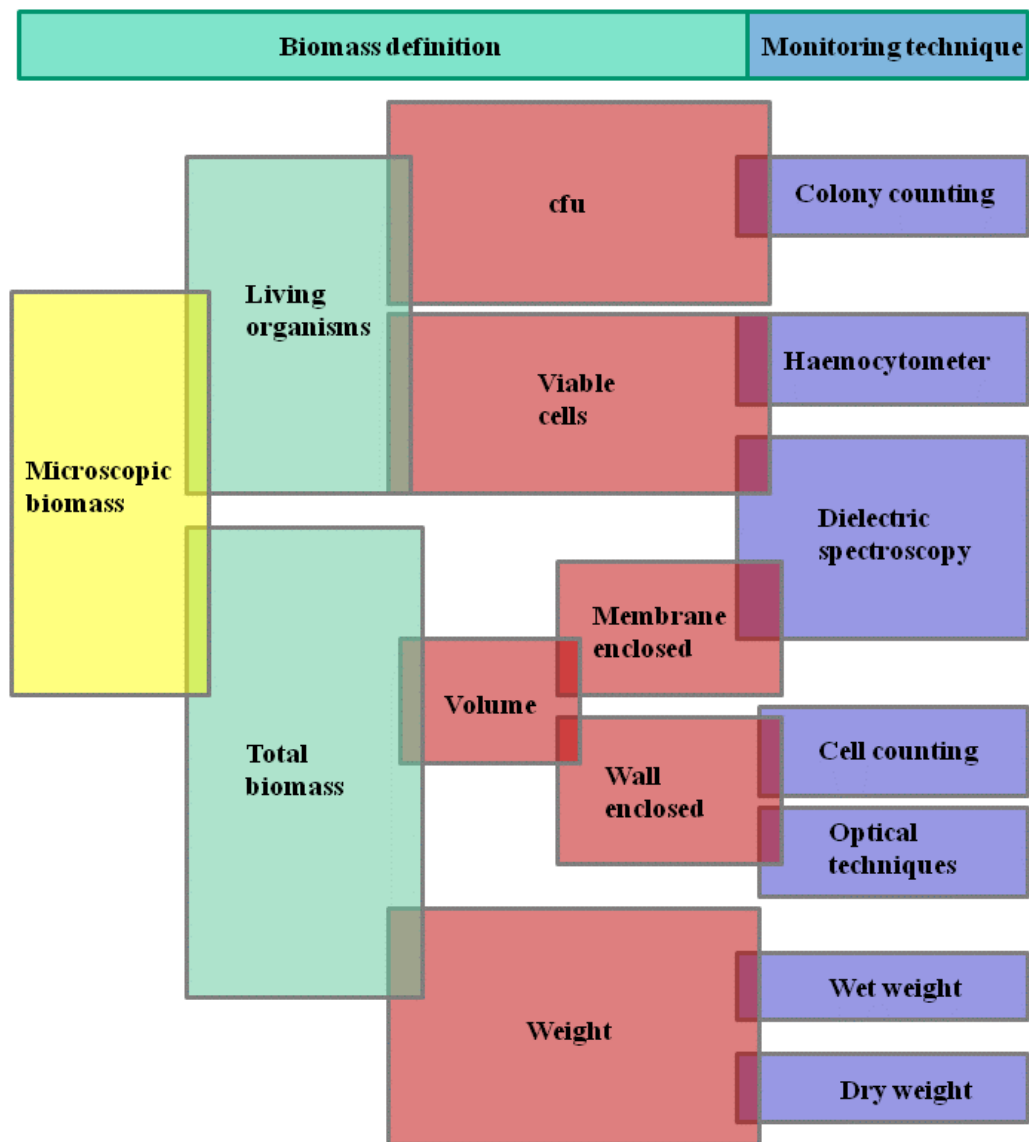
Figure 2.3 Proposed classification of biomass monitoring techniques based on the definition of biomass.

A first division is proposed on the basis of the definition of biomass as the biomass of *living* organisms or as a total *physical* bulk of biomass. The first division is therefore one on the basis of a biological definition of biomass and a physical definition of biomass. Straddling the two is dielectric spectroscopy which is a physical technique which also gives information on cell viability.

Only direct monitoring techniques have been included. Other methods for biomass monitoring are the indirect methods which are based on the developing of relationship between the biomass and some easy to measure attribute. Indirect monitoring techniques are usually based on the measurement of some chemical activity such as rate

of O_2 production or consumption, ATP concentration, metabolite production and changes in the medium among others. A relationship using regression analysis should be established between the biomass and the sampling. Among the disadvantages of the indirect methods are the restriction of the relationship between the indirect attribute and biomass to the time and place where the data were collected.

2.1.3.1 Living microorganisms

Growth and division are usually seen as key criteria for microbial biomass. Information about cell viability is required information for clinical analyses, ecological studies and most fermentations. However, what is actually meant by a "living organism" is still unclear and involves some philosophical and biological arguments (Harris and Kell, 1985).

Viability is a term often used to describe the ability of an organism to live and develop and therefore for microorganisms to divide and form colonies. Viability can be defined as the ability of a cell to multiply under controlled conditions. A methodology based on this definition is colony counting in which the colony forming unit (CFU) is an estimate of viable cells present in a cell suspension. The methodology is based on the ability of a (single) viable cell to raise colonies under specific conditions. Theoretically, one viable cell can originate one colony. However, this methodology becomes difficult to use when describing non-culturable or dormant microorganisms which are unable to form colonies but are otherwise intact (Patel and Markx, 2008). Also it becomes difficult to use with filamentous organisms. Added to this, in certain microorganisms a change in growth rate can induce a change in the morphology of the cells, accompanied by a reduction or increase in the number of cells. This means that the total amount of biomass may change independently of the number of cells. Another problem with the plate colony count is that one is supposed to use the suspension immediately as the inoculum. However, even if you use the suspension immediately, the plate count will still be unavailable for at least a day.

Other available methodologies for determining the number of viable cells are based on different assays that quantitatively give measures of cell viability such as the measurement of membrane leakage (Propidium iodide, Trypan blue, Methylene blue),

mitochondrial activity (MTT and XTT assays); or other functional assays (Gurr, 1965; Wang *et al*., 2011). Each of the methodologies give different answers to the question of what is the amount of viable cells in a suspension since they are all based on different definitions of cell viability (Patel and Markx, 2008).

2.1.3.2 Total physical amount of biomass

While cell viability may provide the information needed for some industrial and research processes, in some cases it is the total amount of biomass including necromass which is important. This is the case for certain fermentations for the production of glycerol and proteins. If the total amount of biomass is calculated from the number of viable cells, the error can be as high as 50% (Harris and Kell, 1985). Over the years many methodologies for the estimation of the total microbial biomass have been developed based on physical principles. These methodologies are generally based on the weight and the volume of the biomass.

Among the conventional off-line physical monitoring methods, dry and wet weight measurements are amongst the more commonly used in industry and research. These methods rely on the taking of samples, and are therefore neither *in situ* nor online. During sampling there is a risk of contamination. The methodologies can be time consuming in preparation. They determine the total amount of suspended biomass, and the presence of non-cellular material can create interference in the data. The methodologies are not suitable for continuous monitoring but are useful for providing one-off spot checks, which is a desirable good laboratory practice in order to avoid errors (Harris and Kell, 1985).

Direct counting of cell numbers is both possible both online and off-line, and can be done both by hand and automated. Some of the problems associated with direct counting have already been discussed when discussing cell viability. The presence of non-cellular particles can create high levels of errors (Harris and Kell, 1985).

Photometric systems are based on the amount of light that is absorbed, transmitted (turbidimetry) or scattered (nephelometry) by a sample and related to the cell concentration (Harris and Kell, 1985; Salgado *et al*., 2001; Griffiths et al., 2011). These

optical techniques are very useful for cell suspensions with a clear medium without suspended non cellular particles. A major problem with measurements based on the turbidity of a cell suspension is that they are unable to distinguish viable cells from non-viable cells and non-cellular particles without previous preparative procedures (Harris and Kell, 1985). Optical techniques only work in a limited range of cell concentrations (See Figure 2.4). The relation between optical density and cell concentrations often becomes non-linear already at low cell concentrations. Photometric systems do not measure cell numbers nor do they measure CFU, the measurement are systems more closely related to the dry weight of the cells (Sutton, 2011).
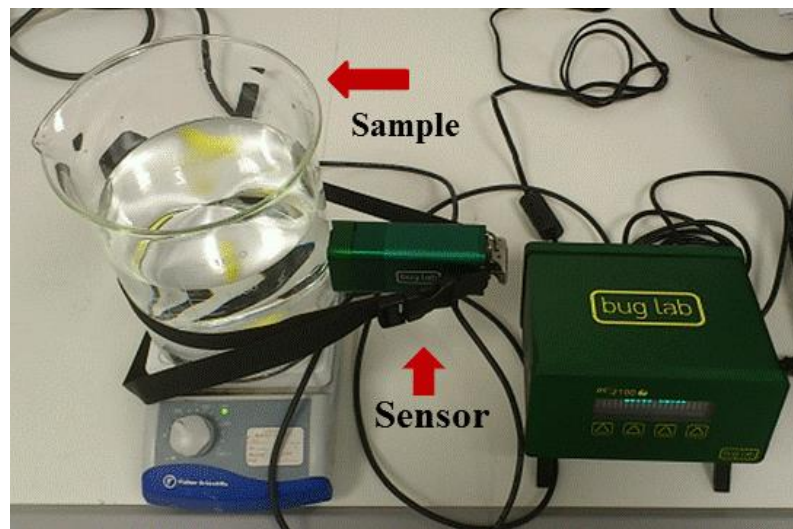
Figure 2.4 Infrared optical sensor from Buglab attached to a glass beaker.

One operational definition of microbial biomass which has been proposed is the volume fraction of the fermenter fluid which is enclosed within the boundary of the cell membrane. Dielectric spectroscopy determines biomass levels on the basis of this definition. When the cell is exposed to an electric field a polarisation process occurs across the cell membrane and this polarisation is accompanied by the formation of a strong dipole. When the volume fraction of cells increases, there are more polarised membranes, and the measured biomass concentration increases. Since dead cells and non-biomass solids do not possess intact plasma membranes there will not be a significant polarisation when the cells are dead and therefore the interference by dead cells should be minimal (Carvell and Dowd, 2006). However, this is valid only in situations where the mechanism causing death leads rapidly to gross cell lysis (Davey *et*

al., 1993). Also, cells have a strong ability of self-repair and even when the membrane is broken the cell can repair itself and is not actually non-viable, just injured (Patel and Markx, 2008).
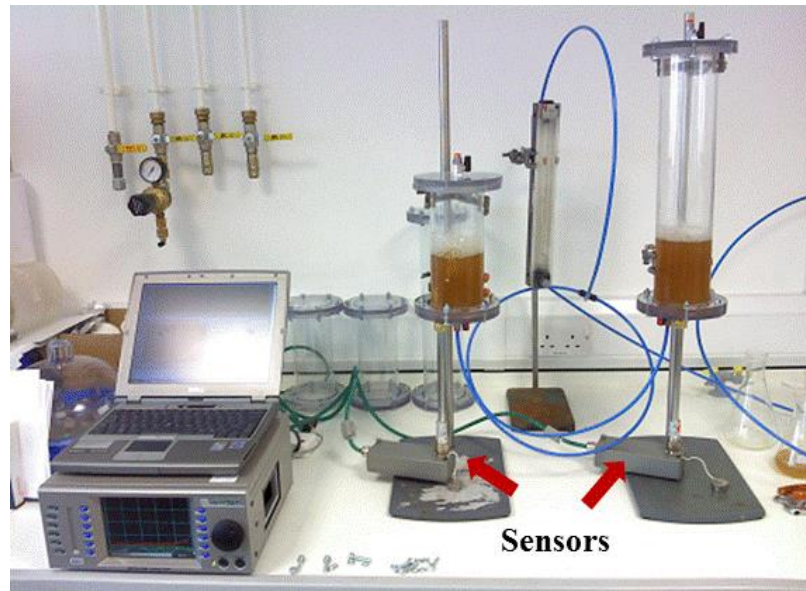
Figure 2.5 Dielectric biomass monitor from Aber Instruments being used to monitor two fermentations at the same time.

Dielectric spectroscopy is a most interesting technique not only because it measures biomass directly, continuously, on-line and in real time, but also because it is a physical technique which gives information on cell viability which otherwise can only be obtained with biological techniques (See Figure 2.5).

2.2 Dielectrics

"Dielectric" is the name given to a material that has the ability to support charge without conducting it to a significant degree. Therefore, on the basis of this description, all insulators are dielectrics, but they may have differences in their capacity to support charge (Maxwell, 1873). The name dielectric was first proposed by William Whewell ("dia-electric" from Greek prefix dia- "through, across, by over") in a response to a request from Michael Faraday.

Every material consists of positively and negatively charged atomic particles. Because of the bonds that keep these particles together, and the mutual attraction of the positive and negative particles, the average or total charge in any area of a material is normally zero. When a material is placed between electrodes that generate an electric field, the particles that form the material that carry a charge experience electrical forces created by the electric field (Pethig, 1979). If the material contains charged atomic particles with weak bonds which are free to move throughout the entire material then the material is called an electric conductor. But if the bonds between particles are strong and they move only slightly away from their normal position in the material then the materials is called an electric insulator. A pure dielectric is a pure insulator; however, although the term insulator implies low electrical conduction, the term dielectric only refers to the polarizability of a material. A dielectric can therefore be (slightly) conductive, as long as it polarises. Materials that polarise but conduct are called "lossy dielectrics". For simplicity, we will only discuss pure dielectrics (Fricke, 1931).

In a pure dielectric, when an electric field is applied, no electric charge transfer occurs; instead a wave of polarisation that travels through the material when an electric field is changed is the cause of the charge. The net result is that a dielectric supports charge separation by acquiring a polarity due to the application of an electric field, i.e. one surface develops a net negative charge while the opposite surface develops a net positive charge – see Figure 2.6 (Von Hippel, 1954b).
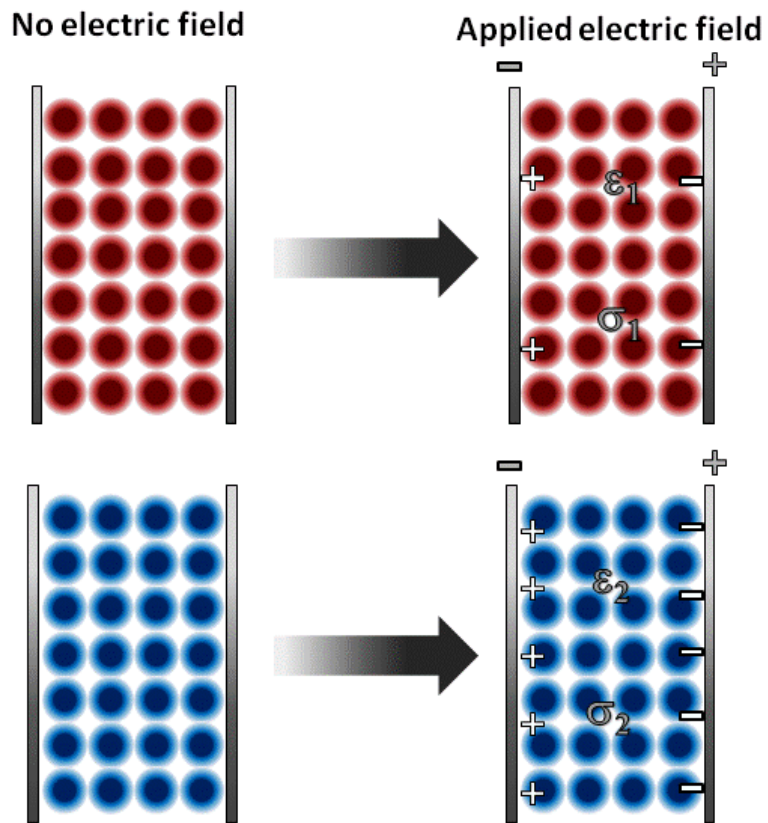
Figure 2.6 A comparison of two materials with different polarisabilities. When the materials are placed between electrodes and an electric field is applied, the charge accumulation on the surface is different, depending on the material's polarisability.

The development of this polarisation is possible because of the presence of electric dipoles.

2.2.1 Polarisation and dipoles

A dipole is the result of the presence of two opposite charges separated by a certain distance. A dipole can be defined in two ways:

a. A dipole moment (denoted μ) can arise if two charged particles of opposite charges become separated by a certain distance as seen on Figure 2.7, where d is the distance and q is the charge.
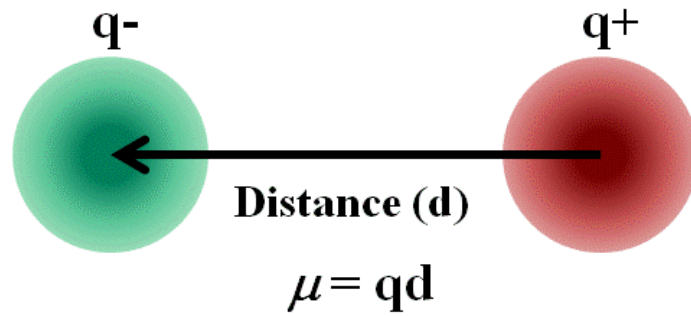
Figure 2.7 Dipole moment due to the distance between two charged particles.

b. A dipole moment arises as well when the centres of the positive and negative charges within a region are not in the same position. This definition is more useful since it can be applied to an area containing many charges.

Dipoles may be permanent, instantaneous or induced. Typical of permanent dipoles are molecules in which one atom attracts electrons more than another, becoming more negative, while the other atom becomes more positive. Instantaneous dipoles occur when due to chance electrons in a molecule happen to be more concentrated in one place than another. This creates a temporary dipole. Induced dipoles are dipoles that are induced by external electric fields causing a spatially uneven distribution of charges (Von Hippel, 1954a).

The net polarisation of a material is the total dipole moment per unit of volume. Since the dipole moment (μ) is a vector, the vector sum of the dipole moments may cancel out each other. A material may therefore contain dipoles but have no net polarisation.
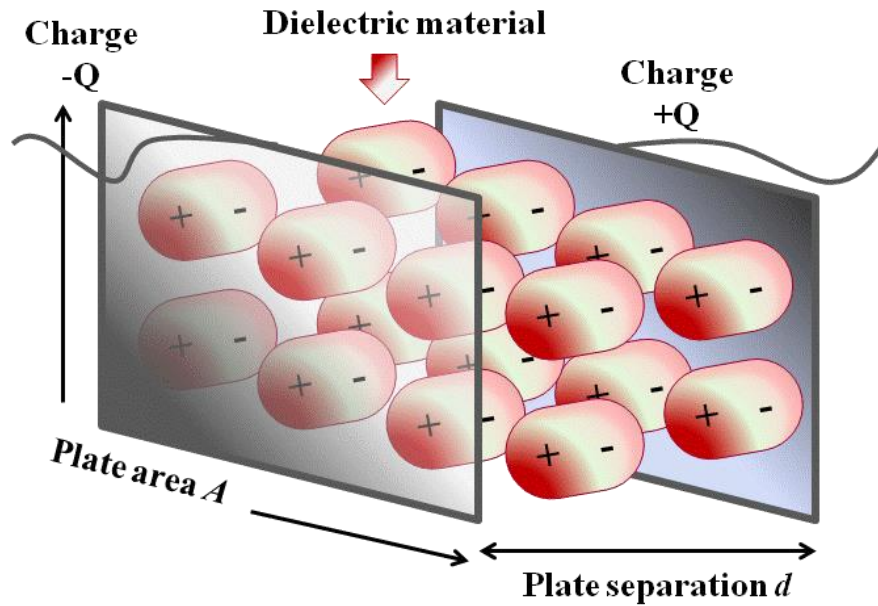
Figure 2.8 Charge separation in a parallel-plate capacitor causes an internal electric field. A dielectric (material) reduces the field and increases the capacitance.

When a (pure) dielectric is placed in an electric field, electric charges shift from their average equilibrium positions but remain bound. Positive charges (+Q) are displaced toward the negative electrode and negative charges (-Q) shift in the opposite direction. Because the charges are bound to the molecules or atoms forming the material, the overall effect is that the (induced or permanent) dipoles in the material align in the electric field as shown in Figure 2.8. Within the material the dipoles will cancel each other, but at the surface the dielectric will attain a net positive charge opposite the negative electrode, and a net negative charge opposite the positive electrode. The charges at the surface negate some of the charges on the electrodes, and which reduces the overall field within the dielectric itself (Davey and Kell, 1995).

The mechanism by which polarisation occurs is dependent on the nature of the material. The polarisation of a material in an electric field does not occur instantaneously when the electric field fluctuates; it takes some time to the material to react to the changes in the field. There is a delay in time between the fluctuation of the electric field and the polarisation of the material; this momentary delay is known as a relaxation (Ishikawa *et al*., 1981). Due to this relaxation, the permittivity and conductivity are frequency dependent. The way the conductivity and permittivity changes along the frequency

range are like steps and these steps changes are called dispersions. Each dispersion has its own characteristic frequency (See Figure 2.9) (Cole and Cole, 1941).

Dielectric polarisation mechanisms can be divided into four kinds: electronic, atomic, orientational and interfacial polarisation. Some authors mention ionic polarisation as well (Markx and Davey, 1999).
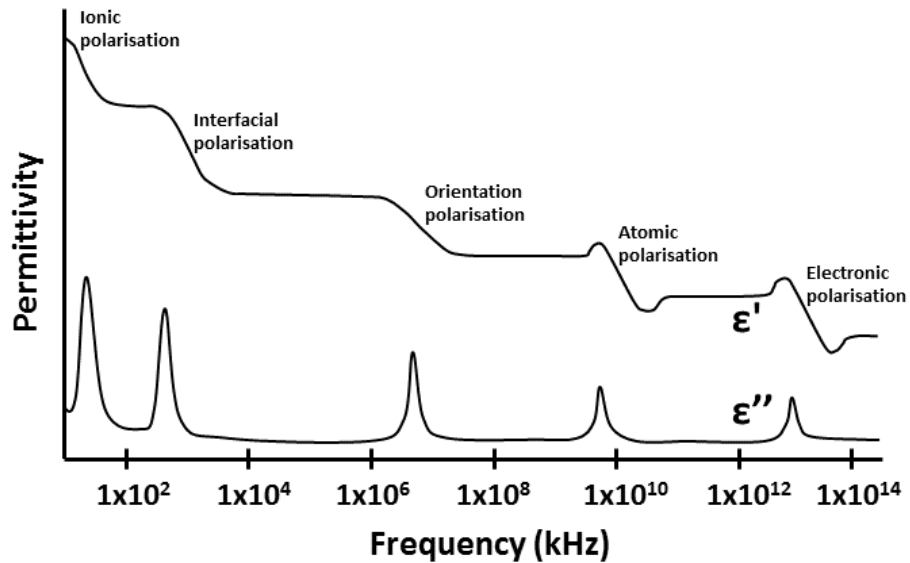
Figure 2.9 Spectrum showing the different dielectric polarisation mechanisms as a function of frequency. ε' and ε'' denote the real and the imaginary part of the complex permittivity, respectively.

2.2.1.1 Electronic polarisation

Electronic polarisation refers to the distortion or displacement of the cloud of electrons (electron density) in an atom in response to an electric field. Because the electrons are very light, this polarisation can occur at very high frequencies, around 10^{12} kHz (Salsman, 1991; Markx and Davey, 1999). See Figure 2.10.
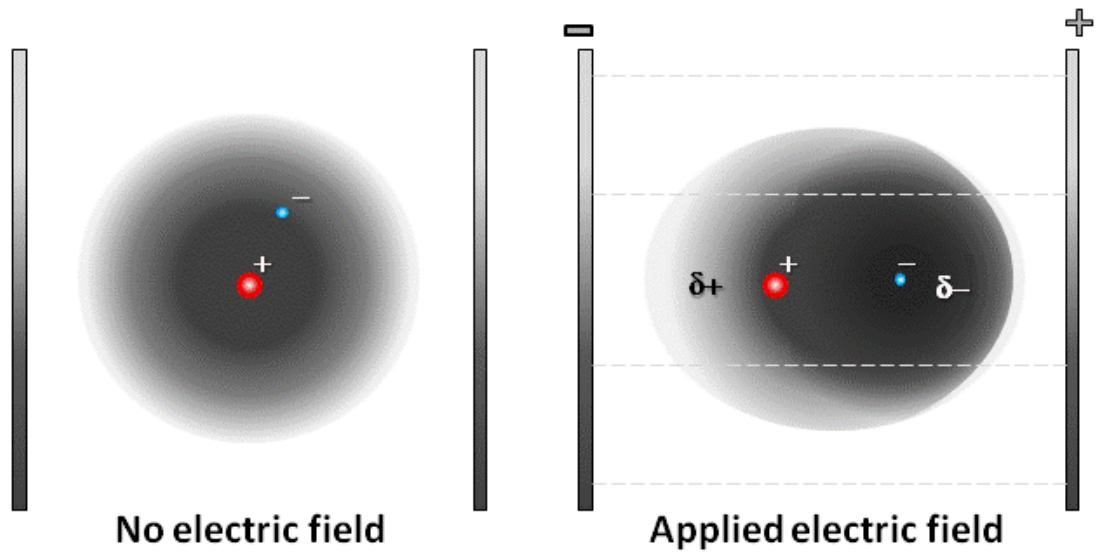
Figure 2.10 Electronic polarisation.

2.2.1.2 Atomic polarisation

Atomic polarisation refers to the displacement of whole atoms or atom groups in the molecule due to the influence of an applied electric field. This polarisation occurs at frequencies around 10^9-10^{10} kHz (Schwan, 1985). See Figure 2.11.
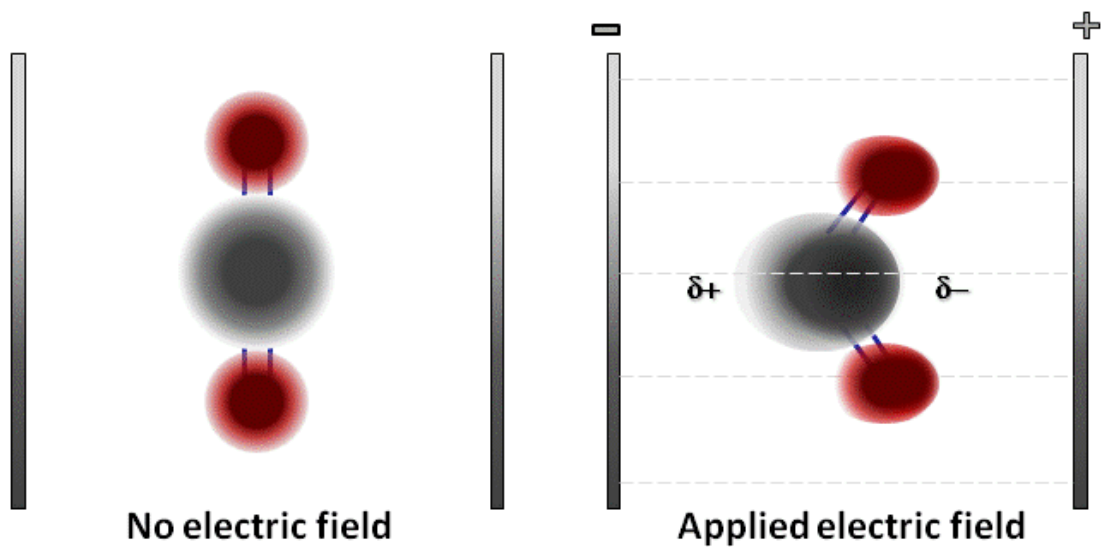
Figure 2.11 Atomic polarisation.

2.2.1.3 Orientational polarisation

Orientational polarisation refers to the physical alignment of permanent or induced dipoles to an applied electric field by the rotation of the molecule. Some molecules (like water) possess a permanent dipole due to the separation of charge within the molecule. These molecules are normally randomly arranged, and their net polarisation is zero, as the dipole moments from the different molecules cancel each other out; however, when an electric field is applied the dipoles rotate in order to align with the electric field and the material develops a net polarisation due to the sum of the dipole moments of the molecules. This polarisation is sometimes called dipolar polarisation (Haggis *et al*., 1952; Castro-Giraldez *et al*., 2011). This polarisation is proportional to the strength of the electric field and is influenced by the shape and weight of the molecules, and the composition of the medium such as viscosity and temperature (Fernandez *et al*., 1995). See Figure 2.12.
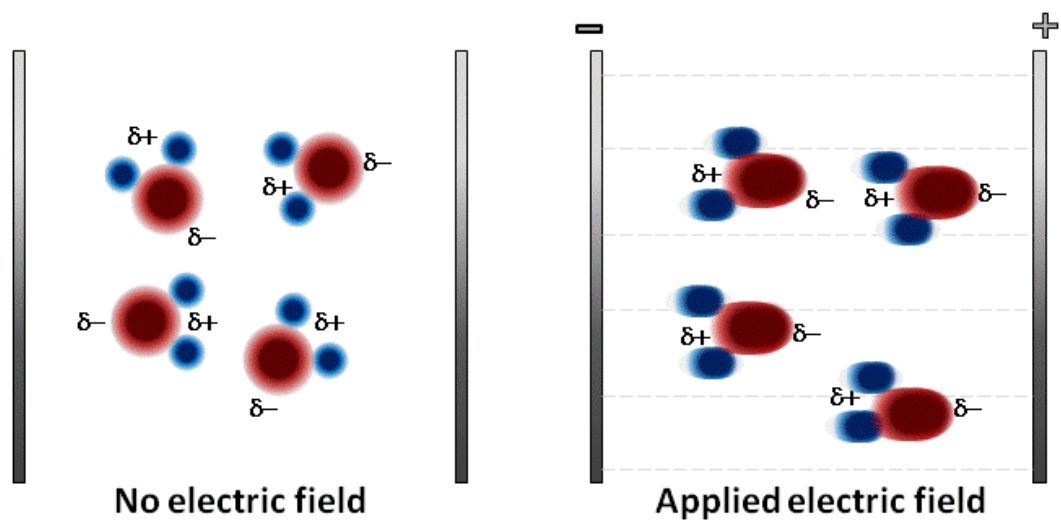
Figure 2.12 Orientational polarisation. Without an electric field Brownian motion will cause the H_2O molecules to have random orientations. When an electric field is applied on average the molecules will be oriented in the electric field. If temperature is increased the molecules Brownian motion will be stronger and the molecules will be less oriented; as a result, the permittivity will decrease

2.2.1.4 Ionic polarisation

To get ionic polarisation a material must be composed of cations and anions (i.e. have an ionic structure); typical are salt crystals. If we just have a single cation and anion,

with equal but opposite charge, held together by an ionic bond (see Figure 2.13), then a dipole moment can be observed before the application of and electric field. However in a crystal the net polarisation, which is the result of the sum of dipole moments over the whole material, is zero. An external electric field can induce a net dipole by slightly displacing the ions from their original position. The application of an alternating electric field will cause the ionic bond to stretch and compress alternately increasing and decreasing the dipole moment (Ueda *et al*., 1992).
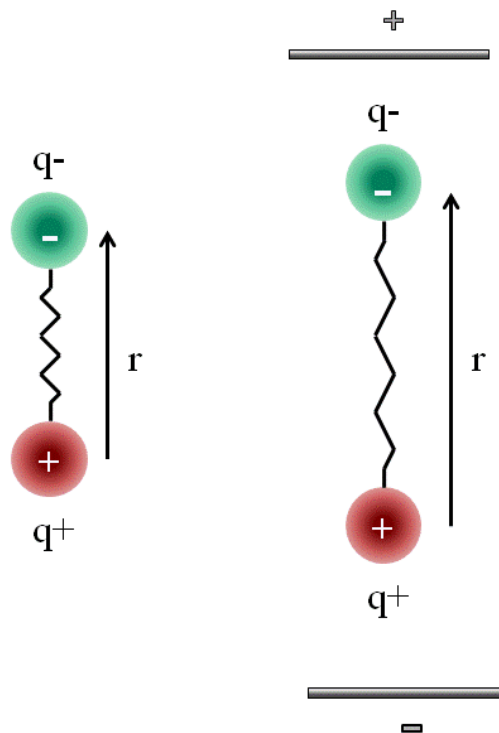
Figure 2.13 Ionic polarisation

2.2.1.5 Interfacial polarisation

Interfacial polarisation refers to an accumulation of charges on the surfaces of structures *within* a material. It should therefore not be confused with the accumulation of charges on the *outside* surface of a material due to the polarisation of a material in local areas due to the interference in the motion of charge carriers (electrons, ions or charged molecules) that move under the influence of an external electric field either because they become trapped; or because there is a limit to the extent or rate at which they are discharged or replaced at an interface (Markx and Davey, 1999).

Different mechanisms can lead to interfacial polarisation. The best-known mechanism is the so called Maxwell-Wagner polarisation. This model is based on the polarisation that occurs at the interface between materials with different dielectric properties (conductivity and permittivity). If we place two different materials one next to the other in the middle of an electric field, accumulation of charge in the interface will occur as a result of the difference in conductivity that will create a difference in current density on both sides of the interface and a different amount of charge stored on the two sides of the interface will be created due to the difference in the permittivity (Maxwell, 1873; Schwan and Morowitz, 1962).

2.2.2 The dielectric properties of materials

The dielectric properties of a material refer to the behaviour of this material when it is exposed to an electric field. Every material has electric properties that refer to the general electric properties of the substance such as conductivity, permeability, permittivity and piezoelectric constants; meanwhile the dielectric properties refer to the ability of a material to let an electric field pass through it. In the case of a metal, it has electric properties but it is not a dielectric as an electric field cannot get through it because of the Faraday cage effect. When a material is in an applied electric field, energy in the field is either lost by friction and turned into heat (resistive loss), or stored by polarisation of the material's components (Carstensen, 1967). Theoretically, energy storage in magnetic fields could also occur (induction), but this is negligible in most biological materials. The response of a material to an applied electric field is described by its conductivity (σ, in S/m) and permittivity (ε, in F/m) (Carstensen and Marquis, 1968). The conductivity gives a quantitative measure of the level of charge conduction through a material, irrespectively of the material's dimensions; meanwhile the permittivity gives a measure of the level of charge storage due to the polarisation again irrespective of the material's dimensions. The value of these parameters can be determined by placing a dielectric material in a capacitor. A capacitor can be described as any device used for storing charge, but usually consists of two conducting plates with a dielectric material in between (Davey *et al*., 1992, 1993a). Conductivity and permittivity are determined by measuring the conductance (G, in S) and capacitance (C, in F). The conductance is determined from the magnitude of the electrical current through the material as a function of the applied voltage, whereas the capacitance is

determined from the amount of charge stored on the plates when an electric field is applied (Fricke, 1931).

One way to illustrate the interfacial polarisation which leads to a Maxwell-Wagner dispersion type of polarisation is to envisage two different materials with different dielectric properties (permittivity and conductivity) in series between a capacitor plates (see Figure 2.14). If an equivalent circuit model of the resultant parallel capacitance C_p is calculated, we obtain:

$$C_p = \frac{(C_1 R_1^2 - C_2 R_2^2)}{(R_1 + R_2)^2} \qquad (2.1)$$

$$C_p = \frac{C_1 C_2}{C_1 + C_2} \qquad (2.2)$$

The capacitance at low frequency is higher than the capacitance at higher frequencies, therefore, with a parallel model of two slabs in series, a classical Debye dispersion can be observed even without any dipole relaxation in the dielectric (material). The dispersion is due to a conductance in parallel with a different capacitance for each dielectric (material), therefore a charge in the interface can be obtained due to the conductivity. The dielectric displacement is continuous along the whole interface (Davey *et al.*, 1992).
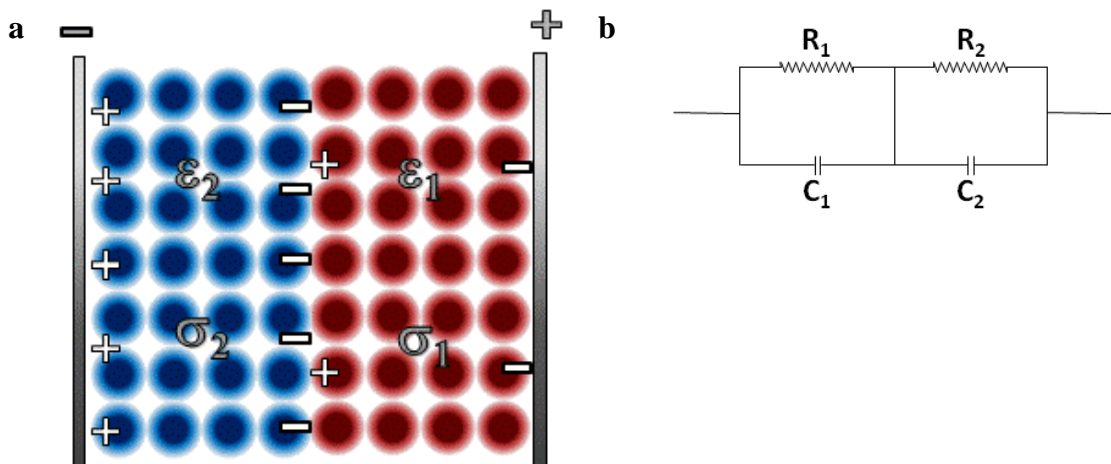
Figure 2.14 a) Interfacial polarisation occurs in the interface between materials with different dielectric properties in the presence of an alternate electric field b) equivalent circuit.

The theory establishes that the strength of the electric field will be lower on the high-permittivity side (material). In Fig. 2.14a; if $\sigma_1\varepsilon_2 \neq \sigma_2\varepsilon_1$ the difference in current densities implies that the interface will be charged. It will also be charged if $\sigma_1=0$ and $\sigma_2>0$. In the case where $\sigma_1\varepsilon_2 = \sigma_2\varepsilon_1$, the interface will have zero density of free charges and no Maxwell-Wagner polarisation will be observed, even though the materials had different dielectric properties (Pethig and Kell, 1987).

If the electrodes that create the electric field are plane-parallel plates or sheets of area A separated by a distance d, the capacitance and conductance measured will be a function of permittivity and conductivity following the equations:

$$\sigma = G\frac{d}{A} \tag{2.3}$$

$$\varepsilon = C\frac{d}{A} \tag{2.4}$$

$\frac{d}{A}$ is also known as the cell constant. Capacitance and conductance are proportional to the area and inversely proportional to the separation between electrodes, the closer the electrodes, the greater the capacitance; meanwhile, conductivity and permittivity are proportional to the separation between electrodes and inversely proportional to the area (Pethig, 1979).

Capacitance can be described as well with the equation:

$$C = \varepsilon_r\varepsilon_0 \frac{A}{d} \tag{2.5}$$

where C is the capacitance, A is the area between plates or electrodes; d is the separation between plates; ε_r is the relative permittivity (sometimes called as relative static permittivity or also known as the dielectric constant of the material); ε_o is the permittivity of free space (also known as the electric constant) with a value of 8.854 $\times10^{-14}$ F/cm. From the previous equation it can be derived that:

$$\varepsilon = \varepsilon_r\varepsilon_o \tag{2.6}$$

where ε_o (permittivity of free space), is equal to the capacitance of 1 cm^3 containing vacuum. ε_r (relative permittivity) is the ratio of the amount of electrical energy stored in a material when placed in an electric field, relative to that stored in a vacuum. In other words, it is the ratio of the capacitance of a capacitor using certain material as a dielectric; compared to a similar capacitor that has a vacuum as its dielectric. Therefore, ε (permittivity or absolute permittivity), measures how easily a dielectric (material) polarizes in response to an electric field. In other words, permittivity relates to a material's ability to transmit (or "permit") an electric field. The relative permittivity (ε_r) is dimensionless and is also known as the dielectric constant (sometimes denoted as K). See Table 2.1. Whilst in most publications dielectric constant and relative permittivity are the same, in some the term dielectric constant is reserved for the relative permittivity of a material when the frequency is zero (when the direction of the electric field is fixed, i.e. static). The term relative permittivity may refer to both the static and the frequency-dependent relative permittivity (Davey *et al*., 1993b).

Material	K	Temp (F)
air (standard conditions)	1.0005	68
nylon	2	75
paper	2	75
polyethylene	2.3	68
quartz	4.3	75
pyranol oil	5.3	68
mica	7	75
water	80	68

Table 2.1 Dielectric constant of some common materials. (source: http://www.deltacnt.com/99-00032.htm).

2.2.2.1 Complex permittivity

If a dielectric material becomes polarized in the presence of an electric field and the direction of the field is switched, the direction of the polarisation will also switch following the electric field in order to align. This change does not occur instantaneously and some time is needed for the dipoles to align. The time needed for the dipoles to

align with the electric field is called the relaxation time. The relaxation time causes a delay between changes in the external electric field fluctuates and the polarisation induced in the material. The dielectric displacement and the external electric field will therefore be out of phase, and there is a necessity to have another parameter to describe the changes' frequency-dependency (Pethig and Kell, 1987). The usual way to do this is to describe this situation in terms of a complex permittivity:

$$\varepsilon^* = \varepsilon' - j\varepsilon''$$

(2.7)

where ε' is the real part of the complex permittivity related to the amount of stored energy ($\varepsilon' = \varepsilon$) and ε'' is the imaginary part related with the loss of energy and $j = \sqrt{-1}$.

It can be derived that the imaginary part of the permittivity is related to the conductivity by:

$$\varepsilon'' = \frac{\sigma}{\omega}$$

(2.8)

where σ is the conductivity of the material in S/m. and ω is the radial frequency (in rad/s). Therefore

$$\varepsilon^* = \varepsilon' - \frac{j\sigma}{\omega}$$

(2.9)

2.2.3 Dielectric dispersions

2.2.3.1 Debye relaxation theory

The relaxation (or time delay) in the polarisation process produces a dispersion which exhibits itself as changes in the permittivity as a function of frequency. This relaxation was extensively studied by Peter Debye (Debye, 1929). Debye proposed that this dielectric relaxation could be expressed in terms of the complex permittivity as a function of the frequency of the external electric field by the following equation:

$$\varepsilon^*(\omega) = \varepsilon_\infty + \frac{\varepsilon_L - \varepsilon_\infty}{1 + i\omega\tau} \tag{2.10}$$

ε_∞ is the permittivity measured at a frequency sufficiently high that the polar or polarisable entity is unable to respond to the electric field; ε_L is the limiting low-frequency permittivity (sometimes called 'static' permittivity) where the polarisation is fully manifest, ω is the angular frequency of the (sinusoidal) electric field (in rad/s) and τ is the characteristic response time or relaxation time (see Figure 2.15). The magnitude of the dielectric dispersion can be defined as:

$$\Delta\varepsilon = \varepsilon_L - \varepsilon_\infty \tag{2.11}$$
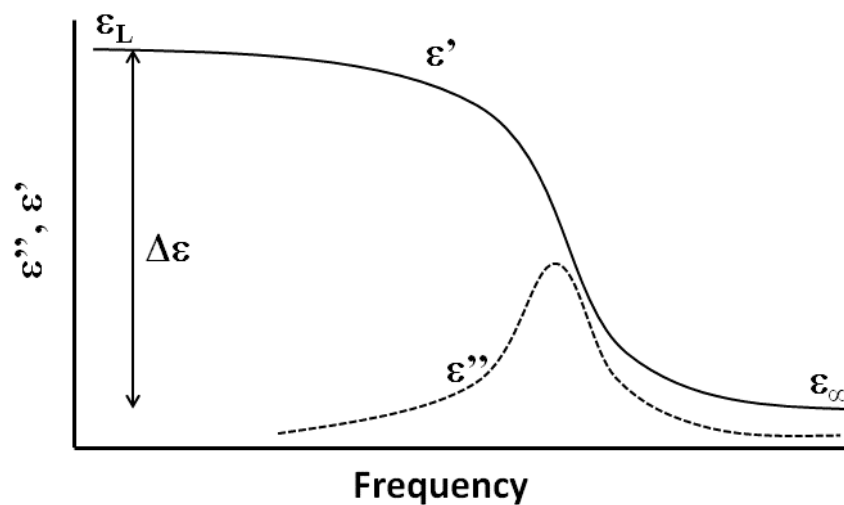
Figure 2.15 The dielectric dispersion illustrated in terms of the change in the real (ε') and imaginary (ε''; dielectric loss) parts of the permittivity (Davey and Kell, 1995).

This model is based under the assumption that the sum of different polarisation contributions due to different step potentials gives the total polarisation. In a previous equation it was explained that the complex permittivity ε^* may also be expressed in the form of its real and imaginary parts as:

$$\varepsilon^* = \varepsilon^{'} - j\varepsilon^{''}$$

(2.12)

in which the real part $\varepsilon^{'}$, can also be described following the Debye theory as:

$$\varepsilon^{'} = \varepsilon_{\infty} + \frac{\varepsilon_L - \varepsilon_{\infty}}{1 + (\omega\tau)^2}$$

(2.13)

and the imaginary component $\varepsilon^{''}$, known as the dielectric loss, corresponds to the dissipative loss associated with the movement of polarisable charges in phase with the electric field and can also be described by:

$$\varepsilon^{''} = \frac{(\varepsilon_0 - \varepsilon_{\infty})\omega\tau}{1 + (\omega\tau)^2}$$

(2.14)

The Debye theory describes a fall in the permittivity (real part; ε') and a peak in the dielectric loss (imaginary part; $\varepsilon^{''}$) (Pethig and Kell, 1987). In the next figure an idealized model can be seen of the real and imaginary part of the permittivity and dielectric loss as a function of frequency for experimental data and those obtained by Debye model. It can be observed that the predicted values deviate from the experimental values.
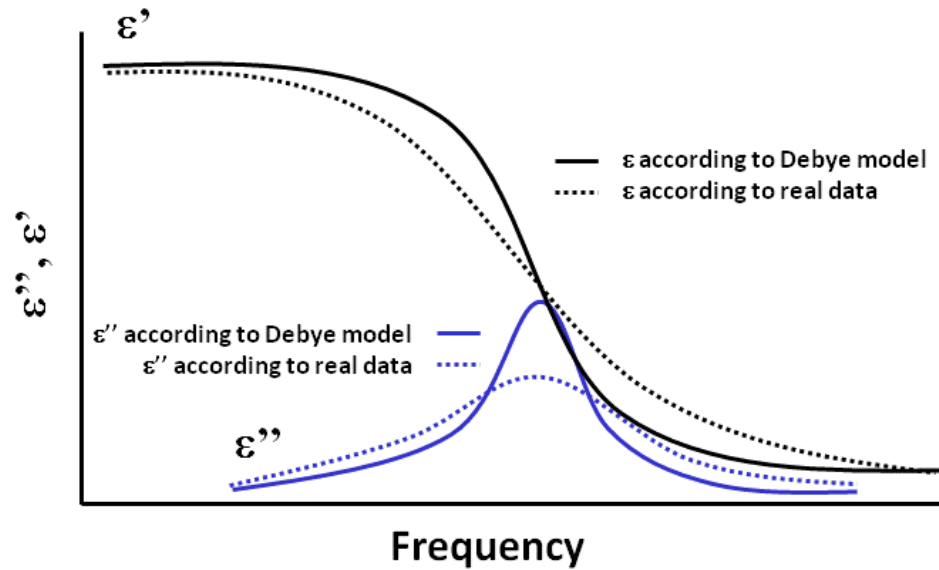
Figure 2.16 Real (ε') and imaginary (ε'') parts of the dielectric constant plotted against frequency. The solid curves are following the Debye model; and the dashed curves indicate the behaviour commonly found in real data (Davey and Kell, 1995).

In complex systems, such as biological materials, the dispersion of the permittivity as a function of frequency usually occurs in a broader band than that described by the Debye model (see Figure 2.16). This is usually interpreted to be due to a distribution of relaxation times. Biological materials can also show more than one dispersion when several relaxation mechanisms are involved and their time constants are different (Carstensen and Marquis, 1975; Harris and Kell, 1985).

2.2.3.2 The Cole-Cole model

In 1941, Kenneth S. Cole and Robert H. Cole proposed a model which could be used to make the Debye theory fit more closely to data found in experiments (Cole and Cole, 1941). This model is now known as the Cole-Cole model. It proposes a new parameter (α) which has been called the Cole-Cole alpha and gives a measure of the distribution of relaxation times and modifies the Debye equation as follows:

$$\varepsilon^{*}(\omega) = \varepsilon_{\infty} + \frac{\varepsilon_{L} - \varepsilon_{\infty}}{1 + (\iota\omega\tau)^{(1-\alpha)}} \qquad (2.15)$$

Cole and Cole based their findings on the Argand diagram or complex plane locus in which the imaginary part of the complex dielectric constant (ε'') is plotted against the real part (ε'), each point being characteristic of one frequency of measurement. This chart gives a semicircle with its centre on the real (ε') axis and intercepts at ε_{∞} and ε_{L} on this axis.
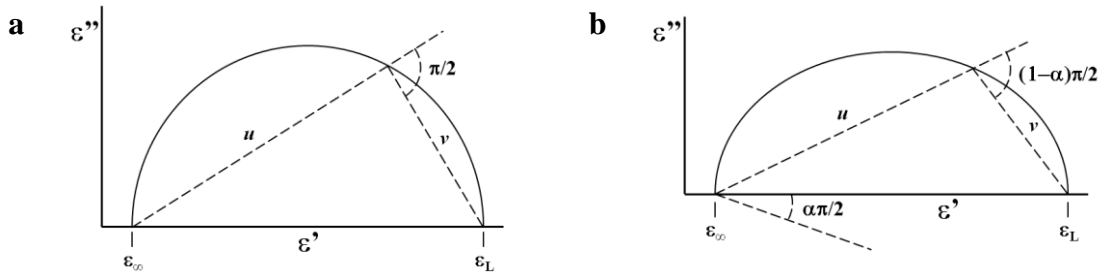
Figure 2.17 Theoretical complex plane loci (Argand diagram) showing the imaginary part of the complex dielectric constant (ε'') plotted against the real part (ε') for a) Debye theory and b) as required by experimental evidence (Asami, 2002).

In figure 2.17 an Argand diagram can be seen with ε'' plotted against ε' where u and v are perpendicular vectors in the complex plane with $u+v=\varepsilon_{L}-\varepsilon_{\infty}$. The right angle included by these vectors is therefore inscribed in a semicircle of diameter $\varepsilon_{L}-\varepsilon_{\infty}$. This semicircle is then the locus of the dielectric constant as w varies from 0 to ∞. Using geometry, an analytical expression for the angle between u and v can be found which is $(1-\alpha)\pi/2$. This expression is independent of the frequency and equal to half the central angle subtended by the arc. Therefore, parameter α can take values between 0 and 1 and allows us to describe different spectral shapes. When α takes values above 0, the relaxation is extended over a wider range of frequencies than the Debye relaxation. The Cole-Cole model can be reduced to the Debye equation when $\alpha = 0$ (Cole and Cole, 1941). The Cole-Cole α parameter is an empirical parameter introduced by Cole and Cole to reflect and heterogeneity of dielectric properties within a cell suspension. The α parameter could in theory be related to cell size distribution, cell shape, and budding cell fraction or to the presence of organelles. However, in practice these relations are

still not fully understood (Foster *et al*., 1989; Markx *et al*., 1991; Davey *et al*., 1996; Asami, 1999).

Cole and Cole were not the only ones to propose a theory to explain the deviation of the real data compared with the Debye model. Various other empirical equations have been proposed by Davidson and Cole, Havriliak and Negami, von Schweidler, Williams and Watts, Fuoss and Kirkwood, Jonscher and others (Asami, 2002). These models have been used to classify the dielectric relaxations of various materials and to extract the relaxation parameters from dielectric relaxation data. Some of these theories are summarized next.

Debye (semicircular arc rule)

$$\varepsilon^*(\omega) = \varepsilon_\infty + \frac{\varepsilon_L - \varepsilon_\infty}{1 + i\omega\tau} \tag{2.16}$$

Cole-Cole (circular arc rule)

$$\varepsilon^*(\omega) = \varepsilon_\infty + \frac{\varepsilon_L - \varepsilon_\infty}{1 + (\iota\omega\tau)^{(1-\alpha)}} \quad (0 < \alpha < 1) \tag{2.17}$$

Davidson-Cole (skewed arc rule)

$$\varepsilon^*(\omega) = \varepsilon_\infty + \frac{\varepsilon_L - \varepsilon_\infty}{(1 + \iota\omega\tau)^\beta} \quad (0 < \beta < 1) \tag{2.18}$$

Havriliak-Negami

$$\varepsilon^*(\omega) = \varepsilon_\infty + \frac{\varepsilon_L - \varepsilon_\infty}{[1 + (\iota\omega\tau)^{(1-\alpha)}]^\beta} \quad (0 < \alpha < 1, 0 < \beta < 1) \tag{2.19}$$

2.3 Electrical properties of biological cells and tissues

Cells are the basic unit of life. Some cells are shown in Figure 2.18. All cells have the same basic structure. They all have a phospholipid bilayer membrane (with some exceptions found in archaea) enclosing a cytoplasm which is complex and contains many small and large molecules and dissolved ions, but is mainly composed of water. In some organisms the cell is surrounded by a cell wall basically formed by glycoproteins and polysaccharides (Salton *et al*., 1951). The cell wall can be compared to an ion exchange resin because it is readily permeable to small molecules and ions (Carstensen *et al*., 1965). Because of its high salt content the cytoplasm is highly conducting. Many studies have been carried out on the electrical properties of cell membranes with real and artificial bilayer lipid membranes (Asami, 2002). In a static electric field the membrane acts as a good insulator as there are no free ions in the membrane to act as carriers transporting charges. However, the conductance of cell membranes is higher than that of a pure insulator due to pores and ion channels that allow current to flow through (Foster and Schwan, 1989; Cevc, 1990; Coster *et al*., 1996).
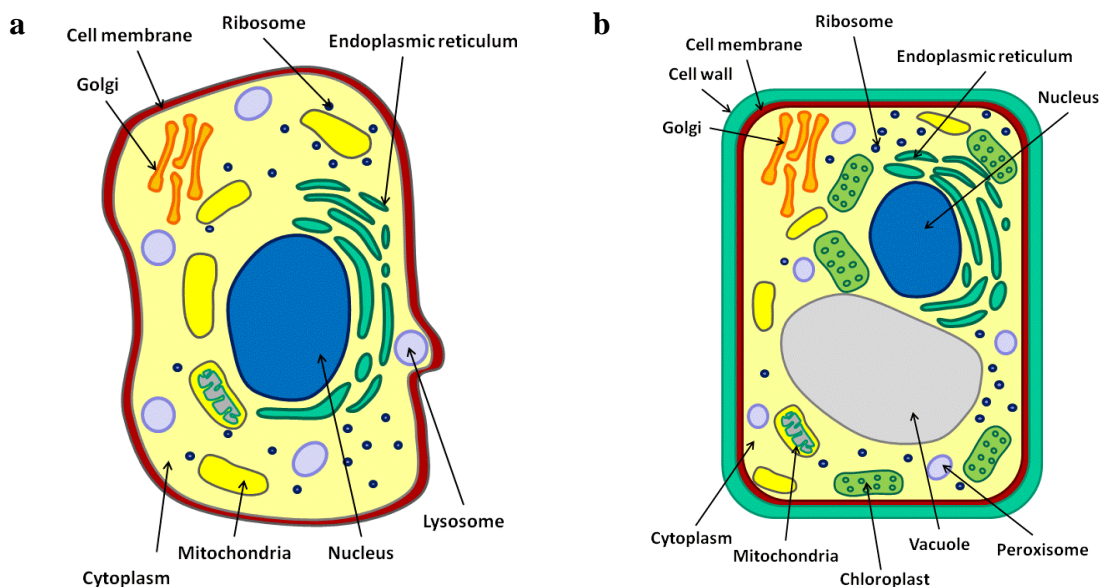
Figure 2.18 a) Typical animal cell b) Typical plant cell

2.3.1 Dielectric dispersions in biological materials

The dielectric properties of biological cells are frequency dependent. This exhibits itself as a series of broad steps in the permittivity and conductivity called dispersions (see

Figure 2.19) (Davey *et al*., 1992; Asami, 2002; Di Biasio *et al*., 2007). Three kinds of dispersions are typically observed in biological materials which contain cells: the *α*-dispersion, which occurs at lower frequency values, the *β*-dispersion, which occurs at middle frequency values and the *γ*-dispersion which occurs at high frequency values. In certain materials a *δ*-dispersion can also be observed which occurs between mid and high frequency values (Pethig, 1979; Schwan, 1985; Davey *et al*., 1995). The *α*-dispersion is due to the tangential flow of ions across cell surfaces, the *β*-dispersion results from the build-up of charge at cell membranes due to the Maxwell-Wagner effect, the *δ*-dispersion is caused by the rotation of macromolecular side-chains and "bound" water, and the *γ*-dispersion is due to the dipolar rotation of small molecules particularly water (Markx and Davey, 1999).
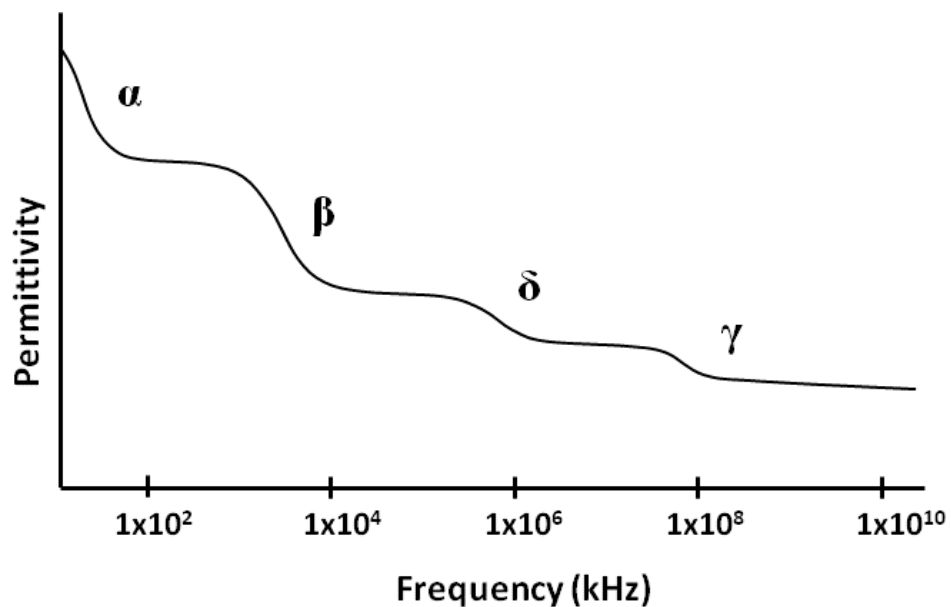
Figure 2.19 Theoretical chart showing the different dispersions observed on biological materials.

2.3.1.1 α-dispersion

The α-dispersion occurs at frequencies around 0.1 MHz. It is still not clear what phenomena cause the α-dispersion; several possible mechanisms have been proposed including gating of ion permeation in excitable membranes, gap junctions and holes in membranes, intracellular membrane systems connecting with the plasma membrane; and displacement of counterions around charged cell surfaces (Pauly and Schwan, 1959;

Schwan, 1985; Asami, 2006; Grosse and Delgado, 2010). One of the reasons why so little is known about the α-dispersion is that occurs in the same frequency range as the electrode polarisation. Electrode polarisation is caused by counter ions in the medium which are attracted by the charged electrode, forming a capacitative layer on the electrode surface. The descriptive literature on electrode polarisation is voluminous and has been studied since the last century (Schelder, 1975; Schwan, 1992; Davey and Kell, 1998a&b; Bordi *et al*., 2001).

2.3.1.2 β-dispersion

The β-dispersion can typically be found at frequencies between 0.1 to 100 MHz (i.e. in the radio frequencies). This dispersion occurs due to the large differences in dielectric properties between the different cell components (cell wall, membrane, and cytoplasm) and the medium. The polarisability of the low conductivity membranes is much smaller than that of the cytoplasm or the cell wall/medium, leading to the occurrence of build-up of charges at the surfaces of the cell membrane by a Maxwell-Wagner type of interfacial polarisation as shown in Figure 2.20.
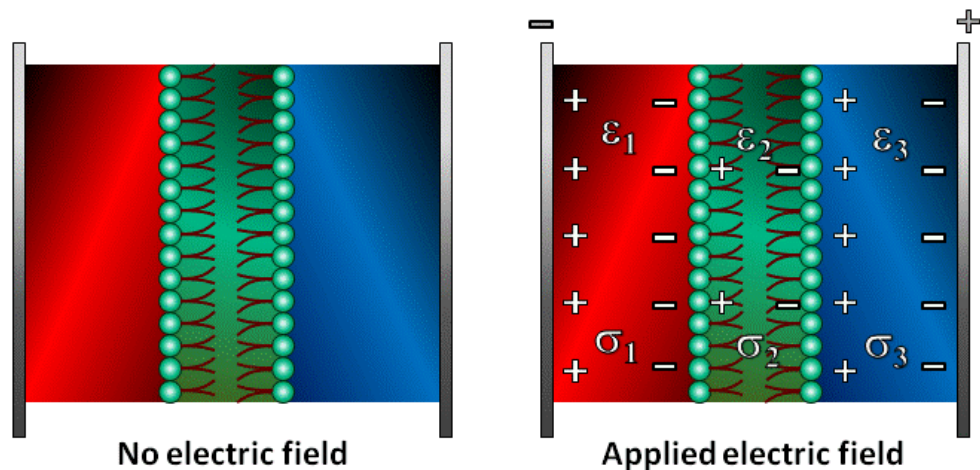
Figure 2.20 Interfacial polarisation across a cell membrane. For simplicity the cell wall has been omitted. The different dielectric properties of the media, cell membrane and cytoplasm results in polarisation of the membrane interface when an electric field is applied across the membrane.

The result of the polarisation process is an increase of the permittivity at lower frequencies which declines with increasing frequency. The dispersion associated with this Maxwel-Wagner type of interfacial polarisation at the cell membrane has been

extensively analyzed due to the fact that the increase in the permittivity linearly varies with the concentration of viable cells. Study of the β-dispersion can therefore give a reliable estimate of the volume fraction of viable cells (Schwan, 1957; Asami, 2002; Carvell *et al*, 2006).
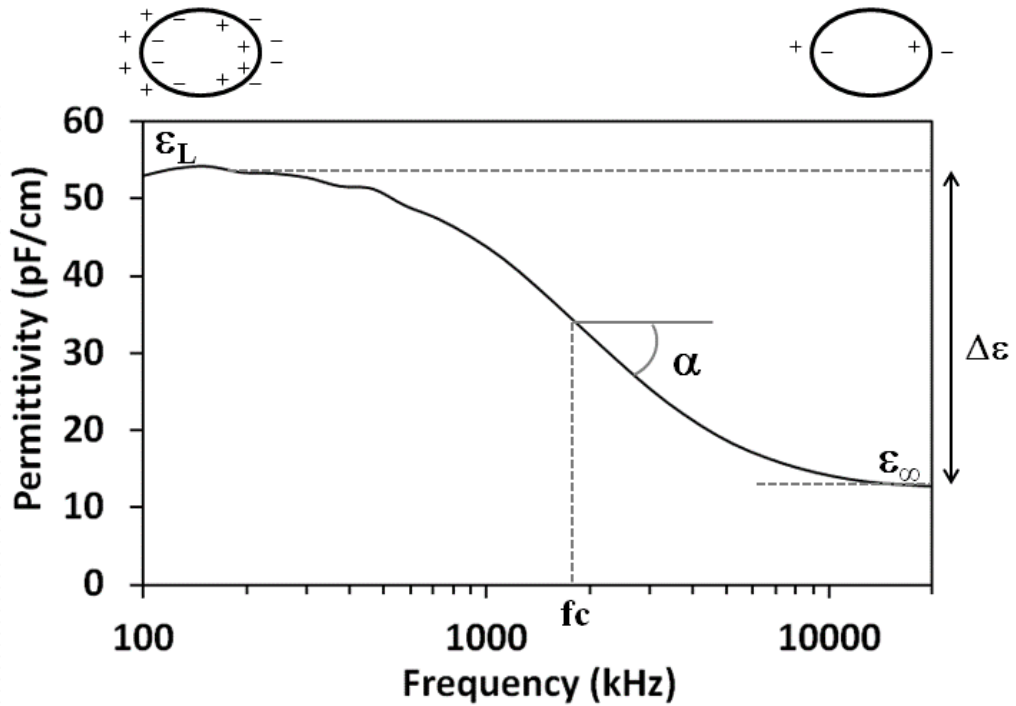
Figure 2.21 Typical β-dispersion curve for cell suspensions (Carvell and Dowd, 2006).

Figure 2.21 shows a sketch of a β-dispersion. A low frequency plateau can be seen which declines with increasing frequency to reach another plateau at high frequencies. The plateau in the high frequency permittivity is known as the residual permittivity (ε_{∞}). The dielectric increment ($\Delta\varepsilon$) is the difference between the low frequency plateau in the permittivity (ε_{L}) and the residual permittivity (ε_{∞}). The dielectric increment can be described by the equation:

$$\varepsilon_{L} - \varepsilon_{\infty} = \Delta\varepsilon = \frac{9}{4\varepsilon_{0}} PRC_{m} \tag{2.20}$$

where P is the volume fraction of (membrane enclosed) biomass; C_{m} is the membrane capacitance per unit area; R is the radius of the cell and ε_{o} the permittivity of free space.

The characteristic frequency f_c is the frequency at the inflection point, where $\varepsilon = (\Delta\varepsilon + \varepsilon_\infty)/2$ The Cole-Cole factor α determines the slope at f_c. The shape of the β-dispersion is influenced by various biological parameters other than the volume fraction of cells such as cell size and shape, internal conductivity and others. Apart from the polarisation of cellular membranes, other factors that contribute to the β-dispersion are thought to be the polarisation of proteins and other organic macromolecules (Gabriel *et al*., 1996)

In the previous discussion the effect of the presence of a cell wall on the β-dispersion has been ignored. Carstensen reported for *Escherichia coli* and *Micrococcus luteus* (formerly *lysodeikticus*) that when the conductivity of the media is low, the conductivity of the cells is dominated by the fixed charges in the cell wall. It has been suggested that for bacteria, the value of the conductivity at low frequencies are due to the properties of the cell wall rather than the cell membrane (Carstensen, 1967). At higher conductivities however, the ions from the medium invade the cell wall, causing the effective conductivity of the wall to take a value similar to that of the medium (Carstensen *et al*., 1965). As a result at high medium conductivities, as are often found in fermentation media, the contribution by the cell wall to the cell dielectric properties is usually minimal.

2.3.1.3 δ-dispersion

The δ-dispersion occurs at frequencies just above the β-dispersion and is believed to be mainly caused by rotation of macromolecular side-chains, proteins, cell organelles, and bound water. The α, β and γ-dispersions where discovered in earlier stages of research, and recently, when more sensitive devices to measure the permittivity have been developed, other dispersions with smaller magnitude have been observed, among them, the δ-dispersion (Schwan, 1957).

2.3.1.4 γ-dispersion

The γ-dispersion is due to the dipolar rotation of small molecules, particularly water. This dispersion was noted for a variety of tissues and protein solutions above 1 GHz (Schwan, 1957).

2.3.2 Dielectric properties of tissues

Whilst the previous discussion has concentrated on the dielectric properties of cells in general, the dielectric properties of tissues are also worth mentioning. Tissues are formed by different layers of different cells. The cells are surrounded by an extracellular matrix which can vary widely in function and formation. In principle, biological tissues have similar electrical properties as cell suspensions. Among the biological tissues that have been previously investigated we can find blood, bone, fat, grey matter, white matter, kidney, spleen, heart, liver, lung, muscle, and skin. Big differences can be found when measuring the electric properties of tissues. These differences can be due to the fluid content of the tissue, cell shape and size, the tissue orientation relative to the applied field; also changes may occur in the tissues over time. Analysis of tissues is difficult due to the variety of cell shapes and their distribution inside the tissue (tissue inhomogeneity), physiological state of the tissue, anisotropy of the tissue (orientation of the cells) as well as differences in the extracellular material (Miclavcic *et al*., 2006). The Cole-Cole model with several variations has been applied to describe the variation of dielectric properties of tissues as a function of frequency (Gabriel *et al*., 1996). Some problems are found when measuring the dielectric properties of biological tissues at low frequencies due to electrode polarisation and the strong dependency of the dielectric properties on the physiological state of the tissues. Therefore, some studies have been done at high frequencies (microwave frequencies) to identify different sources of errors (Peyman, 2011).

2.4 Strategies for modelling the dielectric properties of cells

Models can help interpreting experimental data. However, cells have a complex and heterogeneous structure with many different materials with different dielectric properties, and modelling is therefore difficult.

2.4.1 Modelling of dielectric phenomena

Maxwell established in 1873 the first model of interfacial polarisation. Maxwell stated that "for every particle of the dielectric is electrified with equal and opposite charges on its opposite sides, if it would not be more correct to say that these electrifications are only the manifestation of a single phenomenon, which we may call Electric Polarisation". When talking about the medium, Maxwell stated "A dielectric medium, when thus polarized, is the seat of electrical energy, and the energy in unit of volume of the medium is numerically equal to the electric tension on unit of area, both quantities being equal to half the product of the displacement and the resultant electromotive force, or

$$p = \frac{1}{2} DE = \frac{1}{8\Pi} KE^2 = \frac{2\Pi}{K} D^2 \qquad (2.21)$$

where p is the electric tension, D the displacement, E the electromotive force and K the specific inductive capacity. If the medium is not a perfect insulator, the state of constraint, which we call electric polarisation, is continually giving away" (Maxwell, 1873).

In 1850, Ottaviano-Fabrizio Mossotti analysed the distortion of the electric field in a continuous medium by a particle with a different dielectric constant. Further work was done by Rudolf Clausius in 1879, and the combined model is now known as the Clausius-Mossotti law. The law establishes that:

$$\left(\frac{\varepsilon - \varepsilon_0}{\varepsilon + 2\varepsilon_0} \right) \left(\frac{M}{d} \right) = \frac{4\Pi N_A \alpha}{3} \qquad (2.22)$$

where ε is the material's dielectric constant, ε_o is the permittivity of free space (vacuum), M is the material's molar mass, d is the material's density, N_A is Avogadro's number and α is the molecular polarizability.

The left hand term in equation 2.22 is often referred to as the Clausius-Mossotti factor. Instead of the form in 2.22 is often expressed in terms of complex permittivities:

$$K(w) = \frac{\varepsilon_p^* - \varepsilon_m^*}{\varepsilon_p^* + 2\varepsilon_m^*} \qquad (2.23)$$

with:

$$\varepsilon^* = \varepsilon_r \varepsilon_0 - j\sigma/w \qquad (2.24)$$

where ε^* is the complex permittivity and subscripts s, p and m refer to the suspension, particle (cell or microorganism) and suspending medium, respectively, $j = \sqrt{-1}$ (imaginary unit), w is the angular frequency of the applied electric field, σ the conductivity, ε_r the relative permittivity and ε_o the permittivity of free space ($8.854 \times 10^{-12}\,\text{Fm}^{-1}$).

From the Clausius-Mossotti relation several other models have been derived. This has included the Lorentz-Lorentz equation which relates the refractive index of a material to its polarizability. The Lorentz-Lorentz equation is:

$$\frac{n^2 - 1}{n^2 + 2} = N\alpha \frac{4\Pi}{3} \qquad (2.25)$$

where n is the refractive index (a measure of the speed of light in the medium) of the substance, N is the number of molecules per volume and α is the polarizability.

Based on the Clausius-Mossotti theory, in 1914 Wagner modelled the conductivity of a diluted suspension of randomly distributed spherical particles:

$$\left(\frac{\sigma_s - \sigma_m}{\sigma_s + 2\sigma_m}\right) = P\left(\frac{\sigma_p - \sigma_m}{\sigma_p + 2\sigma_m}\right) \tag{2.26}$$

where σ_s is the conductivity of suspension, σ_m the conductivity of the medium, σ_p conductivity of the particle and P the volume fraction of particles in the suspension. For interfacial polarisation of spherical particles within a matrix (i.e. a suspension of spherical particles with homogeneous dielectric properties in a homogenous suspending medium with different dielectric properties), Wagner proposed the following equation for the complex permittivity of the suspension:

$$\varepsilon_s^* = \varepsilon_m^* \frac{\left[1 + 2P\left(\frac{\varepsilon_p^* - \varepsilon_m^*}{\varepsilon_p^* + 2\varepsilon_m^*}\right)\right]}{\left[1 - P\left(\frac{\varepsilon_p^* - \varepsilon_m^*}{\varepsilon_p^* + 2\varepsilon_m^*}\right)\right]} \tag{2.27}$$

in which ε^* is the complex permittivity, P the volume fraction and subscripts s, p and m refer to the suspension, particle (cell or microorganism) and suspending medium, respectively, with $\varepsilon^* = \varepsilon_r \varepsilon_0 - j\sigma / w$, where $j = \sqrt{-1}$, σ the conductivity, ε_r the relative permittivity and ε_0 the permittivity of free space ($8.854 \times 10^{-12} \text{Fm}^{-1}$).

In 1923, Hugo Fricke suggested a model for electric capacity of cell suspensions. He wrote two articles in 1924 and 1925 about a mathematical treatment of the electric conductivity and capacity of disperse systems. In the first document, in 1924, he proposed a model for the electric conductivity of a suspension of homogeneous spheroids; and in 1925 he proposed a model for the capacity of a suspension of conducting spheroids surrounded by a non-conducting membrane for a current of low frequency. Fricke established that conductivity measurements may give values for (1) the specific conductivity, (2) the concentration of cells and (3) eccentricity of form of the suspended particles. The derived equation was:

$$\frac{(k/k_1) - 1}{(k/k_1) + x} = p \frac{(k_2/k_1) - 1}{(k_2/k_1) + x} \tag{2.28}$$

where k, k_1 and k_2 are the specific conductivities of the suspension, suspending medium and the suspended particles; p is the volume fraction of the particles and x is a function of the ratio k_2/k_1 and the ratio a/b of the axis of symmetry of the spheroids to the other axis. This equation is valid only for dilute suspensions and when the particles are spheres, $x = 2$ and the formula reduces to that of Lorentz-Lorentz and Clausius-Mossotti.

Schwan established in 1954 and 1957 that for a homogeneous cell suspension with spherical cells that are enclosed by a cell membrane the dielectric properties of the suspension can be described by the following equations.

$$\varepsilon_L - \varepsilon_\infty = \Delta\varepsilon_r = \frac{9}{4\varepsilon_o} \frac{PRC_m}{1 + RG_m \left(\dfrac{1}{\sigma_i} + \dfrac{1}{2\sigma_m} \right)^2} \tag{2.29}$$

$$\sigma_L = \sigma_m \left[1 - \frac{3}{2} P \frac{1 + RG_m \left(\dfrac{1}{\sigma_i} - \dfrac{1}{\sigma_m} \right)}{1 + RG_m \left(\dfrac{1}{\sigma_i} + \dfrac{1}{2\sigma_m} \right)} \right] \tag{2.30}$$

$$\sigma_\infty = \sigma_m \left[1 + 3P \frac{\sigma_i - \sigma_m}{\sigma_i + 2\sigma_m} \right] \tag{2.31}$$

$$\tau = \frac{RC_m}{\left(\dfrac{1}{\sigma_i} + \dfrac{1}{2\sigma_m} \right)^{-1} + RG_m} \tag{2.32}$$

where $\Delta\varepsilon_r$ is the dielectric increment (change in the relative permittivity); ε_L is the permittivity at lower frequency; ε_∞ is the permittivity at higher frequency; σ_L is the conductivity at lower frequency; σ_∞ is the conductivity at higher frequency; σ_i is the cell interior conductivity; σ_m is the conductivity of suspending medium; ε_r is the relative permittivity; P is the biomass volume fraction; C_m is the membrane capacitance

per unit area; R is the radius of the cell; τ is the relaxation time; G_m is the membrane conductance per unit area.

Some assumptions can be made about in the previous model to simplify it further. If the membrane conductance is sufficiently low and the radius of the cell is very large compared with the membrane thickness (assume that there is no wall present) and if the cells have random orientation, the previous equations will be reduced to the following forms:

$$\varepsilon_L - \varepsilon_\infty = \Delta\varepsilon_r \approx \frac{9}{4\varepsilon_o} PRC_m \qquad (2.33)$$

$$\sigma_L \approx \sigma_m \left(1 - \frac{3}{2}P\right) \qquad (2.34)$$

$$\tau \approx RC_m \left(\frac{1}{\sigma_i} + \frac{1}{2\sigma_m}\right) \qquad (2.35)$$

The previous assumptions are valid for most cells; however, they fail where there is a thick cell wall, when cells are markedly non-spherical, when cells do not have random orientation (tissues), and when P gets much above 0.15 (adjacent cells disturb the field impinging on their neighbours). Equation 2.33 we have seen before (eq. 2.20), and is the one that is most often used to relate dielectric (capacitance) measurements with biomass levels. Other models have been suggested for use when these assumptions are no longer valid (Markx *et al.*, 1999).

When cells are alive, the plasma membranes are intact and the polarisation can be related with the previous models. When cells are dead, the membranes are lysed, and then the equation implies that one can measure viable cell concentrations only (Markx *et al.*, 1999).

All the previous equations have been modelled for dilute systems where the volume fraction is low ($P \leq 0.15$) and the particles are spherical. Several equations have been derived for higher volume fractions, among these are included those of Bruggeman in 1935 and Hanai in 1968. Bruggeman's equation established that:

$$\frac{\sigma_s^{'}}{\sigma_m^{'}} = (1-P)^{2/3} \tag{2.36}$$

where $\sigma_s^{'}$ and $\sigma_m^{'}$ are respectively the conductivity of the cell suspension and conductivity of the suspending medium at low frequencies (100-465 kHz).

In Hanai's equation:

$$\left(\frac{\varepsilon_p^* - \varepsilon_m^*}{\varepsilon_p^* - \varepsilon_s^*}\right)\left(\frac{\varepsilon_s^*}{\varepsilon_m^*}\right)^{1/3} = 1-P \tag{2.37}$$

where ε_m, ε_p and ε_s are respectively the complex permittivity of the medium, particle and suspension.

All the previous mathematical models can be used to calculate the dielectric properties of the suspension, but to use them we still need to know the dielectric properties of the suspended particles. One method that has been used extensively is the multishell model (Fricke, 1924; Irimajiri, 1979), which is an extension of the work by Maxwell (1873). The multishell model proposes that for a single particle composed of (N+1) concentric spheres, with N shells, each of radiuses R_{N+1}, R_N, etc, the complex permittivity can be calculated with the equation:

$$\varepsilon_{peff}^* = \varepsilon_{(N+1)}^* \frac{\left[\left(\frac{R_{N+1}}{R_N}\right)^3 + 2\left(\frac{\varepsilon_{(N-1)eff}^* - \varepsilon_{(N+1)}^*}{\varepsilon_{(N-1)eff}^* + 2\varepsilon_{(N+1)}^*}\right)\right]}{\left[\left(\frac{R_{N+1}}{R_N}\right)^3 - \left(\frac{\varepsilon_{(N-1)eff}^* - \varepsilon_{(N+1)}^*}{\varepsilon_{(N-1)eff}^* + 2\varepsilon_{(N+1)}^*}\right)\right]} \tag{2.38}$$

where $\varepsilon_{(N+1)}^*$ is the complex permittivity of the outermost shell, and $\varepsilon_{(N-1)eff}^*$ represents the effective complex permittivity of the inner most N spheres after they have been smeared together. See Figure 2.22.
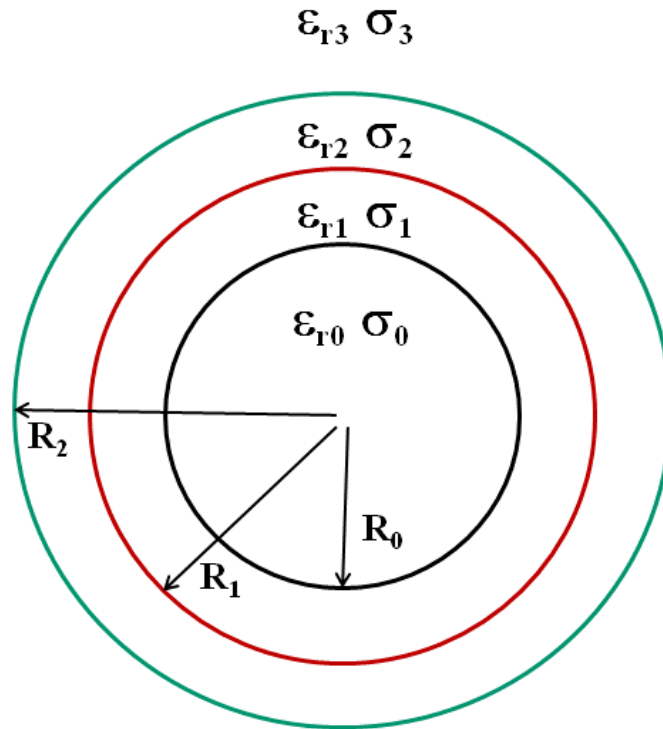
Figure 2.22 Multishell model of a cell. Spherical concentric shell with radius R_i, having shell conductivity σ_i and permittivity ε_{ri}. Different values have been given to these parameters and from these values the overall permittivity and conductivity of the cell can be calculated, where suffix 0 corresponds to internal cell; 1, membrane; 2, cell wall; and 3, medium. The permittivity and conductivity of the suspending media can vary depending on the experiment.

In this model we start with the two innermost spheres and calculate the complex permittivity for an equivalent homogeneous sphere. This procedure is repeated for subsequent shells until the outermost sphere is calculated (see Figure 2.23). Typical values for the conductivity and permittivity have been given and are: $\sigma_{internal}$: 2-10 S/m; $\varepsilon_{r\ internal}$: 50-120; $\sigma_{membrane}$: 10^{-8}-10^{-4} S/m; $\varepsilon_{r\ membrane}$: 2-10; σ_{wall}: 0.01-1 S/m; $\varepsilon_{r\ wall}$: 60 (Markx *et al.*, 1999).
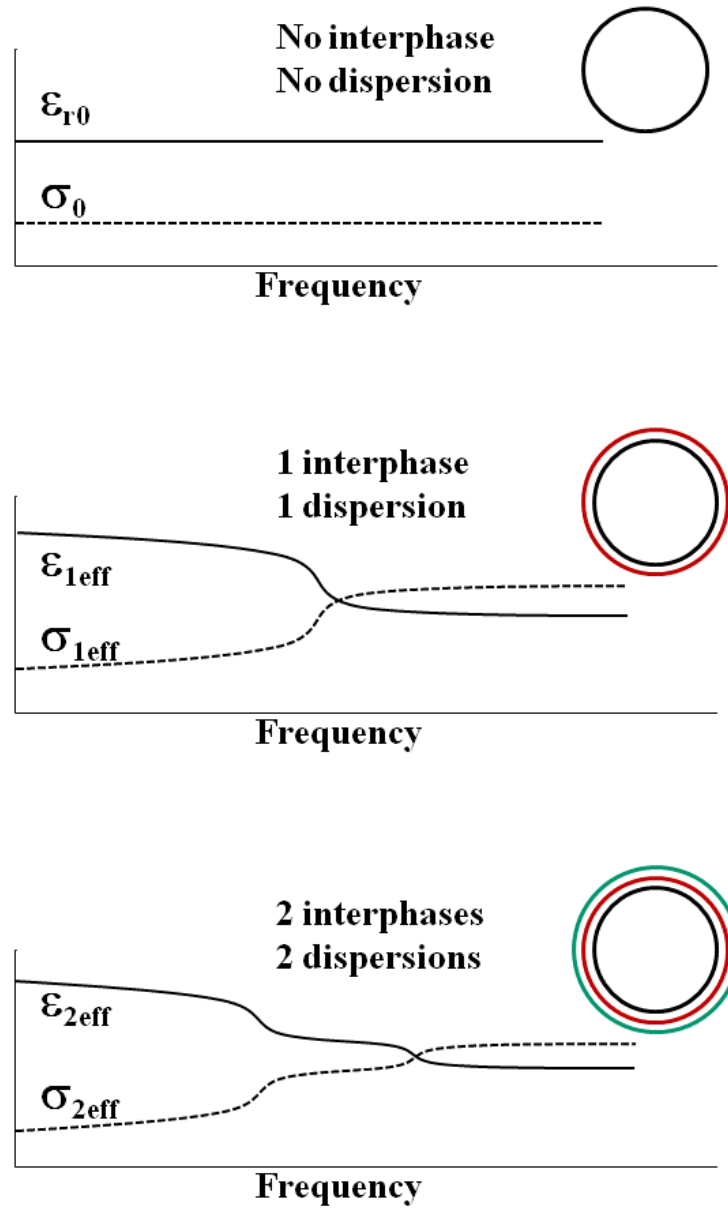
Figure 2.23 The multishell model. It is based in the fact that for every layer present in the cell there is an interphase between them creating a dispersion or change in the levels of conductivity and permittivity.

Different models have been proposed for non-spherical particles and for tissues. For an ellipsoidal shaped particle:

$$\varepsilon_{effp}^{*} = \varepsilon_{3}^{*} \frac{\varepsilon_{3}^{*} + (\varepsilon_{ieff}^{*} - \varepsilon_{3}^{*})[A_{1\alpha} + v_{1}(1 - A_{0\alpha})]}{\varepsilon_{3}^{*} + (\varepsilon_{ieff}^{*} - \varepsilon_{3}^{*})(A_{1\alpha} - v_{1}A_{0\alpha})} \tag{2.39}$$

where ε^*_{effp} is the effective complex permittivity of the two-shelled ellipsoid along the a ($a=x,\ y$) axes, and ε^*_{ieff} represents the effective complex permittivity of the inner-most ellipsoids after they have been smeared together:

$$\varepsilon^*_{ieff} = \varepsilon^*_2 \frac{\varepsilon^*_2 + (\varepsilon^*_1 - \varepsilon^*_2)[A_{2\alpha} + v_2(1 - A_{1\alpha})]}{\varepsilon^*_2 + (\varepsilon^*_1 - \varepsilon^*_2)(A_{2\alpha} - v_1 A_{1\alpha})} \qquad (2.40)$$

with

$$v_j = \frac{a_j b_j c_j}{a_{j-1} b_{j-1} c_{j-1}} (j = 1,2) \qquad (2.41)$$

where the subscripts 1, 2 and 3 represent the internal phase, cytoplasmic membrane and wall of a yeast cell, respectively, and $A_{i\alpha}$ ($i=0,\ 1,\ 2;\ \alpha=x,\ y$) is the depolarising factor along the x and y axes (Zhou $et\ al.$, 1996).

2.5 Dielectric measuring techniques

The different techniques will be reviewed by which the dielectric properties of materials can be measured and subsequently used to obtain valuable information.

2.5.1 Dielectric spectroscopy

As seen previously, dielectric spectroscopy involves the direct measurement of the dielectric properties (permittivity and conductivity) of a material in terms of its polarisation when the material is exposed to an electric field of varying frequency.

In recent years dielectric spectroscopy and dielectric based monitoring techniques have found increasing use in several fields and industries as a means of assessing the structure and composition of a material. Dielectric spectroscopy is used in a wide range of applications including food analysis (Bohigas *et al*., 2008; Lizhi *et al*., 2008; Al-Muhtaseb *et al*., 2010; Castro-Giraldez *et al*., 2010 and 2011; Castro-Giraldez, 2011; Guo *et al*., 2011; Smith *et al*., 2011) plastics and other polymers (Asami, 2002; McCrystal *et al*., 2002; Kalakkunnath *et al*., 2007; Christensen and Keiding, 2008; Singha and Thomas, 2008; Chen *et al*., 2011; Christensen *et al*., 2011), ceramics (Kolodiazhnyi *et al*., 2006; Silva *et al*., 2009), analysis of novel glasses and crystals (Costa, 2011; Hanumantharao and Kalainathan, 2012), oil analysis (Guan *et al*., 2009; Guan *et al*., 2011), drug analysis (Masoud *et al*., 2005), emulsions (Hanai *et al*., 1962); aging effects on insulation systems (Mopsik and Martzloff, 1990; Zaengl, 2003); proteins (Bonincontro and Risuleo, 2003) and other biological systems (Schwan and Foster, 1980; Pethig and Kell, 1987; Gabriel *et al*., 1996; Richter *et al*., 2007; Hayashi *et al*, 2008; Maskow *et al*., 2008; Bryant *et al*., 2011; Tibayrenc *et al*., 2011; Colella *et al*., 2012), and even water detection on the lunar surface (Nurge, 2012).

Other dielectric based techniques have focused on the nature of the materials and their applications such as the free space dielectric measurement technique for wires and ceramics (Free and Henry, 2007), the HYMENET probe for soils (Frangi *et al*., 2009), the broadband dielectric relaxation spectroscopy (DRS) and the thermally stimulated depolarisation currents (TSDC) for water mixtures (Kremer, 2002; Panagopolou *et al*.,

2011) and other techniques focused on low-frequency dielectric measurements (Krupka, 2003; Sorichetti and Matteo, 2007).

A reduction in the electric field will lead to a relaxation process which will follow with some delay or retardation to the reduction of the electric field. This event can be quantified in the time and in the frequency domain and dielectric spectroscopy monitoring equipment can be based in any of them. Most of the equipment developed has based on the dielectric response in frequency domain (Cole *et al*., 1989; Zaengl, 2003). In recent years, time-domain spectrometers have improved in accuracy and time response, enabling faster phenomena to be investigated.

Among the probes used for the measurements, a parallel-plate capacitor type is commonly used for frequencies below 10 MHz. However, the measurements require corrections due to the residual inductance and capacitance from the measuring cell and the connecting leads. When a fringing field exists at the edges of the parallel plate electrodes this can cause errors; a three-terminal method can be used to effectively eliminate this effect. For higher frequency work open-ended coaxial probes are typically used that are suited for measurements with network analyzers and time domain reflectometers at frequencies above 100 MHz (Asami, 2002).

In recent years, various new dielectric measurement techniques have been developed. Among them are various resonance measurement techniques which have been applied to the measurement of the dielectric constant and dielectric loss at microwave frequencies. These techniques can be divided into two groups. In the first group (called dielectric resonance), the resonance is supported by the dielectric itself. The sample acts as a dielectric resonator in which different geometries of metal shields are introduced to prevent radiation loss. Three of the most widely used dielectric resonance techniques to measure the dielectric properties of dielectric samples are the Post Resonance technique, the Cylinder Cavity Resonance technique and the Waveguide Reflection Resonance technique. The difference between the three techniques is basically the geometrical arrangement of the metal shields (Sheen, 2005). In the second group of the resonance measurement techniques (called cavity perturbation technique), the resonance is supported by the metal walls of a metal cavity. Samples placed in the cavity cause a perturbation on the field distribution in the metal cavity (Sheen, 2009). The main advantage of the dielectric resonance methods is the high accuracy of the dielectric

properties measurements, however among the principal disadvantages of these techniques it can be mentioned the complicated calculations for the dielectric properties, the sample dimensions and the fact that only a single frequency point can be measured for each sample (Krupka *et al*., 2001; Sheen, 2005).

The measurement of the dielectric properties of biological materials has focused on the measurement of the dielectric properties of cell suspensions because of the ability of cells to accumulate charges across the cell membrane when exposed to an electric field. Because each cell acts as a capacitor, the overall permittivity reflects the biomass levels in the suspension which can be monitored over a period of time for different applications. The use of the dielectric spectroscopy for the monitoring of biomass has been widely studied to use for different cell types under different conditions demonstrating a high level of reliability and accuracy. The direct linear relation between changes in permittivity and volume fraction has been proven for many cell types, such as bacterial cells (Asami *et al*., 1980), yeast (Asami *et al*., 1976; Markx *et al*., 1991; Markx, 1995; Davey *et al*., 1996), mammalian cells (Wang *et al*., 2002; Cannizzaro *et al*., 2003), plant cells (Markx *et al*., 1991; Asami *et al*., 1992). This methodology has been used and studied as an effective method for on-line measurement of biomass for many years (Schwan, 1957; Pethig *et al*., 1987; Asami *et al*., 1990; Davey *et al*., 1990; Asami *et al*., 2000; Asami, 2006; Carvell, 2006). The dielectric properties of biological cell suspensions are typically measured in a frequency range between 0.1 and 100 MHz using rapid, automated, frequency-domain, high precision spectrometers. To reduce problems associated with the high conductivity of the samples the four-electrode method (Schwan and Ferris, 1968) is often used, or the electromagnetic induction method with a pair of toroidal coils (Wakamatsu, 1997).

2.5.2 Electrokinetic techniques

Dielectric spectroscopy is not the only technique used to measure the characteristics of cells. In recent years, single-particle analysis techniques have been developed and they have become increasingly important methodologies especially in medical and biotechnological researches (Asami, 2002). For single-particle analysis, electrokinetic techniques are mostly preferred instead of conventional dielectric spectroscopy (Jones,

1995). Alternatively, imaging techniques with a scanning fine probe are also available for the single-particle analysis (Asami, 1994).

The electrokinetic techniques include DC electrokinetic techniques such as electrophoresis and electro-osmosis and AC electrokinetic techniques such as dielectrophoresis, electro-rotation, electro-orientation and travelling wave devices. Electrokinetic techniques are based on the movement of particles in electric fields. Many of these techniques can work with single cells, and it is therefore not necessary to make a suspension with a high concentration of cells as is the case with dielectric spectroscopy. Because they can work with single cells electrokinetic techniques have the advantage of being able to do measurements without cell-cell interactions. The technique can be used for cell characterization as well as cell manipulation (Markx and Davey, 1999).

2.5.2.1 DC electrokinetic techniques

This refers to those techniques that are based in the behaviour of a particle in the presence of a DC electric field. The most important DC electrokinetic technique is electrophoresis (see Figure 2.24). In electrophoresis the movement of a particle originates from the presence of electrical charge on the surface of the particle. The interaction between this charge and the electric field produces a migration of the particle. Electrophoresis is a useful tool for the separation of large molecules (nucleic acids, proteins) as well as microscopic particles (Zewert and Harrington, 1993; Szoke *et al*., 1999; Shendruk *et al*., 2012).
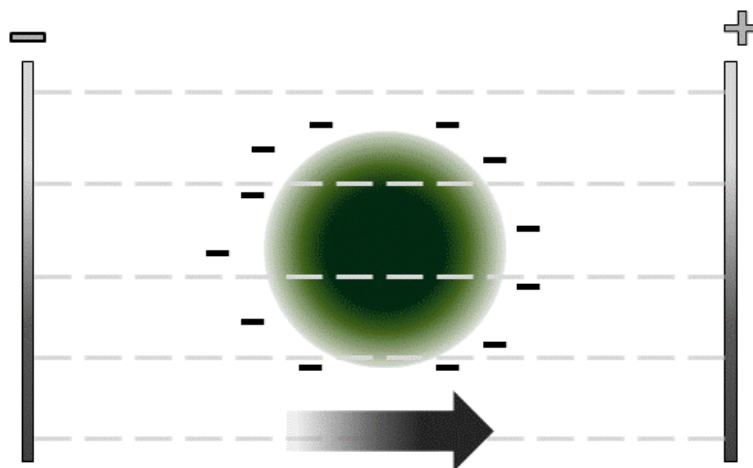
Figure 2.24 Electrophoresis

2.5.2.2 AC electrokinetic techniques

The term "AC electrokinetic techniques" refers to those techniques that are based in the behaviour of a particle in the presence of an alternate electric field. To observe AC electrokinetic effect it is necessary to apply a high strength field, which can be achieved by high voltages with large electrodes or low voltages with small electrodes. The last approach is generally used more often because of the simplicity. Some of the most well-known techniques are the following.

2.5.2.2.1 Dielectrophoresis

Dielectrophoresis is the induced movement of a particle in a non-uniform AC electric field. An explanation of dielectrophoresis can be seen in Figure 2.25. When a polarisable particle is present in an electric field the applied electric field induces a dipole in the particle. Due to the non-uniform nature of the electric field, the Coulomb force on one side of the particle is stronger than on the other side, and as a result there is a net motion. In the Figure shown the particle is more polarisable than the medium and the particle moves to the higher field near the smaller electrodes; this effect is called positive dielectrophoresis. If the particle is less polarisable than the surrounding medium, the dipole will align in the opposite direction to the field and the particle will be repelled from the high electric field region. This is called negative dielectrophoresis. Several attempts have been made in the modelling of the dielectrophoretic forces in 2D and 3D (Kua *et al*., 2008; Shi *et al*., 2011; Sun *et al*., 2011).

The dielectrophoresis has found many applications in cell separation and trapping and also in cell characterization (Wang *et al*., 1993; Becker *et al*., 1994; Markx *et al*., 1994, 1995, 1996; Stephens *et al*., 1996; Gascoyne *et al*., 1997; Song *et al*., 2011; van den Driesche *et al*., 2012). Dielectrophoresis has been used for separation of live and dead yeast cells (Markx *et al*., 1994; Fuhr *et al*., 1995; Patel *et al*., 2008) and bacteria of different species (Markx *et al*., 1996), for separation of human and animal cells (Becker *et al*., 1994; Stephens *et al*., 1996; Gascoyne *et al*., 1997; Cen *et al*., 2004), and for separation and manipulation of different solid particles (Batton *et al*., 2007; Jeong *et al*., 2009; Chen *et al*., 2010; Shi *et al*., 2011).
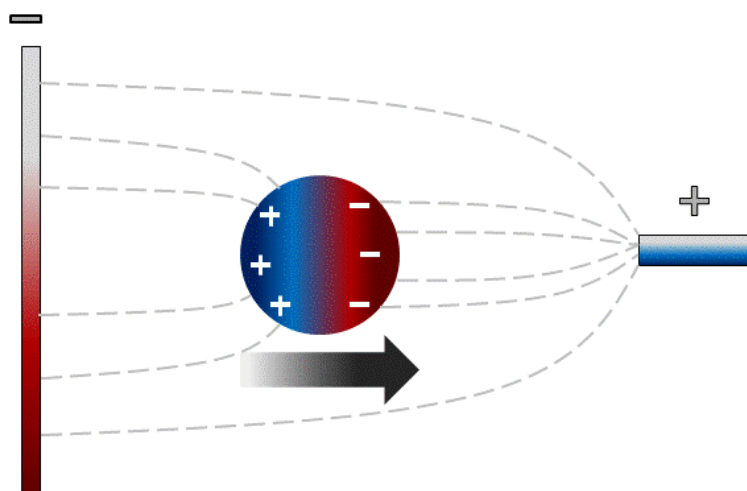
Figure 2.25 Dielectrophoresis

2.5.2.2.2 Electro-rotation

Electro-rotation refers to the rotation of particles in the presence of an applied electric field. The measurement of the electro-rotation rate as a function of the frequency can be used to obtain information about the electrical properties of single particles. Even though this technique can be used for a wide variety of particles, the measurement of the electro-rotation speed is better for those particles between 1 and 100 microns due to the fact that for small particles is very difficult to observe and measure the rotation, especially for those with spherical shape while it is hard to apply strong enough forces to big particles to overcome friction. This technique has been used for measurement of cell properties (Zhou *et al*., 1995; Chan *et al*., 1997; Falokun and Markx, 2007; Voyer *et al*., 2010) and to measure the effects of chemicals on cells (Arnold, 1988). This technique has a lot of potential in toxicology testing and drug screening (Zhou *et al*., 1996), particle characterization (Morganti and Morgan, 2011), and cell characterization (Zimmerman and Grosse, 2002; Wu *et al*., 2005).

2.5.2.2.3 Electro-orientation

Electro-orientation is the frequency-dependent orientation of particles in the presence of an electric field. The orientation of the particles varies according to their dielectric properties and shapes and the frequency of the electric field. This technique has biological applications in the fields of particle characterization (Iglesias, 1985; Jones,

1990; Bunin, 1996; Gimsa, 2001), production of structured materials (Pohl, 1978) and cell characterization (Markx *et al*., 2002; Bunin *et al*., 2004).

2.5.2.2.4 Travelling wave dielectrophoresis

Travelling wave dielectrophoresis is a technique in which the movement of particles over the electrodes is due to the application of phase-shifted electric fields applied to a railway sleeper-like electrode system. It has a large potential in developing "biofactory-on-a-chip" devices (Pethig, 1998) and for cell characterization (Wu *et al*., 2005).

2.6 Factors that can influence the dielectric signal during biomass monitoring

Dielectric spectroscopy is a powerful tool for monitoring biomass during fermentation; additional information can also often be obtained about cell properties. However, fermentation processes are difficult environments to do impedance measurements in. Often the medium is complex and may contain high concentrations of materials. The composition of the medium may change considerably as media components are taken up by the cells and converted, or material is added during fed batch operations, leading to changes in the medium permittivity and conductivity. Not all materials present in the medium may be soluble. The materials may also be solids, oil droplets, etc. Such materials have their own dielectric dispersions which contribute to the overall spectrum. Other factors may also be important. Large temperature changes may occur. Objects in the vicinity of the sensor may disturb the electric field emanating from the sensor. Bubbles may be generated (CO_2, air) which can lead to a decrease in the signal when the bubbles come close to the sensor. Cells may accumulate on the sensor. The electrical or magnetic environment of the sensor may vary due to fluctuation in the ground potential, electric motors, magnetic stirrers etc.

Clearly a lot of factors may interfere in a biomass measurement. An attempt will now be made to give an overview, dividing them into internal factors that are related to the electronic equipment used for biomass measurements, and external factors that are associated with the measurement environment.

2.6.1 Internal factors that influence dielectric measurements

All electronic measurement systems contain elements that can affect the signal integrity, and Biomass Monitors are no exception. Poor signal integrity will affect system reliability. The aim is therefore a design which minimizes detrimental effects on signal integrity. Many internal factors can interfere with the signal in an electronic system, the most significant factors being the cross-talk, EMI and lead inductance.

2.6.1.1 Cross-talk

Cross-talk is a term used in electronics to refer to the disturbance or interference caused when the signal from one circuit or channel becomes superimposed on another circuit or channel, creating an undesired signal in the electrical circuit as a result of electrical coupling. The line the signal is coupled from is usually referred to as the active (or aggressor) line, and the signal line the signal is coupled into is called the passive (or victim) line. A common cause of crosstalk in electronic devices is the current induced in a wire by the magnetic field created by the changing current in another wire when both wires run parallel or when two or more twisted wire cables are bundled together.

Cross-talk coupling generates two types of effects: forward and reverse cross-talk. Forward cross-talk refers to the current coupled onto a passive line away from the active line driver, as shown in Figure 2.26. The current is the result of capacitively coupled current (I_C) minus the inductively coupled current (I_L).
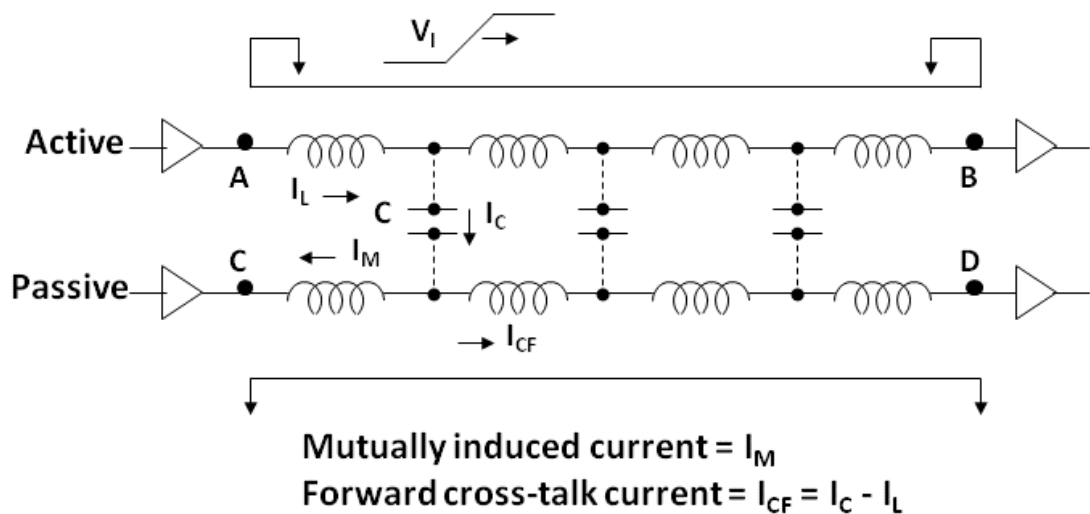
Figure 2.26 Illustration of forward cross-talk.

Reverse cross-talk refers to the current coupled onto a passive line toward the active line driver, as shown in Figure 2.27. The current is the result of capacitively coupled current (I_C) plus the inductively coupled current (I_L).
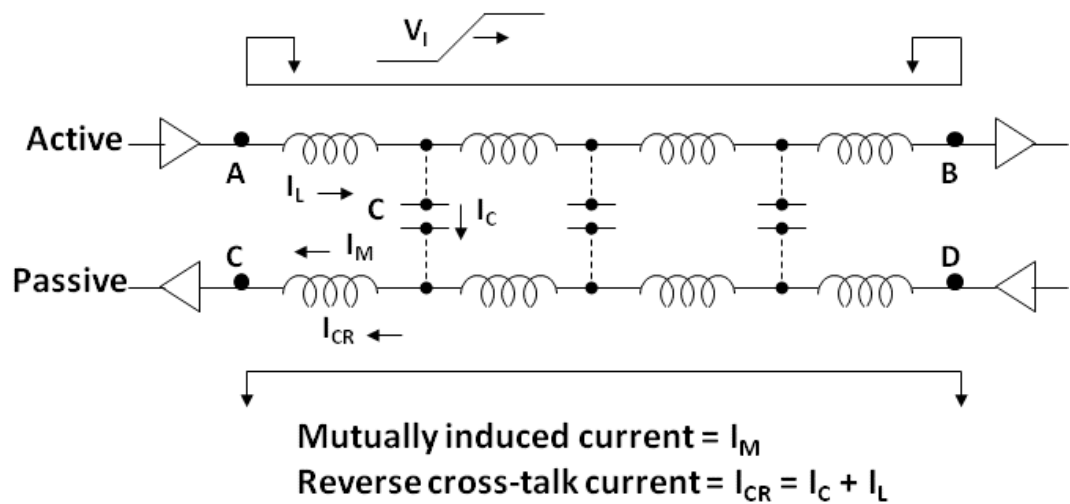
Figure 2.27 Illustration of reverse cross-talk.

Cross-talk in integrated circuits can be reduced by using insulated or shielded cables or by increasing the distance between conductors or by wire re-ordering. However, even when cross-talk normally refers to a signal affecting another nearby signal due to capacitive or inductive coupling, other forms of coupling and effects on signalling can be found (Fairchild Semiconductor, MS-566, 2002; Moser *et al*., 2002). In biosensors, cross-talk can be due to the miniaturization of the sensor device, and the design and geometry of the biosensors can help to reduce cross-talk. Several methodologies have been proposed to eliminate the phenomenon in such sensors (Palmisano *et al*., 2000; Suzuki and Akaguma, 2000; Moser *et al*., 2002).

2.6.1.2 Electromagnetic Interference (EMI)

Electromagnetic Interference (EMI) refers to any unwanted spurious, conducted or radiated signals of electrical origin that can cause interference and degradation of the system signal integrity and performance. This interference can result in data errors and system faults and can cause problems in the connections, inside the actual system or outside the system like in cables or nearby systems. Overall board and system layout have a significant effect on EMI since current flowing in a path within the system can generate EMI (Fairchild Semiconductor, MS-566, 2002).

2.6.1.3 Lead inductance

Inductance is a phenomenon that occurs when a change in the current in a conductor induces or creates a voltage in both the conductor itself and on any nearby conductors. For steady currents, a steady magnetic field is created following Oersted's law. With time-varying i.e. changing electric currents changing magnetic field are associated which following Faraday's law of induction and Lenz's law lead to an induced voltage which is opposed to and proportional to the change in the current The varying field in a circuit may also induce voltage in a neighbouring circuit.

In biosensors lead inductances are often introduced when the wires are connected at a small distance from the edge of a chip. When AC current is flowing in the electrode it generates a magnetic field surrounding the wires. This time-varying magnetic field induces voltage in the leads. This behaviour is observed at high frequencies.

Several strategies have been proposed to eliminate inductance effects but because the effect is magnetic, using shielded wires do not eliminate the effect completely. The behaviour can often be minimized by twisting the wires or by re-ordering. Many electronic systems have already made corrections for this effect in their software (Rodgers and Eggers, 1993).

The inductance of the probe and connecting cable adds another factor to the errors of measured dielectric properties of materials. It affects the dielectric properties of lossy media. Its value could be determined from measurements on standard salt solutions and applying an equivalent circuit analysis (Gabriel *et al*., 1996).

2.6.2 External Factors that influence dielectric measurements

External factors are factors that are not directly associated with the measurement system itself. They can include soluble and non-soluble media components, temperature, the presence of non-viable cells, carriers, bubbles and other factors.

2.6.2.1 Temperature

Changes in temperature have a significant effect on the dielectric properties of any material. Many studies have also looked at changes in the dielectric properties of polymers, ceramics and other materials over the years (Wang *et al*., 2002; Zhang *et al*., 2006; Lizhi *et al*., 2008; Saltas *et al*., 2008; Gokcen and Altuntas, 2009; Du, 2010; Okiror and Jones, 2012). In certain materials there is a U-shape frequency response in the dielectric loss factor (Roebuck and Goldblith, 1972).

Generally, the dielectric loss factor in water increases with increasing temperature at low frequencies due to ionic conductance and decreases with increasing temperature at high frequencies due to free-water dispersion (Tang *et al*., 2002). At lower frequencies the changes in the temperature in water directly impacts on the movement of the ions, producing a rise in conductivity levels when the temperature rises (Fernandez *et al*., 1995). The effect of the temperature on the permittivity is particularly high for water because it has permanent dipoles. When the temperature is raised the molecules have more energy (thermal energy) and move more strongly. This makes it more difficult to achieve orientational polarisation, and the relative permittivity of (pure) water value goes down by 0.38%/K (Fernandez *et al*., 1995). When other materials are dissolved in water, the changes in the relative permittivity with temperature can be quite complex. For example in glucose solutions the dielectric constant may increase when temperature rises (Liao *et al*., 2003)

While measuring the dielectric properties of biological tissues temperature is an important factor to be aware of. In general an increase of about 2%/°C is observed in the conductivity of tissues in the frequency range below 1 GHz up to a temperature of around 40 °C due to the decrease of the viscosity of the fluids with increasing temperature. At higher temperatures the cell membrane begins to deteriorate (Foster and

Schwan, 1989; Soley *et al*., 2005). Extrapolation from experimental data on temperature effects in tissue is difficult (Gabriel *et al*., 1996).

2.6.2.2 Soluble media components

Media can be made from a wide range of different soluble and non-soluble components. All these components contribute to overall dielectric properties of the medium (Haggis *et al*., 1952). Media components such as salts, sugars, enzymes and other organic and inorganic compounds affect the dielectric spectra in different ways. Salts are ionic compounds that when dissolved in a solvent make it more electrically conductive. There is a linear relationship between the increase in the concentration of ionic compounds and the increase in the conductivity of the medium. However, the concentration of ions normally has little effect on the capacitance of the medium (Hasted *et al*., 1948; Arnoux *et al*., 2005) (though it will affect electrode polarisation). In contrast, an increase in the level of reducing sugars causes a decrease in the capacitance of a medium, but has little effect on the conductivity (Liao *et al*., 2003; Bryant *et al*., 2011).

The composition of the medium can change remarkably as the cells grow and consume its components. The conductivity of the medium can change considerably due to consumption or formation of organic compounds, though it depends on the species used. During yeast fermentation changes in medium conductivity are often small because the concentration of ions remains almost invariable and the main products of the metabolism are not ionized (Soley *et al*., 2005). In contrast, during fermentations of lactic acid bacteria large charges occur in the medium conductivity due to the formation of lactic acid.

2.6.2.3 Electrode polarisation

One of the main sources of error while measuring the dielectric properties of biological materials is electrode polarisation, which occurs at the lower frequency range (Gabriel *et al*., 1996). The magnitude of the electrode polarisation is highly dependent on the ion concentration and increases with increasing conductivity of the sample. Electrode polarisation decreases with increasing frequency. Electrode polarisation is due to a

charge organization that occurs at the interface of the electrode and the sample in the presence of water molecules and hydrated ions (Schwan, 1992). The nature of the ions in the layer is determined by the nature of the suspension and the material of the electrode. Therefore, changing the nature of the suspension or the electrode material will modify the levels of response of the electrode polarisation. Several methods have been suggested to overcome the effect of the electrode polarisation. Different mathematical modelling methods have been proposed which determine the contribution of the electrode polarisation to the spectrum and then eliminate it (Davey and Kell, 1998 a&b; Yardley *et al*., 2000). Changing the electrode material or the properties of the electrode surface can improve the electrode polarisation and move it to lower frequencies, thus permitting better measurements of the β-dispersion to be obtained (Gabriel *et al*., 1996). For example, more noble metals have been reported to be better at reducing electrode polarisation than less noble metals (Stoneman *et al*., 2007). Also, the deposition of platinum black on a platinum surface can greatly increase the surface area of the electrode and thereby reduce the current density, thereby reducing electrode polarisation.

The use of two electrodes with varying distance has been suggested as one method to eliminate the electrode polarisation. By varying the separation of the electrodes, the levels of the electrode polarisation can be determined and eliminated. This method is suitable only for alternating current measurements. An alternative method for reducing electrode polarisation is the four electrode method. Here two pairs of electrodes are used: the outer (current) electrodes and the inner (voltage) electrodes. Some authors recommend the two electrode system with an electrode polarisation correction as the better option to measure the dielectric properties of materials since the four electrode method does not completely eliminate the electrode polarisation on the inner (voltage) electrodes (Miklavcic *et al*., 2006).

2.6.2.4 Insoluble media components

2.6.2.4.1 Liquids

In many fermentations oils or fats are added; also many compounds used in biotransformations are insoluble liquids, or the compounds are dissolved in solvents

such as hexane and then added to the medium. In the highly stirred environments used in most fermentations the presence of liquids in the medium that are insoluble in water leads to the formation of emulsions.

An emulsion is a mixture of liquids which are immiscible; one liquid (the dispersed phase) is dispersed in another (the continuous phase) (see Figure 2.28). Many studies have been done to understand the dielectric properties of heterogeneous liquid systems such as emulsions (Hanai *et al*., 1962; Feldman *et al*., 1997; Asami, 2002).
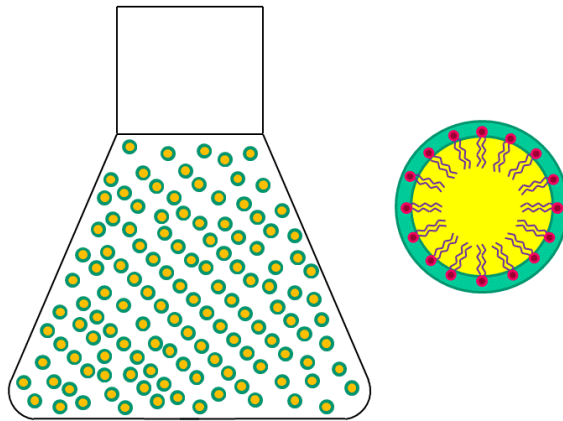
Figure 2.28 Emulsion of two immiscible liquids with the surfactant around the oil drops stabilizing the emulsion. A surfactant acts as emulsifier, leading to the formation of a micelle.

Emulsions are well studied using dielectric spectroscopy because the two immiscible materials often have very different dielectric properties and interfacial polarisation can therefore be readily observed. Emulsions are particularly good for examining the validity of dielectric mixture equations (Asami, 2002). For water-in-oil emulsions it can be assumed that the conductivity of the oil phase is much lower than that of the water. For concentrated suspension of spherical droplets, the following approximate equations have been derived from Hanai's equation:

$$\Phi = 1 - (\varepsilon_a / \varepsilon_1)^{1/3} \tag{2.42}$$

$$\kappa_a = \kappa_1 (1 - \Phi)^3 \tag{2.43}$$

$$\varepsilon_p = \varepsilon_a + \frac{\varepsilon_h - \varepsilon_a}{1 - (\varepsilon_h / \varepsilon_1)^{1/3}} \tag{2.44}$$

$$\kappa_p = \kappa_h \frac{3 - (2 + \varepsilon_a / \varepsilon_h)(\varepsilon_h / \varepsilon_1)^{1/3}}{3[1 - (\varepsilon_h / \varepsilon_1)^{1/3}]^2} \tag{2.45}$$

where Φ is the volume fraction of the water droplets, κ_a the conductivity of the oil phase, ε_p the relative permittivity of the water droplets, κ_p the conductivity of the water droplets, ε_a relative permittivity for the oil phase and ε_1, ε_h, κ_1 and κ_h are dielectric relaxation parameters.

For oil-in-water emulsions, in which oil droplets are dispersed in water, the conductivity of the oil droplets is negligibly small compared with the water. Therefore, assuming that $\kappa_p \ll \kappa_a$ we can obtain the following equations from Hanai's equation:

$$\varepsilon_1 = \frac{3}{2}\varepsilon_p + \left(\varepsilon_a - \frac{3}{2}\varepsilon_p\right)(1-\Phi)^{3/2} \tag{2.46}$$

$$\left(\frac{\varepsilon_h - \varepsilon_p}{\varepsilon_a - \varepsilon_p}\right)\left(\frac{\varepsilon_a}{\varepsilon_h}\right)^{1/3} = 1-\Phi \tag{2.47}$$

$$\kappa_1 = \kappa_a(1-\Phi)^{3/2} \tag{2.48}$$

$$\kappa_h = \kappa_a \frac{\varepsilon_h(\varepsilon_h - \varepsilon_p)(2\varepsilon_a + \varepsilon_p)}{\varepsilon_a(\varepsilon_a - \varepsilon_p)(2\varepsilon_h + \varepsilon_p)} \tag{2.49}$$

Emulsions encountered in biotechnology are usually simple oil-in-water emulsions. The dielectric constants of fats and oils present low values (2-4) and are relatively independent of frequency and temperature (Kent, 1987; Lizhi *et al*., 2008). Such emulsions do not have interfacial dispersion, and the compensation of the dielectric spectra for the presence of organic phase is generally straightforward. Dielectric spectroscopy can be used to evaluate the dielectric properties of the emulsions even when complete phase separation occurs (Asami, 2002). Other more complicated systems such as liposomes have also been described (Schwan *et al*., 1970).

2.6.2.4.2 Suspended non-cellular materials

Among the solid materials commonly found along with cells in different processes we can mention solid organic materials of biological origin such as starch granules, cellulose and similar materials, and plastics, ceramics, glasses, and minerals used as support for cell immobilisation.

Many theoretical and experimental studies have been performed to understand the dielectric properties of suspension of particles and coarsely dispersed systems (Hanai *et al*., 1959; Noll and Biselli, 1998; Asami, 2002; Bonincontro and Cametti, 2004; Christensen and Keiding, 2008). Spherical particle, single-shell and multishell models have been applied to analyse the dielectric properties of solids (Asami, 2002).
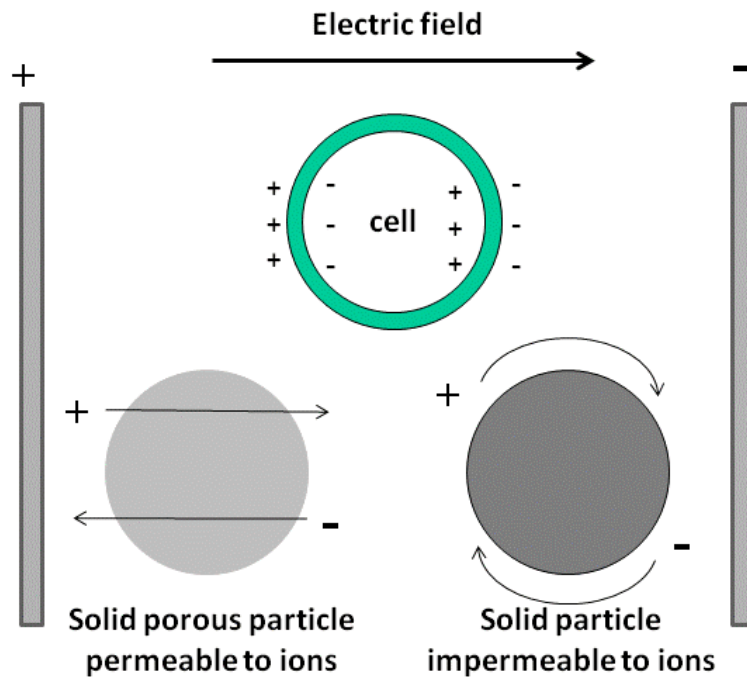
Figure 2.29 Schematic diagram showing the principle of dielectric measurements of biomass in the presence of suspended non-cellular material.

Most solid materials actually are not easily polarisable and have little or no dispersion in the radiofrequency range. In contrast cells, because they have a membrane enclosing the highly polarisable cell interior, are easily polarisable (Figure 2.29). The dielectric signal in this frequency range is therefore often dominated by cells with an intact plasma membrane if present (Davey *et al*., 1993). The most important effect of the presence of solid particles is commonly only a displacement of cell-containing suspension which will lead to a slight reduction of the measured capacitance dependent on the volume fraction of the solid particles (Noll and Biselli, 1998).

2.6.2.4.2.1 Solid organic materials of biological origin

Many fermentation contain significant amounts of solid organic material of biological origin, either as a byproduct of the production process of the medium (e.g. spent grain) or as an additional or major nutrient source (e.g. starch) . Concentrations can range from a few particles dispersed in an otherwise homogeneous liquid to the substrate of solid state fermentations in which there is little free water.

Numerous data have been reported in literature on the dielectric properties of food and other agricultural products (Kent, 1987; Ikediala *et al*., 2002). Salt, water and oil content can influence the dielectric properties of these materials. In general, the dielectric constant increases with increasing moisture content and conductivity rises linearly with salt concentration (Bengtsson and Rirman, 1971; Feng *et al*., 2002). The main mechanism for the interaction between electric fields and organic materials is the oscillation of polar water molecules and ions as well as interfacial polarisation when cells are present (Bengtsson and Rirman, 1971; Kent, 1987).

Many fermentations have been reported in which solid biological particles interfered in dielectric measurements. For example, Ng *et al*. (2007) showed that spent grain that the real part of the relative complex permittivity of suspensions of brewer's spent grain was dependent on the concentration; however, the imaginary did not vary with concentration. Equally Nicholson *et al*. (1996) described the interference of wheatgerm on dielectric measurements. They showed that artificial neural networks and multivariate statistical methods could be used to deconvolute the dielectric spectra of mixtures of yeast cells and wheatgerm. Bryant *et al*. (2011) described the use of dielectric spectroscopy for the monitoring of both the hydrolysis of lignocellulosic fibre and the accumulation of organic acids. During enzymatic hydrolysis, dielectric spectroscopy capacitance due to the presence of fibre decreased along with a subsequent increase in conductivity resulting from the production of organic acids during microbial growth. It was possible to determine the level of enzymatic hydrolysis of the fibre fractions using this method (Bryant *et al*., 2011).

Solid state fermentation is a process involving microorganisms growing on solid or semi-solid immobilized or fluidized supports that have been traditionally exploited in the manufacture of a wide variety of products. Solid substrates can be characterized as

gas-liquid-solid mixtures, in which the aqueous phase is intimately associated with both the solid surface and the gaseous environment (Davey *et al*., 1991). Monitoring and controlling biomass and metabolite production during solid state fermentation is a challenge because of the the complexity and heterogeneity of the media and the variety of reactors used (Bellon-Maurel *et al*., 2003). However, dielectric spectroscopy is one of the few methods that can be used to obtain information on biomass levels during a solid state fermentation. For example, Peñaloza and co-workers used dielectric spectroscopy to investigate changes in biomass levels during the production of tempe, a traditional soya bean product (or any other cereal) fermented by *Rhizopus oligosporus* (Davey *et al*., 1991; Peñaloza *et al*., 1992). They showed there was an excellent linear relationship between the increase in capacitance and the amount of biomass as estimated from the hyphal length (Davey *et al*., 1991).

2.6.2.4.2.2 Polymers

The dielectric properties of polymers are well studied (Von Hippel, 1954; Schwan *et al*., 1962; Hanai *et al*., 1964; Kazarnovskiy and Yamanov, 1972; Ishikawa *et al*., 1981; Zhang *et al*., 1983; Liu *et al*., 1996; Christensen and Keiding, 2008; Singha *et al*., 2008). Plastics have weak interactions with electric fields because of their non-polar molecular structure. Resins and plastics like polyurethane foam are commonly used as inert supports in solid state fermentations (Bellon-Maurel *et al*., 2003). The use of dielectric spectroscopy for monitoring biomass in immobilized cell cultures has been reported previously. For example, the growth of Vero cells on Cytodex 1 carriers and tissue growth within microporous polymer scaffolds (Dziong *et al*., 2005; Rourou *et al*., 2010). All these publications have reported that dielectric spectroscopy is very well capable of measuring biomass in the presence of a plastic support.

2.6.2.4.2.3 Ceramics, glass, and similar materials

Ceramics are widely used in many areas of research and engineering because of their unique characteristics such as high temperature stability, physical properties, thermal conductivity and weight. The dielectric properties of several ceramic materials have been previously studied (Von Hippel, 1954). The dielectric constant of ceramic

materials is usually low (<10) though some ceramics show higher values (Xi and Tinga, 1993; Hamlin *et al*., 1995). Most minerals exhibit increasing values of the dielectric constant when temperature is increased with some exemptions showing some more complicated dependencies (Salsman, 1991).

Ceramics and glass have previously been used as support for cell immobilization. It has been shown that dielectric spectroscopy can be used for the monitoring of biomass growing immobilized inside porous glass carriers (Noll and Biselli, 1998) or inside ceramic carriers (Salter *et al*., 1990). The presence of the glass or ceramic carriers has an effect on the dielectric signal, but because the concentration of the carriers was constant an increase in the permittivity could be directly attributed to cell growth.

Dielectric properties of many soils are closely dependent of their moisture content (Hipp, 1974; Hoekstra and Delaney, 1974). Some sandy soils have been classified according to the value of their loss factor (Gonchariva *et al*., 1991). Soil bioremediation is a process involving microorganisms growing on solid or semi-solid substrates or supports, and the use of dielectric spectroscopy for measuring cell concentrations during soil bioremediation could be considered.

2.6.2.5 Non viable cells

If a cell is dead, the membrane is often broken and charges may pass through the holes in the membranes, causing a failure of polarisation across the membranes (Davey *et al*., 1993). Residual polarisation however remains across the remnants of the cell structures that cause dead cells to have a small but measurable polarisation. This residual polarisation contributes to the overall dielectric signal and can cause estimates of viable cells counts with dielectric spectroscopy to be too high. This is complicated by the fact that the actual value of the residual polarisation of dead cells depends on the method by which the cells have been killed (Patel and Markx, 2008). In fact under certain circumstances, the cells could be dead, but the membrane intact; dead cells would then give the same signal as live cells.

Changes that occur in the dielectric properties of cell suspensions during cell death under different environmental stresses have been described by many authors (Stoicheva

et al, 1989; Huang *et al*., 1992; Davey *et al*., 1993; Patel and Markx, 2008). To describe the changes in the dielectric behaviour when the cells are dying, Equation 2.33 has been often used. However, for cells with a high membrane conductivity, Equation 2.29 should be used instead since it could be wrongly concluded that a fall in the capacitance of a cell suspension upon cell death is mainly caused by a drop in the value of C_m when most likely, this change is actually mainly due to an increase in the membrane conductance G_m (Patel and Markx, 2008).

2.6.2.6 Gases

Air, or more general gas bubbles are non conductive, and have a very low permittivity (dielectric constant ~1). The presence of air bubbles has a negative effect in the capacitance and conductance values (Davey *et al*., 1993; Soley *et al*., 2005). This is the consequence of the replacement of a fraction of the volume previously occupied by a polarisable and conductive material (such as cells or other materials) with the non-polarisable and non-conductive gas bubbles. In cell suspensions with a low volume fraction of cells the interference due to the cell displacement by the presence of gas bubbles is an important source of error. Algorithms to reduce the noise generated by gas bubbles have been proposed (Sonnleitner *et al*., 1992). Other source of variation during measurements can be gas bubble trapping on electrodes.

2.6.2.7 Wall effects

Sometimes during the monitoring of biomass at laboratory scale the vessels used for holding the sample are quite small and the probes or electrodes are placed close to the walls. This creates an interference with the electric field, producing a reduction in the capacitance. It is therefore important not to have the probe close to the wall or near the surface of the liquid as this may also interfere with the electric field distribution around the dielectric probe. Also, during stirring, vortex can create an impact similar to wall or surface effect. Other sources of variation can be biofilm formation and cell clumping.

CHAPTER 3

A METHOD FOR COMPENSATING BIOMASS MEASUREMENTS DURING BARLEY-BASED FERMENTATIONS FOR INTERFERENCE BY THE PRESENCE OF SPENT GRAIN

ABSTRACT

Non-cellular particles can interfere during biomass monitoring during fermentation using dielectric spectroscopy. This study investigated the level of interference caused by the presence of spent grain from the malting process during barley based fermentations. Two methods were developed for successfully overcoming the interference by spent grain. One was based on mathematical modeling, and one on physically keeping the spent grain from the measuring probe using filters. Although further development is needed, both methods made it possible to obtain estimates of the biomass level in the presence of unknown concentrations of non-cellular particles.

3.1 Introduction

All cells have a cellular membrane. The presence of this membrane causes a frequency-dependent interfacial polarisation process to occur across the membrane. At low frequencies this makes the cells highly polarisable, increasing the overall suspension permittivity. As the frequency is increased the capacitor formed by the cell membrane becomes more permeable for the electric field. As a result the polarisation of the cells becomes less, and the permittivity of a cell suspension goes down as the frequency increases (Pethig, 1979; Schwan, 1985; Davey *et al*., 1995) (see figure 3.1).
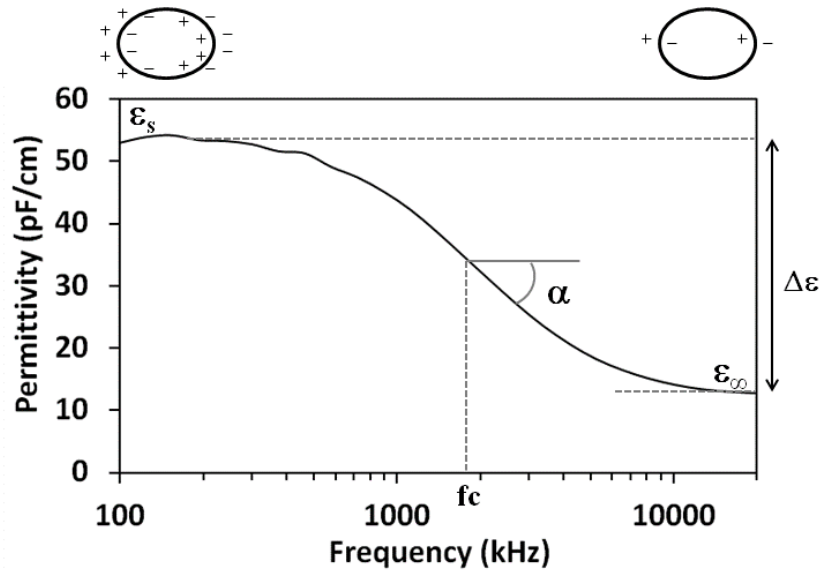
Figure 3.1 Typical β-dispersion curve for cell suspensions

As shown by Schwan (1957), there is a linear relation between the dielectric increment ($\Delta\varepsilon$) (i.e. the difference between the maximal suspension permittivity at low frequency (ε_L) and the residual permittivity at high frequency (ε_∞) and the volume fraction of membrane enclosed biomass P which is given by the equation:

$$\varepsilon_L - \varepsilon_\infty = \Delta\varepsilon = \frac{9}{4\varepsilon_s} PRC_m \qquad (3.1)$$

In which C_m is the membrane capacitance per unit area, R is the radius of the cell, and ε_0 is the permittivity of free space. This linear relationship between the dielectric increment and cell concentration has allowed dielectric spectroscopy to become one of the most useful technologies for measuring biomass levels (Schwann, 1957; Kell *et al.*, 1990; Markx and Davey, 1999; Asami, 2002; Carvell *et al*, 2006). The method has also been used to obtain additional information about cellular properties such as the conductivity and content of the cytoplasm, cell morphology and cell size (Kell *et al.*, 1990; Markx and Davey, 1999; Ferreira *et al.*, 2005; Ansorge *et al*, 2010 a & b). Application of dielectric spectroscopy in biological materials have also spread to different fields, from studies in tissues (Pethig and Kell, 1987; Gabriel *et al.*, 1996 a, b & c; Miklavcic *et al*, 2006; Peyman, 2011) to food technology (Tran *et al.*, 1984; Liao *et al.*, 2003; Bohigas *et al.*, 2008; Al-Muhtaseb *et al.*, 2010; Guo *et al.*, 2010 & 2011; Smith *et al.*, 2011).

Dielectric spectroscopy is relatively insensitive to the concentration of dissolved medium components. Unfortunately, in many fermentations particulate matter can be found at high concentrations that also can show interfacial polarisation in an applied electric field, and their signal in many cases contributes significantly to the overall dielectric signal. Such particulate matter includes agents used for immobilisation of the cells such as ceramics or polymer beads, precipitated medium components, and solid substrates such as starch and (ligno) cellulose. This can make biomass measurements with dielectric spectroscopy difficult, especially when the actual cell concentration is low, and the concentration of the non-cellular material varies during the fermentation. The dielectric properties of many non-cellular particles have been well studied (O'Konski, 1960; Hanai *et al*., 1962; Bone and Pethig, 1979; Hill and Jonscher, 1983; Wang *et al*., 1993; Barker *et al*, 1994; Carrique *et al*, 1994; Asami, 2002; Bonincontro and Cametti, 2004; Christensen and Keiding, 2008; Singha and Thomas, 2008). Often materials are polarized by different polarisation mechanisms, showing frequency dependent permittivities with different relaxation times (Asami, 2002).

The fact that the frequency dependency of the permittivity of non-cellular particles may be different from that of cellular material potentially offers on the possibility to separate the signal coming from viable cells from that of interfering non-cellular particles. This will be explored in this chapter. As a model system a barley-based fermentation with baker's yeast was used with spent grain as the noncellular interferent. Spent grain can be present in distilling fermentations in significant concentrations. Also explored is a physical technique, in which the medium and cells are separated from the larger non-cellular particles.

3.2 Materials and methods

Media

100 g of malted barley was crushed in a disc mill at mesh number 7 (0.7 mm particle) and 400 ml of hot water added to start the mashing process. The malted barley was kept in a stirred receptacle at 65°C for one hour. After the mashing process had finished the product was filtered over a filter paper (Munktell 006 folded, pore size: 3 to 4 μm) for 2½ hours. The clear liquid obtained after filtration (the wort) was used as the medium in all the experiments. The spent grain remaining on the filter was used in the experiments

as the source of non-cellular particles (density: 1.068 g/ml). Wort was used for all the experiments immediately after the filtration.

Cells

To inoculate the fermentations, yeast (*Saccharomyces cerevisiae,* DCL "M" strain) was cultivated for 48 h in 250 ml conical flasks containing 200 ml of wort in a stirred fermentation (200 rpm). The initial yeast concentration used to start the fermentations was the same as in a usual brewing fermentation, i.e. 10×10^6 cells/ml. Fermentations were performed in 600 ml glass beakers containing 400 ml of wort as medium with a magnetic stirrer at 200 rpm. Cells were harvested by centrifugation for 15 min at 5000 rpm and the pellet was resuspended with wort to obtain 160 ml of yeast suspension with a cell concentration of 375×10^6 cells/ml. These cells were then used for further measurements.

Dielectric measurements

An Aber Instruments Biomass monitor model 220 with a 1.2 cm diameter 30 cm long annular probe, connected to a PC with Aberscan software version 2.2 (Aber Instruments, Aberystwyth, UK) was used for recording the dielectric frequency spectra (see Figure 3.2). The freerun option was used to measure the dielectric properties of the suspensions at 25 frequency points distributed over the frequency range 0.1 to 20 MHz. Each spectrum took approx. 10 seconds to record. Spectra obtained during one minute were averaged. All spectra were automatically corrected for electrode polarisation. All data are given as pF/cm, i.e. capacitance $\times$ cell constant (in /cm). Where appropriate measurements were corrected for dilution effects.

Figure 3.2 Biomass monitor model 220 from Aber Instruments using three probes at the same time.

Fitting procedure

Measurements were taken at different frequencies f_i. By taking measurements on suspensions with yeast and grist at a known total concentrations P_Y for yeast and P_G for the spent grain, proportionality constants K_{Yi} (for yeast) and K_{Gi} (for the spent grain) can be determined similar to the molar absorptivity in spectrophotometric measurements:

$$K_{Yi} = (\varepsilon_{Yi} - \varepsilon_{0i})/P_Y \qquad (3.2)$$

And

$$K_{Gi} = (\varepsilon_{Gi} - \varepsilon_{0i})/P_G \qquad (3.3)$$

in which ε_{Yi} is the permittivity at frequency i of a suspension of yeast at cell concentration P_Y, and ε_{Gi} is the permittivity at frequency i of a suspension of the spent grain at concentration P_G. ε_{0i} the permittivity of the background at frequency i.

Assuming linearity, the overall (calculated) permittivity ε_{ic} of a mixture of yeast and spent grain at frequency i can be calculated from:

$$\varepsilon_{ic} = \varepsilon_{0i} + K_{Yi} P_{cY} + K_{Gi} P_{cG} \qquad (3.4)$$

in which P_{cY} is the calculated concentration of yeast (in cells/ml) and P_{cG} the calculated concentration of the spent grain (in gr/ml) in the mixture. Suspension permittivities ε_i were then obtained at different frequencies f_i for different total concentrations of yeast and spent grain. Data were fitted to equation (3.4) using Excel Solver as described in Harris (2007) by minimising the distance between calculated (ε_{ic}) and measured (ε_i) values of the suspension permittivity for different frequency combinations and values.

$$\sum_{f_1}^{f_n} (\varepsilon_i - \varepsilon_{ic})^2 = \text{minimal} \qquad (3.5)$$

3.3 Results and discussion

The dielectric properties of different suspensions were measured at different frequencies (100 kHz to 20 MHz). A first set of experiments was done with increasing yeast and spent grain concentrations in pure wort. 20 ml of yeast suspension was added every 15 min to 400 ml of wort and changes in dielectric properties recorded. In a different experiment 20 ml of spent grain was repeatedly added every 15 min to 400 ml of wort. Comparison of the dielectric spectra obtained (Figure 3.3) shows that the shape of the dispersions is quite different for the spent grain and the yeast.
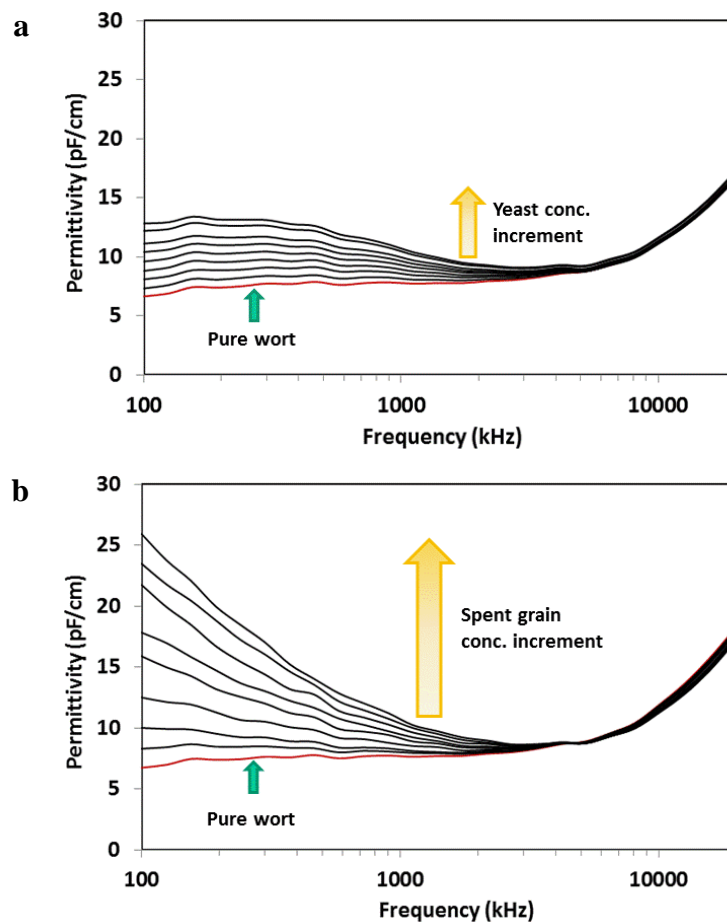
Figure 3.3 Permittivity in function of frequency at different concentrations of a) yeast and b) spent grain. Each line indicates an increment of a)17.8×10^6 cell/ml and b)0.05 g/ml.

The spectra of yeast are those of a β-dispersion with a low frequency plateau between 200-300 kHz and a characteristic frequency (f_c) around 1000 kHz. With spent grain there is no low-frequency plateau. As can be seen in Figure 3.4, both the yeast and spent grain permittivity signals were linearly dependent on the concentration of yeast and spent grain.
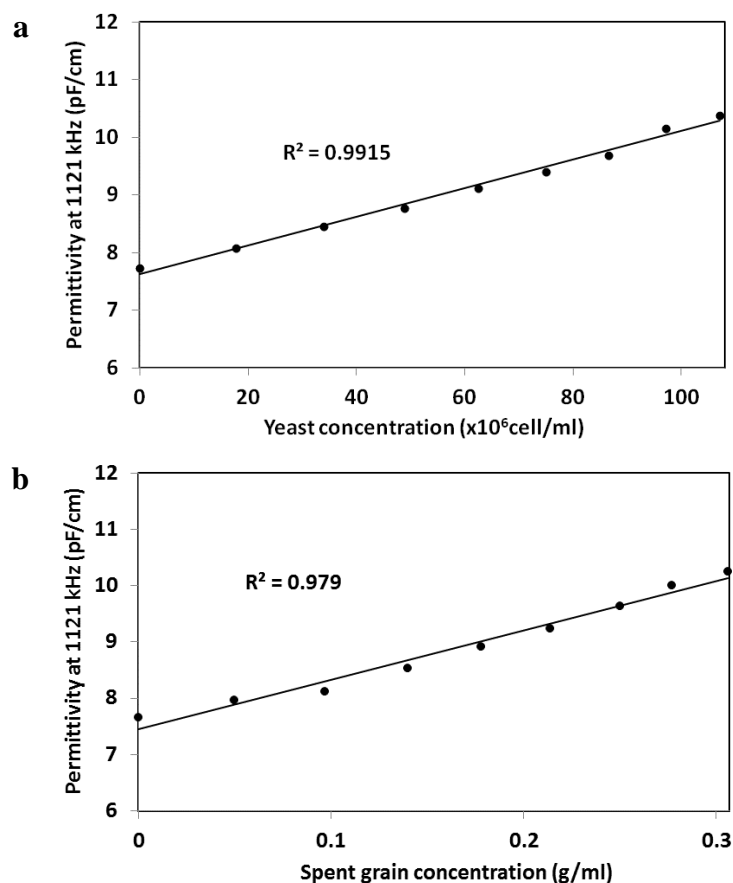
Figure 3.4 Permittivity at 1121 kHz frequency in function of the concentration of a) yeast and b) spent grain.

This linearity, combined with the different frequency-dependent behaviour of the spectra led us to explore the possibility of the developing a mathematical model in order to separate the signal from yeast and the spent grain and calculate the different concentrations of yeast and spent grain in a unknown sample.

Spectra were obtained of suspensions of different but known yeast and spent grain concentrations. Data covered the whole frequency range (25 frequencies between 100 kHz and 20 MHz) were used. The spectra obtained were analysed using the fitting procedure described previously in Materials and Methods. Results are shown in Figure 3.5, showing the known spent grain and yeast concentrations and comparing them with the ones calculated from the spectra.
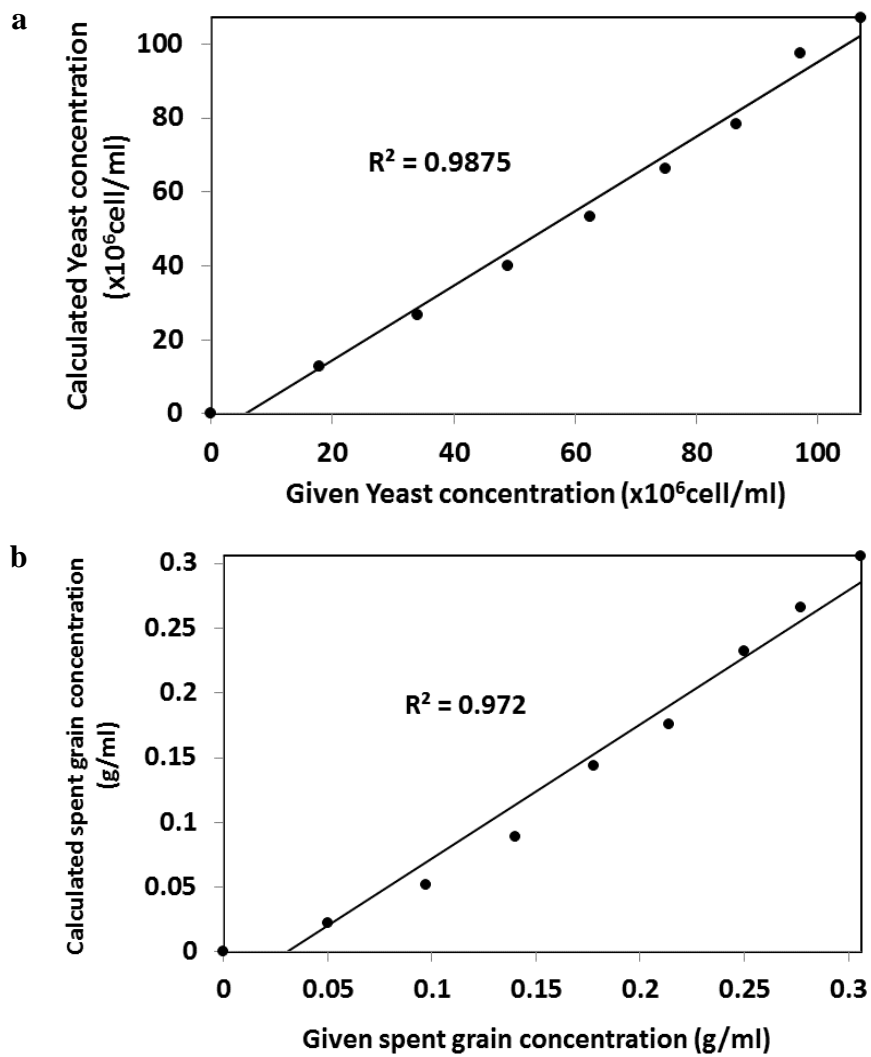
Figure 3.5 Comparison of known ("Given") yeast and spent grain concentrations and those calculated from the dielectric spectra ("Calculated"). a) Yeast. b) Spent grain.

The results show that the procedure allows separating the signal from yeast and the spent grain in order to obtain a good estimate of the yeast cell concentration from a mixed suspension of yeast and spent grain. However, it is more difficult to obtain a good estimate of the concentration of the spent grain.

To explore if the procedure is able to obtain estimates of the concentrations of yeast and spent grain during fermentation, fermentations were done with wort with different known concentrations of spent grain. Yeast was inoculated at an initial concentration of 10×10^6 cell/ml, and cell concentrations were measured by cell counting using methylene blue staining technique (Gurr, 1965) for the fermentation with no spent grain only. Dielectric spectra were recorded throughout the fermentation. Figure 3.6 shows the

change in the permittivity at 1121 kHz during the fermentations. The presence of the relatively large spent grain particles resulted in a significant amount of noise during the measurement.
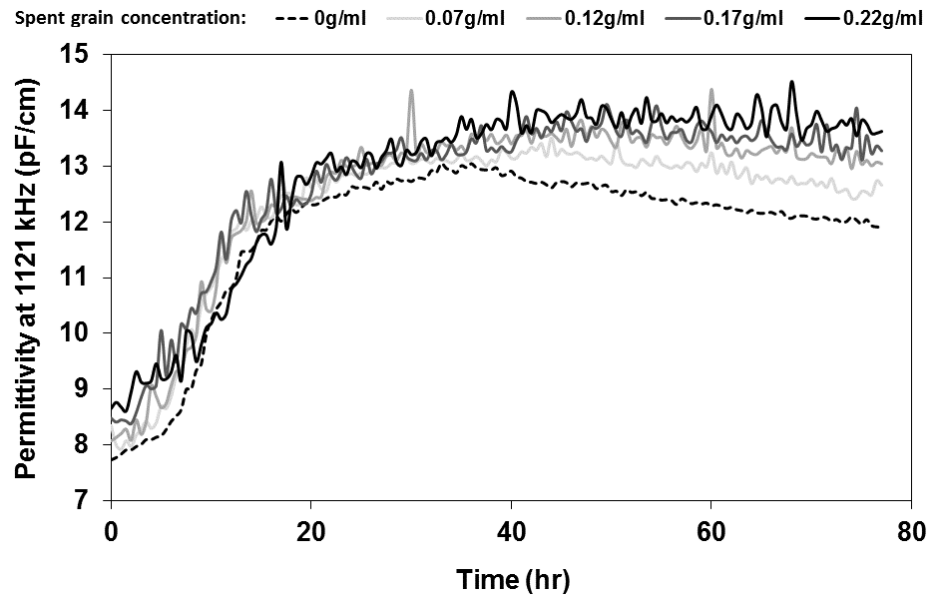
Figure 3.6 Permittivity in function of time during stirred fermentations with 400 ml wort and different concentrations of spent grain. Initial cell concentration: 10×10^6 cells/ml.

Dielectric spectra of the fermentation with only yeast and no spent grain, and with yeast and 0.22 g/ml of spent grain can be observed in Figure 3.7.
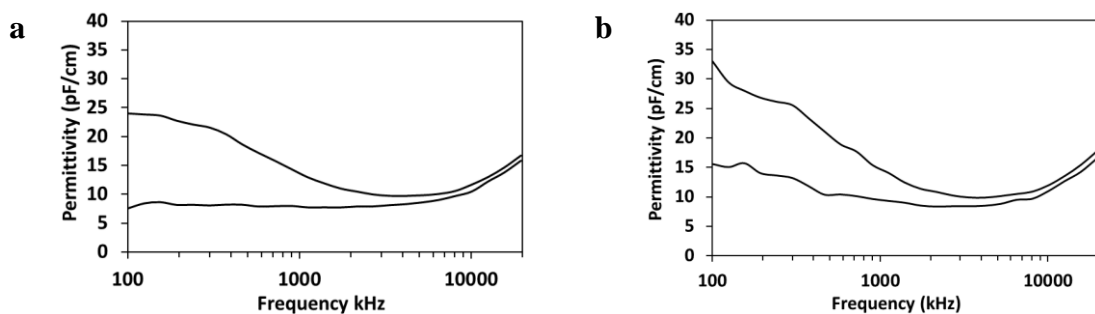
Figure 3.7 Permittivity as a function of frequency for stirred fermentation showing the dielectric spectra for a) yeast only, with no spent grain, and b) yeast and 0.22 g/ml of spent grain. Bottom line is at the beginning of the fermentation and the upper line is 38 h later when cell concentration reached its maximum value.

The spectra obtained at 10, 20, 40 and 60 h during the fermentations were analysed using the procedure described before in order to estimate the concentrations of the spent grain and yeast during the fermentation. As it was difficult to perform accurate cell counts when spent grain was present, it was assumed that the cell concentration during the fermentations in which spent grain was present followed the same time course as the one without spent grain and the spectra obtained without spent grain was used for all the calculations. The results are shown in the Figure 3.8.
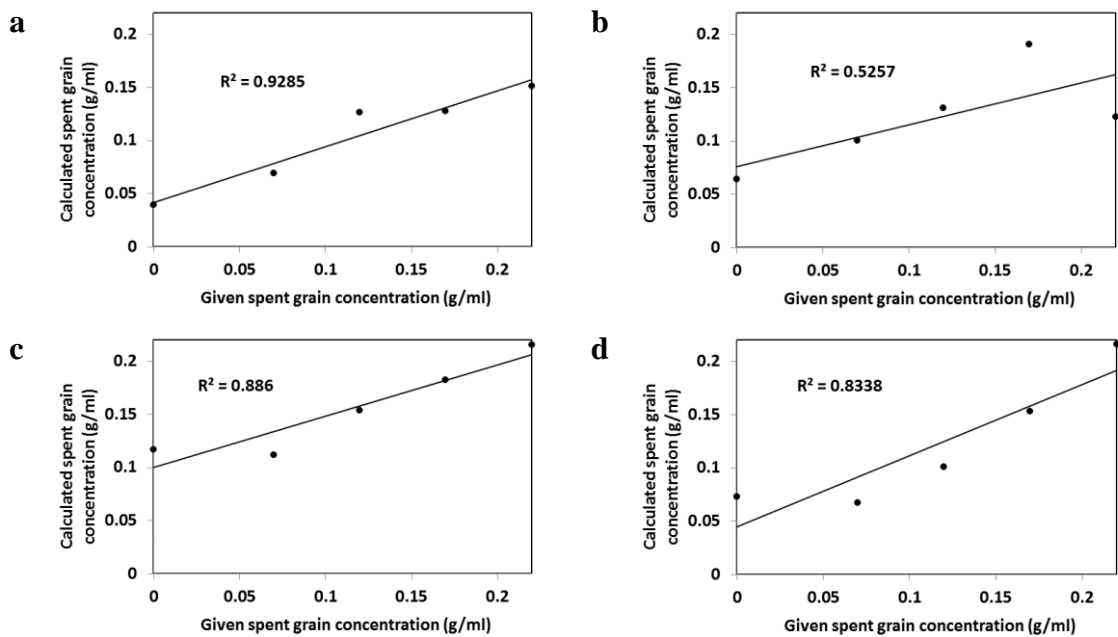
Figure 3.8 Comparison of yeast concentration measured with a haemocytometer and spent grain concentration based on how much spent grain was added ("Given") with those obtained from the analysis of the dielectric spectra ("Calculated") a) After 10 h of fermentation time, b) 20 h, c) 40 h, d) 60 h. Cell concentration was a) 83, b) 175, c) 190 and d) 170×10^{6} cell/ml.

It can be observed that the mathematical model is able to estimate the concentration of spent grain at the beginning of the fermentation. However, since the spectra used for the yeast in the mathematical model was the one without spent grain, data obtained at 20, 40 and 60 h shows low correlations.

Physical separation technique

As an alternative method, a series of experiments were performed in which the spent grain was separated from the yeast using a filter. In the experiments two dielectric probes were used at the same time. One probe was left uncovered and the second probe was placed inside a perforated plastic casing made from a centrifuge tube covered with filter paper (Munktell 006 folded, pore size: 3 to 4 μm). In the first part of the experiments the concentration of the spent grain was gradually increased by adding small aliquots of spent grain to 400 ml of wort and simultaneously recording the impedance at both probes. In the second part of the experiments the yeast concentration was gradually increased.
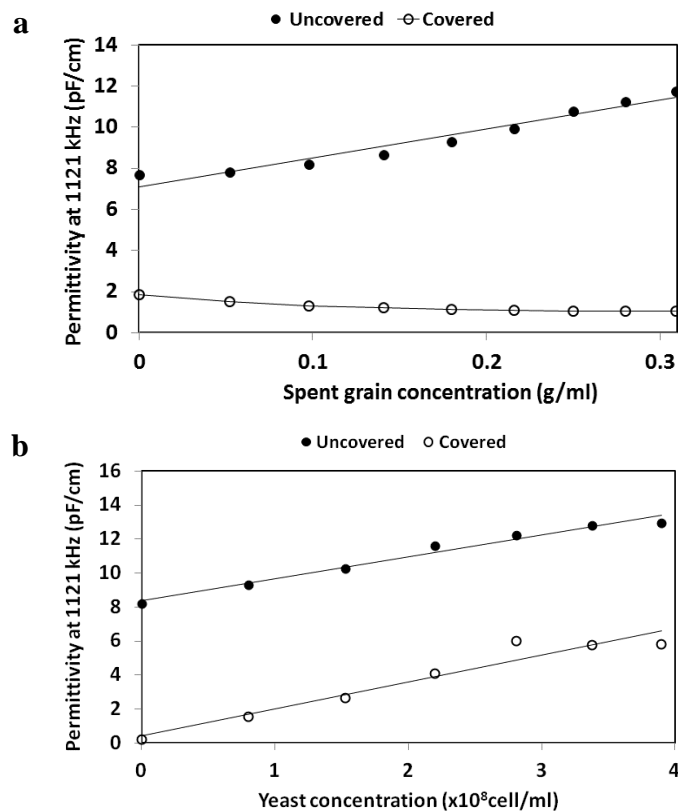
Figure 3.9 Permittivity as a function of concentration of a) spent grain and b) yeast. Two probe technique was used. One probe covered with filter paper and the other probe left uncovered.

As can be seen in Figure 3.9, the probe left uncovered shows a linear response to the addition of spent grain, whilst the probe covered by a filter paper shows little response to the addition of spent grain. Addition of yeast raises the permittivity level at both probes, showing that the paper filter effectively shields the probe from the spent grain in the bulk suspension, whilst still allowing yeast to pass through.

3.4 Conclusions

It was shown that the difference in the frequency dependency of the dielectric spectrum of spent grain and yeast is a large enough to deconvolve the spectra to obtain accurate estimates of the relative contributions of the spent grain and the yeast. Thus it is possible to use this technique in order to obtain good estimates of the concentration of yeast cells despite the presence of significant amounts of spent grain. However, accurate estimation of the yeast spectra alone is needed. Therefore, a two probe system has been developed in which the spent grain is separated from the suspension using filtration. This allowed one to measure the dielectric properties of the suspended yeast only at one of the probes, and suspended yeast plus spent grain at the other, allowing one to obtain accurate measurements of both.

By varying the size of the pores of the membrane it should be possible to keep particles with different sizes away from the probe, indicating the possibility to separately measure and resolve the dielectric properties of the suspending medium, the cells, non-cellular particles of different sizes, and cellular aggregates. The methods developed are generally applicable, and the findings have relevance for any process where biomass is monitored using dielectric spectroscopy and interference occurs by the presence of non-cellular particles.

CHAPTER 4

USE OF DIELECTRIC SPECTROSCOPY FOR MONITORING CELLULAR BIOMASS DURING LIGNOCELLULOSIC FERMENTATIONS

ABSTRACT

Dielectric spectroscopy could potentially be used to measure the level of viable biomass during lignocellulosic fermentation for bioethanol production. However, during lignocellulosic fermentations the solid material used as the substrate can potentially interfere during the measurement. It is shown that if pretreated birch wood is used as the substrate the contribution to the suspension permittivity is minimal, indicating that dielectric spectroscopy may be an excellent method for monitoring changes in cellular biomass during lignocellulosic fermentations on wood.

4.1 Introduction

Lignocellulosic materials potentially constitute a relatively abundant and renewable feedstock for the chemical industries. Chemicals derived from them include carbohydrates, primary metabolites obtained through photosynthesis, which can be converted into biofuels. Other products include those derived from secondary metabolites such as gums, resins, rubber, waxes, terpenoids, steroids, triglycerides, tannins, alkaloids and others. Such materials can be used for the production of very high value biochemicals such as food flavours, feeds, pharmaceuticals, chemicals for cosmetic industry and nutraceuticals among others (Naik *et al*., 2010; Limayem and Ricke, 2012). Of particular interest is bioethanol production (Wyman *et al*., 1992). Different processes have been developed for the production of ethanol from lignocellulosic feedstocks including separate hydrolysis and fermentation (SHF), simultaneous saccharification and fermentation (SSF) and direct microbial conversion (DMC) (Wyman *et al*., 1992). At the moment, however, production is not competitive compared with the cost of gasoline with the technology available. This, combined with

other considerations such as environmental concerns will determine the extent of use of ethanol as a fuel in the future (Keim and Venkatasubramanian, 1989; Sun and Cheng, 2002).

The SSF process has received more attention because the yield of ethanol is relatively high and the cost of equipment relatively low. Various studies have been performed in order to improve biomass pretreatment and process conditions (Nguyen and Saddler, 1991; Hinman *et al*., 1992; Wyman *et al*., 1992; Olsson and Hahn-Hagerdal, 1996). This has included testing different enzymes and microorganisms for their ability to resist the high temperatures during the production process and the presence of inhibitors such aromatics and acetic and formic acids (Palmqvist and Hahn-Hagerdal, 2000; Krishna *et al*., 2001; Ballesteros *et al*., 2004; Sanda *et al*., 2011).

Direct measurement of the cellular biomass during the lignocellulosic fermentations could be of significant benefit during optimisation of the production process. Of the different methods available for measuring biomass, dielectric spectroscopy is potentially one of the most useful (Schwann, 1957; Kell *et al*., 1990; Markx and Davey, 1999). Dielectric spectroscopy involves the measurement of the overall dielectric properties (permittivity and conductivity) of a material as a function of frequency. When the material is a suspension then any material that is suspended that has different electrical properties from that of the suspending medium will attain a frequency-dependent dipole in the applied electric field caused by a process called interfacial polarisation (Maxwell, 1873; Schwann, 1957; Pethig, 1979). Cells, because they have a cellular membrane surrounding a highly conductive aqueous cytoplasm, attain particular high dipoles which are highly frequency dependent. The tendency is for the permittivity to go down as the frequency increases, caused by interfacial polarisation at the cellular membranes and walls (Schwan, 1985; Davey et al., 1995). A linear relationship exists between the dielectric increment and cell concentration which holds over a wide concentration range for different types of cells (Asami, 2002). Because the accumulation of charges at the cell membrane is reduced when the cell membrane is permeabilized the dielectric increment declines when a cell dies, and the dielectric signal therefore gives a measure of the concentration of viable cells mainly.

Non-cellular particles which do not have a membrane do not in the main attain as high a dipole moment as cells, but they still do. The presence of such materials at high

concentrations will contribute to the overall suspension conductivity and permittivity, and can therefore make the direct measurement of cellular biomass concentrations with dielectric spectroscopy more difficult. This is particularly true for lignocellulosic fermentations in which the concentration of lignocellulosic particles is usually very high (Bryant *et al*., 2011). In the research presented, an evaluation will be made of the ability of the dielectric spectroscopy to measure yeast biomass concentrations during lignocellulosic fermentations for biofuel production with pre-treated wood (white birch) as the substrate.

4.2 Materials and methods

Cells

Yeast (*Saccharomyces cerevisiae,* DCL "M" strain) was cultivated for 48 h at 22 °C in a stirred fermentation (200 rpm) in malt extract as medium (Oxoid Ltd, 20 g/L) in 250 ml conical flasks containing 200 ml of medium. Cell cultures obtained were stored at 0-4º C for 2 hrs and then decanted to obtain a highly concentrated sample of yeast of about 6×10^8 cells/ml. Cell concentration was tested using methylene blue staining technique (Gurr, 1965). The concentration of yeast used as inoculum to start the fermentation was the same as in a usual brewing fermentation which is 10×10^6 cells/ml.

Medium

Fermentations were performed in 600 ml glass beakers containing 400 ml of medium. Sterile IFM medium (Mascoma Ltd) with added nutrient salts was used as the fermentation medium. Pre-treated hardwood (white birch) (Mascoma Ltd) was used as the lignocellulosic substrate. Cellulase from *Aspergillus niger* was obtained from Sigma-Aldrich Company Ltd to enzymatically convert the lignocellulosic particles. The enzymatic digestion was done adding 2 mg commercial cellulase/g total solids to the fermentation (simultaneous saccharification and fermentation process, SSF). 100 g of malted barley was crushed in a disc mill at mesh number 7 (0.7 mm particle) and 400 ml of hot water was added. The water and malted barley were left in a stirred receptacle at 65 °C for one hour. After this the product was filtered with a filter paper (Munktell 006 folded, pore size: 3 to 4 μm) during 2 and half hours to obtain the wort.

Dielectric measurements

A Biomass monitor model 220 with a 1.2 cm diameter 30 cm long annular probe, connected to a PC with Aberscan software version 2.2 (Aber Instruments, Aberystwyth, UK) (Figure 4.1) was used for recording the dielectric frequency spectra. The Aber Instruments Biomass Monitor automatically corrects for differences in cell constants between probes, and all data are given as pF/cm, i.e. capacitance × cell constant (in /cm). One spectrum (25 frequency points distributed over the frequency range 0.1 to 20 MHz) was measured every 10 seconds. For fermentations one spectrum was measured every 30 min. The results shown are averages. All spectra were automatically corrected for electrode polarisation. To calculate ΔPermittivity data at 10 MHz was subtracted from data at 1121 kHz.
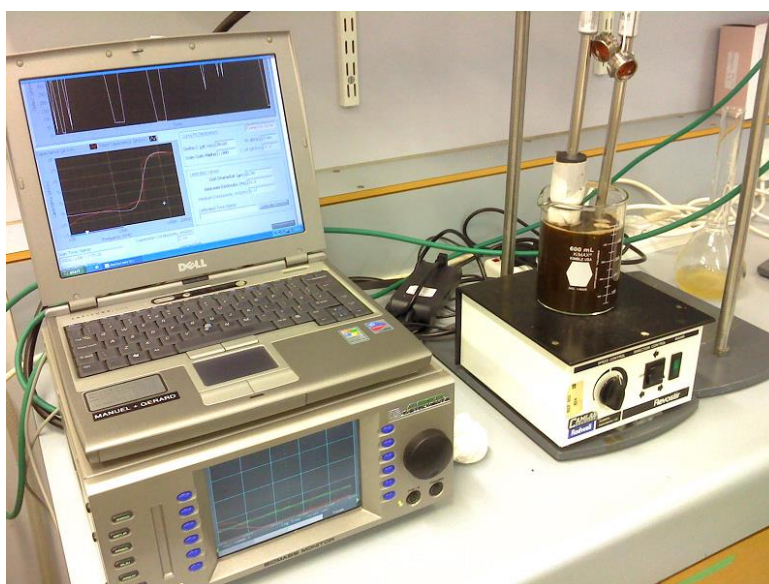
Figure 4.1 Experimental set up showing the Aber biomass monitor

4.3 Results and discussion

Experiments were performed at 22 °C in 600 ml glass beakers. The dielectric properties of 400 ml of sterile IFM medium (Mascoma Ltd) with added nutrient salts were measured and recorded for 50 min, and then 0.05 g/ml of pre-treated wood was added 5 times every 20 min. Following this, yeast was added to the medium containing 0.25 g/ml of lignocellulosic particles. The yeast concentration was increased four times. The results are shown in Figure 4.2.
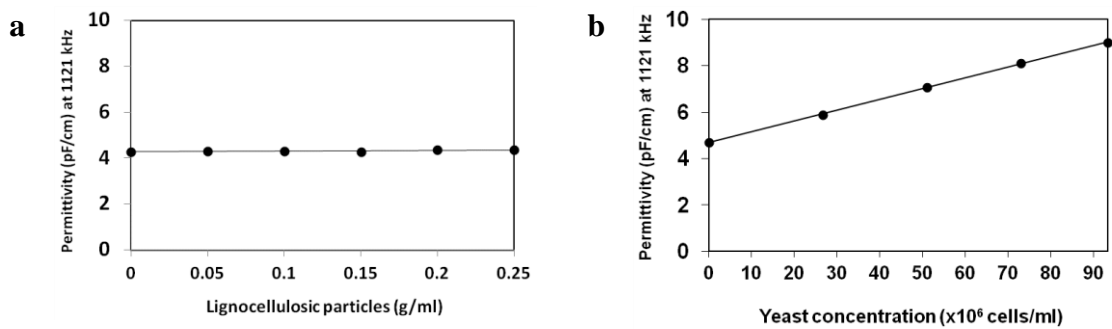
Figure 4.2 Permittivity as a function of a) concentration of lignocellulosic particles and b) yeast concentration containing 0.25 g/ml of lignocellulosic particles.

As can be seen in Figure 4.2a, when the lignocellulosic particles were added to the medium, the changes in the permittivity levels were very small. When the yeast was added to the medium containing lignocellulosic particles (see Figure 4.2b), the permittivity went up immediately. The dielectric properties of wood depend on type of wood, density, moisture content and temperature (Torgovnikov, 1993). In this case the wood was birch which had received an unknown treatment to make it more easily digestible. The presence of lignocellulosic particles appears to have a minimal impact on the permittivity signal, and did not create any major interference when measuring the changes in dielectric properties of the suspension due to an increase in yeast concentration.

Figure 4.3 shows the effects of the addition of lignocellulosic particles and yeast on the conductivity of the medium. Addition of lignocellulosic particles and yeast decreased the conductivity.
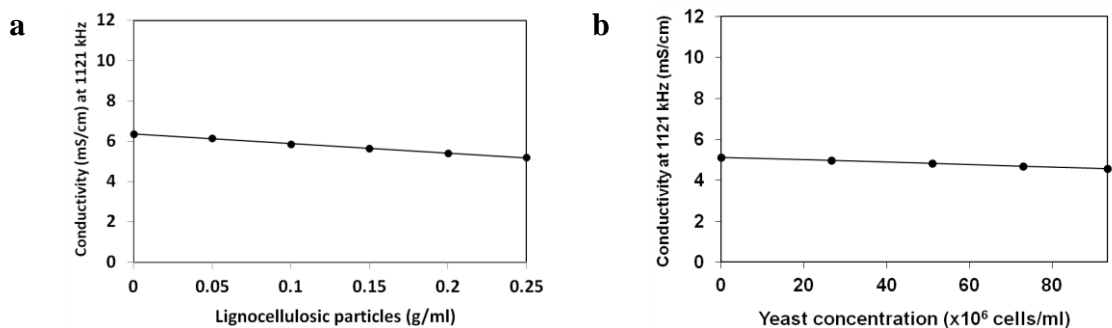
Figure 4.3 Conductivity as a function of a) lignocellulosic particles and b) yeast concentration in a medium containing 0.25 g/ml of lignocellulosic particles.

In the next experiment, fermentation of yeast was performed at room temperature (22 °C) with lignocellulosic particles as the substrate (simultaneous saccharification and fermentation process, SSF). 400 ml of sterile IFM medium (Mascoma Ltd) with added nutrient salts was placed in a 600 ml glass beaker, and monitored for 1 hr. After 1 hr; 0.03 g/ml of lignocellulosic particles were added along with commercial cellulose (2 mg/g total solids). After 15 min; yeast was added to an initial concentration of 10×10^6 cells/ml to start the fermentation along (See Figure 4.4).
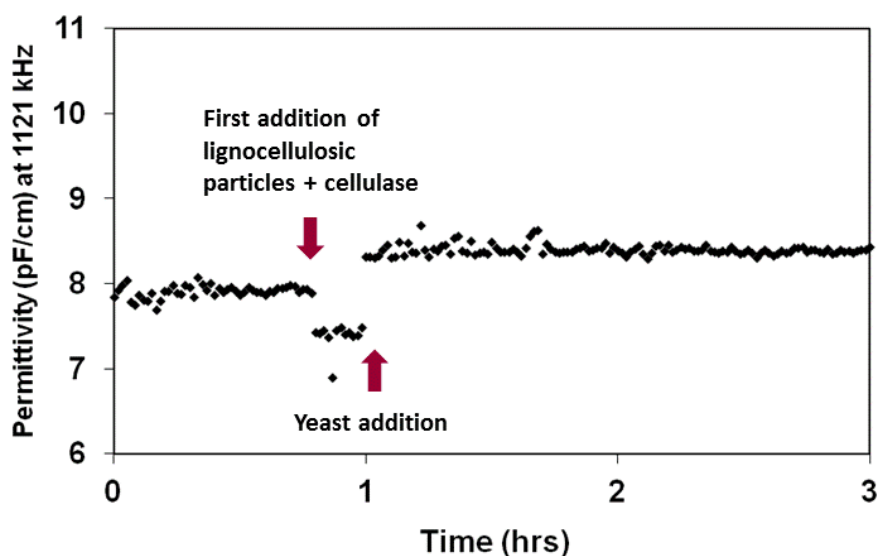
Figure 4.4 First 3 hours of lignocellulosic fermentation. Addition of cellulase influences the level of permittivity signalling by going down, while the addition of yeast increases the permittivity levels.

In the next 3 days lignocellulosic solids were fed in five equal increments to a total concentration of 0.15 g/ml whilst the dielectric properties of the suspension were continuously monitored. At the end of the third day, 80 ml of wort were added to the fermentation (0.16 ml wort/ml final volume). As can be seen in Figure 4.5, the increase in the permittivity during the first 3 days was quite low. This is most likely caused by the fact that little substrate was released that was suitable for yeast growth.
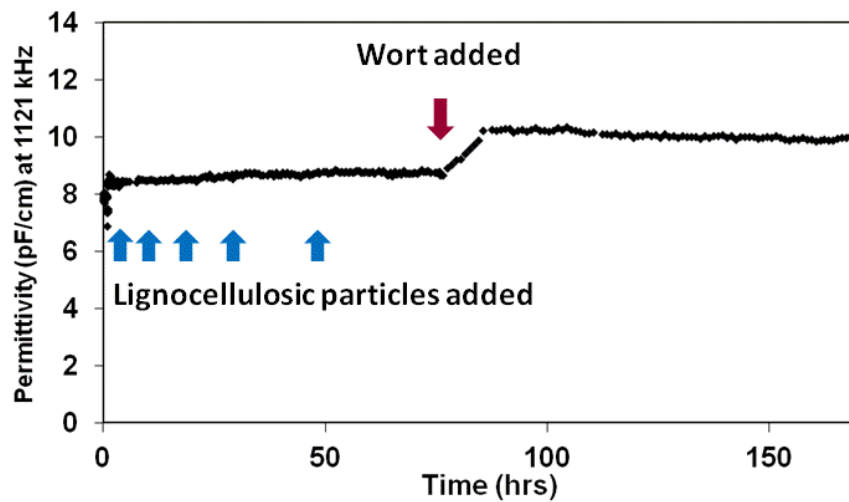
Figure 4.5 Permittivity as a function of time during lignocellulosic fermentation with pretreated hardwood. Lignocellulosic solids were added in five equal increments to a total concentration of 0.15 g/ml. 0.16 ml/ml of wort was added after 3 days.

The optimal temperature for saccharification would be 50 °C degrees whilst the optimum for most fermentations would be near 35 °C (Olsson and Hahn-Hagerdal, 1996; Krishna *et al*., 2001). The temperature used in our experiments was 22 °C degrees, considerably lower. The fact that little fermentable material was released was confirmed when after 3 days 80 ml wort was added to the medium. Wort is rich in fermentable sugars, and the permittivity levels rapidly went up in the next 10 hours due yeast growth in the more favourable medium.

To determine whether the small increase in the permittivity during the first 3 days was due to cell growth and not drift, the drift of the instrument was measured by monitoring the permittivity of a NaCl solution with the same conductivity as the growth medium for 3 days. As drift would normally affect the low and high frequency, the high frequency signal (10 MHz) in a spectrum was also subtracted from the low frequency signal (1121 kHz). The results, shown in Figure 4.6 shows that the change in the Δpermittivity during the first 70 hours of the fermentation was larger than the drift. The small increase in the Δpermittivity is therefore likely to be due to yeast growth, though because of the lack of conversion of the substrate yeast growth is not a strong.
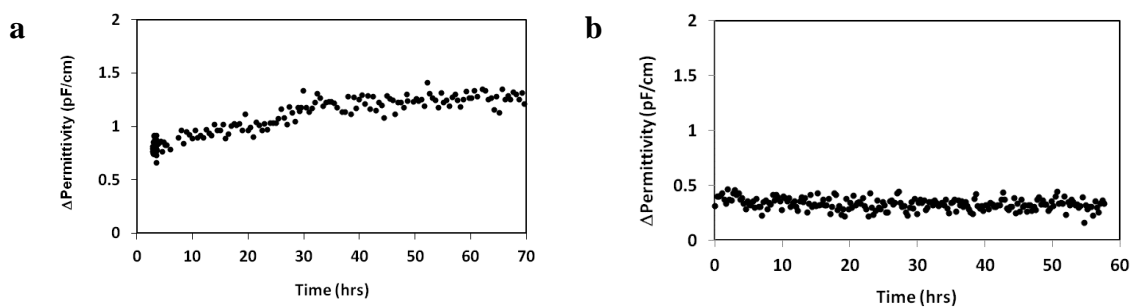
Figure 4.6 a) First 70 hours of the lignocellulosic fermentation. An increase in the Δpermittivity can be seen, indicating some yeast growth occurred. b) ΔPermittivity of a NaCl solution for a similar period. ΔPermittivity is calculated as the difference between data at 1121 kHz and 10 MHz frequency.

4.4 Conclusions

The presence of non-cellular particles can complicate the measurement of the cellular biomass during fermentation using dielectric spectroscopy. Pre-treatment of the lignocellulosic particles along with the enzyme treatment can play an important role during fermentations and good care should be taken to obtain good results. The enzymatic treatment could have not been effective enough in making wood digestible for the yeast and that could cause a poor growth rate at the beginning of the fermentation. However, in the system studied, the presence of pre-treated hardwood had little effect on the permittivity readings during fermentation, and only small changes in the conductivity occurred. Rapid changes were observed when cellulase and yeast were added. Otherwise, the changes in the magnitude of the permittivity signal appear to depend on yeast growth mainly. Dielectric spectroscopy therefore appears to be a good method for monitoring the cellular biomass concentration during simultaneous saccharification and fermentation of hardwood. However, the signals are small, and great care needs to be taken during measurements and their interpretation as many factors other than the yeast concentration can affect the capacitance signal (Asami, 2002). However, if these problems can be overcome then dielectric spectroscopy could play an important role in optimising microbial growth during fermentations of lignocellulosic feedstocks and studying adverse effects of processing conditions on cell viability during production.

CHAPTER 5

CORRECTION OF DIELECTRIC SPECTRA OBTAINED IN HIGHLY CONDUCTIVE MEDIA FOR NEGATIVE ELECTRODE POLARISATION

ABSTRACT

Negative electrode polarisation was observed below 1000 kHz when working with highly conductive media. A mathematical method based on the rate of change in the permittivity as a function of the frequency and the medium conductivity was developed and successfully used to compensate spectra of yeast and microalgae for the negative electrode polarisation. This allowed estimates of the intracellular conductivity and membrane capacitance of baker's yeast and microalgae to be determined.

5.1 Introduction

Dielectric spectroscopy involves the measurement of the dielectric properties of materials as a function of frequency. Dielectric spectroscopy is a non-invasive technology that can provide very useful information about the structures and electrical properties of the system at molecular and macroscopic levels (Maxwell, 1873; von Hippel, 1954). The dielectric properties of cell suspensions have been particularly well studied because interfacial polarisation processes that occur between the structures that form the cell lead to frequency-dependent behaviour of the permittivity and conductivity in the low radio-frequencies (0.1-100 MHz). Particularly well studied is the β-dispersion which is caused by the presence of the cell membrane. The low permittivity, low conductivity membrane separating the high conductivity, high permittivity cell interior and medium leads to an increment in the low radio-frequency permittivity whose magnitude is linearly correlated with the volume of membrane enclosed material (biomass) (Schwann, 1957; Harris *et al*., 1987). This linear relation has been shown to be valid for many different cells types, including bacteria, yeasts,

moulds and other microorganisms, as well as animal and plant cells, and has made dielectric spectroscopy one of the most used technologies for measuring cellular biomass (Kell *et al*., 1990; Markx and Davey, 1999; Ferreira *et al*., 2005; Ansorge *et al*., 2010a&b). Detailed analysis of the dielectric spectra can provide additional information about cellular properties, and dielectric spectroscopy has been be used to determine other changes in the cells such as size, shape and lipid accumulation among others (Asami *et al*, 1980; Asami, 2002; Di Basio and Cametti, 2007; Maskow *et al*., 2008; Di Basio *et al*., 2010).

Microalgae have in recent years attracted increased attention due to their ability to produce a wide type of useful products for diverse industries. Among these products are chemicals and bioactive compounds for cosmetic and pharmaceutical applications and proteins and lipids for food and biofuel industries (Carballo-Cardenas *et al*., 2003; Spolaore *et al*., 2006, Garcia-Casal *et al*., 2009, Demirbas, 2010; Harun *et al*, 2010; Nigam and Singh, 2011). The high conductivity of the media used for growing marine microalgae combined with their small size, makes monitoring of the biomass level during their culture with dielectric spectroscopy challenging. As a result, optical methods have been preferred to date (Sandnes *et al*., 2006; Griffiths *et al*., 2011). Dielectric spectroscopy can, however, potentially give additional information about algal cell properties which are difficult to obtain on-line and in real-time with other methods, including information about cell viability and lipid content. It may therefore be useful to explore the use of dielectric spectroscopy in algal cultures in high conductivity media further.

The challenge of using dielectric spectroscopy to measure the concentration of biomass of microalgae in high medium conductivity media is one that is common with many other types of fermentation. During many fermentations the properties of the medium change over time as different compounds are generated and released to the medium, changing the chemical and electrical properties of the suspension (Palmqvist and Hahn-Hagerdal, 2000, Bryant *et al*., 2011, Tibayrenc *et al*., 2011).

Working with dielectric spectroscopy in media with high conductivity levels presents two challenges. The first challenge is crosstalk. The other challenge is electrode polarisation (Schwann, 1992; Davey and Kell, 1998 a&b; Yardley *et al*., 2000).

Crosstalk is caused by the inability to resolve the imaginary and real part of the impedance, causing a change in the measured capacitance when the conductance changes. Crosstalk is a problem that is caused by the limitations of the electronic circuitry, and can be solved –or at least reduced - by electronic design.

Electrode polarisation is thought to be produced by the build-up of charge at the interface between the electrode and the electrolyte (medium) which results in frequency-dependent contributions to the measured permittivity and conductivity (Schwan, 1992). Electrode polarisation causes a distortion of the β-dispersion producing high (positive) or low (negative) values of permittivity and occurs at the low frequency end (below 1000 kHz).

Several methods have been proposed for reducing electrode polarisation. One approach is to change the measurement system. For example, the use of inductively coupled electrodes makes it possible to do dielectric measurements without direct contact with the liquid, and can completely eliminate electrode polarisation (Siano, 1997). Four electrode measurements, in which only a small voltage drop is induced at the inner set of electrodes, and the majority of the current (and hence the electrode polarisation) occurs at the outer electrodes can be used to significantly reduce (but not eliminate) electrode polarisation (Harris *et al*., 1987; Schwan, 1992). This method is used in the commercially available Aber and Fogale Biomass Monitors. The amount of electrode polarisation is dependent on the material of the electrode and the current density through the surface. Noble metals tend to produce much less electrode polarisation, and platinum, which can be induced to form a layer of highly porous platinum with a very high surface area ("platinum black") is particularly useful. A move from pure gold to platinum electrodes can result in a reduction in electrode polarisation of 2-4 orders of magnitude (Stoneman *et al*., 2007). Precise measurement of the contribution of the electrode polarisation is possible by taking admittance measurements with different distances between the measuring electrodes (Schwan, 1992). Taking measurements with different distances is impractical for on-line biomass measurements due to the introduction of movable parts and concomitant problem with sterility, though a vibrating electrode system has been proposed (Davey and Kell, 1998).

The other approach is to use mathematical models to describe and then compensate for electrode polarisation. Among methods that have been proposed is the substitution

method (Davey *et al.*, 1990; Schwan, 1992), in which a low frequency scan is made of the capacitance of a sample of the suspending medium and subsequently subtracted from the low frequency scan of the cell suspension (Davey *et al.*, 1990; Schwan, 1992; Davey and Kell, 1998a&b; Yardley *et al.*, 2000; Bordi *et al.*, 2001; Stoneman *et al.*, 2007; Prodan and Bot, 2009;). Davey and Kell (1998) proposed a mathematical model which allowed compensation of a spectrum for the electrode polarisation by using the fact that electrode polarisation declines rapidly from at increasing frequencies. By fitting the low frequency part of a spectrum to a power law they were able to remove electrode polarisation from a spectrum without having to separately measure the polarisation of medium without cells (Davey and Kell, 1998b). However, this method can overcompensate for electrode polarisation, especially where the signal that is being measured is very small, or where the signal from the material that is being measured itself is frequency dependent (for example where low-frequency dispersions occur).

Here we will describe a method for the removal of (negative or positive) electrode polarisation in system combining the relative uses of the substitution method and the Davey and Kell's mathematical modelling approach. The method was applied to the measurement of the dielectric properties of microalgae and yeast in highly conductive media.

5.2 Materials and methods

Cells

High activity, pressed baker's yeast. (*Saccharomyces cerevisiae*) was obtained from DCL Craftbake and stored at 0-4° C for a maximum of 12 days. The viability of fresh yeast was tested using methylene blue staining (Gurr, 1965) before each experiment, and was not less than 98%. 100 g of pressed yeast was resuspended with deionised water and artificial sea salt (Instant Ocean) was added at different concentrations to a final volume of 150 ml to obtain a thick suspension with 7×10^9 cells/ml.

Nannochloropsis oculata is a marine micro alga with a diameter of around 2.7 ± 0.3 μm during the stationary phase. *Nannochloropsis oculata* was cultivated in four 10 L culture flasks (Carbuoys) in f/2 artificial sea medium (see http://www.ccap.ac.uk/media/documents/f2.pdf) at 20° C with 16 hrs of light and 8 hrs

of darkness until stationary phase was reached (Day *et al*., 2012). Centrifugation of the 40 L of cells was done in 500 ml flasks (15 min centrifuge spin at 5000 rpm, 5311 g) and resuspended in the same medium to obtain a volume of 150 ml with about 2.3×10^9 cells/ml. Previous experiments made with this micro alga show it has a strong wall which makes it difficult to break it down making it very resistant to the treatments for concentration and preservation (Gwo *et al*., 2005). A 5 µl sample was diluted to 1 ml and cell concentration was determined by haemocytometer counting. Cell concentration after centrifugation was 2.3×10^9 cell/ml

Dielectric measurements

For the experiments with microalgae, 700 ml of f/2 artificial sea medium was prepared and placed in a 1000 ml glass flask. 15 ml of a concentrated microalgae suspension (2.3×10^9 cell/ml) was added to the medium 10 times every 5 min, and the dielectric properties of the suspension continuously monitored. In the next experiment, 100 ml of medium was diluted 10 times to 1 L final volume with deionised water. Cells from previous experiment were centrifuged, washed twice and resuspended to 150 ml final volume with the same 10 times diluted medium. 700 ml of the 10 times diluted medium was placed in a 1000 ml glass flask. Again, 15 ml cell suspension (with 2.3×10^9 cell/ml) was added to the dilute medium 10 times every 5 min, and the dielectric properties of the suspension recorded.

For the experiments with baker's yeast (*S. cerevisiae*), small aliquots (15 ml) of the concentrated yeast suspension (7×10^9 cells/ml) were added to a 1 litre beaker with 500 ml medium containing deionised water with different concentrations of artificial sea salt. In all experiments an Aber Instruments Biomass Monitor model 220, shown in Figure 5.1, was used, with a 1.2 cm diameter 30 cm long annular probe with 4 platinum electrodes, connected to a PC with Aberscan software version 2.2 (Aber Instruments, Aberystwyth, UK) to record the dielectric frequency spectra. The freerun option was used to measure the dielectric properties of the cell suspension at 25 frequency points evenly distributed over the frequency range 0.1 to 20 MHz. One spectrum was measured every 10 seconds, and then an average spectrum was calculated from the data from 30 spectra. All data were corrected for dilution effects.
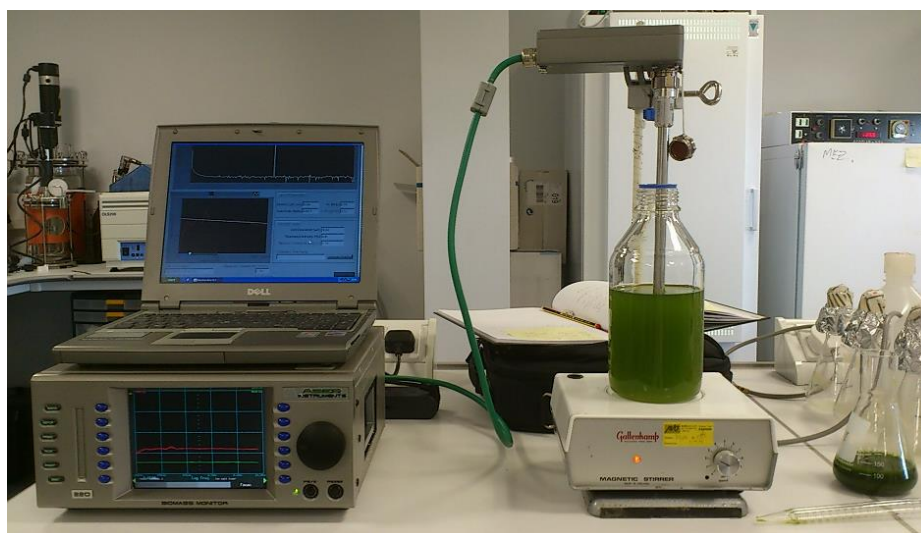
Figure 5.1 Experimental set up showing the Aber biomass monitor.

5.3 Results and discussion

Cross-talk

At frequencies above 1 MHz electrode polarisation effects were minimal, and for this reason the amount of cross-talk at 1121 kHz was measured by measuring the permittivity of deionised water at different medium conductivities. As can be seen in Figure 5.2, when the permittivity of deionised water without salt was measured an anomalously high permittivity was observed. However, when the medium conductivity was increased by increasing the amount of artificial sea salt (Instant Ocean) in the medium, the permittivity remained near constant for conductivities until a value of 54 mS/cm was reached. Above this level, no increase in conductivity could be measured, and the measured permittivity declined strongly.
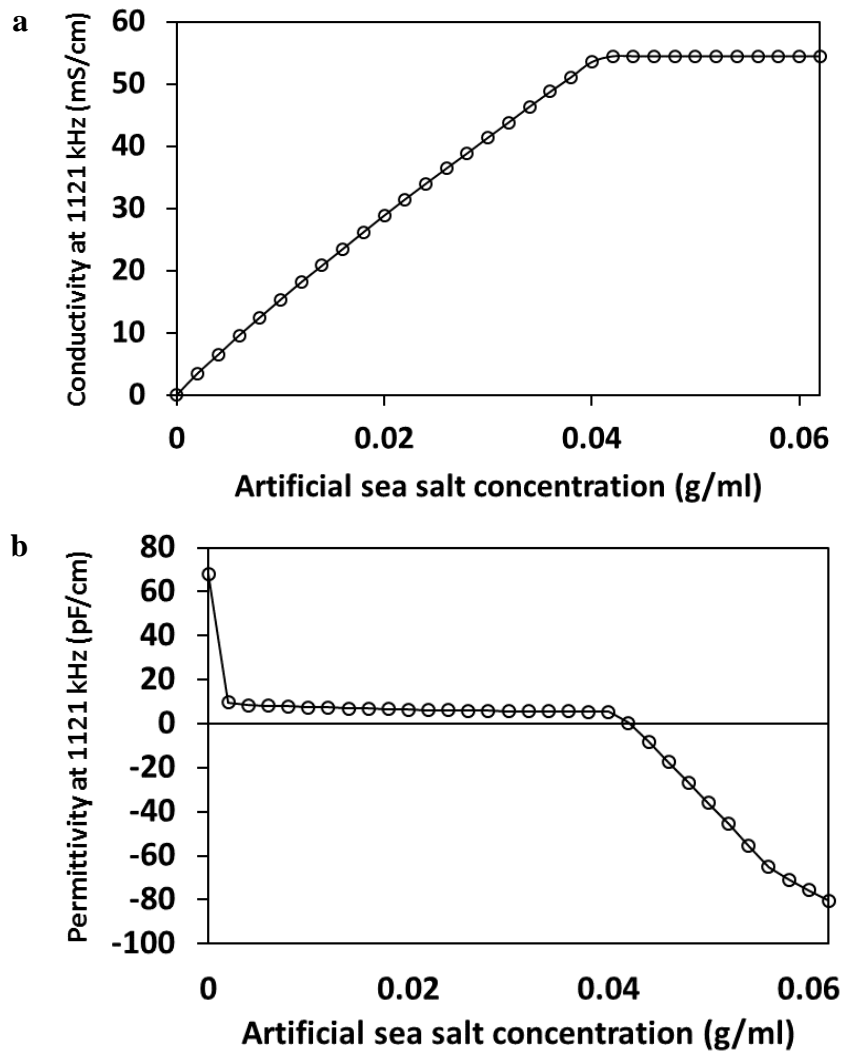
Fig. 5.2 a) Conductivity and b) Permittivity at 1121 kHz as a function of artificial sea salt concentration.

As can be seen in Figure 5.3., when the experiment was repeated in a suspension which contained yeast, for an artificial sea salt concentration between 0.001 – 0.04 g/ml, the linear correlation between cell concentration (yeast) and permittivity at 1121 kHz remained nearly constant and was only slightly influenced by the conductivity in the medium.
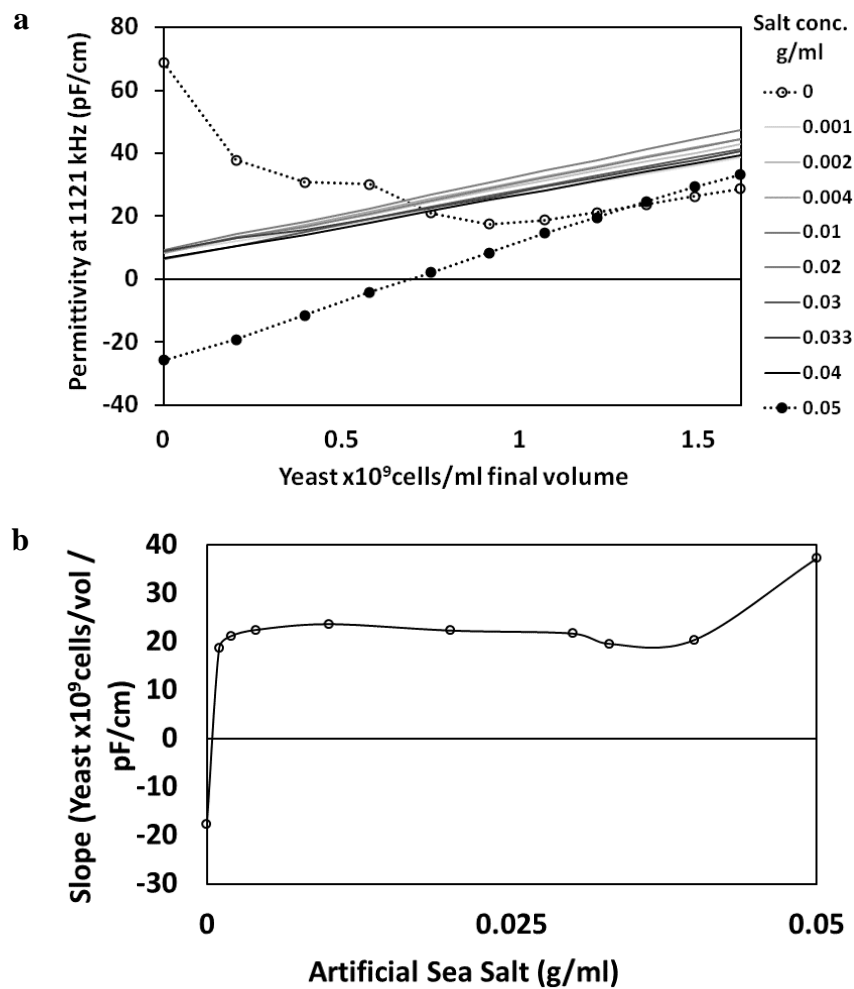
Fig. 5.3 a) Permittivity (pF/cm) as a function of cell concentration for media with different artificial sea salt concentrations. b) Slope of permittivity as a function of cell concentration for different artificial sea salt concentrations.

Electrode polarisation

As can be seen in Figure 5.4, at low frequencies (below 1000 kHz) significant electrode polarisation was observed. Although electrode polarisation is commonly positive, i.e. it increases the permittivity, negative electrode polarisation which decreases the permittivity does commonly occur (M. Lee, Aber Instruments, personal communication). As expected the difference between the expected and measured permittivity due to electrode polarisation increased at lower frequencies and higher conductivities.
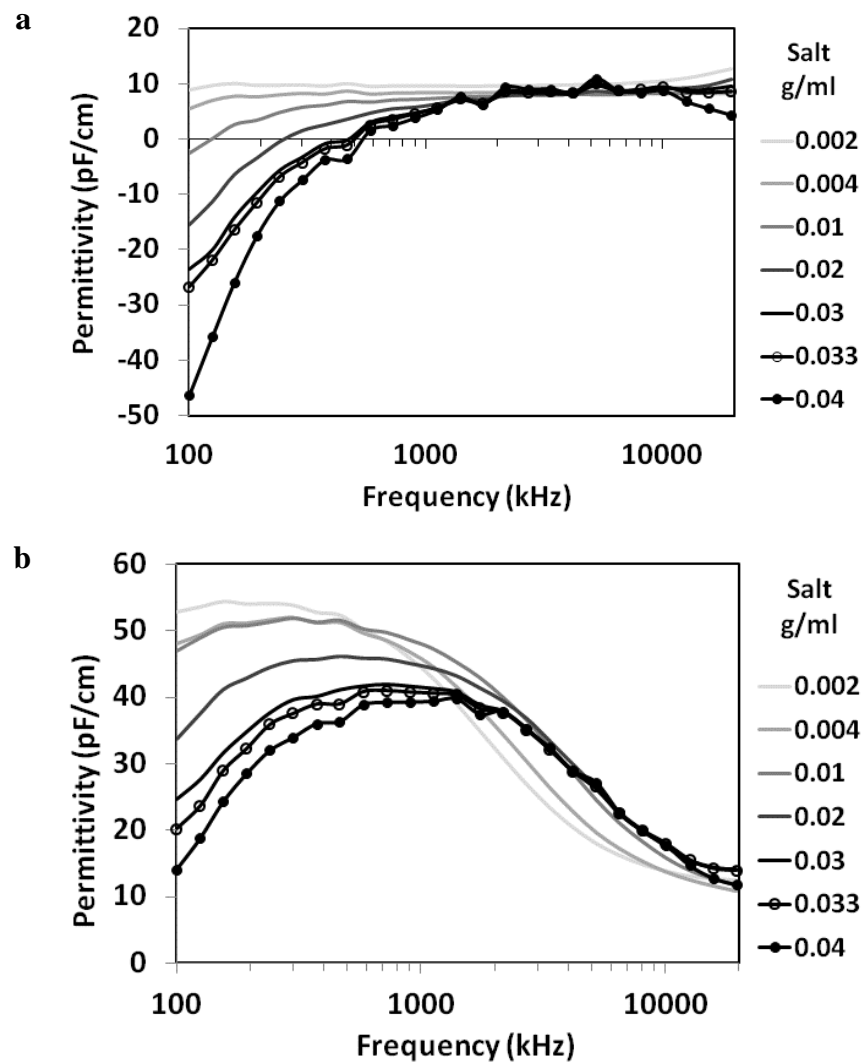
Fig. 5.4 Dielectric spectra of permittivity (pF/cm) as a function of frequency for different artificial sea salt concentrations a) in water without cells and b) in water with 1.6×10^9 yeast cells/ml.

Compensation for electrode polarisation

A new methodology was developed to overcome electrode polarisation whilst working with highly conductive media. The protocol was as follows:

Permittivity measurements were taken in water at different frequencies f_i from 100 kHz to 20 MHz for different concentrations of artificial sea salt. For each frequency and salt concentration the data were plotted in a graph as shown in Figure 5.5.
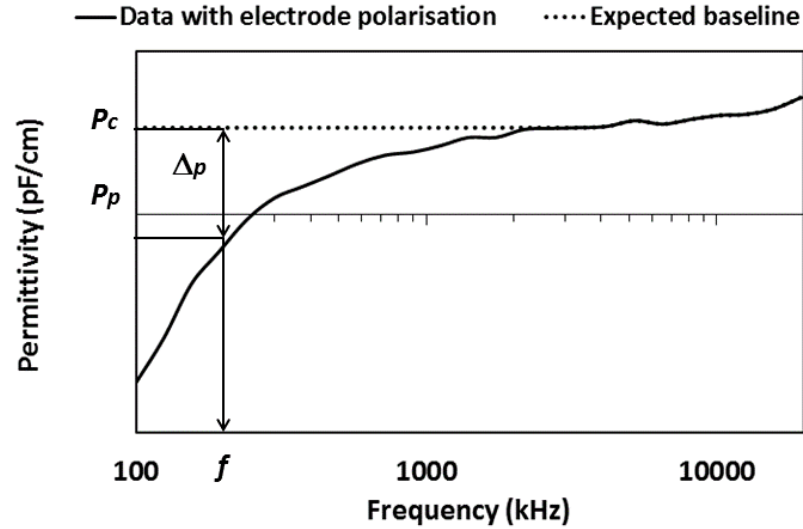
Figure 5.5 Permittivity spectrum as a function of frequency showing the expected baseline P_c and electrode polarisation P_p.

The contribution by the electrode polarisation to the spectrum reduces as the frequency increases, and becomes negligible at frequencies over 3 MHz. Dielectric spectra usually show an increase in the permittivity at the highest frequencies, but typically there is a flat baseline around 3-4 MHz. From the experiments on crosstalk we know that the baseline is relatively constant over a large frequency range and at different medium conductivities. Assuming that the baseline has the same value at all frequencies below 3 MHz, we can assign the baseline a value P_c based on the measured permittivity between 3 and 4 MHz. For a given salt concentration (X_i) and a given frequency (f_i) the contribution by the electrode polarisation ΔP to the spectrum can then be estimated:

$$\Delta P = \mathrm{Abs}(P_p - P_c) \tag{5.1}$$

where P_p corresponds to the experimental permittivity values showing electrode polarisation and P_c is the baseline permittivity, i.e. the expected permittivity when there is no electrode polarisation. The electrode polarisation was estimated for different salt concentrations, and the results are shown in the next Figure 5.6.
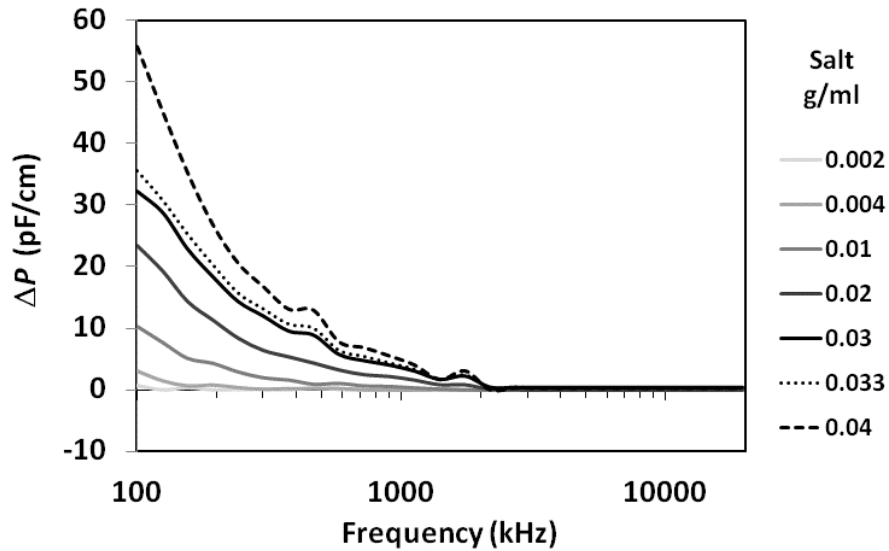
Figure 5.6 Contribution of electrode polarisation to the spectra at different artificial sea salt concentrations.

The shape of curve of ΔP as a function of frequency (Figure 5.6) suggests that a power law model, as previously observed in other work (Onaral *et al*., 1984; Davey and Kell, 1998; Yardley *et al*, 2000), could be applied. The power law establishes that:

$$^{f}C_{p} = {}^{1\,Hz}C_{p}f^{p} \qquad\qquad (5.2)$$

or

$$\log(^{f}C_{p}) = \log({}^{1\,Hz}C_{p}) + p\log(f) \qquad\qquad (5.3)$$

where $^{1\,Hz}C_{p}$ is the capacitance due to polarisation at 1 Hz, f is the applied frequency (Hz), $^{f}C_{p}$ is the capacitance (pF) due to electrode polarisation at a given frequency and p is a dimensionless power term.

According to Eq. 5.3, when data are plotted in a log-log plot, then the intercept with the y-axis will give $\log(^{1\,Hz}C_{p})$, and the slope the power p. $^{1\,Hz}C_{p}$ gives a measure of the magnitude of the polarisation, and p a measure or the rate of fall of polarisation as a function of frequency

As can be seen in Figure 5.7 the power law described the polarisation data well, and a value for p was found of -1.1. For further analysis a more practical values of -1 was used.
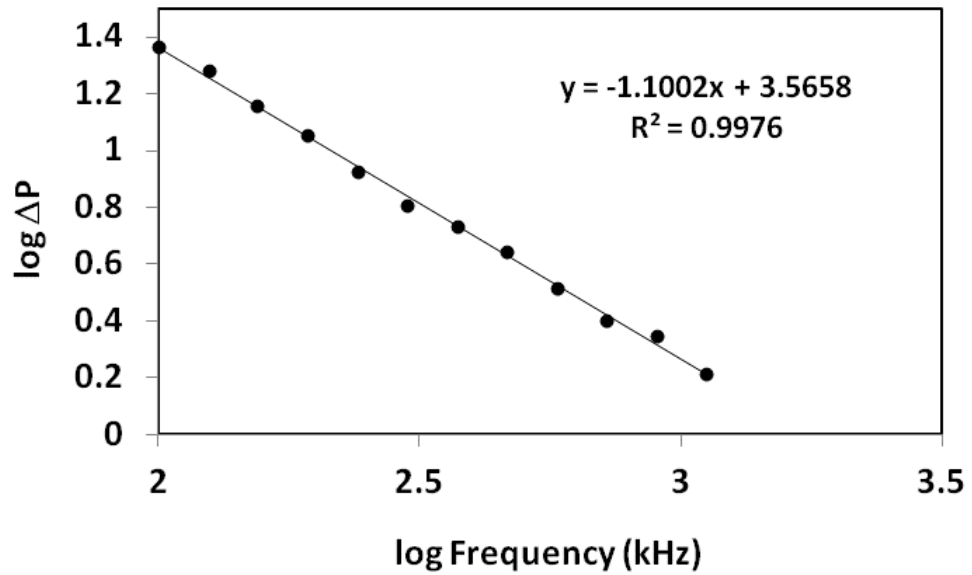
Figure 5.7 ΔP values replotted on a log/log plot to show the correlation with the frequency following the power law model on Eq. 5.3.

Thus, following the previous results, the frequency dependent polarisation ΔP can be described by:

$$\Delta P = M/f \tag{5.4}$$

The value of M is dependent on the salt concentration. A plot of the values of M as a function of the salt concentration (Figure 5.8) showed that M is linearly dependent on the salt concentration. This is most likely due to the fact that the electrode polarisation is dependent on the current density, and hence the medium conductivity. Medium conductivity will be linearly correlated with salt concentration.
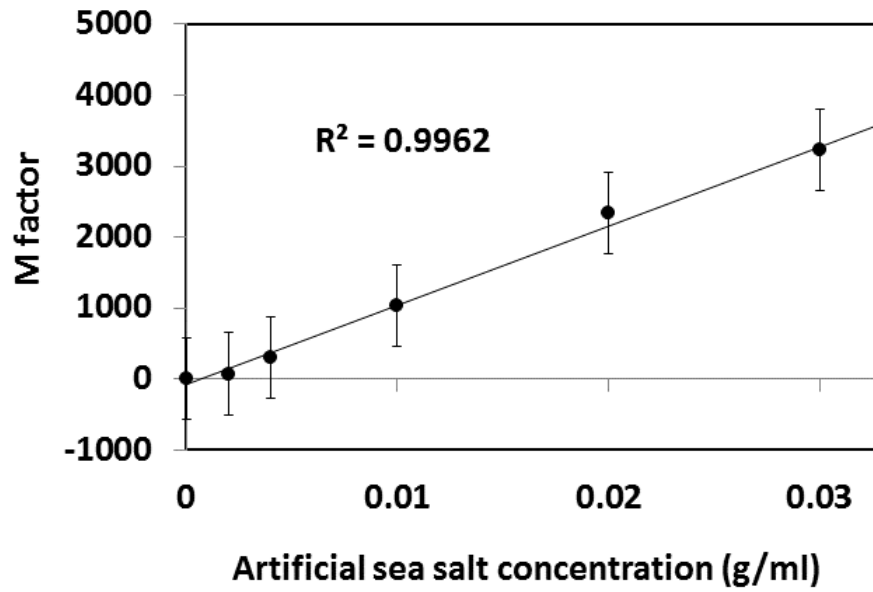
Figure 5.8 Factor *M* as a function of artificial sea salt concentration obtained experimentally based on data with electrode polarisation.

Factor *M* for a known artificial sea salt concentration can therefore be estimated with the linear relation:

$$M = 105000X_i \qquad\qquad (5.5)$$

where X_i is the salt concentration in g/ml.

In Figure 5.9 predictions of the electrode polarisation based on equation 5.4 and 5.5 are plotted as a function of the measured electrode polarisation. Predicted values of the electrode polarisation correlate strongly with the measured values.
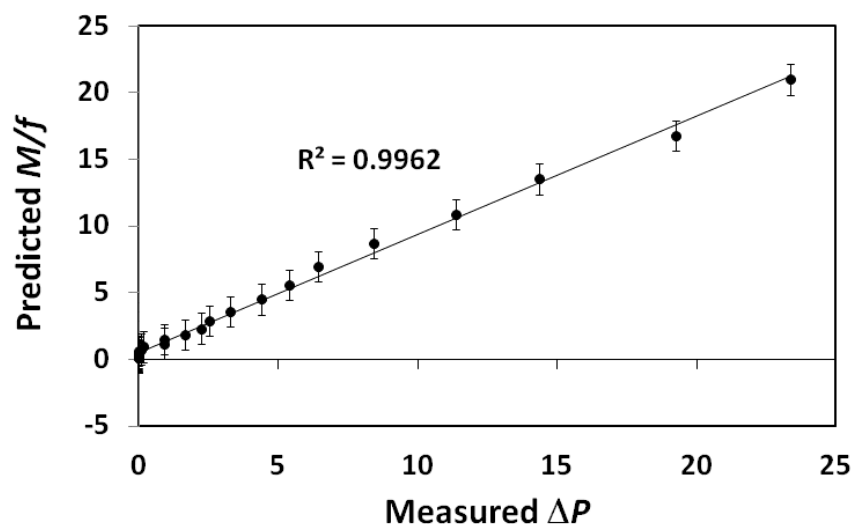
Figure 5.9 Predicted values of electrode polarisation as a function of measured values of electrode polarisation.

Application of the electrode polarisation compensation method to the measurement of the electrical properties of baker's yeast

Having established a simple protocol to estimate the contribution by the electrode polarisation to a dielectric spectrum, measurements were taken of suspensions of yeast cells at different cell concentrations and at different medium conductivities.

The measured permittivity values from a yeast suspension with electrode polarisation (P_e) can be corrected for electrode polarisation to obtain the corrected permittivity (P_c) using the equation:

$$P_c = P_e + M/f \tag{5.6}$$

Figure 5.10 shows the dielectric spectrum of a cell suspension of 1.6×10^9 cells/ml of yeast in water with a salt concentration of 0.02 g/ml before and after correction for electrode polarisation using equation (5.6). Figure 5.11 shows all corrected spectra.
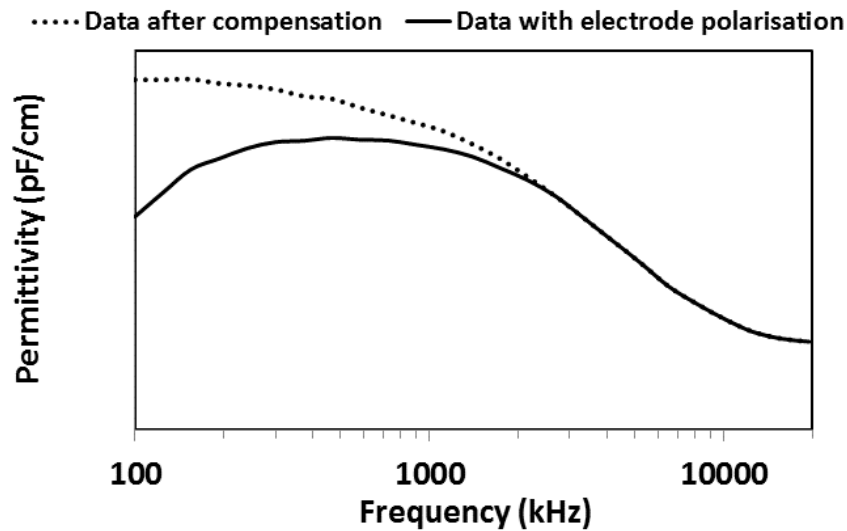
Figure 5.10 Original and corrected permittivity spectra for a yeast suspension with a cell concentration of 1.6×10^9 cell/ml. The artificial sea salt concentration in the medium was 0.02 g/ml.
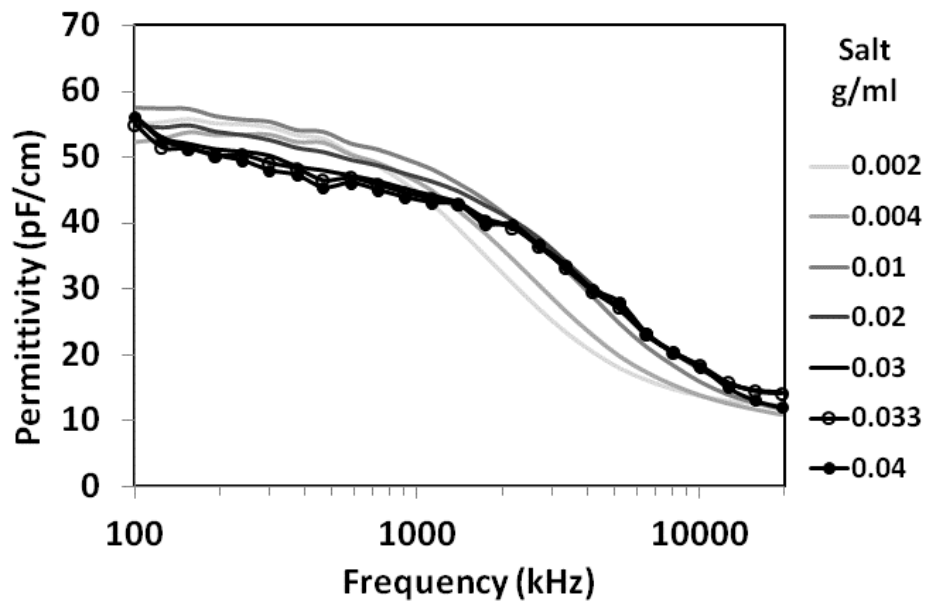
Figure 5.11 Dielectric spectra with of suspensions with 1.6×10^9 yeast cells/ml with different artificial sea salt concentrations in water after compensation for electrode polarisation.

With the corrected data it was possible to determine the change in f_c of the yeast suspensions as a function of the salt concentration. It was found (Figure 5.12) that the characteristic frequency f_c moved to higher values when salt concentration was increased, but at certain point, around 0.02 g/ml the f_c stabilized.
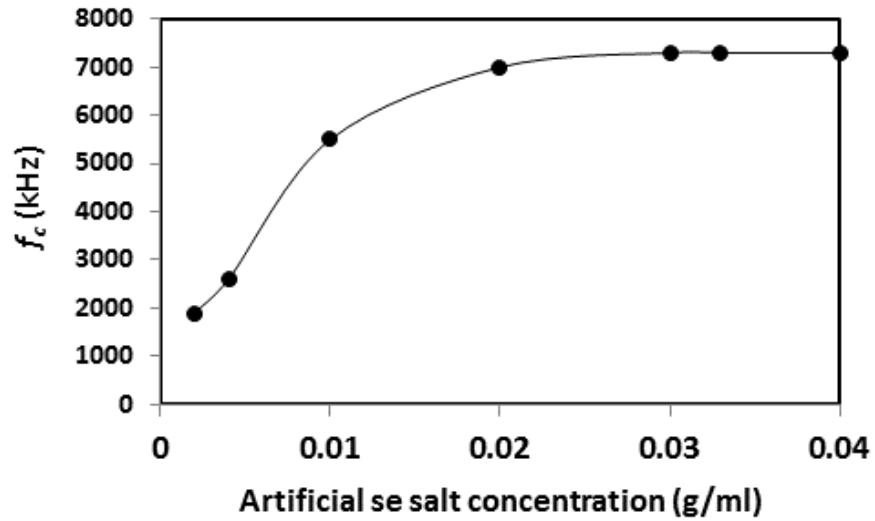
Figure 5.12 Characteristic frequency f_c as a function of artificial sea salt concentration for cell suspension of yeast with concentration of 1.6×10^9 cell/ml.

For diluted suspensions of viable cells, when the viable cell volume fraction (P) is low ($P<0.2$) and the electrical interactions between cells in negligible, f_c can be effectively related with the internal conductivity of the cells following an equation developed by Pauly and Schwan (Harris *et al*., 1987), in which the relaxation time for a Maxwell-Wagner dispersion (β-dispersion) is described by:

$$\frac{1}{2\pi f c} = r C_m \left(\frac{1}{\sigma_i^{'}} + \frac{1}{2\sigma_o^{'}} \right) \tag{5.7}$$

where r is the cell radius (cm); C_m, specific membrane capacitance ($\mu F/cm^2$); σ_i', intracellular conductivity (mS/cm) and σ_o', medium conductivity (mS/cm). For yeast with a radius of 3 μm in a suspension with 1.6×10^9 cells/ml P can be estimated to be 0.18, i.e. smaller than 0.2. The external conductivity can be estimated from the salt concentration in water. Though the medium conductivity was slightly frequency dependent (Figure 5.13), in the frequency range in which the f_c occurred its value was relatively constant, and the conductivity of the medium at 1121 kHz was chosen as the most appropriate.

101
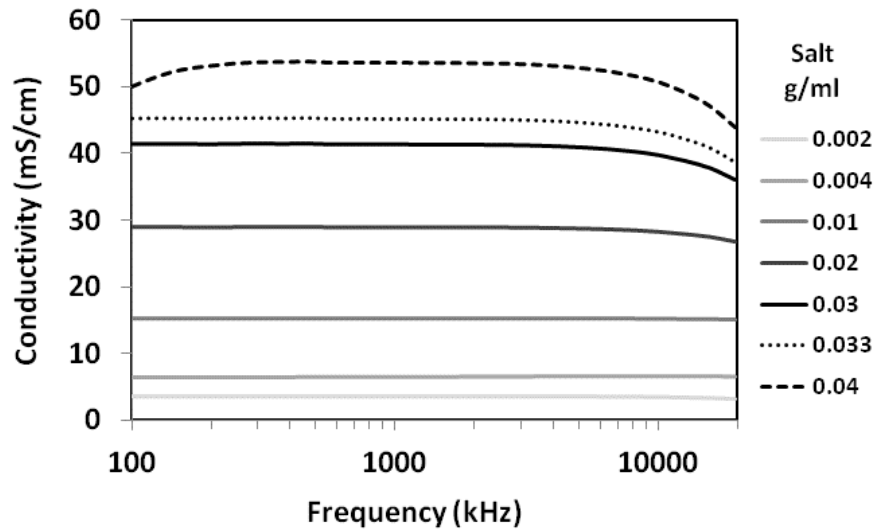
Figure 5.13 Conductivity as a function of frequency for increasing artificial sea salt concentration in deionised water.

A plot of $1/f_c$ as a function of $1/\sigma_o$' is shown in Figure 5.14.
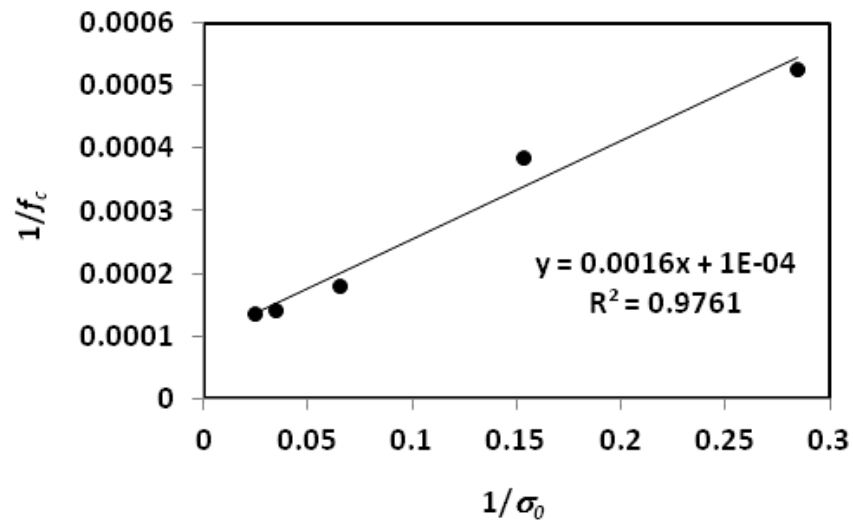
Figure 5.14 Characteristic frequency as a function of medium conductivity for yeast suspension of 1.6×10^9 cell/ml at different artificial sea salt concentrations.

σ_i' can be obtained from the intersection with the x axis and C_m from the slope of the line. C_m was calculated to be 1.35 μF/cm^2 and σ_i' 32 mS/cm.

The C_m gives a measure of the cell's ability to build-up electrical charges across the cell membrane. Its value is dependent not only on the permittivity and thickness of the

membrane, but also whether folds occur in the membrane. A value of 1 ± 0.5 μF/cm^2 is commonly attributed to it (Harris *et al.*, 1987), but its value can vary. For halophilic bacteria values for C_m have been reported varying between 1 and 4 μF/cm^2 (Morgan *et al.*, 1987). Using a similar method as the one employed here, Patel reported values for the C_m for yeast between 2.8 and 3.8 μF/cm^2 (Patel, 2009). Typical values for the value of the intracellular conductivity for yeast are between 1 and 6 mS/cm (Tibayrenc *et al.*, 2011). Patel, using a similar method as the one used here, reported measured values of the internal conductivity of yeast cells in the range of 25 ± 3 mS/cm (Patel, 2009).

Application of the electrode polarisation compensation method to the measurement of the electrical properties of microalgae

The next set of experiments was performed with the marine microalga *Nannochloropsis oculata.* Figure 5.15 shows the cell count as a function of time in a batch culture. Cells were harvested when they were in the stationary phase. The cell size at that time was around 2.7 ± 0.3 μm.
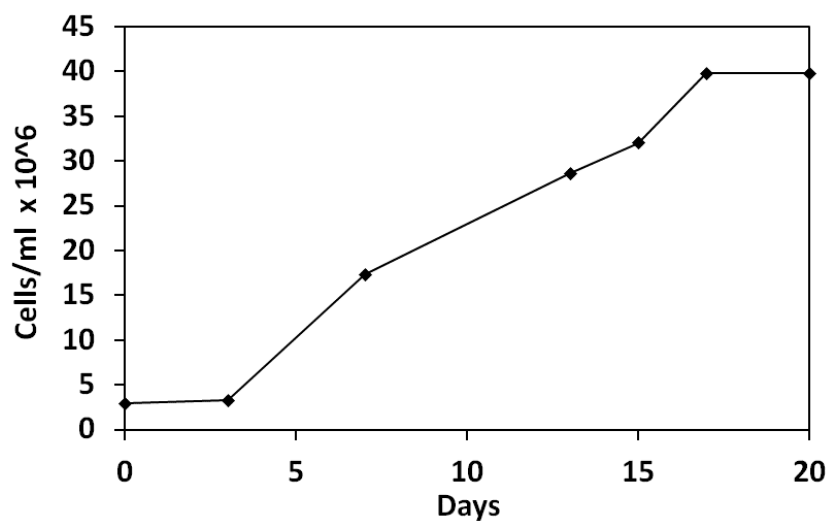
Figure 5.15 *Nannochloropsis oculata* culture.

A concentrated microalgal suspension was created and in small aliquots added to a medium with a sea salt concentration of 0.0335 g/ml, and also to a ten times diluted medium with a sea salt concentration of 0.00335 g/ml. The salt concentration of the growth medium for the microalgae was around 0.0335 g/ml. the high medium conductivity at these salt concentrations creates a large amount of electrode polarisation, causing serious interference during the monitoring of microalgal biomass levels.

Equation 5.6 was applied and Figure 5.16 shows the results of the correction for electrode polarisation for a cell suspension with a concentration of 0.3×10^9 cells/ml in seawater.
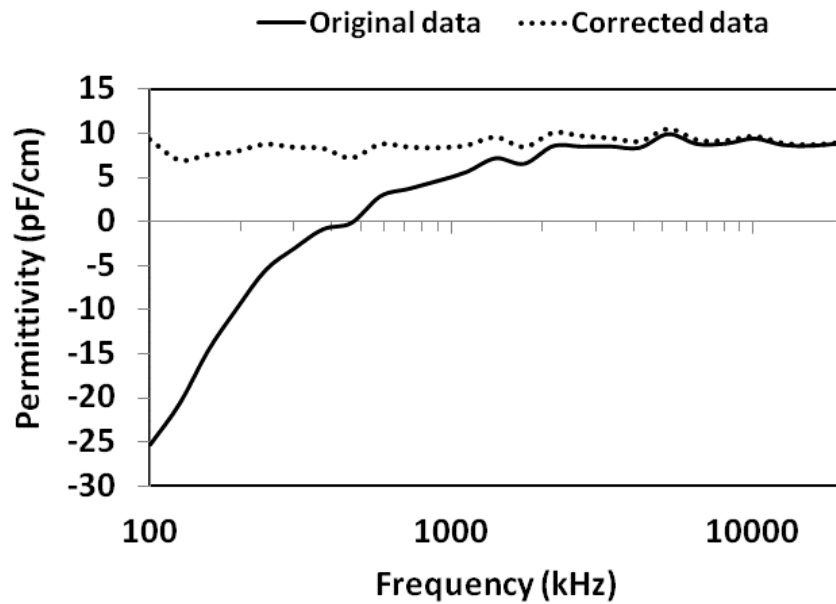
Figure 5.16 Original and corrected permittivity spectra as a function of frequency for microalgae suspension with a concentration of 0.30×10^9 cell/ml. Artificial sea salt concentration in the medium was in the order of 0.033 g/ml.

Figure 5.17 shows the results of the correction of the data of microalgae suspension in 10 times diluted media.
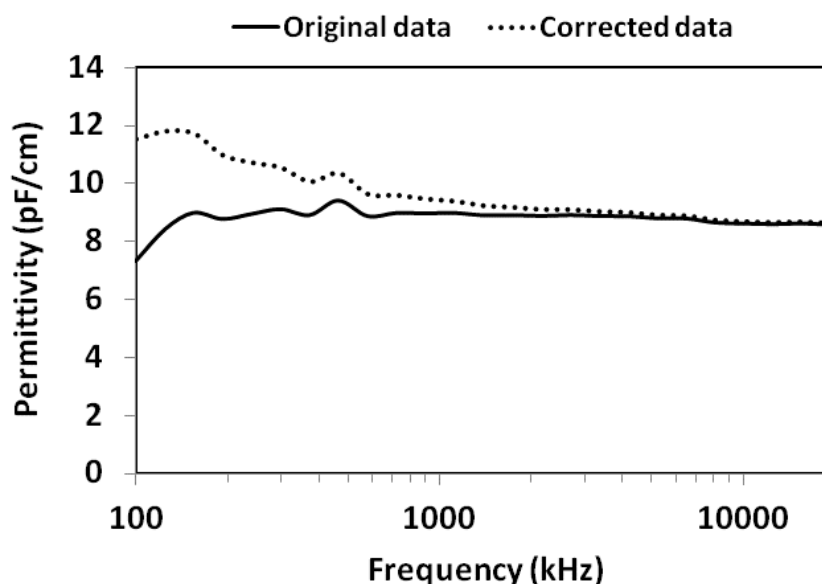
Figure 5.17 Original and corrected permittivity spectra as a function of frequency for microalgae suspension with a concentration of 0.30×10^9 cell/ml. Artificial sea salt concentration in the medium was in the order of 0.0033 g/ml.

Comparison of Figure 5.16 and 5.17 shows that in Figure 5.16 there is no sign of a dispersion caused by the presence of the cells, whilst in Figure 5.17 there is. This indicates that even thought the method eliminates the negative electrode polarisation successfully, when changes in the permittivity caused by the presence of the cells are small (due maybe to a small cell diameter), the method may not be sensitive enough to identify these small changes in the biomass levels since the high conductivity of the medium creates a strong interference.

The electrode polarisation method was applied to all the cell concentrations for the two media conductivities. Data at 1121 kHz were then abstracted. Figure 5.18 shows the correlation between permittivity and cell concentration for a) usual medium and b) diluted medium at 1121 kHz. The experimental data without electrode polarisation correction indicate that linear relations exist between cell concentration and dielectric increment for both mediums at frequencies above 1000 kHz as seen before with yeast suspensions. The results show that there is no significant difference in the slopes of the permittivity as a function of cell concentration (1.3 cell/ml per dielectric increment) when cells are added to a usual media or to a 10 times diluted media.
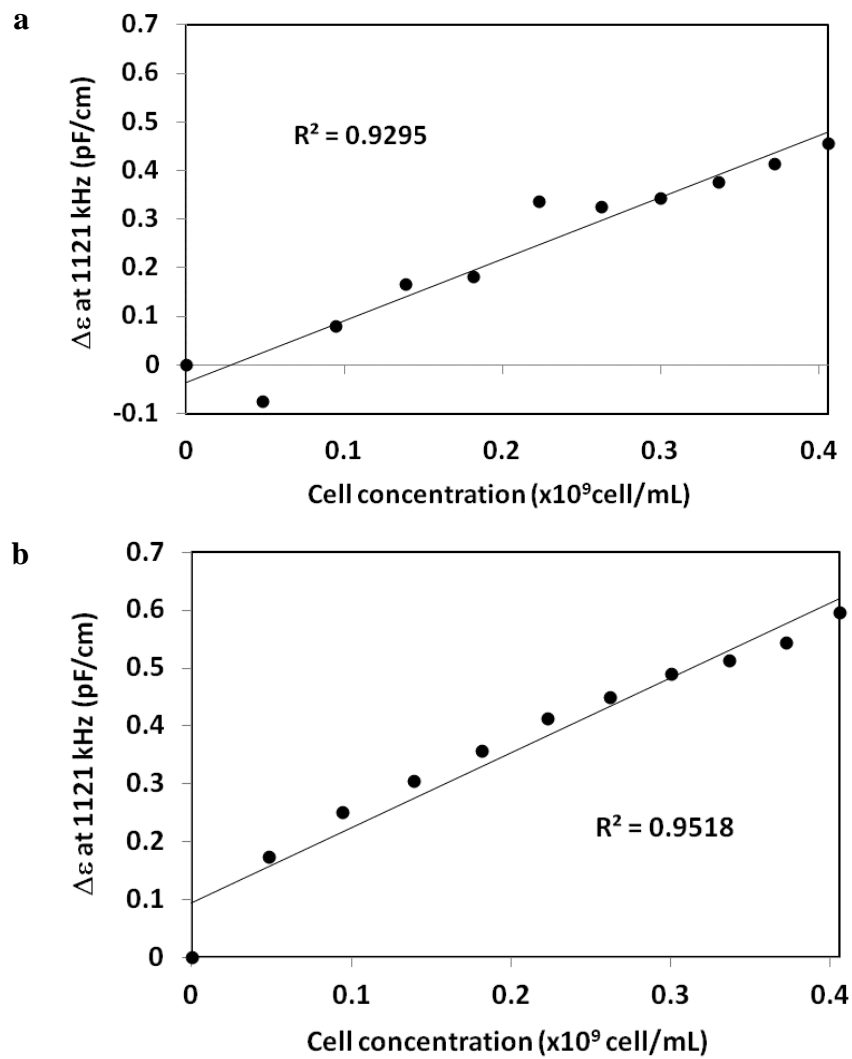
Figure 5.18 Permittivity (pF/cm) as a function of cell concentration for a) usual media, and b) 10 times diluted media.

C_m and σ_i' were calculated following the same procedure as that used for yeast. In this case, only two different salt concentrations were available. The results are shown in Figure 5.19.
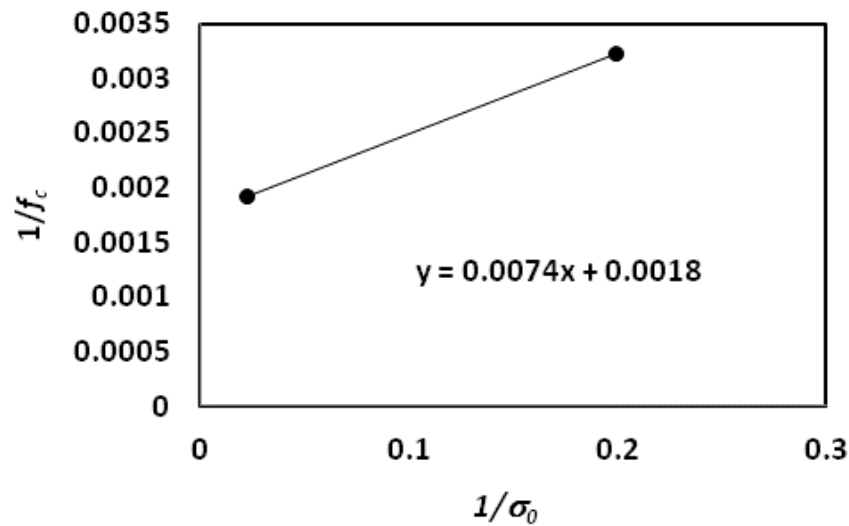
Figure 5.19 Inverse of the characteristic frequency as a function of the inverse of the medium conductivity for microalgal suspension of 0.3×10^9 cells/ml at different artificial sea salt concentrations.

σ_i' can be obtained from the intersection with the x axis and C_m from the slope of the line. C_m for marine microalga *(Nannochloropsis oculata)* was calculated to be 15.6 $\mu F/cm^2$ and the intracellular conductivity (σ_i') of the microalgae to be 8.2 mS/cm. The values of σ_i' and C_m have never been previously reported for this microalga and there is therefore no direct reference value; however the values obtained are relatively high compared to those previously reported in literature for other microorganisms (Harris *et al*., 1987; Morgan *et al*., 1987; Patel, 2009; Tibayrenc *et al*., 2011). More experiments with different medium conductivities should therefore be done.

5.4 Conclusions

The Biomass Monitor model 220 has an upper limit for the medium conductivity of 54 mS/cm. Below this conductivity values crosstalk between the conductivity and capacitance signal was minimal, but strong electrode polarisation could be observed at high medium conductivities which could affecting biomass measurements.

A simple relation was found to exist between the salt concentration in the medium and the level of electrode polarisation. This allowed spectra to be corrected for electrode

polarisation, and the internal conductivity and membrane capacitance of baker's yeast and microalgae (*Nannochloropsis oculata)* to be determined. The signal for microalgae however was quite small. Although the use of dielectric spectroscopy for measuring biomass levels during microalgal cultivation is a possibility, an increase of the sensitivity of the biomass monitor of an order of magnitude would be needed to consistently obtain reliable data. This should enable one to obtain better estimates of the internal conductivity of the cells, which in turn could provide information of the lipid content of the cells (Maskow *et al*., 2008).

CHAPTER 6

MICROELECTRODES FOR MEASURING THE DIELECTRIC PROPERTIES OF CELL SUSPENSIONS

ABSTRACT

The use of microelectrodes for the measurement of the biomass during fermentation was explored. Interdigitated microelectrodes were fabricated from indium tin oxide (ITO) on glass with different electrode widths and distances between the electrodes. Spectra in a frequency range 100 kHz to 24 MHz were obtained of yeast suspensions in malt extract. The results show that it is feasible to use ITO microelectrodes for monitoring biomass levels in suspensions. Reduction of the electrode width reduces the signal; also the signal may become unstable. Reduction of the distance between the electrodes generally improved the signal.

6.1 Introduction

The study of electrical phenomena in biological materials goes back many centuries. The use of electrical phenomena in biotechnology is nowadays an extensive field with many different applications. Common amongst these experiments is the use of electrodes to either apply electric fields or measure electric fields. Whilst traditionally large electrodes have been used, the use of microelectrodes, rather than macroelectrodes can have many advantages. They include the ability to generate high electric field strengths with relatively small voltages, the ability to pick up small signals, and perform measurements on smaller systems, and to produce disposable electrodes. The use of microelectrodes increases the portability of devices, makes it easier to work in parallel, increasing the throughput, and allow the simultaneous production of many devices simultaneously. Applications of microelectrodes include their use as sensing elements in biosensors (Rodrigues *et al*., 2004; Morin *et al*., 2005; Marrakchi *et al*., 2007; Laczka *et al*., 2009; Jungreuthmayer *et al*., 2012) and to generate electric fields for cell

manipulation (Markx *et al*., 1999, Cen *et al*., 2004). Microelectrodes have been also been used before in the study of changes in the electrical properties of cells (Hause *et al*., 1981; Giaever *et al*., 1992; Ehret *et al*., 1997; Rodrigues *et al*., 2004; Morin *et al*., 2005; Natarajan *et al*., 2006; Burmeister *et al*., 2008; Varshney *et al*., 2008).

Dielectric spectroscopy, also referred to as impedance or admittance spectroscopy, is an effective technique for the characterization and enumeration of cells. The technique can be used online, and there is no need for labels or any other pre-treatment of the cells before a measurement. Measurements of biomass levels using dielectric spectroscopy are based on the fact that in the frequency range between 0.1 and 100 MHz interfacial polarisation occurs at the cell membrane interfaces, causing large dipoles to be induced in the cells (Markx *et al*., 1999). As shown by Schwan (Schwan, 1957), the resulting increase in the capacitance at low frequencies is directly related to the volume fraction of membrane–enclosed material. When a cell dies, the membranes are often damaged. When a membrane becomes permeable charges cannot accumulate at the interface, and interfacial polarisation will be reduced. The accompanying reduction in the capacitance can be used to monitor cell death on-line and in real-time (Markx *et al*., 1999; Yang *et al*., 2008).

It is well recognised that the magnitude of the electric field generated by the microelectrodes depends on the applied voltage and electrode geometry (Morgan *et al*., 2001; Wakizaka *et al*., 2004; Wang *et al*., 2010). However, relatively little attention has been given to the way the electric field generated by the electrodes extends away from the electrode surface, and how this affects dielectric measurements. Also, it has been little explored how this can be used to advantage (Olthuis *et al*., 1995; Krommenhoek *et al*., 2006). The aim of the present study is to explore the use of microelectrodes made by photolithography for improving dielectric measurements on cell suspensions. The findings will help in developing techniques for improving the accuracy of the impedance readings and optimising the measurement of biomass levels during.

6.2 Materials and Methods

Microelectrodes

Microelectrodes were fabricated from ITO-coated (100 nm ITO) microscope glass slides (Delta Technologies Ltd, USA) using photolithography. Prior to photolithography the slides were cleaned with acetone or propanol to remove any contamination, then dried using compressed air, baked at 115 ºC for 20 min to evaporate all the adherent water molecules and to enhance the adhesion of photoresist to the substrate. After cleaning, the slides were placed in the centre of the spin coater ensuring balance. A layer of photoresist (Microposit 1813, Shipley) was added with a pipette, covering the whole surface of the slide. It was then spin-coated at 400 rpm for 20 sec with an acceleration of 100 rpm/sec and then at 3000 rpm for 30 sec with an acceleration of 500 rpm/sec. The coated ITO wafer was placed in contact with a hot plate set at 115 ºC for 1 min to strengthen the photoresist.

Photomasks were designed using Protel 99 software and printed on polyacetate sheet externally (JD Photo Tools Services, Oldham, UK). A photomask with the design of the electrode in black was placed on the top of the photoresist and UV light (150 J for 5 sec) applied using a mask aligner (Tamarack 152R). The microelectrode wafer was then washed with a developer (Microposit MF26) which removes the UV-exposed photoresist layer leaving the mask-protected patterns. The microelectrode wafer was then washed with acid (fresh aqueous solution of HCl 5 M and HNO_3 1 M at 4:1 ratio v/v) which etched away the unprotected ITO, leaving behind the photoresist-protected areas. The photoresist was then removed with acetone. See Figure 6.1.
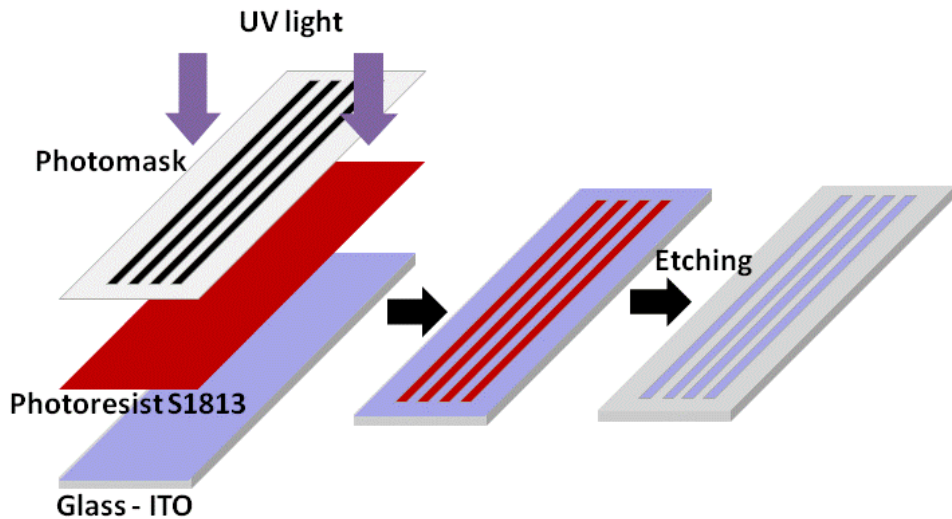
Figure 6.1 Protocol of fabrication of ITO microelectrodes.

Dielectric measurements

A Biomass monitor model 220, connected to a PC with Aberscan software version 2.2 (Aber Instruments, Aberystwyth, UK) was used for recording the dielectric frequency spectra. The microelectrodes were connected to the biomass monitor headamp using a PCB clip-on connector connected to an Amplikon 10 pin connector. See Figure 6.2. During the measurements, the microelectrodes were covered with black insulating tape. Unless specified otherwise, 1 cm of the microelectrodes were left exposed. The exposed area was immersed in the liquid and the height was then fixed for the rest of the experiments. High activity, pressed baker's yeast was obtained from DCL craftbake, and stored at 0-4 ºC for a maximum of 12 days. Malt extract was obtained from Oxoid Ltd. 500 ml of malt extract at 20 g/L was prepared with water. 100 g of pressed yeast was resuspended with malt extract to a final volume of 150 ml obtaining a thick suspension of 7×10^9 cells/ml. 15 ml of this concentrated yeast suspension was added to 500 ml malt extract medium every 2 min ten times. The freerun option was used for measuring the capacitance and conductivity of a cell suspension. The automatic electrode polarisation correction procedure was on throughout all the experiments. Every measurement was done three times. The results shown are averages.
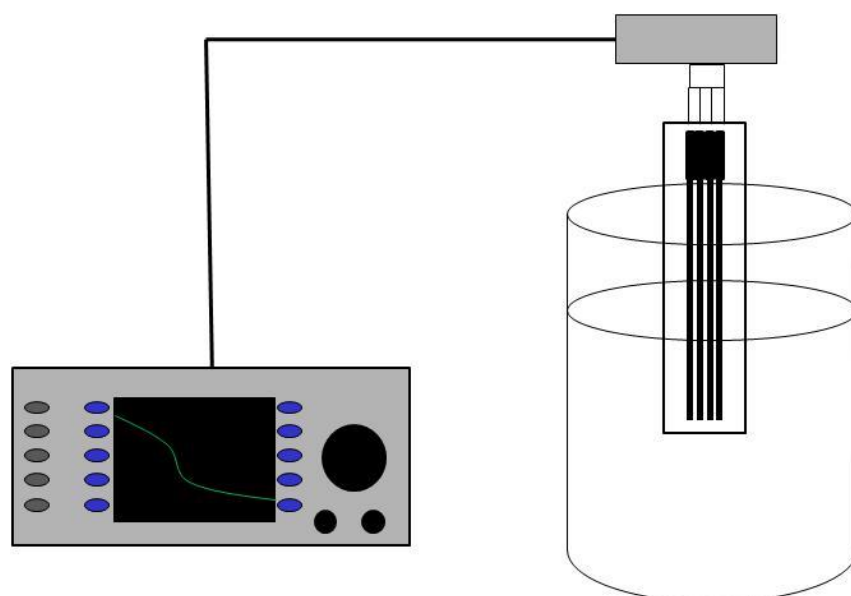
Figure 6.2 Experimental setup using ITO microelectrodes.

6.3 Results

Electrode design

Different microelectrode designs were tested. Interdigitated microelectrodes were fabricated from indium tin oxide (ITO) on glass with different widths of electrodes and distances in between the bars of the electrodes. An example is shown in Figure 6.3.
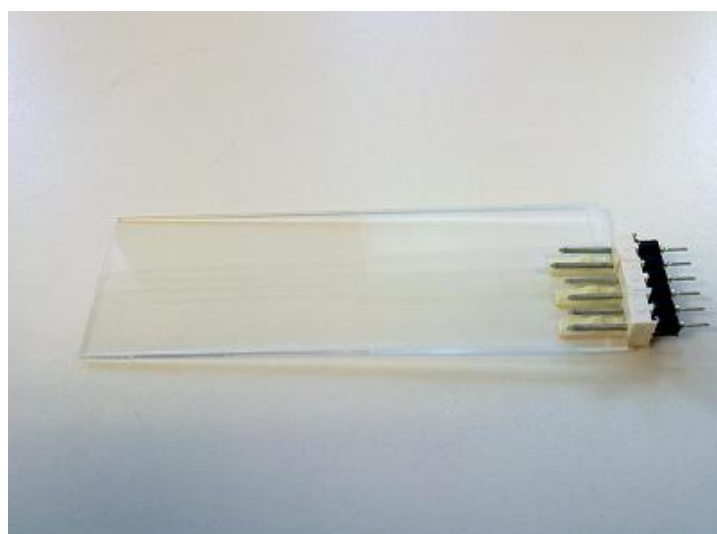
Figure 6.3 Microelectrode with connectors.
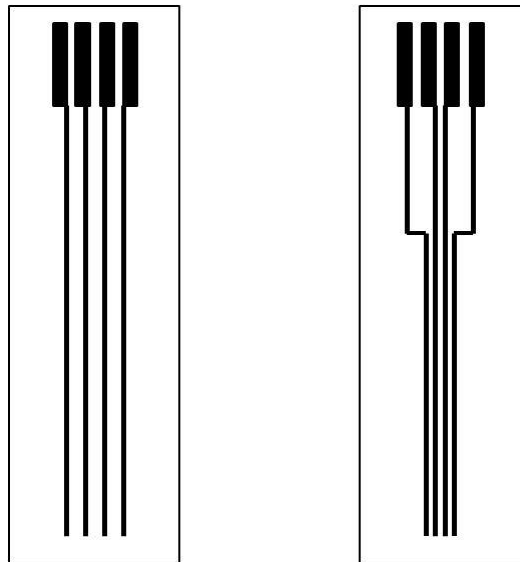
Figure 6.4 Typical microelectrode designs.

Figure 6.4 shows typical microelectrode designs. All designs had 4 interdigitated electrodes of the same width and the same distance in between bars. A total of 10 microelectrodes were fabricated as listed in Table 6.1.

Microelectrode number	Electrode width (mm)	Distance between bars (mm)
1	0.5	1.2
2	0.5	0.8
3	0.5	0.5
4	0.1	0.2
5	0.8	1
6	0.8	0.8
7	0.3	0.8
8	0.3	0.2
9	1.2	0.8
10	1.2	0.5

Table 6.1 Microelectrodes fabricated showing the correspondent electrode width and distance in between bars.

The permittivity as a function of the frequency is shown in Figure 6.5 for the different microelectrodes with 1 cm exposed to the liquid.
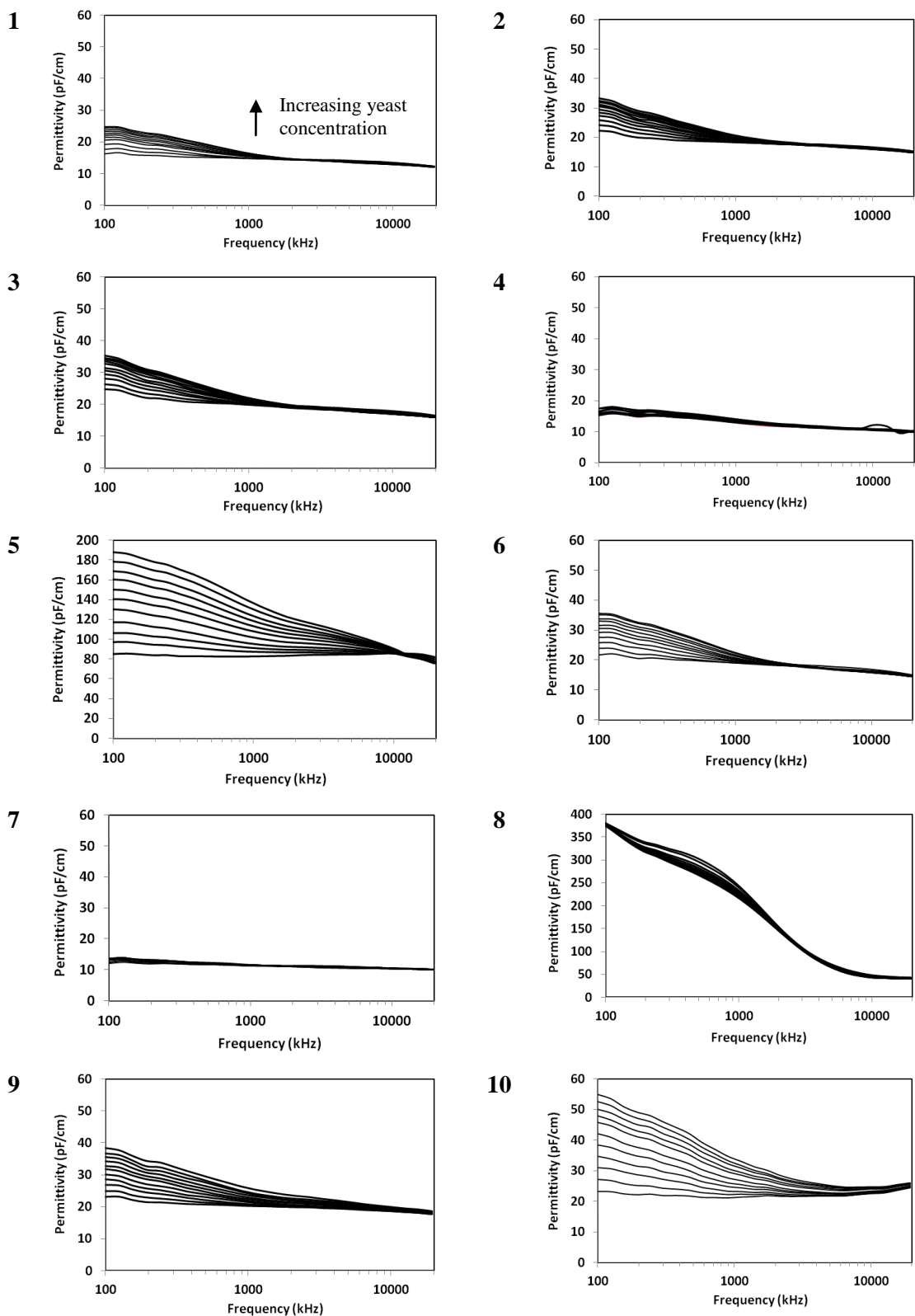
Figure 6.5 Permittivity as a function of frequency at increasing concentrations of yeast cells. 1 cm of the microelectrodes was exposed to the suspension.

Large differences can be observed in the shape of the frequency scan at different microelectrode sizes. Smaller electrode widths give smaller signals. Electrode polarisation is generally limited, though Microelectrode 8 showed very high baseline polarisation which may be due to electrode polarisation, with permittivity values close to the limit of the biomass monitor. Microelectrodes 5 and 10 appear to give the best response.

Figure 6.6 shows the permittivity as a function of yeast concentration for different microelectrodes.
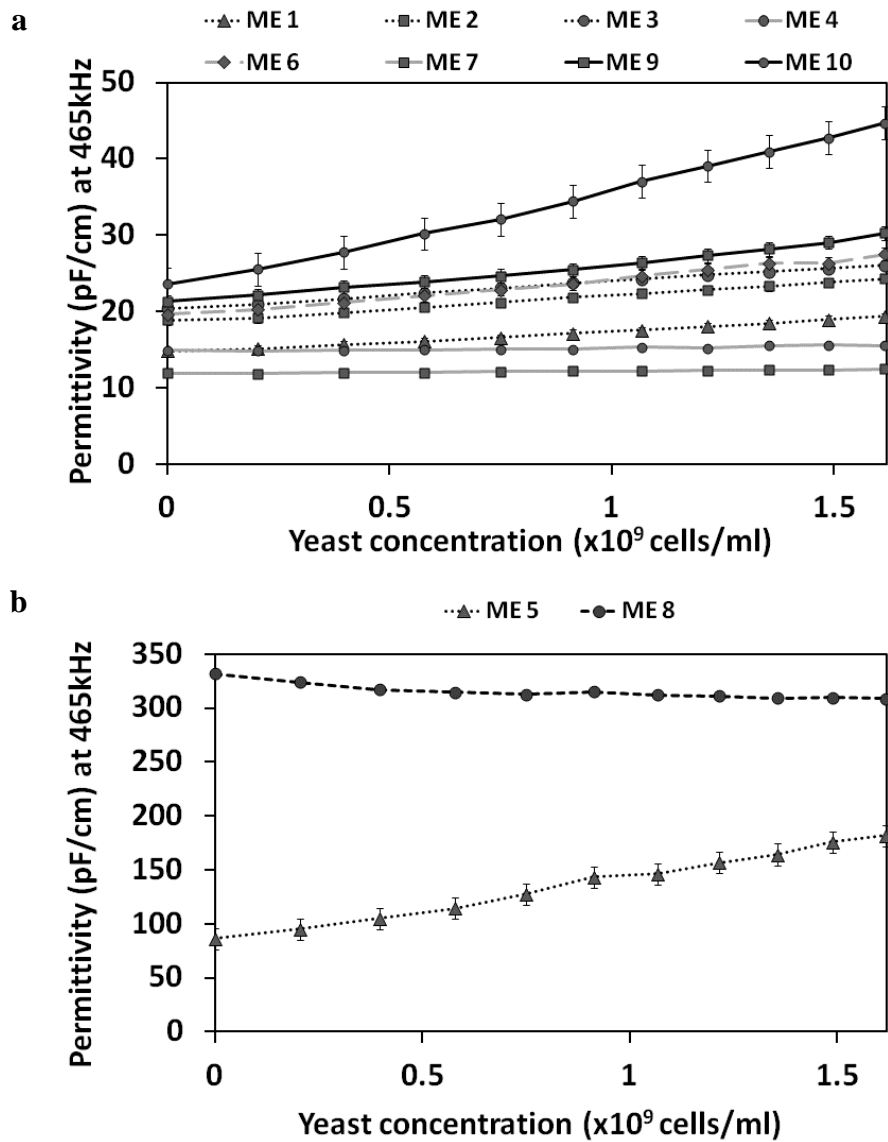
Figure 6.6 Permittivity as a function of the yeast concentration for a) 8 microelectrodes with different electrode bar widths and distances in between bars b) ME5 and ME8.

Surprisingly, ME8 shows a decline in the permittivity with increasing yeast concentration rather than an increase. This finding is commensurate with the notion that the high signal shown by ME8 is caused by electrode polarisation. The presence of yeast near the electrode surface may well lead to a local decrease in the current density, leading to a decrease in the electrode polarisation and hence overall permittivity signal.

Figure 6.7 shows data for the three microelectrodes with the same bar width (0.5 mm), but different distances between the electrode bars. It can be seen that the permittivity signal becomes larger when the distance in between the bars is smaller.
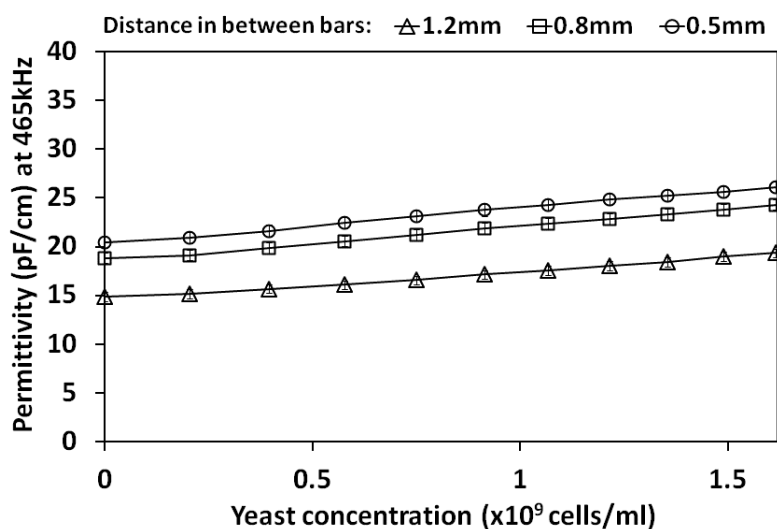
Figure 6.7 Permittivity as a function of yeast concentration for microelectrodes with 0.5 mm bar width and different distances in between bars.

Figure 6.8 shows the slopes of the three microelectrodes with the same bar widths but different distance in between the electrodes. It can be observed that the slope is higher when the distance in between the bars is smaller.
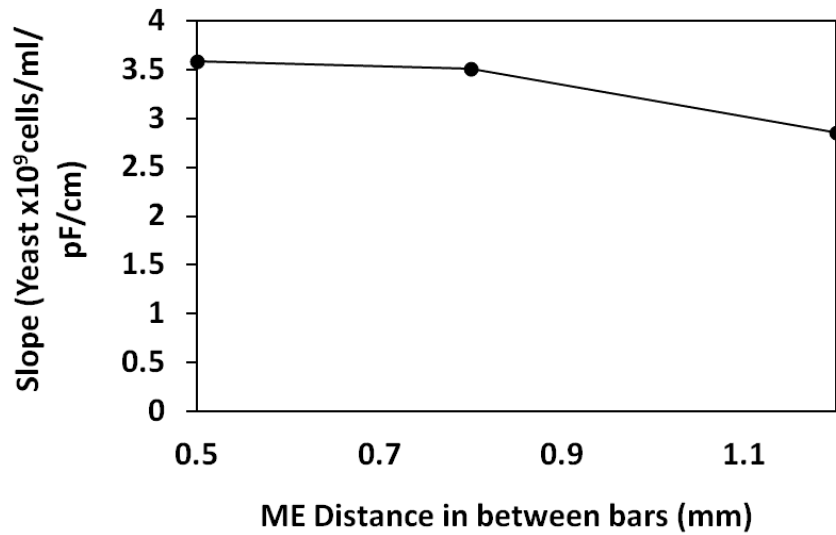
Figure 6.8 Slope (permittivity / yeast concentration) as a function of the distance between the microelectrodes for microelectrodes with a 0.5 mm bar width.

As shown in Figure 6.9 the same behaviour was observed for the microelectrodes with 1.2 mm bar width. However in contrast with the previous electrodes, the increase of the permittivity with cell concentration at these microelectrodes was higher.
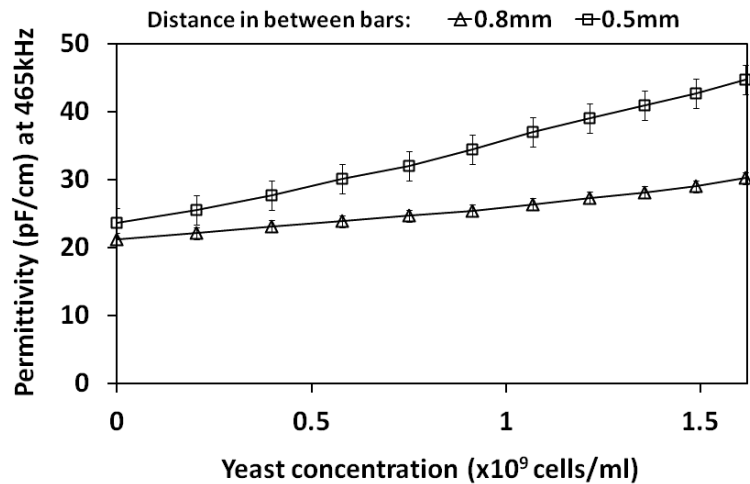
Figure 6.9 Permittivity as a function of yeast concentration for microelectrodes with a bar width of 1.2 mm bar and different gaps in between bars.

When different microelectrodes with the same distance in between the electrodes but different bar widths are compared it is observed that the microelectrodes with the wider bars give higher capacitance readings. This can be seen in Figure 6.10.
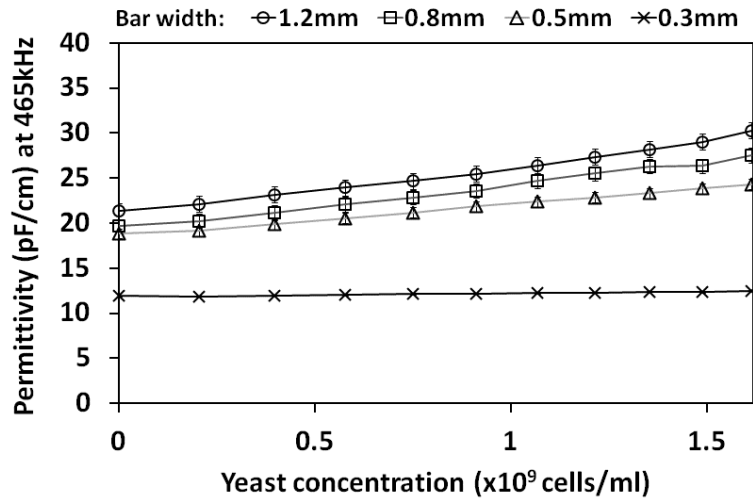
Figure 6.10 Permittivity as a function of yeast concentration for microelectrodes with 0.8 mm distance in between bars and different bar widths.

In Figure 6.11 it can be seen that when microelectrodes with 0.8 mm of distance in between bars and different bar widths are compared, the microelectrodes with the wider bars give higher slopes.
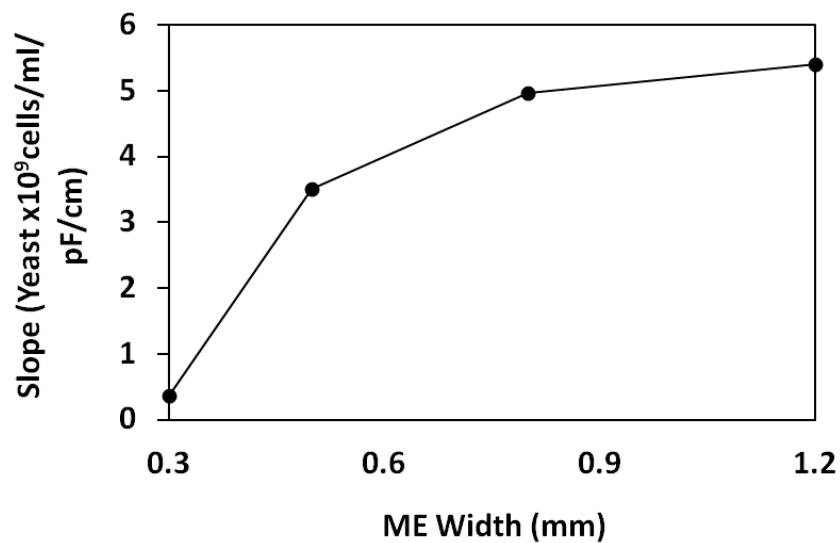
Figure 6.11 Slope (permittivity / yeast concentration) as a function of microelectrode bar width for a microelectrode with 0.8 mm distance in between bars.

Influence of the area exposed for measuring the dielectric properties of cells

In the next set of experiments, microelectrode number 5 (ME5), with a width of 0.8 mm and a gap of 1.0 mm, was used. Every measurement was done three times and the results shown are averages. To investigate the effect of the length of the microelectrode slides with microelectrode design ME5 were covered with insulating tape, but different areas were exposed by leaving 5, 4, 3, 2, 1, 0.5 and 0 cm from the end uncovered (see Figure 6.12). Initially only the exposed area was immersed into the suspension. However, as yeast was added, the liquid volume increased, and the liquid also started to cover the tape.
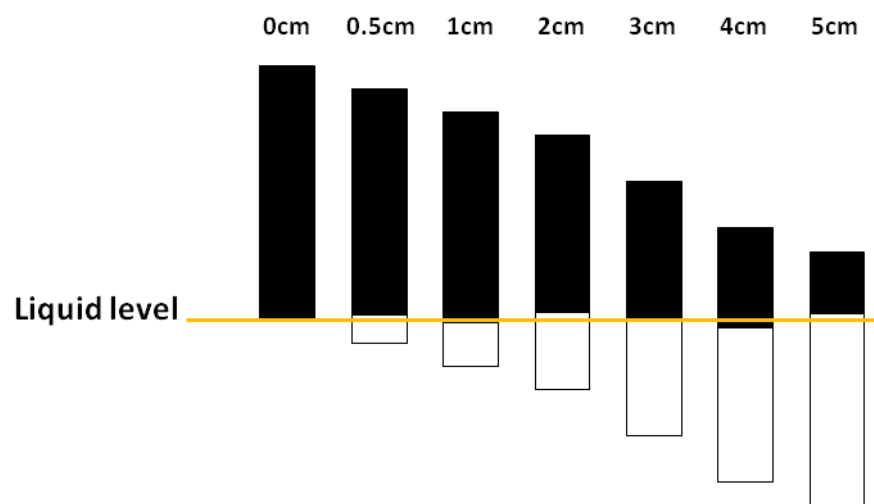
Figure 6.12 Diagram showing how the area of the microelectrodes was initially exposed to the liquid.

Figure 6.13a shows the permittivity at 465 kHz for different yeast concentrations. The slopes of the lines are shown in Figure 6.13b. It can be observed that when the area of the microelectrode exposed is increased the permittivity rises. When the microelectrodes were totally covered with black tape small changes in the permittivity values could still be observed as the yeast suspension was added. This indicates that changes in the capacitance (and volume as the amount of liquid in the beaker increased as yeast was added) can be detected across the black tape. It also can be observed that exposure of larger areas corresponds to higher slope values. However, it is not a linear relation.
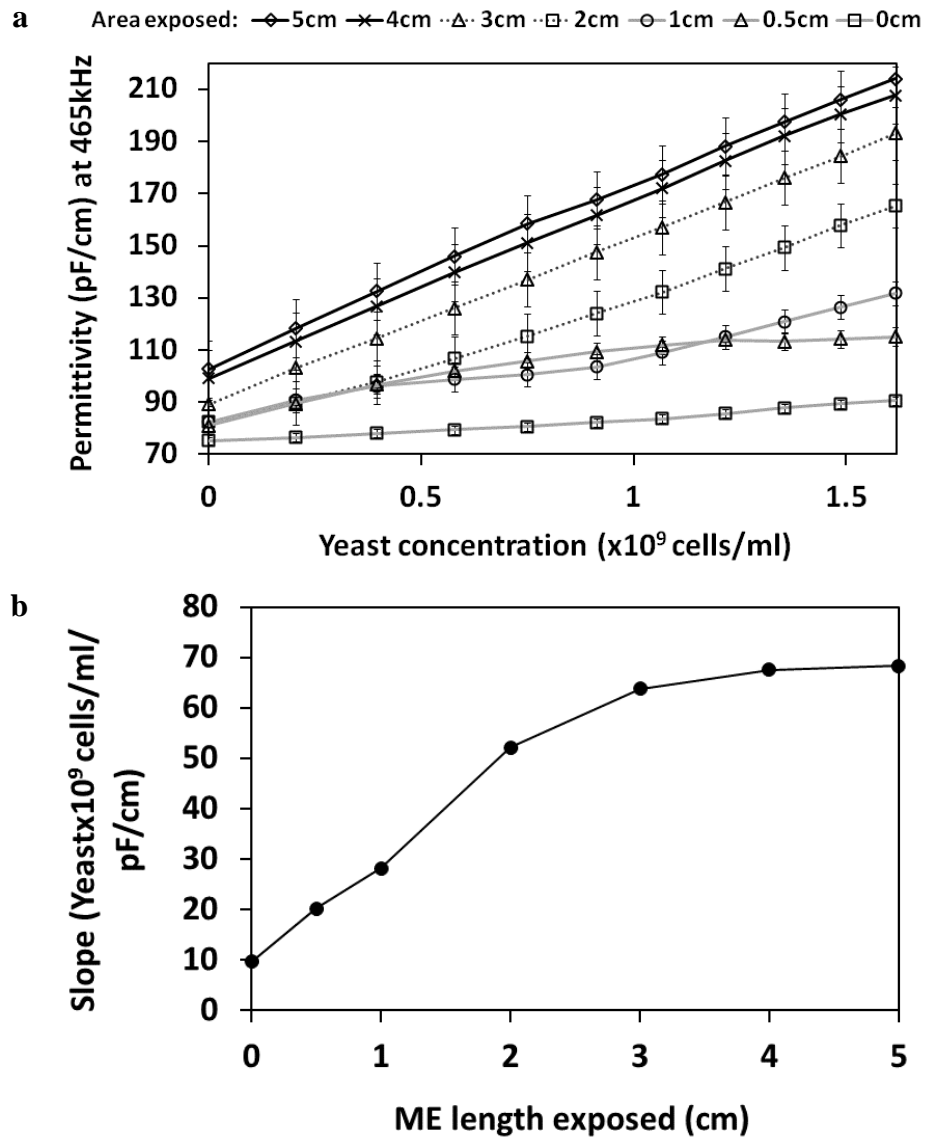
Figure 6.13 ME5 with different areas exposed to the yeast suspension according to the method shown in Figure 6.12. a) Permittivity as a function of yeast concentration; b) Slope (permittivity / yeast concentration) as a function of the length of electrode that was exposed.

When a small area was exposed (0.5-1.0 cm) permittivity readings were sometimes unstable and could jump within experiments between higher to lower values as shown in Figure 6.14. This did not happen when larger areas were exposed.
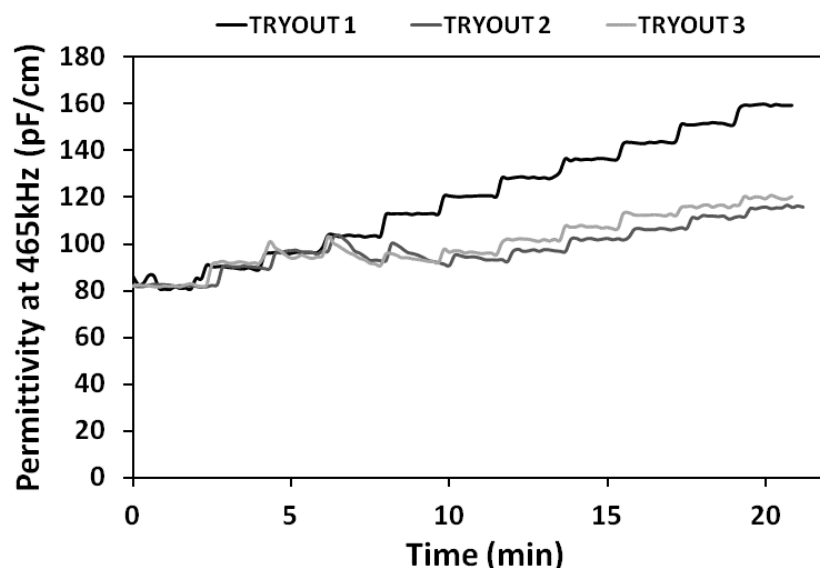
Figure 6.14 Comparison of three tryouts with ME5. 1cm of the microelectrode was exposed according to the method shown in Figure 6.12.

6.4 Discussion and Conclusions

The results show that it is entirely feasible to use microelectrodes made using photolithography from ITO to measure biomass levels using dielectric spectroscopy. Many of the smaller electrodes generally gave quite small signals, but large signals could still be obtained with some of the microelectrodes.

Biomass measurements with microelectrodes of different designs clearly indicate in what direction optimisation of the electrode size should go. The wider the microelectrode bars were, the higher the capacitance values and slopes; for microelectrodes with the same width, the closer the bars, the higher the signal. This correlates well with theory (Schwan, 1957; Olthuis *et al.*, 1995), as the capacitance signal is inversely proportional to the cell constant *d/A*. For parallel plates *d* is the distance between the electrodes, and *A* the area of the electrodes. More complex relations would be expected for other geometries. Despite this, both theory and experiments indicate that a sensible approach would be to make the distance between electrodes small, but the width (and length) of the electrodes large to increase the measured capacitance signal. Large electrode widths would also be beneficial for

electrode polarisation effects. The use of larger electrode areas would lead to smaller current densities, and hence smaller levels of electrode polarisation.

Finally, the extent to which the electric field penetrates into the surroundings can be expected to decrease as the gap between the electrodes becomes smaller. An electric field that reaches far into a fermenter is more likely to be disturbed by the proximity of other items such as walls, baffles and stirrers. For this reason also the gap between electrodes needs to be kept small as a system with a smaller gap between electrodes is likely to suffer less from interference. Too small gap, however, may possible lead to irreproducibility as minor events in the gap could have large effects on the signal. Some optimisation is therefore still needed.

CHAPTER 7

DEVELOPMENT OF A MICROFABRICATED REFERENCE ELECTRODE FOR THE SEPARATE MEASUREMENT OF THE DIELECTRIC PROPERTIES OF SUSPENDED CELLS AND MEDIUM

ABSTRACT

To measure the electrical properties of cells during fermentation more accurately it was attempted to measure the electrical properties of the suspending medium without a contribution by the cells by selectively preventing cells but not medium to reach an electrode surface. The use of microelectrodes with small distances between the electrodes would confine the electric field to the area within the gel or behind a membrane. Microelectrodes were made from indium tin oxide (ITO) on glass with different electrode widths and distances between the electrodes, and dielectric spectra in a frequency range 100 kHz to 24 MHz were measured using the Aber Instruments Biomass Monitor. It was shown that both agar gels and membranes could effectively keep cells away from the electrode surface, and that the measurement of medium electrical properties with cell interference was possible. However, the minimum response time of both systems to step changes in the conductivity was in the order of 3 hours, which is too slow for most practical applications.

7.1 Introduction

To provide for the ever increasing demands for more information during production processes based on fermentation new technologies are constantly needed to monitor changes in cell properties as well as those of the suspending medium. Understanding the interaction between biomass and their environment is of fundamental importance to gain insight into how cellular systems respond to changes in the medium (Richter *et al*., 2007; Bryant *et al*., 2011).

Some of the best techniques for studying fermentations are based on impedance measurements. Impedance measurements involve the exposure of a material to electric fields. From the relation between voltage and current the electrical properties of the material can be determined. Of particular interest has been the measurement of the electrical properties of cell suspensions in the radiofrequencies range as a linear relationship exists between the low-frequency dielectric increment and the cell concentration (Schwan, 1957). This has allowed impedance technology to be developed into a useful technology for measuring biomass levels (Kell *et al.*, 1990; Markx and Davey, 1999; Asami, 2002; Carvell *et al.*, 2006). The main advantage of this technique is that it enables online monitoring and there is no need to label or use any form of pre-treatment of the cells for the measurement. However, a major disadvantage of this technique is that polarisation of the electrode can distort the low frequency signal (Asami, 2002; Krommenhoek *et al.*, 2006). This amount of electrode polarisation is dependent on the properties and composition of the medium, in particular the conductivity (see also chapter 5). It therefore would be beneficial to measure the electrical properties of the medium separate of that of the suspension.

The aim of the work described in this chapter is the development of an impedance reference probe which is insensitive to biomass. The insensitivity will be achieved by concentrating the electric field to an area near the electrode surface, and at the same time preventing cells but not medium from approaching the electrode surface using gels or membranes. The reference sensor will allow one to measure changes in the medium composition and electrode polarisation separate from that of the suspension. In addition, by comparing the signal at the reference probe with that of a standard probe which measures directly in the suspension improved estimates can be obtained of biomass levels. Miniature planar interdigitated electrodes can be expected to be particularly well suited for the construction of the reference probe. Micro-electrode technology has previously proven useful in monitoring impedance changes of biological samples (Krommenhoek *et al.*, 2006; Ertl and Heer, 2009). Impedance microelectrodes are commonly used as medical biosensors (Morin *et al.*, 2005; Marrakchi *et al.*, 2007; Laczka *et al.*, 2009; Colella *et al.*, 2012) and for the evaluation of microbial growth (Rodrigues *et al.*, 2004; Krommenhoek *et al.*, 2006; Richter *et al.*, 2007; Gottschamel *et al.*, 2009), among others. Among the advantages of microelectrodes we can mention that they are not only inexpensive to manufacture but their design is also simple,

making it possible to use analytical and mathematical techniques to optimise their design (Olthuis *et al*., 1995; Ertl and Heer, 2009; Jungreuthmayer *et al*., 2012).

7.2 Materials and Methods

Development of a reference electrode

Agar was obtained from Sigma (A7002) and prepared at 10 g/L in deionised water. It was either simply poured onto the microelectrode surface to different thicknesses, or poured into a preassembled chamber to a defined height. Membranes were glued onto chambers covering the microelectrode surface. The membranes tested were: Whatman Cyclopore Track Etched membrane 7060-4702 0.2μm; Millipore Durapore PVDF GVWP09050 0.22μm; Millipore Express Polyethersulfone HPWP04700 0.45μm; Millipore Durapore PVDF DVPP04700 0.65μm; Dialysis Membrane Medicell International Ltd MWCO-12-14000Da. In all the experiments the electrical properties of pure malt extract medium (20 g/L) was measured first, and then 0.2 g of NaCl was added. Measurements were taken until the readings were stable. In some experiments it was attempted to improve diffusion by using acoustic streaming; this was done by applying ultrasound by applying a 1 MHz 10 V_{pk-pk} signal to a 2 mm thick PZT piezoelectric ultrasound transducer using a TG120 Function Generator (Thurlby Thandar Instruments). Same microelectrodes and dielectric measurement techniques showed in Chapter 6 were used (See Materials and Methods and Table 6.1). See Figure 7.1.

Figure 7.1 Microelectrode showing the connections to an Amplikon 10 pin connector.

7.3 Results

Modelling of the electric field distribution around the microelectrodes

The choice of microelectrodes was guided by the expectation that the electric field would extend less or further away from the electrode surfaces with different electrode designs. The extent to which the electric field distribution extended was determined by simulation of the electric field distribution using the finite element software COMSOL FEMLAB. In Figure 7.2 all the parameters can be seen that were used to simulate the microelectrodes. The size parameters were changed according to the design of the individual electrode but the electric potential remained the same.
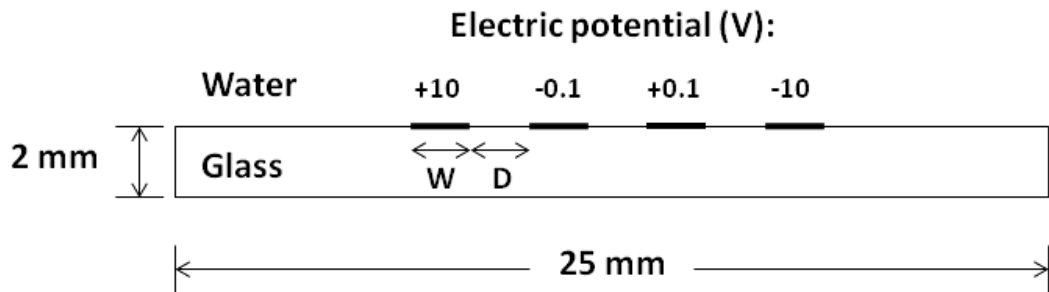
Figure 7.2 Parameters used to simulate the electric field with software COMSOL FEMLAB. The distance between the electrodes (*D*) and the width of the electrode (*W*) were different for all the electrode designs.

Figure 7.3 shows the calculated distribution of the electric field around the microlectrodes.
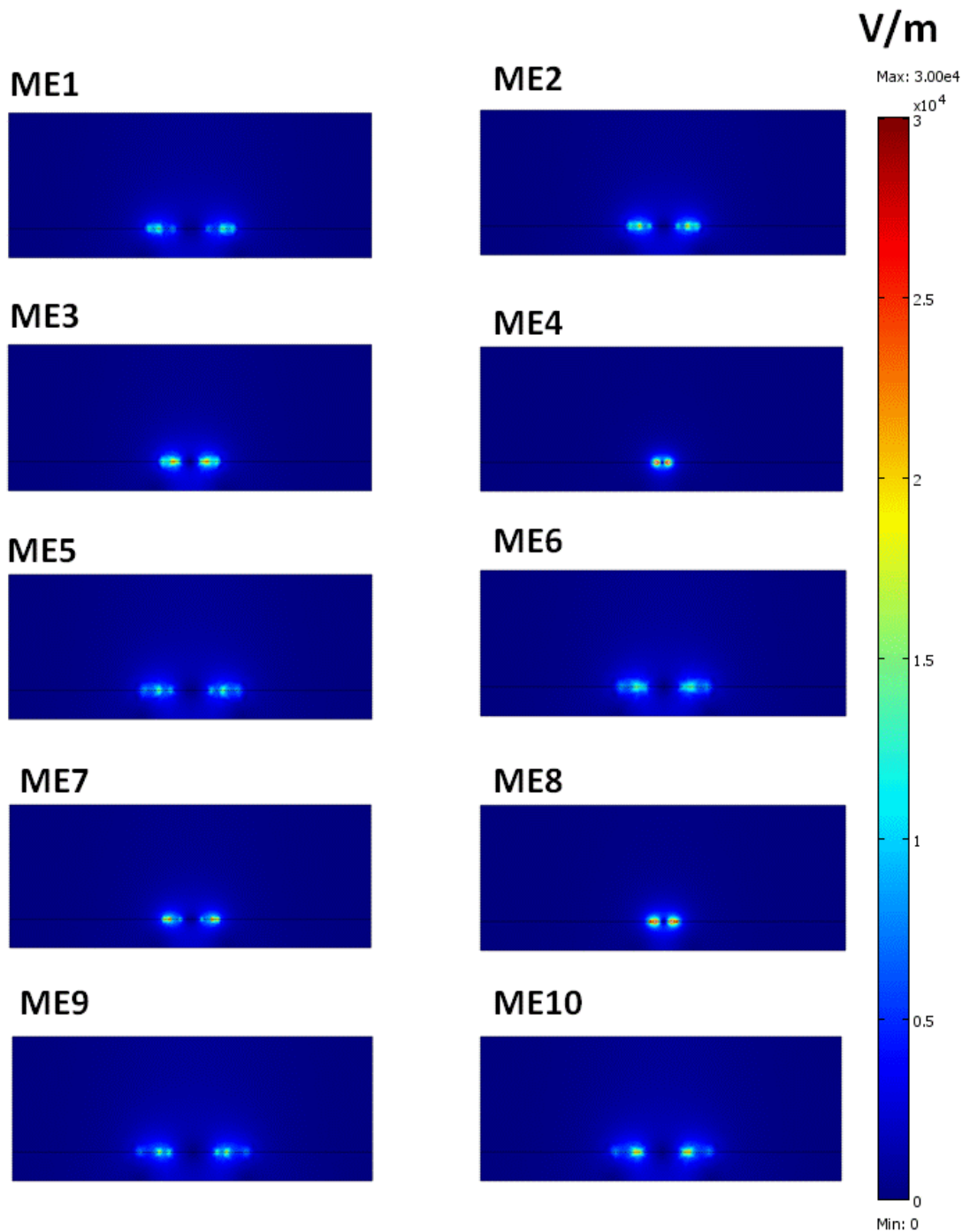
Figure 7.3 Electric field distributions around microelectrodes, simulated using modelling software COMSOL FEMLAB.

As can be seen in Figure 7.3, the electric field distribution is different for all the microelectrodes. For microelectrodes with the same bar width, the electric field is stronger when the distance in between bars is smaller. For electrodes with wider bars

the electric field is more extended but weaker. For electrodes with slimmer bars the electric field is stronger but confined to a smaller area.

ME10 (1.2 mm width/0.5 mm distance in between) and ME7 (0.3 mm width/0.8 mm distance in between) were selected for the next set of experiments based on the level of response when measuring permittivity signalling (see Figure 6.5 Chapter 6). ME10 has wider bars and therefore the electric field extends beyond 3 mm. For ME7 the field is confined within 3 mm.
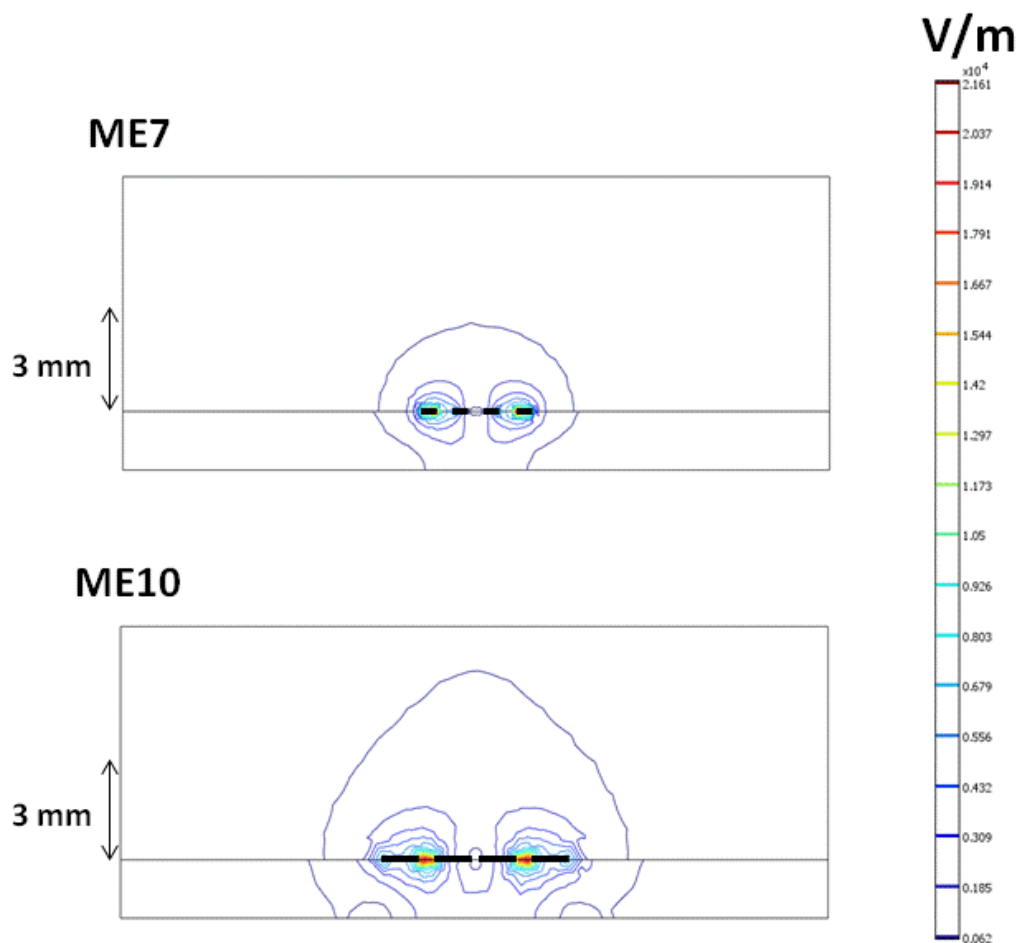
Figure 7.4 Cross section of ME7 and ME10 showing the strength and extension of the electric field into the medium.

Microelectrodes covered with agar

Microelectrodes were covered with insulating black tape, leaving 3 cm of the measurement area exposed to the medium. The electrode surface that was exposed was

covered with agar gel with different thicknesses (Figure 7.5). It was expected that the gel would keep cells from the electrode surface, but that ions would still be able to diffuse through the gel.
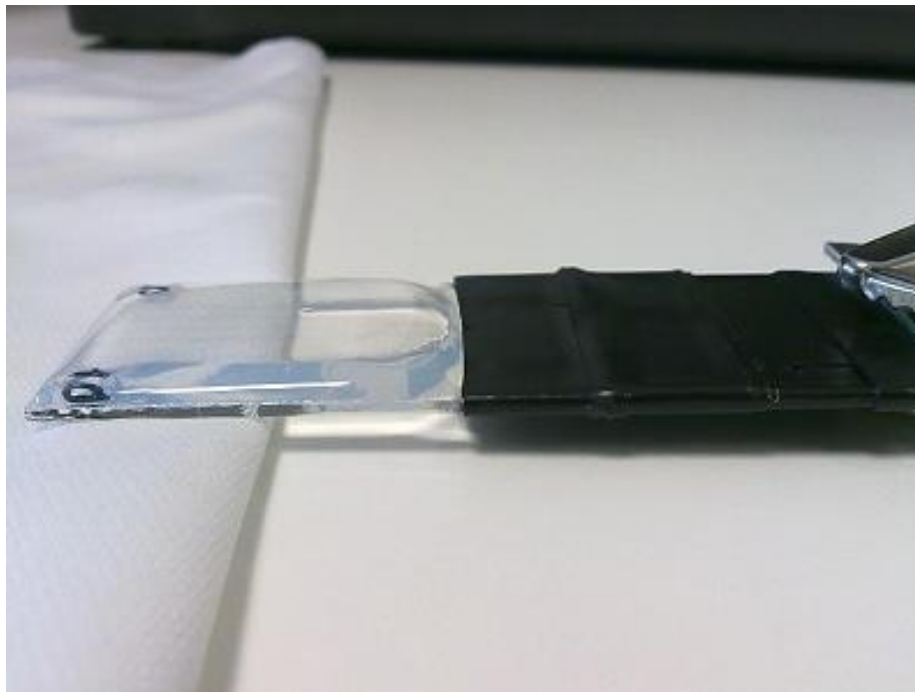
Figure 7.5 Microelectrode with agar layer.

Yeast was added in increasing concentrations, and the permittivity measured. The results, for different thicknesses of agar, are shown in Figure 7.6. The slopes of both ME7 and ME10 can be seen in Figure 7.7. As it was expected, according to Figure 7.4, the data shown indicate that ME7 stops detecting the presence of cells with a 2 mm thick agar layer, meanwhile ME10 still senses the cells with 3 mm of agar.
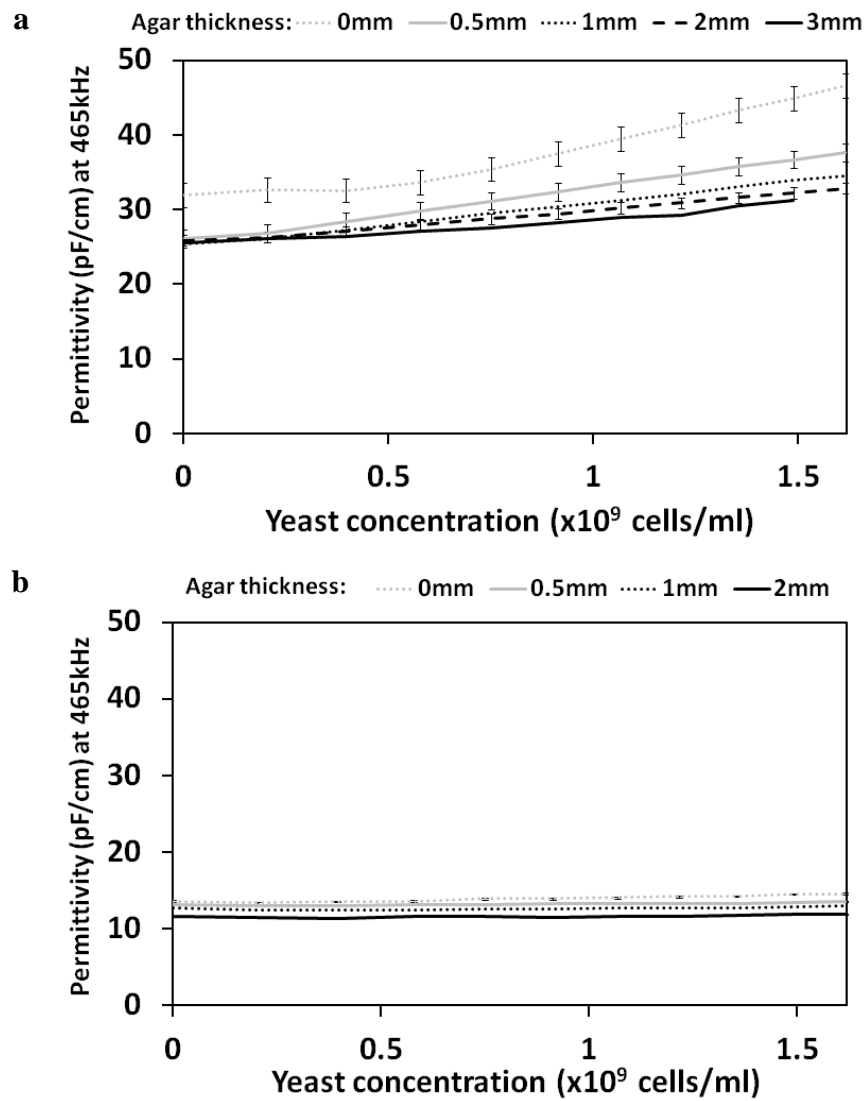
Figure 7.6 Permittivity as function of yeast concentration for microelectrodes with different agar layer thicknesses. a) ME10 (1.2 mm electrode width/0.5 mm distance in between electrodes); b) ME7 (0.3 mm electrode width/0.8 mm distance in between electrodes).
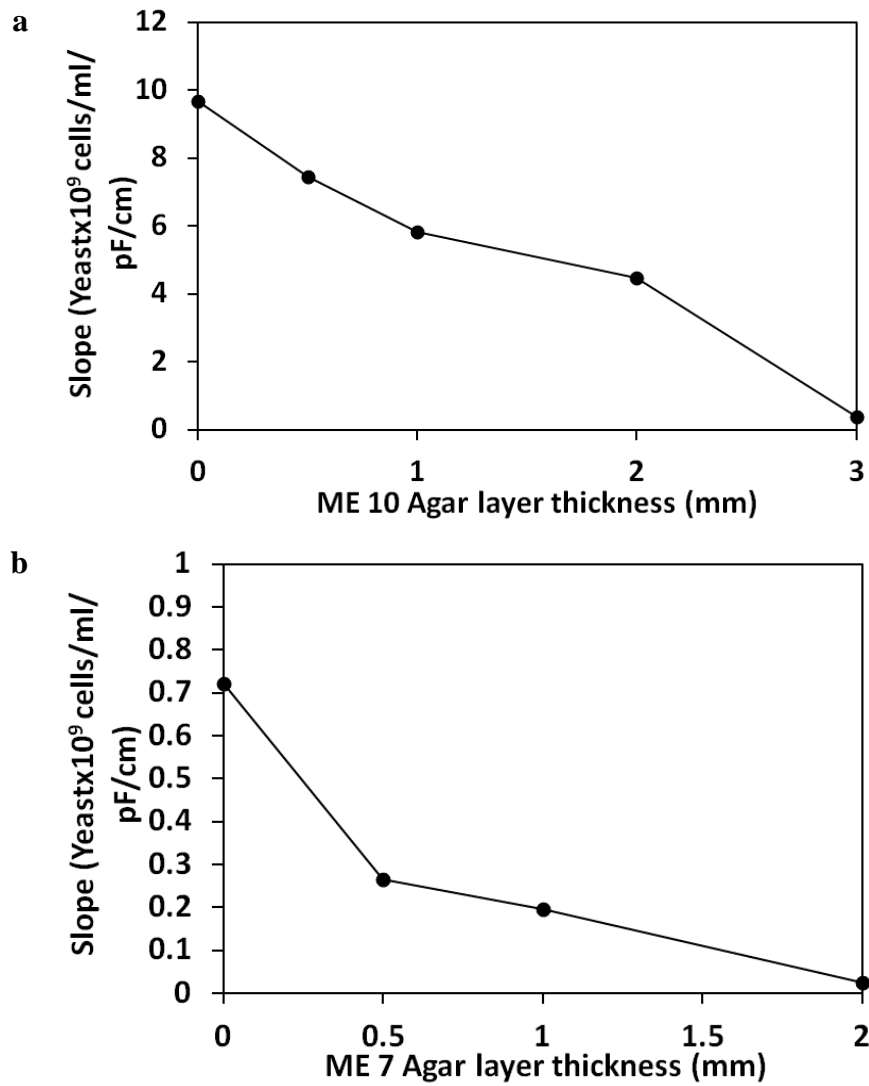
Figure 7.7 Slope of permittivity as a function of yeast concentration as a function of the agar layer thickness for a) ME10 and b) ME7.

The next step was to measure changes in the electrical properties of the medium. This was achieved by adding NaCl to the malt extract to change the conductivity. During initial experiments it was found that, when changing the medium conductivity, the agar layer often readily came off. An improved chamber was therefore created which a chamber with a plastic mesh to prevent the agar layer from coming off, this can be seen in Figure 7.8. ME1 (0.5 mm electrode distance, 1.2 mm bar width) was used in this experiment.
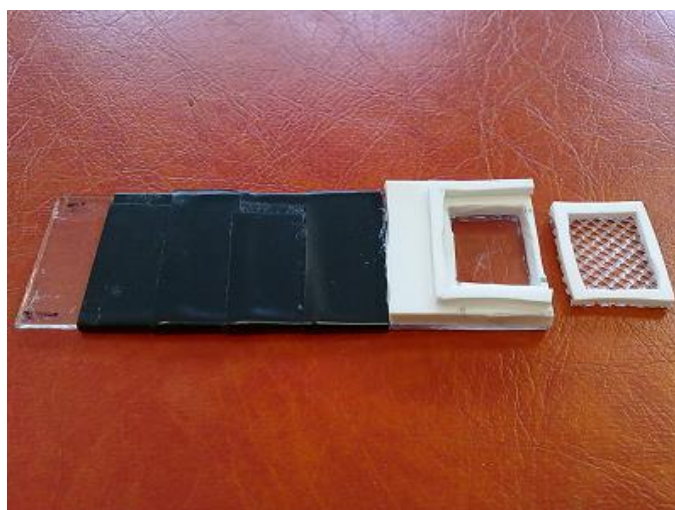
Figure 7.8 Microelectrode with Teflon chamber with mesh to prevent agar layer to come off.

The chamber was filled with a 3 mm agar layer and covered with the plastic mesh. An agar thickness of 3 mm was selected based on previous results (Figure 7.7) that showed that with an agar layer of 3 mm as thickness the presence of cells in the suspending medium cells was barely sensed or not sensed at all. First the conductivity of 500 ml malt extract solution (20 g/L) was measured for 1 h, and then 0.2 g of NaCl was added. The experiments were repeated without an agar layer. The results of these experiments can be seen in Figure 7.9.
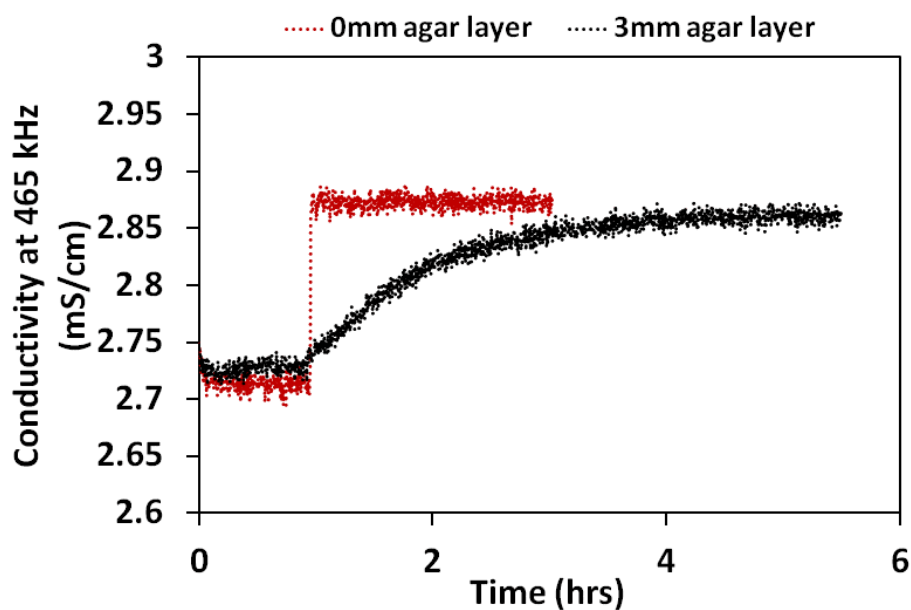
Figure 7.9 Conductivity as function of time for microelectrode number ME1 with and without agar layer.

It can be observed that when NaCl was added the conductivity went up immediately when no agar was present, but in the presence of 3 mm of agar layer it took over 3 hours for the conductivity signal to stabilise. This can be expected to be too long for practical purposes. Further analysis with different agar concentrations should be done.

Microelectrodes covered with a membrane

Another set of experiments was done using different membranes to prevent the cells from coming near to the microelectrode surface. Many different designs of chambers were made and tested. The most useful and practical design was found to be a polycarbonate chamber into which a glass slide with microelectrodes could be inserted, as can be seen in Figure 7.10. The chamber had an orifice where the electrode surface was exposed. The membrane was glued to this area with silicon rubber. An alternative design was also made in which an ultrasound transducer was connected to the outside of the polycarbonate chamber, as shown in Figure 7.10a. It was expected that the fluid flow induced by the ultrasound would induce mixing of the fluid inside the chamber, speeding up the transfer of ions from the membrane surface to the electrode surface.
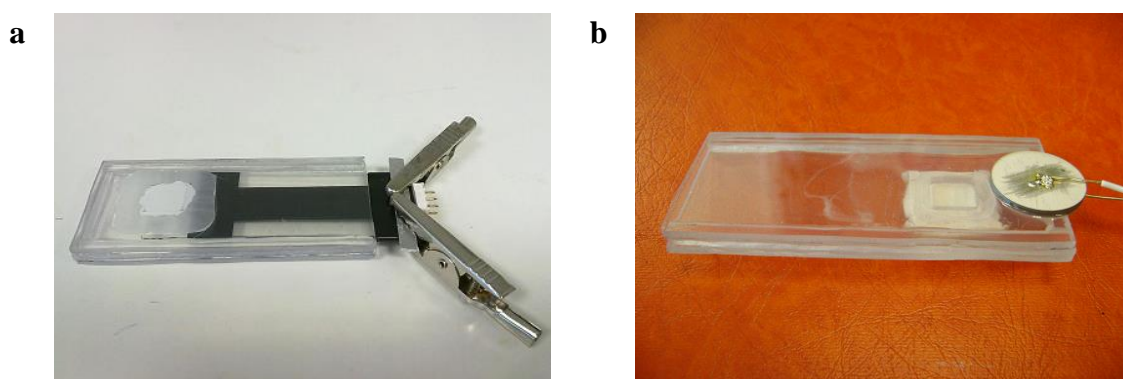
Figure 7.10 Chamber with membrane a) standard chamber without ultrasound and b) chamber with ultrasound.

The first set of experiments was done as control experiments, using an electrode of design ME9. Conductivity measurements were taken in malt extract (20 g/L) for 30 min with just a microelectrode. Following this, 0.2 g of NaCl was added and measurements were continued for 1 hour. The next control experiment was done with the

microelectrode inserted into a polycarbonate chamber without any membrane. No ultrasound was used. After 30 minutes of taking readings of the malt extract, 0.2 g of NaCl was added, and measurements taken for a further hour. In the last experiment measurements were first taken with the microelectrode in a chamber without a membrane for half an hour (no ultrasound). The ultrasound was then put on and measurements taken for another 30 minutes. Then 0.2 g of NaCl was added and the conductivity measured for 1 hour. The results can be seen in Figure 7.11.
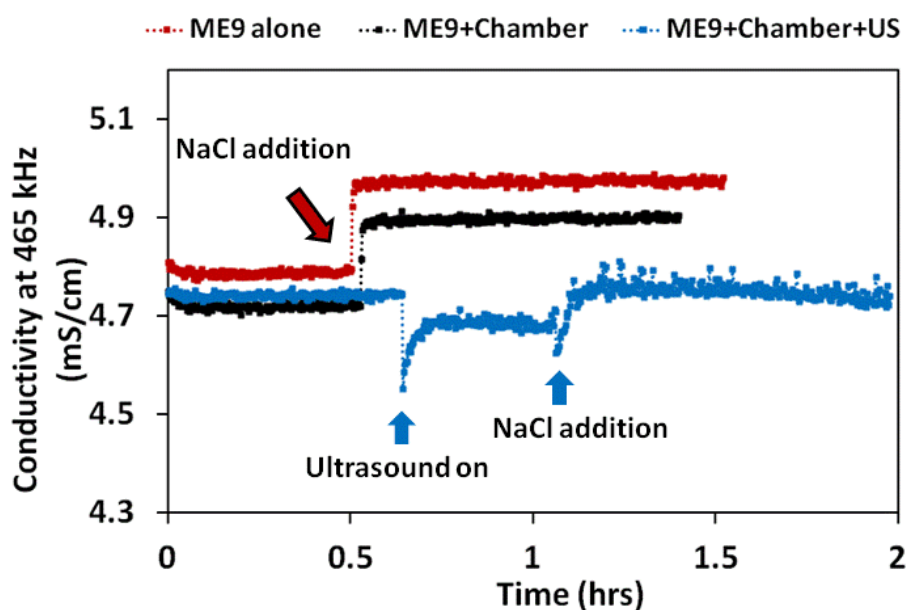
Figure 7.11 Conductivity as function of time for microelectrode ME9 on its own, ME9 inserted into the polycarbonate chamber without ultrasound, and ME9 inserted into a polycarbonate chamber with an ultrasound transducer. No membranes were used in these experiments.

The results indicate that the presence of a chamber reduced the conductivity, but does not affect the overall response to changes in the conductivity. The results also indicate that subjecting the setup to ultrasound at first leads to a change in the measured conductivity, but that the signal eventually stabilises. Addition of NaCl is readily detected, even in the presence of ultrasound.

In the next set of experiments different membranes were tested. The membranes were glued to the polycarbonate chamber, pure malt extract medium was added inside the chamber, and the chamber with the microelectrode and the membrane placed inside

malt extract. After 1 hour the conductivity of the medium 0.2 g of NaCl was added and the conductivity followed for 2 days. The results can be seen in Figure 7.12.
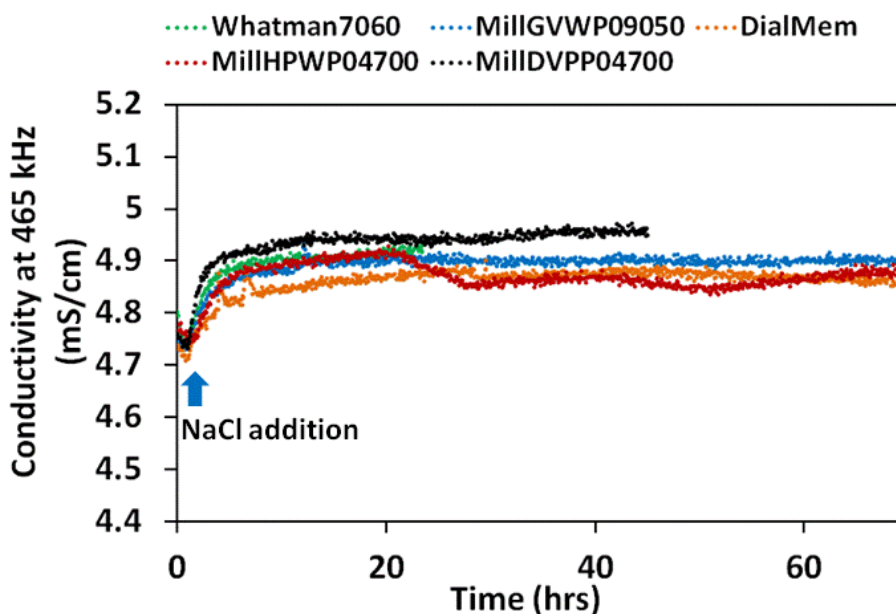
Figure 7.12 Conductivity as a function of time for microelectrode number ME9 and polycarbonate chamber with membrane. 0.2 g of NaCl added and the conductivity measured over 2 days. Different membranes were used to separate cells and medium. No ultrasound was applied.

The results show that when a membrane is used to keep cells from the electrode surface and no ultrasound is applied the time for the microelectrode to sense the changes in the media and reach stabilization is around 10 hours. This is much too long for practical purposes.

In the next set of experiments the conductivity of malt extract was measured for 30 minutes, then the ultrasound was put on and the conductivity of the malt extract measured for another 30 minutes, and then finally 0.2 g of NaCl was added. Results are shown in Figure 7.13.
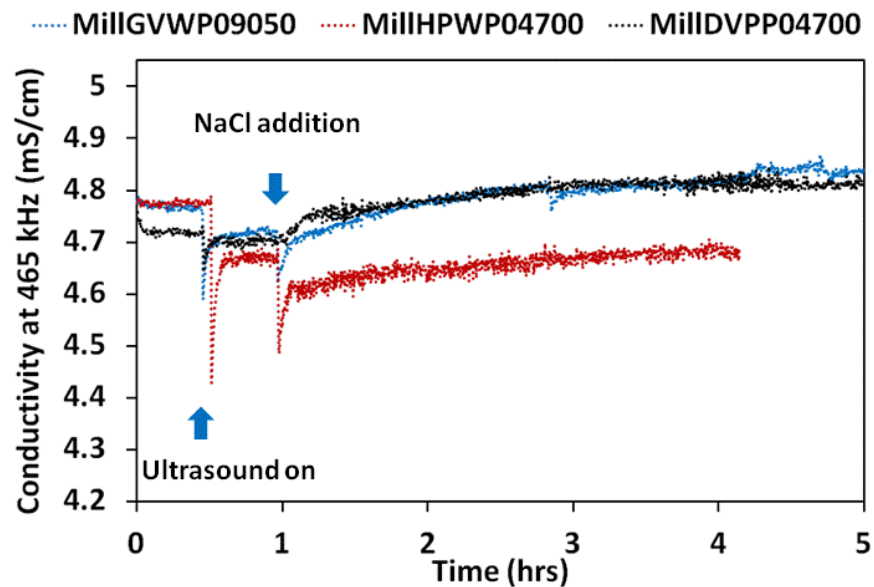
Figure 7.13 Conductivity as function of time for microelectrode number ME9. Different membranes were used to separate cells and medium. Ultrasound was applied.

It can be seen that when a membrane was used to separate cells and medium, and ultrasound was applied, it took 3 to 4 hours for the signal to stabilise after a change in the medium composition. This is less than without ultrasound but comparable with the response time of a gel-based system. In addition, the use of ultrasound causes noise in the signal as well as shifts in the conductivity value. This makes the use of membranes to separate cells from medium at an electrode surface less promising than gel-based systems.

7.4 Conclusions

The experiments have shown that it is possible confine the electric field emanating from a set of electrodes to an area close the electrode surface by decreasing the gap between the electrodes. The experiments have also shown it is possible to use gels and membranes to prevent cells from moving to the area near the electrode surface whilst still allowing medium to pass. This allows the measurement of the dielectric properties (capacitance and conductance) of the suspending medium separate from that of the cell suspension. The presence of a gel or membrane on the electrode surface however does significantly increase the response time of the system. A gel-based system appears to be

better than a membrane-based system as the response time was faster; indicating the flux through the gel is larger than through the membranes. Further optimisation of gel properties (in terms of sterilisability, mechanical strength and permeability) and microelectrode design and gel layer thickness is still needed.

CHAPTER 8

COMPARISON BETWEEN DIELECTRIC AND OPTICAL BIOMASS MONITORING TECHNIQUES

ABSTRACT

A comparison was made between the model 220 Biomass Monitor from Aber Instruments Ltd, which measures biomass levels using dielectric spectroscopy, and the new BE2100 "BugEye" biomass monitor from BugLab Inc which measures biomass optically. The biomass monitors were tested with various different cell types including bacteria (*Micrococcus luteus*) microalgae (*Nannochloropsis oculata, Chlorella vulgaris*) and yeast (*Saccharomyces cerevisiae*). Also, the effect of various interferents (salt, dyes, non-cellular particles, agitation, and temperature) was assessed.

8.1 Introduction

Biomass is one of the most important parameters during fermentation (Soley *et al*., 2005; Krommenhoek *et al*., 2006), but also one of the most difficult to measure (Maskow *et al*., 2008). Conventional off-line methods for measuring biomass, such as cell wet or dry weight measurements are basically manual, time consuming, requiring large sample volumes for accuracy, with a complicated operation and carry a large risk of sample contamination. Also at laboratory scale, the removal of samples could produce the disturbance of steady state conditions when for example the volume changes when samples are taken. To overcome these problems various technologies have been developed which can be used for monitoring of cell concentration on-line and often in real-time. These on-line technologies can be classified as indirect and direct.

Indirect techniques involve the measurement of metabolic activities of the cells such as oxygen uptake, carbon dioxide production, changes in the media and production of metabolites among others and correlating these measurements with biomass levels. These methods are challenging because one needs to know exactly which activities are

due to the cell activity and at what levels, otherwise the results will be far from reliable. Direct techniques measure biomass levels – as the names implies- directly, usually on the basis of a physical phenomenon. Most of the direct measurement techniques are real time. Among the technologies used to measure the biomass concentration directly are optical techniques, acoustic resonance, nuclear magnetic resonance (NMR) spectroscopy, flow cytometry (FCM), fluorescence, real-time imaging, densitometry, particle size analysis and dielectric spectroscopy (Bellon-Maurel *et al*., 2003; Ferreira *et al*., 2005; Sandnes *et al*., 2006).

It is generally expected that on-line sensors should be highly reliable under a wide range of industrial and laboratory applications and fulfil all the requirements in terms of cost, sterilisability and ease of use. A low contamination risk should be associated with their use, and it is generally expected that they are easy to interface and that they are supplied with user-friendly and versatile software. Ideally sensors would also be to be able to work with a wide range of cell types including yeasts, fungi, bacteria, animal and plant cells over a wide range of cell concentrations. Biomass sensors based on optical effects or dielectric spectroscopy are the ones that fulfil most of these requirements, and will be discussed here.

Optical sensors for biomass include devices based on light absorption, turbidimetry, scattering, transmission, reflectance, fluorescence among others (Salgado *et al*., 2001; Griffiths *et al*., 2011). These techniques are very useful for measuring biomass levels in cell suspensions as long as the medium is clear without suspended non cellular particles. Among the manufacturers that offer optical biomass sensors for use in fermentation we can mention Ocean Optics (www.oceanoptics.com), Bfi Optilas (www.bfioptilas.com), Svanholm (www.svanholm.com) and Laboratory Equipment (www.laboratoryequipment.com) among others. To avoid the risk of sample contamination the optical sensors need to be designed with sterilization in mind, along with the prevention of drift due to growth of cells on the sensor. The range of biomass that can be sensed with optical sensors is often quite limited. A non-linear response is often observed in optical biosensors because of saturation effects as the cell concentration increases. Optical sensors that use infrared work typically are based on the absorption of infrared radiation at different wavelengths. Depending on the application the infrared absorption could be at near infrared range (0.7-2.5 μm) and mid-infrared range (2.5-25 μm). Mid-infrared spectroscopy is more sensitive to

molecular traces but more suitable for off-line applications whereas near-infrared is only sensitive to the presence of major compounds and is more suitable for on-line applications (Salgado *et al*., 2001; Bellon-Maurel *et al*., 2003; Krafft *et al*., 2003; Pacifico *et al*., 2003; Petiot *et al*., 2010).

The measurement of biomass using dielectric spectroscopy is based on the frequency-dependent increase in the suspension permittivity by the presence of cells, caused mainly by the accumulation of charges at the boundaries between the cell membrane and the cytoplasm/cell wall/suspending medium. The major manufacturers of biomass monitors based on dielectric spectroscopy for use during fermentations are Aber Instruments (www.aber-instruments.co.uk) and Fogale (www.fogale.fr). Both instruments are very similar. Both devices use a 4-electrode system in which the sterilisable sensor has to be inserted through a port into the fermentation broth. The technique suffers from interference by electrode polarisation which becomes worse at high medium conductivities, which can vary significantly between and even during fermentations (a technique based on inductive permittivity measurement which did not suffer from electrode polarisation was once available commercially from Hewlett-Packard but has since been abandoned). The technique is also not very sensitive to low concentrations of cells, and gives a much lower signal when the cell size is small (Carvell and Dowd, 2006). Linearity, however, is excellent over a very large range of concentrations (Davey *et al*., 1992), and the technique has as a result being proven particularly useful in controlling the pitching of yeast in breweries. (Boulton *et al*., 1989). The technique has been proven to work with a large variety of cell types, and is relatively insensitive to non-cellular materials (Harris *et al*., 1987; Kell *et al*., 1990; Siano, 1997; Markx and Davey, 1999; Asami *et al*., 2002).

Recently, a new non-invasive optical biomass monitor has been developed by Buglab Inc, the BugEye BE2100 (Figure 8.2). To date the device has not been described in the scientific literature, but literature provided by the company on its website (www.buglab.com) claims it is able to measure biomass levels over a wide concentration range similar to that of the Aber or Fogale Biomass Monitors. Although its mode of action is only cursorily described on the company website, the sensor appears to be based on the scattering of infrared laserlight. The BugEye system was designed for use in both research and industrial environments. It consists of an optical sensor head and a monitor. The sensor has to be secured to the outside of the glass

vessel or to the glass viewing port of a stainless steel vessel with. Since no immersion is required, the need for sensor sterilization is eliminated.

The objective of this work was to evaluate the BugEye Biomass Monitor and compare its performance with that of the Aber model 220 Biomass Monitor.

8.2 Materials and Methods

Cells

Chlorella vulgaris was a gift from E. McEvoy, EPS School, Heriot-Watt University. It was grown in 3N-BBM+V medium (Bold basal medium (https://ncma.bigelow.org/node/71) with 3-fold Nitrogen and vitamins; modified) at 20 °C for 1 month previous to the experiment in a 2 L culture flask without agitation with 12 h light and 12 h dark regime. The algal culture was concentrated by decantation and the biomass concentration was measured off-line to be 0.03626 g DW / ml using dry weight technique.

Nannochloropsis oculata was grown in the SAMS laboratories in Oban. It was grown in 2 L artificial sea water medium (f/2) for 20 days at 20 °C with 16 h of light and 8 h dark in 10 L cultures (Carbuoys). Sterile air was bubbled through the culture from the bottom through a 0.2 μm filter. The final algal concentration in the culture was determined to be 37,653 cell/ml using hemocytometer counting. The algal suspension was centrifuged for 10 min at 4500 g and resuspended in centrifuged medium in a final volume of 150 ml, obtaining a suspension with a final concentration of 0.5×10^6 cell/ml.

Micrococcus luteus was a gift from M. Winson, School of Life Sciences, Heriot-Watt University. It was cultured in an orbital shaker (200rpm) at 21 °C in 15 conical 250 ml flasks, each with 100 ml medium (nutrient broth no.1 for microbiology, Sigma-Aldrich, 20 g/L) for 4 days. The cultures were centrifuged at 4500 g for 5 min and resuspended with the same centrifuged medium to a final volume of 150 ml. The dry weight of the concentrated suspension was measured to be 0.2625 g/ml.

High activity, pressed baker's yeast (*S. cerevisiae*) was obtained from DCL craftbake, stored at 0-4 ºC for a maximum of 12 days. 100 g of pressed yeast was resuspended

with malt extract (Oxoid Ltd, 20 g/L) to a final volume of 150 ml to obtain a thick suspension with 7×10^9 cells/ml.

Non-cellular material

For grist experiments, 100 g of malted barley was crushed in a disc mill at mesh number 7 (0.7 mm particle). Grist (ground malt) was added (2 g of grist was added 10 times at 15 minutes intervals) to 1.5 L of malt extract. For salt experiments, NaCl salt from Sigma-Aldrich was used. A red food colouring stain (Super Cook, Tesco, UK) was used for dye experiments. An air diffuser was placed inside 1.5 L of a solution of malt extract and air pumped through in order to observe the impact of the bubbles on the optical and dielectric sensors. Temperature was risen using a hot plate (Corning Inc.).

Biomass measurements

Optical measurements

The Buglab (Bug Eye model BE2100) was used to measure biomass levels optically (see Figure 8.2). The Biomass Monitor consisted of an optical sensor head and a monitor. The sensor head was strapped to a magnetically stirred beaker for the measurements. 15 min were allowed for the biomass monitor to reach stability measuring the media at the beginning of each experiment.

Figure 8.1 Experimental set up showing the Buglab BE2100 optical sensor.

The sensor of the BugEye employs an array of infrared lasers and detectors and it is based on optical reflectance with a detector for multiple source separations. Light from each of the lasers is scattered by the cells or microorganisms, creating "glow balls" of

monochromatic light. The intensity and size of the glow balls are dependent on the biomass within the culture. As the biomass level grows the intensity of the glow will increase and the size of the balls will reduce. The sensor is arranged so as it is able to determine the level of the biomass present by combining the information on both the size and intensity of the glow. The optical biomass monitor is able to detect biomass levels from less than 0.1 to more than 300 OD units. The sensor can be secured to the outside of a glass vessel or can be secured to any kind of vessel with a glass viewing port. Since no immersion is required, the need for sensor sterilization is eliminated.

Figure 8.2 The BE2100 non-invasive biomass monitor by Buglab.

The BE2100 biomass monitoring system includes software which allows tracking the progress of the experiments in real time. The software has an event-marking tool to help keeping the track of different events during the run. The output of the optical biomass monitor works are arbitrary raw "bug units".

Dielectric spectroscopy

An Aber Biomass Monitor model 220, connected to a PC with Aberscan software version 2.2 (Aber Instruments, Aberystwyth, UK) was used for comparison (Figure 8.1). For each measurement the Biomass probe was inserted directly into the suspension in a magnetically stirred beaker.

In all experiments, the response of the BugEye Biomass Monitor and the Aber Instruments were recorded simultaneously in the same sample.

8.3 Results and discussion

Yeast

The first set of experiments was done with baker's yeast. *S. cerevisiae* cells are round to ovoid shaped, 5–8 μm in diameter. 15 ml of yeast suspension (7×10^9 cells/ml) was added to 1.5 L of malt extract 10 times every 15 min. The result of the measurements with the BugEye, shown in Figure 8.3, showed a near linear increase in the BugEye signal with increasing cell concentration. The slight drop in the BugEye output around a yeast concentration of 0.3×10^9 cells however was consistent and reproducible. The signal from the Aber model 220 Biomass Monitor (Figure 8.3b) was similar, but did not have the consistent drop at low cell concentrations.
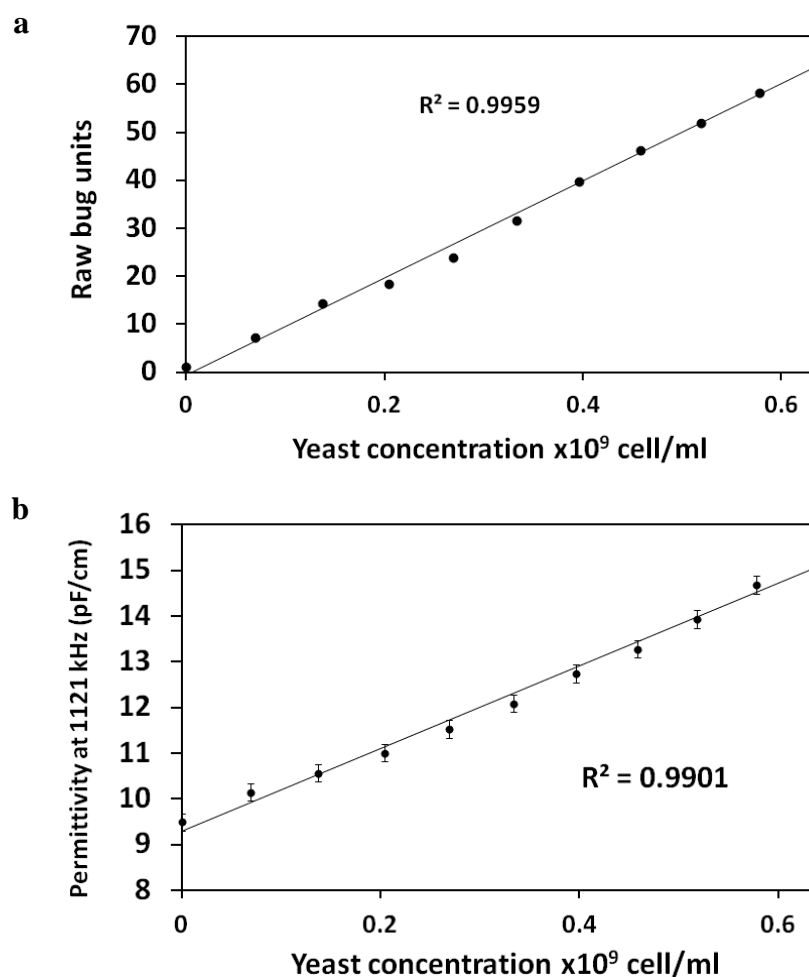
Figure 8.3 a) Raw bug units as function of yeast concentration (*S. cerevisiae*). b) Permittivity at 1121 kHz as a function of yeast concentration. Error bars showed in both results.

Algae

Two different types of algae were evaluated, a marine alga (*N. oculata*) and a fresh water alga (*C. vulgaris*). Both algae are economically relevant for the production of biofuels and in the food industry. *C. vulgaris* is a fresh water green alga which is spherical in shape with a diameter of 2-10 μm. *N. oculata* is a marine alga with cells with a round shape, 2–3 μm in diameter.

The results of the measurement of biomass levels of *N. oculata* with the BugEye optical sensor are shown in Figure 8.4a. Although lower signals overall were obtained with *N. oculata* compared to the measurements with yeast, the concentrations of the algae used were also much lower. Assuming one CFU equals one cell, the signal for algae was approx. 1.6×10^{-5} raw bug units per cell per ml, whilst for yeast it was 1×10^{-7} raw bug units per cell per ml. The algae therefore gave a higher signal per unit (cell), despite the fact that the cell diameter of the algae was smaller than that of the yeast. Further study clearly should be done to evaluate the impact of cell size and shape and other factors on optical signal levels.

The measurement of biomass levels of *N. oculata* with dielectric spectroscopy has already been discussed extensively discussed in chapter 5. Measuring the biomass levels of marine algae presents a challenge for dielectric spectroscopy due to the high salinity of the medium, and the small size of the cells. This is clearly demonstrated in Figure 8.4b, where the dielectric increment actually decreases as a function of algal cell concentration. In comparison the measurement with the optical sensor measurement of biomass of microalgae was straightforward.
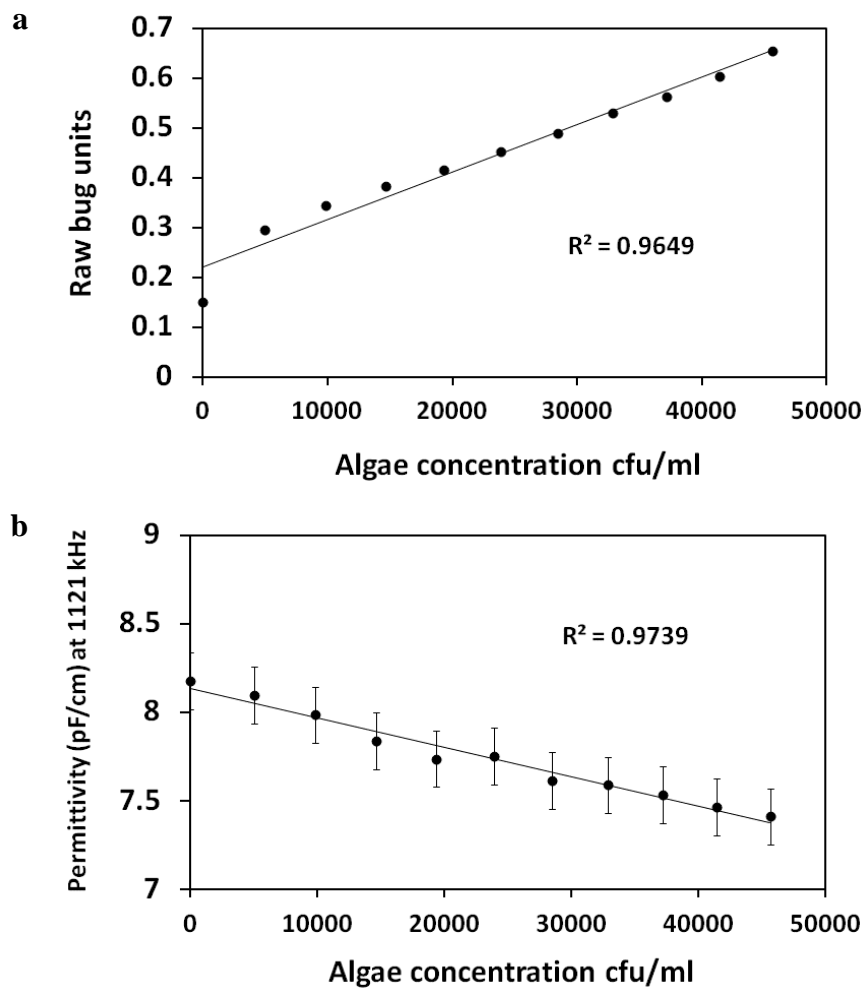
Figure 8.4 a) Raw bug units and b) Permittivity as function of algal concentration (*N. oculata*). Error bars showed in both results.

Results obtained with the freshwater alga *C. vulgaris* can be seen in Figure 8.5. Measurements with the optical biomass monitor were straightforward, giving a strong signal with high linearity Because the medium conductivity is lower the measurements with the dielectric monitor are better than those obtained with the marine microalgae; however because of the small cell size the dielectric signal was small and the noise in the signal large. As a result the linearity still needs to be improved. Further study should be done about the impact of cell size in permittivity signal.
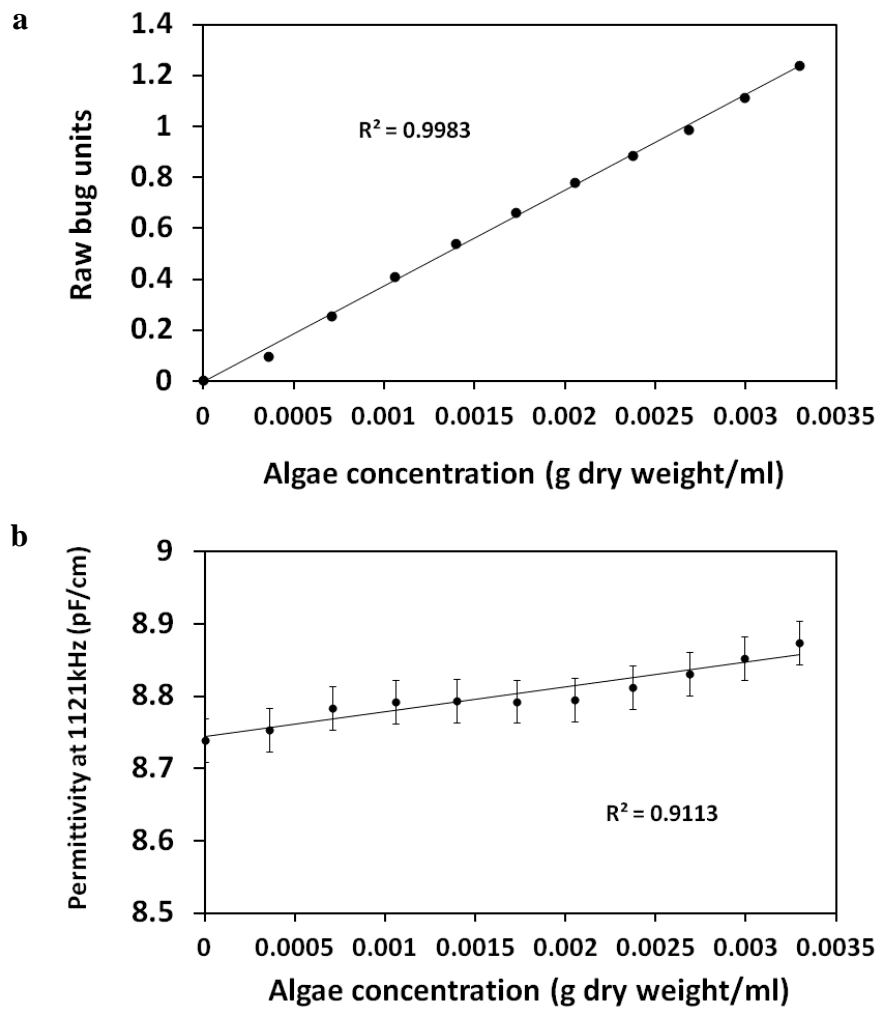
Figure 8.5 a) Raw bug units and b) permittivity as function of algae concentration (*C. vulgaris).* Error bars showed in both results.

Bacteria

M. luteus is an aerobic, Gram-positive, spherical bacterium with a diameter of 0.5-1 μm diameter. Results of the measurement with the optical probe and the dielectric probe can be seen in Figure 8.6. Bacteria have always presented a challenge for dielectric spectroscopy because of the small diameter of the cells. Not surprisingly, data obtained with dielectric spectroscopy showed a lot of noise (Figure 8.6b). However, for the optical biomass monitor the measurement was straightforward, and data showed little noise (Figure 8,6a). Again, a reproducible deviation from linearity was observed at lower cell concentrations, now around a concentration of 0.01 g dry weight/ml, with a noticeably higher signal when no cells are present.
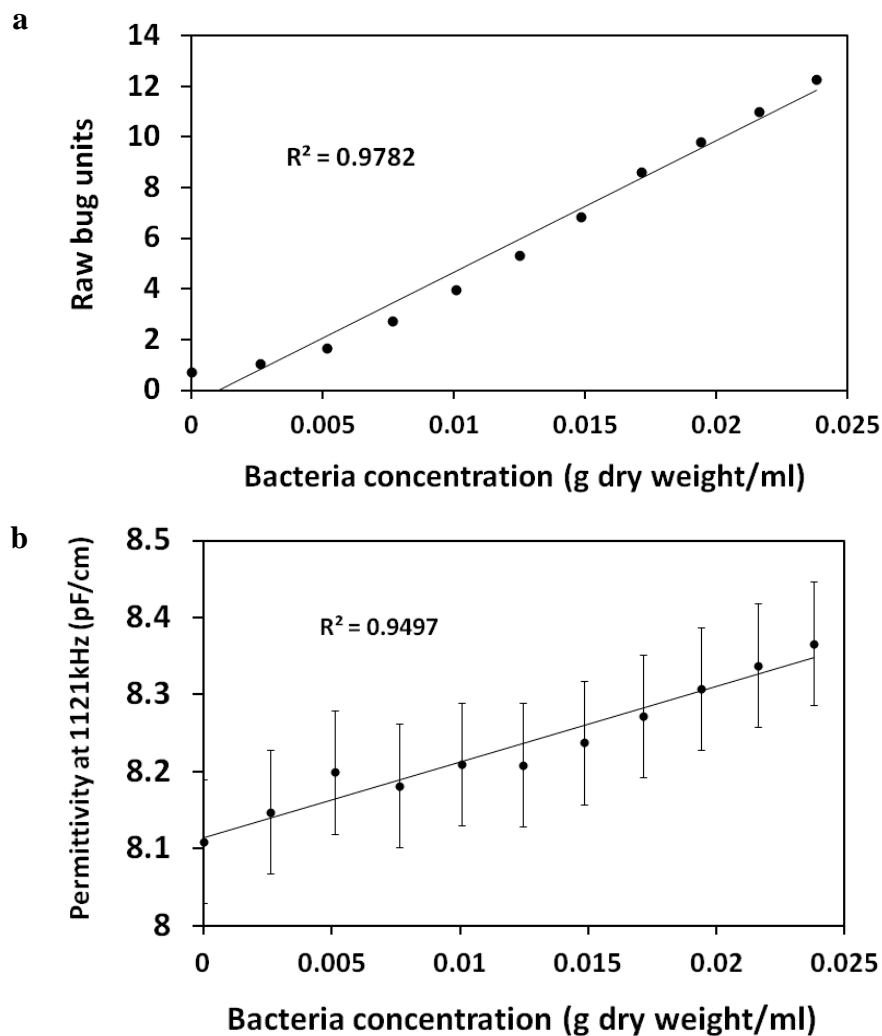
Figure 8.6 a) Raw bug units and b) permittivity as function of bacterial concentration (*M. luteus)*. Error bars showed in both results.

Non-cellular material: Ground malt (grist)

The presence of non-cellular particles in the medium can interfere during biomass measurement; both in optical as well as dielectric measurements (see also chapters 3 and 4 in this thesis). Results with grist are shown in Figure 8.7. The malt extract itself was quite cloudy, indicating it contained a significant amount of particulate material, and pure malt extract itself already gave a strong optical signal. The addition of grist resulted in a significant increase in the optical signal. Apart from the lower concentrations, the signal appears to be linear with grist concentration. In contrast to the optical measurements, the presence of grist particles had little effect on the permittivity signal (Figure 8.7b).
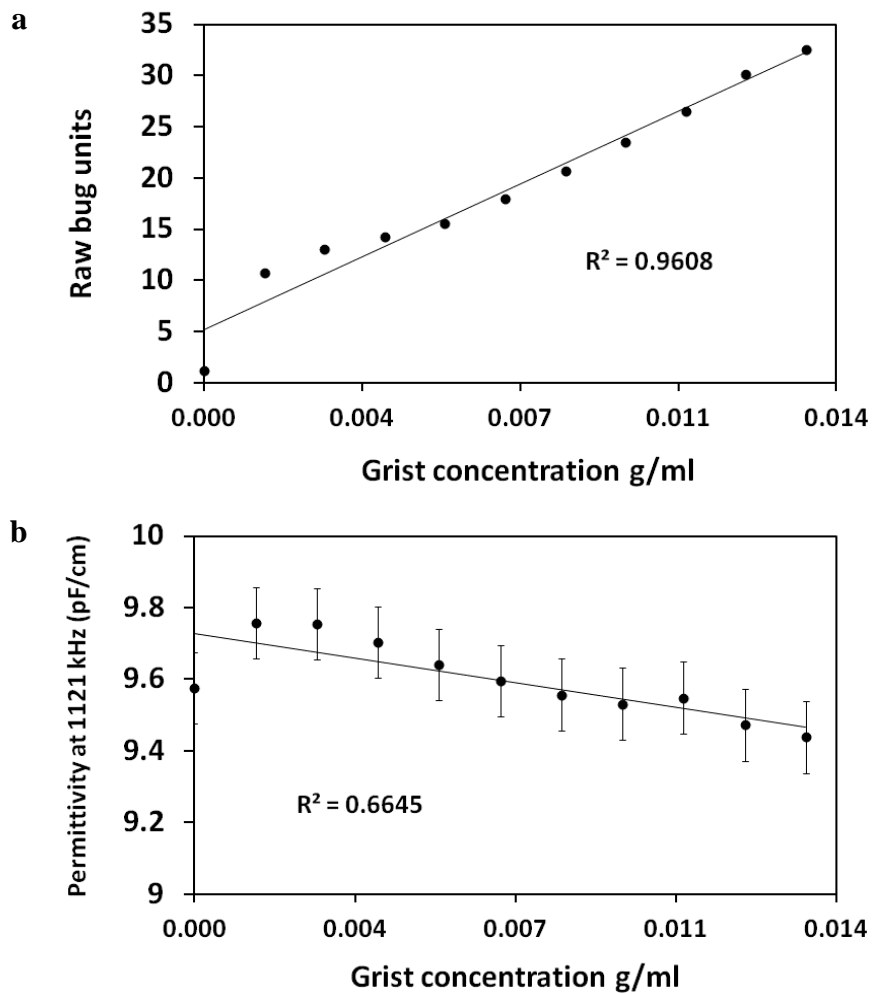
Figure 8.7 a) Raw bug units and b) permittivity as function of grist (ground malt) concentration. Error bars showed in both results.

Salt

The effect of the addition of salt on the dielectric biomass monitor was discussed extensively in chapter 6. The effects are large, especially at the low frequencies, but can be compensated for. To investigate the effect of the addition of salt on the signal from the BugEye optical biomass monitor NaCl salt was added in small aliquots to 1.5 L of water. As can be seen in Figure 8.8 the additions of salt has little effect on output of the optical biomass monitor. At concentrations up to 0.012 g/ml there was no effect, and at higher salt concentrations the effect was very small compared to the signals that can be expected from cellular particles.
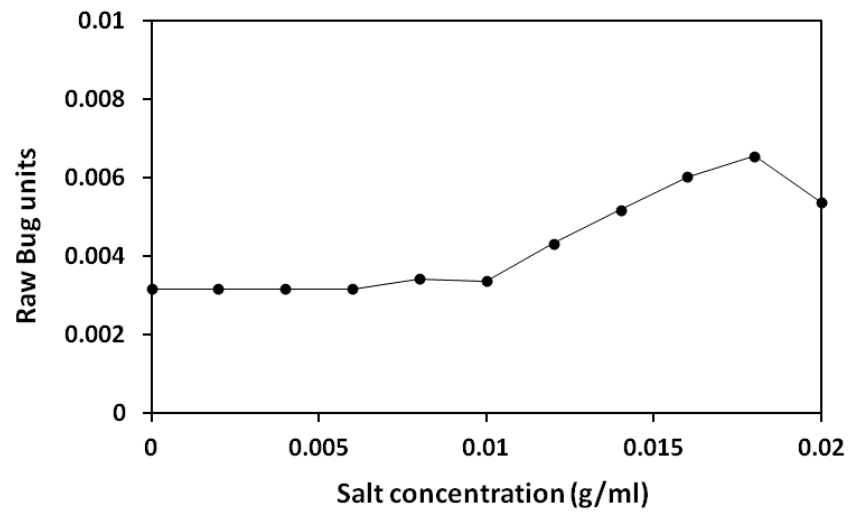
Figure 8.8 Raw bug units as function of salt (NaCl) concentration.

Dye

A red food colouring stain (Super Cook, Tesco, UK) was added to deionised water and the response of the optical sensor observed. Results, shown in Figure 8.9, show that the presence of the dye has no influence on the optical signal. The effect of the dye on the dielectric signal was not measured, but was expected to be nil.
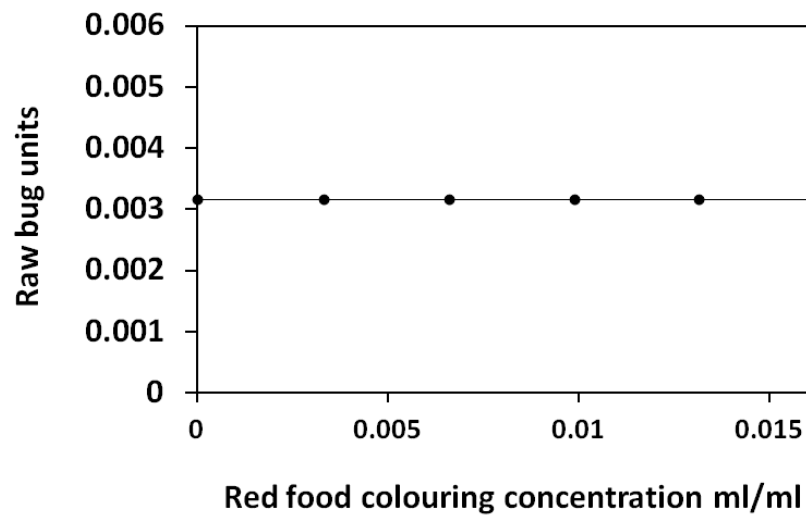
Figure 8.9 Bugeye output as a function of the concentration of red food colouring.

Temperature

In the next set of experiments, the temperature of a solution of malt extract was increased gradually from 22 °C to 80 °C. The results can be observed in Figure 8.10. Changes in temperature produced only a small rise in the signal of the optical sensor.
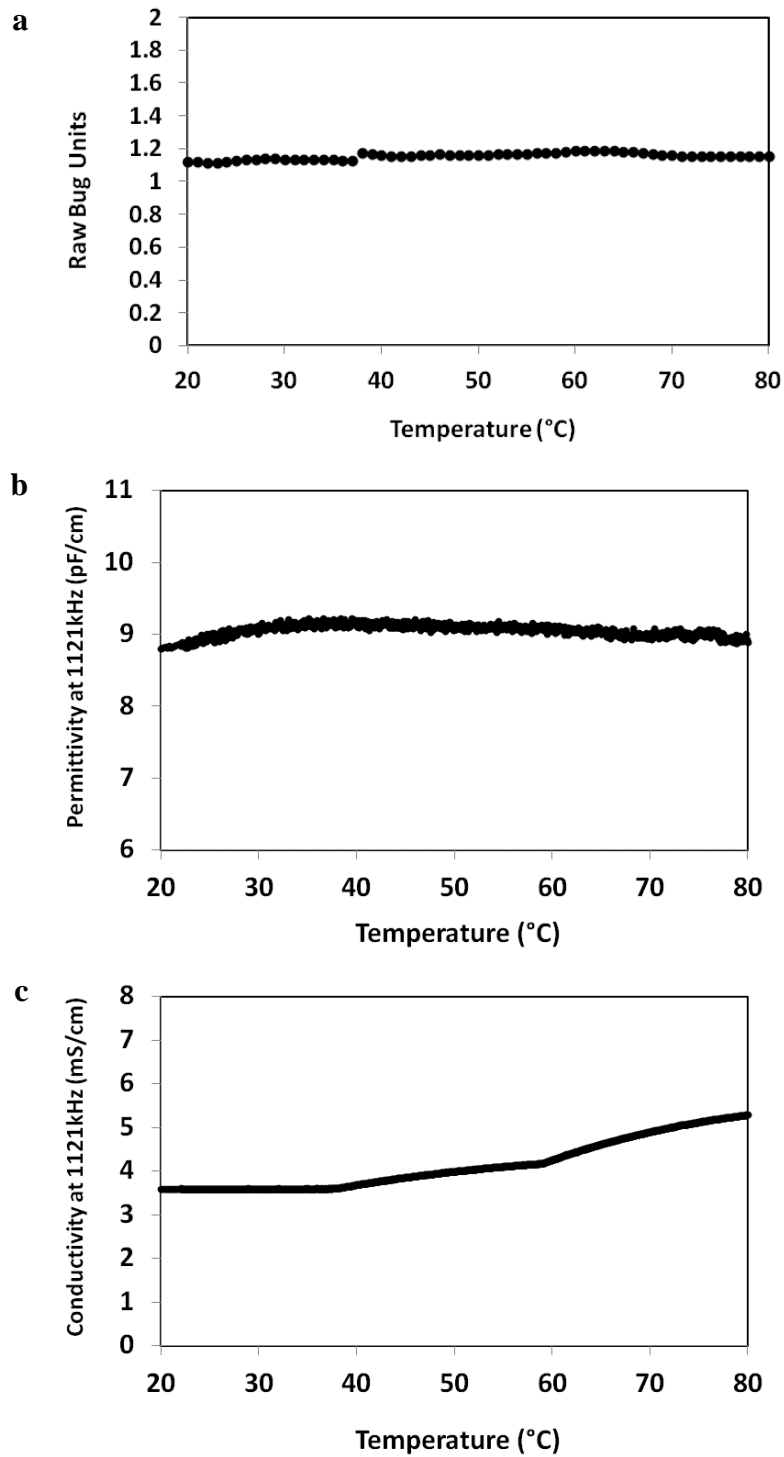
Figure 8.10 a) Raw bug units, b) permittivity and c) conductivity as a function of temperature.

Results obtained with the dielectric monitor were similar. Changes in temperature resulted in only small changes in the permittivity levels. However, changes in the levels of conductivity were large as expected, as can be seen in Figure 8.10c.

Bubbles

As can be observed in Figure 8.11 an increase of the air throughput had some but no major effect on the output of the optical sensor. However, the dielectric sensor showsa decrease in permittivity values.
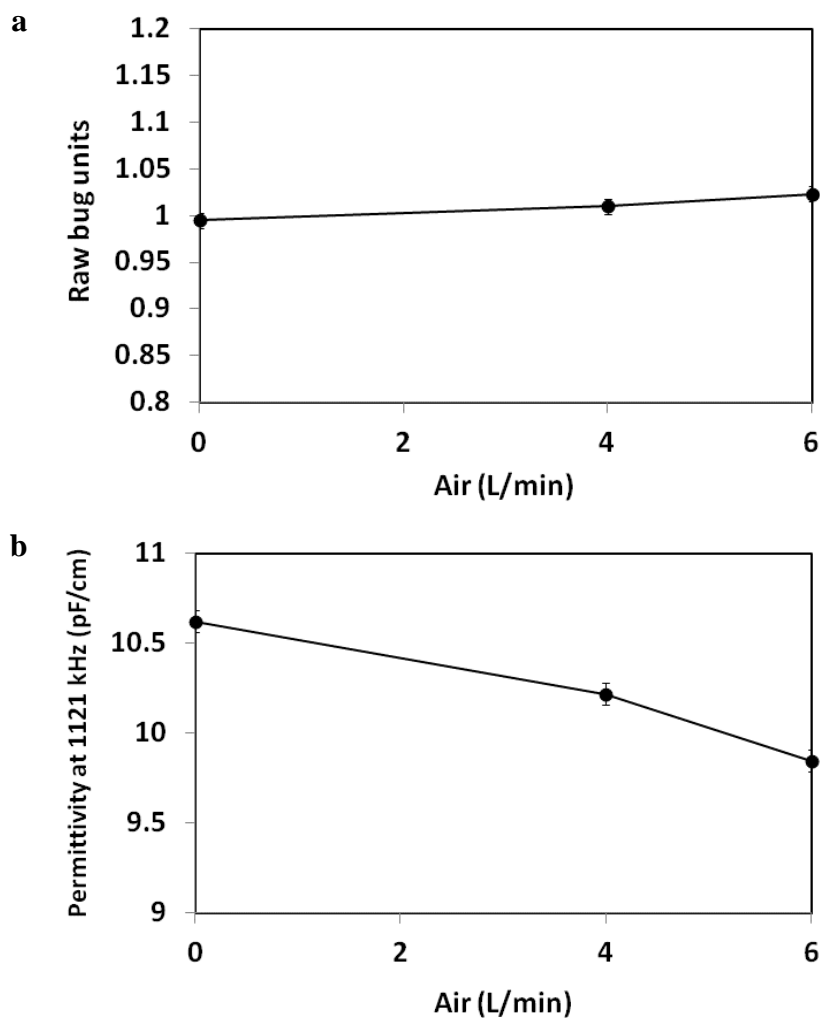
Figure 8.11 a) Raw bug units and b) permittivity as a function of air volume.

8.4 Conclusions

The comparison of the optical and the dielectric sensor biomass sensors showed that each of them has its advantages and disadvantages. The linearity of the optical sensor was less good compared to that of the dielectric biomass monitor, especially at the lower concentrations. However, reproducibility of the optical signal was good, pointing to the possibility of calibrating the response for non-linearities. The sensitivity of the optical probe was generally better than that of the dielectric probe.

The effect of cell size on the signal from the optical sensor was not clear, and further experiments need to be done on this. However, the experiments with different cells types showed that the optical sensor is capable of sensing cells with very different cell sizes with ease. In contrast, the increment of the permittivity is well known to be a direct function of the cell size. For a given cell concentration a large cell gives a much larger dielectric increment. The result was that the dielectric monitor showed much better results when larger cells such as yeast were used in the experiments than if smaller cells were used such as bacteria. These can be noticed by the comparison of the error bars showed in the charts.

For small cells in a high conductive medium such as *N. oculata*, the optical sensor gave better results than the dielectric sensors since it is capable of sensing small cells without any major interference from the medium conductivity. In contrast, cells with a small diameter dispersed in a highly conductive medium present a big challenge for the dielectric monitor.

Neither probes were significantly affected by the presence of dyes, bubbles or changes in temperature.

Where the dielectric monitor played to its strength is when it comes to selectivity. The optical technology measures the presence of particles, - any particle essentially, as long as it reflects light. The dielectric sensor in contrast is quite selective, and the dielectric signal is mainly determined by the concentration of material enclosed by an intact (cell) membrane. This was clearly seen in the experiments with grist, and also in experiments with malt extract, in which the optical sensor responded strongly to the presence of non-

cellular particles, whilst response of the dielectric monitor to these materials was minimal.

Noise levels demonstrated by the dielectric biomass monitor were often quite higher than those from the optical sensor as it can be seen comparing the statistical error bars showed in all the charts.

Finally, it should be noted that because of its non-selectivity the optical sensor measures the total amount of biomass- necromass as well as viable cells- whilst the dielectric signal is much stronger for viable cells than for non-viable cells. This effect will be further explored in chapter 9.

CHAPTER 9

EVALUATION OF METHODS FOR THE ON-LINE AND REAL TIME MEASUREMENT OF CELL VIABILITY USING DIELECTRIC SPECTROSCOPY

ABSTRACT

Dielectric spectroscopy has been used extensively for measuring changes in the biomass levels during fermentation. Both viable and (to a lesser extent) non-viable biomass contribute to the overall dielectric signal, but to date it has not been demonstrated that it is possible to separate their relative contributions. Methods are explored by which the relative contributions of viable and non-viable cells to the overall permittivity signal could be separated. It is shown that viability can be estimated most accurately by combining the dielectric signals with other another on-line (optical) biomass measurement technique which is independent of cell viability.

9.1 Introduction

Biomass is one of the most important parameters during fermentation, and measurement of changes in biomass can greatly assist PAT-based systems for monitoring and controlling cell-culture based production processes (Carvell and Dowd, 2006; Justice *et al*., 2011). Preferably this would be done on-line and in real time, rather than off-line. A variety of techniques have been developed for measuring the biomass concentration on-line and in real time during fermentation including acoustic resonance, nuclear magnetic resonance (NMR) spectroscopy, optical methods including fluorescence and, optical density / turbidity measurements and real-time imaging, and dielectric spectroscopy (Sarra *et al*., 1996; Salagado *et al*., 2001; Bellon-Maurel *et al*., 2003; Sandnes *et al*., 2006; Kivijarju, 2008; Griffiths *et al*., 2011; Hocalar *et al*., 2011; Ronnest *et al*., 2011). However, in practice it is not only the cell concentration that is important, but also their viability. The direct measurement of viability on-line to date has been difficult, though

some success has been achieved mainly with light-based methods (Li *et al.*, 1991; Wei *et al.*, 2007; Tibayrenc *et al.*, 2011). Dielectric spectroscopy, however, could give information about both cell concentration and viability (Davey *et al.*, 1993; Carvell and Dowd, 2006).

Dielectric spectroscopy involves measurement of the dielectric polarisation of a material when it is exposed to an AC electric field of different frequencies (Maxwell, 1873). The measurements give information about the storage and loss of electric field energy in the material, expressed as the respectively the permittivity and conductivity of the material. When the material being measured contains cellular material the presence of a cell membrane around the cell's cytoplasm causes interfacial polarisation to occur which takes the form of a dispersion i.e. a gradual increase in the permittivity and a decrease in the conductivity from high to low frequencies. Typically this dispersion (the so-called β-dispersion) takes place in the frequency range 10 kHz-100 MHz, with a characteristic frequency around 100 kHz-1 MHz, depending on the cell type. (Pethig and Kell, 1987; Asami, 2002) The rise in the permittivity from high to low frequency can be described by (Schwann, 1957; Harris *et al.*, 1987):

$$\Delta\varepsilon = \frac{9}{4} P \, r \, C_{\mathrm{m}} \tag{9.1}$$

In which $\Delta\varepsilon$ is dielectric increment, P is the volume fraction of membrane enclosed biomass, r is the cell radius (or its equivalent sphere), and C_{m} is the membrane capacitance. Equation (9.1) indicates there is a linear relationship between the dielectric increment and cell concentration. This relation has been shown to be valid for many different cells types, including bacteria, yeasts, moulds and other microorganisms, as well as animal and plant cells, and dielectric spectroscopy is now one of the most used technologies is for measuring cellular biomass (Kell *et al.*, 1990; Markx and Davey, 1999; Ferreira *et al.*, 2005; Ansorge *et al*, 2010a&b). As shown by Schwann (1957), and elaborated by Harris *et al.*, (1987); both the permittivity and conductivity can give information about biomass levels. Because large changes can occur in the medium conductivity during many fermentations, the permittivity signal is usually preferred.

For equation (9.1) to be valid the assumptions are made that the cells are completely surrounded by a thin intact plasma membrane which has a low conductivity relative to

that of the cytoplasm and the suspending medium. Whilst that is normally true for viable cells with intact membranes, this situation changes when a cell dies. Cell death is accompanied by many changes in the dielectric properties of the cells (Huang *et al*., 1992; Patel and Markx, 2008). Although the changes that occur in the cells dielectric properties depend on the manner and timing of cell death and the extent of cell damage (Patel and Markx, 2008), when cell death is advanced most commonly permeabilisation of the cell membrane is observed leading to changes in the membrane capacitance and conductance as well as changes the internal conductivity due to an increased exchange between the cytoplasm and the surrounding medium. The overall result is that a massive drop occurs in the dielectric increment, though some residual signal typically remains (Stoicheva *et al*., 1989; Patel *et al*., 2008). Whilst this drop can and has been used for measuring changes in cell viability when the initial cell concentration is known (Stoicheva *et al*., 1989), the technique still poses a problem both the cell concentration and the cell viability are unknown. In this paper we will investigate why this is, and point to some methods that may be used to overcome this problem.

9.2 Materials and methods

Cells

High activity, pressed baker's yeast (*Saccharomyces cerevisiae*) was obtained from DCL craftbake and stored at 4ºC for a maximum of 12 days. 100 g of pressed yeast was resuspended with malt extract (Oxoid Ltd, 20g/L) to a final volume of 150 ml to obtain a thick suspension of 7×10^9 cells/ml for further dilution. To obtain a suspension of non-viable cells a yeast suspension was prepared in a similar way and immersed in a water bath at 85°C for 1 hr. Cell viability was tested using methylene blue staining (Gurr, 1965). The viability of fresh yeast was tested before each experiment, and was not less than 98%; no viable cells could be detected in the heat-killed yeast suspension.

Dielectric and optical biomass measurements

For the experiments a setup was used as shown in Figure 9.1. Suspensions with constant cell concentrations and different ratios of viable and non-viable were made by mixing suspensions of fresh viable yeast cells with suspensions containing heat-killed non-viable cells. Small aliquots (15 ml) of the yeast suspension were added to a magnetically stirred medium in a 1 litre beaker with 500 ml water containing malt

extract (Oxoid) 20 g/L and NaCl 2 g/L. The overall conductivity was 3.5 mS/cm at 1121 kHz. The probe of the dielectric sensor system was immersed in the suspension during measurement. The optical sensor was able to measure through the wall of the beaker and no immersion of the optical sensor was required (see Figure 9.1). Although work with both the dielectric and optical techniques could have been done under sterile conditions, due to the short nature of the experiments no attempt was made to work sterile. All data were corrected for dilution effects.
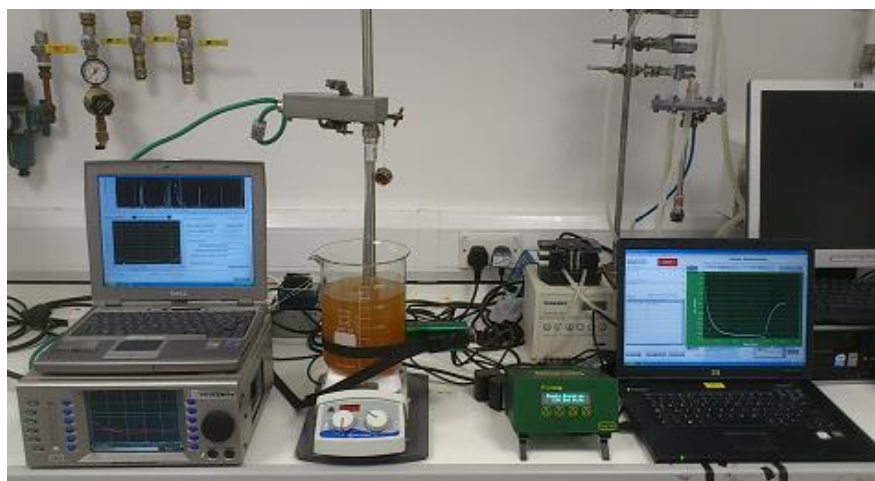
Figure 9.1 Experimental set up showing the Aber biomass monitor (left) and the Buglab BE2100 optical sensor (right).

A Aber Instruments Biomass Monitor model 220, shown in Figure 9.2, with a 1.2 cm diameter 30 cm long annular probe, connected to a PC with Aberscan software version 2.2 (Aber Instruments, Aberystwyth, UK) was used for recording the dielectric frequency spectra. The freerun option was used to measure the capacitance and conductance of the cell suspension at 25 frequency points distributed over the frequency range 0.1 to 20 MHz. One spectrum was measured every 10 seconds, and then an average spectrum was calculated from the data from 30 spectra. All spectra were automatically corrected for electrode polarisation. The Aber Instruments Biomass Monitor also automatically corrects for differences in cell constants between probes, and all data are given as pF/cm, i.e. capacitance $\times$ cell constant (in cm^{-1}).

Figure 9.2 Biomass monitor model 220 from Aber Instruments.

The BE2100 "BugEye" optical Biomass Monitor from BugLab Inc (USA), shown in Figure 9.3, had an optical sensor head which could be secured to the outside of a glass vessel or glass viewing port. Data were logged using software supplied with the instrument. The range of biomass levels that can be detected is comparable to that of the electrical biomass monitor, i.e. 0.1 to 300 OD units.

Figure 9.3 The BE2100 non-invasive optical biomass monitor from BugLab Inc.

Fitting procedure

Measurements were taken at different frequencies f_i. By taking measurements on suspensions with either 100% viable or 100% non-viable cells at a known cell concentrations P_X (viable cells) or P_Y (non-viable cells), proportionality constants K_{Xi} (for viable cells) and K_{Yi} (for non-viable cells) can be determined similar to the molar absorptivity in spectrophotometric measurements (Blanco *et al.*, 1989; Harris 2007).

$$K_{Xi} = (\varepsilon_{Xi} - \varepsilon_{0i})/P_X \qquad (9.2)$$

and

$$K_{Yi} = (\varepsilon_{Yi} - \varepsilon_{0i})/P_Y \qquad (9.3)$$

in which ε_{xi} is the permittivity at frequency i of a suspension of 100% viable cells at cell concentration P_X, and ε_{yi} is the permittivity at frequency i of a suspension of 100% non-viable cells at concentration P_Y. ε_{0i} is the permittivity of the background at frequency i. Assuming linearity, the overall (calculated) permittivity ε_{ic} of a mixture of viable and non-viable cells at frequency i can be calculated by

$$\varepsilon_{ic} = \varepsilon_{0i} + K_{Xi}\, P_{Xc} + K_{Yi}\, P_{Yc} \qquad (9.4)$$

in which P_{Xc} is the calculated concentration of 100% viable cells (in cells/ml) and P_{Yc} the calculated concentration of 100% non-viable cells (in cells/ml) in the mixture. Suspension permittivities ε_i were then obtained at different frequencies f_i for different total cell concentrations and culture viabilities. Data were fitted to equation (9.4) and (9.5) using Excel Solver as described in Harris (2007) by minimising the distance between calculated (ε_{ic}) and measured (ε_i) values of the suspension permittivity for different frequency combinations and values.

$$\sum_{f_1}^{f_n} (\varepsilon_i - \varepsilon_{ic})^2 = \text{minimal} \qquad (9.5)$$

9.3 Results and discussion

In the first set of experiments yeast suspensions of viable and non-viable cells were added to the medium. Figure 9.4 shows in a) the spectra of suspensions of viable yeast cells at different concentrations, whilst b) shows the spectra of non-viable cells.
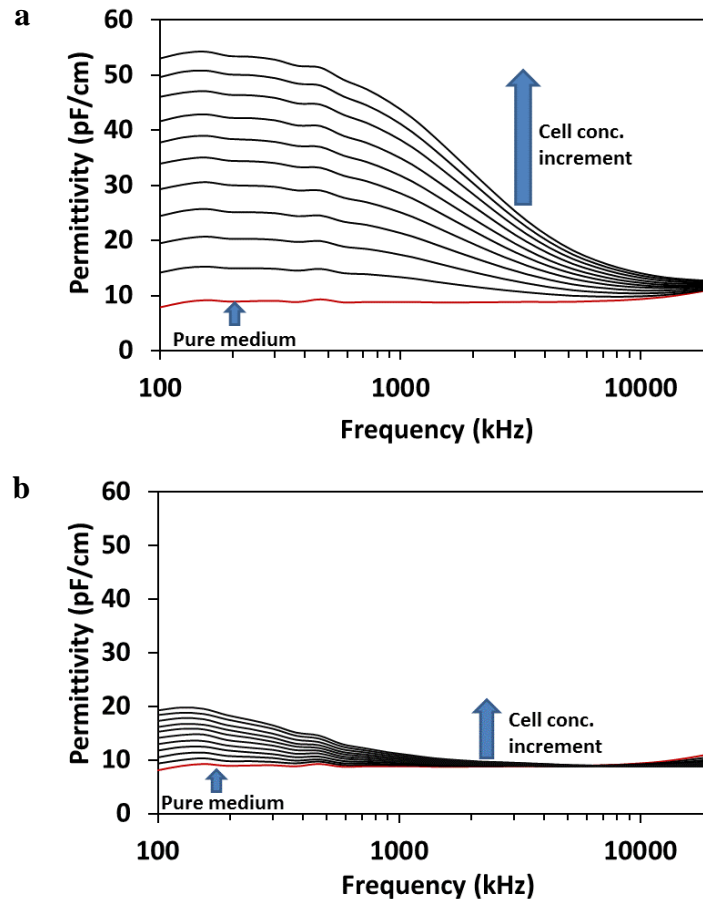
Figure 9.4 Permittivity as a function of frequency for a suspension of a) fresh yeast; b) heat-killed yeast. 15 ml of yeast cell suspension (7×10^9 cells/ml) was added ten times every 5 min to a starting volume of 500 ml. All data were corrected for dilution effects.

The viable cells show spectra with a dispersion with a characteristic frequency (fc) of 1900 kHz. The non-viable cells show spectra with a dispersion with a much lower characteristic frequency of 400 kHz. Both the spectra of the viable and non-viable cells have low-frequency plateaus which depend linearly on the concentration of cells, but a much higher permittivity is obtained with viable cells (around 28 pF/cm per 10^9 cells/ml at the plateau) than non-viable cells (around 6 pF/cm per 10^9 cells/ml).

The data indicate that linear relations exist between cell concentration and dielectric increment for both viable and non-viable cells. This is further confirmed in Figure 9.5.
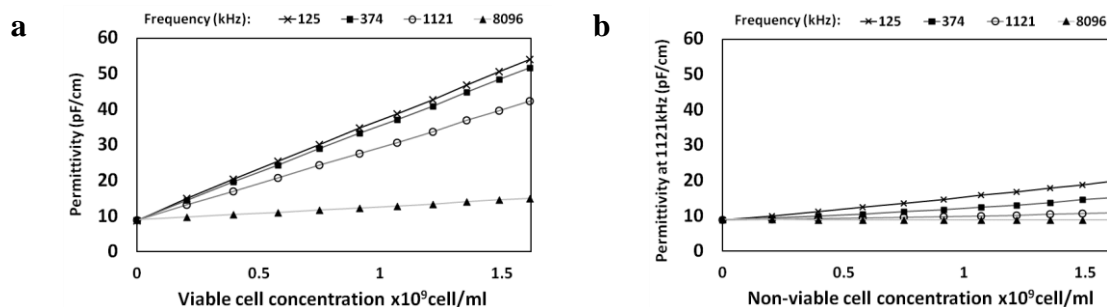
Figure 9.5 Permittivity and best fit as a function of cell concentration for a) 100% viable cells; b) 100% non-viable cells. For clarity only selected frequency data are shown.

In the next set of experiments spectra were obtained of cell suspensions with the same cell concentration but with different ratios of viable and non-viable cells. Figure 9.6 shows spectra for the highest total cell concentration (of both viable and non-viable cells) used.
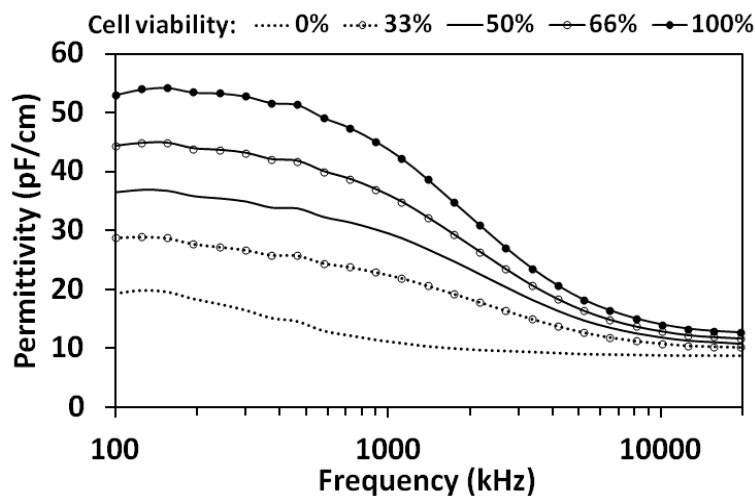
Figure 9.6 Permittivity spectra of suspensions of with the same final concentration (1.62×10^9 yeast cells /ml) and different culture viabilities.

The relation between the permittivity at 1121 kHz and the total cell concentration for suspensions with different cell viabilities is explored in Figure 9.7. Similar results were obtained at all other frequencies.
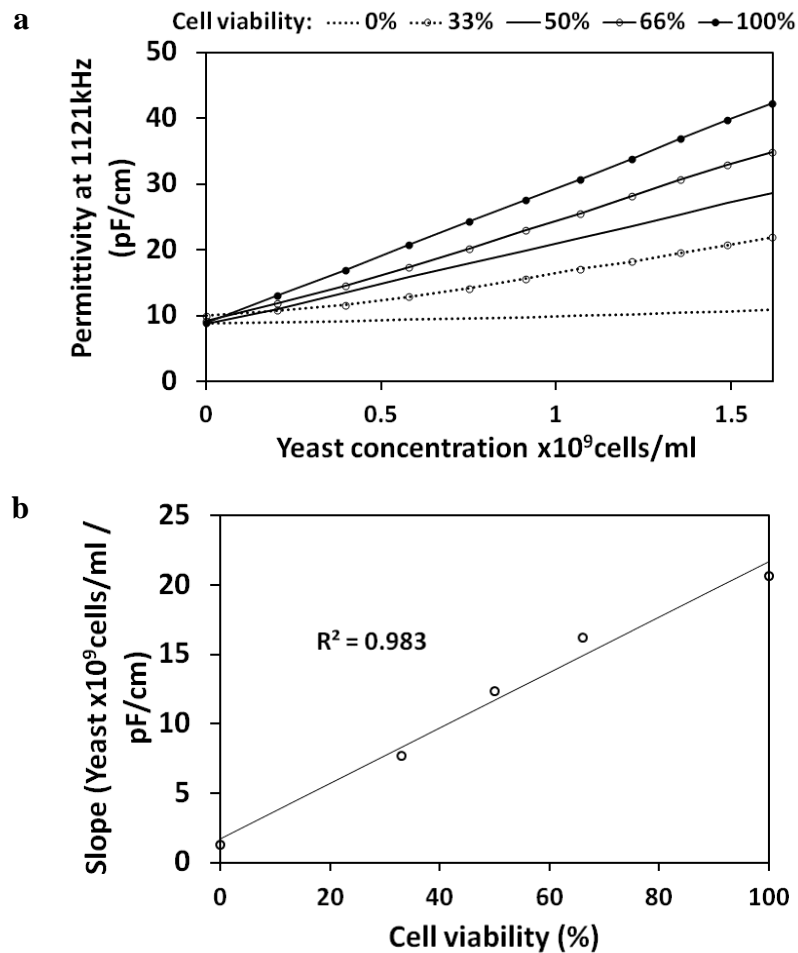
Figure 9.7 a) Permittivity at 1121 kHz as a function of yeast concentration for suspensions with different cell viabilities. b) Slope (permittivity at 1121 kHz divided by cell concentration) for yeast suspensions with different cell viabilities.

The fact that viable and non-viable cells show dispersions with characteristic frequencies that are quite distinct (400 and 1900 kHz, respectively) led us to explore the possibility to separate the signals from viable and non-viable cells on the basis of the frequency dependence, in the same way that the composition of solutions of mixtures of light absorbing compounds can be determined from their overlapping spectra, provided that the a) there is a linear relation between absorbance and concentration, and b) the absorbance of the solution at any wavelength is the sum of the absorbances of all the species in the solution (Blanco, 1989; Harris, 2007).

First, from previous experiments with baker's yeast proportionality constants between the dielectric increment and cell concentration were determined for viable and non-viable cells at different frequencies. Results are shown in Figure 9.8.
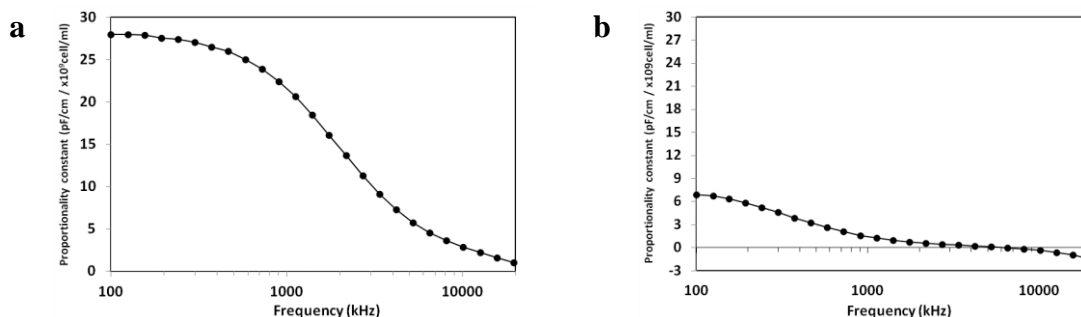
Figure 9.8 Proportionality constants between the dielectric increment ($\Delta\varepsilon$ in pF/cm) and cell concentration (ΔP in 10^9cell/ml) for a) viable and b) non viable cells at different frequencies.

Mixtures were then made with different but known cell viabilities and total cell concentrations, and dielectric spectra recorded. Following this it was attempted to fit the data to equation (9.4), using Excel Solver, with viable cell concentration P_{Xc} and non-viable cell concentration P_{Yc} as the two unknowns.

Different numbers of frequency points and different combinations of frequencies were used in the fitting procedure, but optimal results were obtained using three frequencies (125, 374 kHz and 8 MHz). 125 kHz corresponds to the frequency at which the dispersions of both viable and non-viable cells have reached their low frequency plateau; 374 kHz corresponds to the f_c of the non viable cells and is also the frequency at which the difference in the dielectric increment between viable and non viable cells is at its maximum; at 8MHz the permittivity signal of the non-viable cells has the smallest increment. Results of the fitting procedure are shown in Figure 9.9.
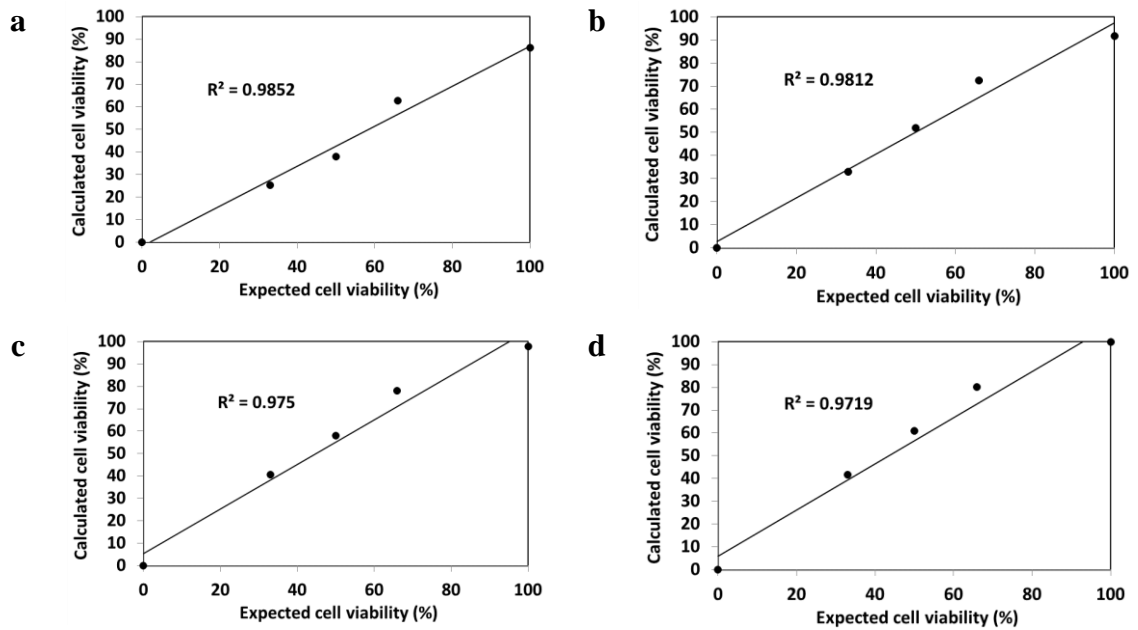
Figure 9.9 Expected and fitted (calculated) cell viabilities for different cell concentrations using permittivity data obtained at 125 kHz, 374 kHz and 8 MHz. a) 0.4 b) 0.91 c) 1.35 d) 1.62×10^9 cell/ml.

The results indicate that despite of the good approximation, it is difficult to estimate simultaneously cell viability and cell concentration directly from dielectric spectra, especially at high cell concentrations, even though the characteristic frequencies of the viable and non-viable cells are quite far apart. The cause of this may arguably lie in the facts that a) the signal of non-viable cells is much smaller than that of the viable cells (by a factor 4 to 5); b) the quality of the data is insufficient to obtain an accurate estimate; and c) there are two unknowns, cell viability and cell concentration.

Factor a) is a consequence of electrical properties of the cells. The electrical properties of cells will vary and depend on species, strain as well as the cell's history (e.g. growth conditions), and for non-viable cells will also depend on method by which the cells have become non-viable (Patel and Markx, 2008), but are not normally under the experimenters' control in most measurements.

Factor b), the quality of the data depends on both the instrumentation and on the method by which the data have been obtained (e.g. averaging/filtering). Permittivity measurements on cell suspensions can be quite noisy (Kiviharju, 2008; Ronnest, 2011), in particular those obtained at the lower frequency ranges where the small contribution of the non-viable cells to the dielectric increment occurs. To a large extend this is probably caused by the need to compensate for electrode polarisation (Schwann, 1992; Davey and Kell, 1998 I&II; Yardley *et al*., 2000). The development of electrodeless measurements systems (Siano, 1997) in which there are no electrodes in direct contact with the medium, and therefore no electrode polarisation and the development of higher resolution dielectric monitors may overcome these problems.

Factor c), the need to fit both the cell viability and cell concentration, could be overcome if one were to obtain a separate measurement of the total cell concentration. In the next set of experiments measurements were done with a NIR probe, the BugEye BE2100 optical Biomass Monitor, on suspensions containing both mixtures of viable and non-viable cells of different concentrations and ratios. Results are shown in Figure 9.10.
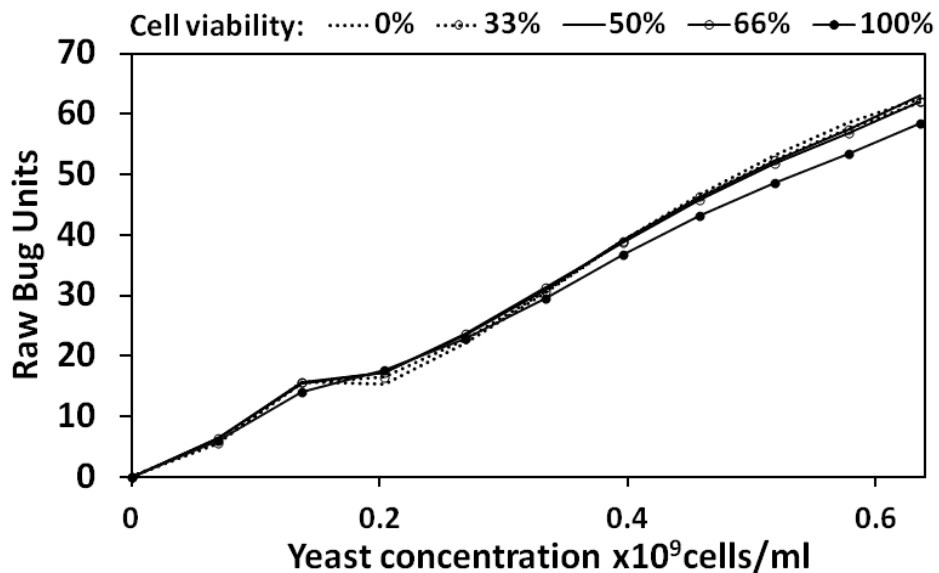
Figure 9.10 Response if the NIR probe (in arbitrary raw bug units) as a function of yeast concentration for suspensions with different cell viabilities.

The response of the BugEye probe (Figure 9.10) to changes in the cell concentration is not as linear as the response of the dielectric probe (Figure 9.5), where the correlation

between biomass level and dielectric increment was typically $R^2 \gg 0.999$ for viable cells (less so for non-viable cells, which had a much lower dielectric increment). However, the correlation between the optical sensor readings and the total amount of biomass is still good ($R^2 = 0.9951$).

Whilst the signal of the dielectric probe is highly dependent on the viability of the cells in the suspension (Figure 9.4), the optical sensor does not distinguish between viable and non-viable cells. Thus, by combining the signals of the NIR probe (to get an estimate of the total cell concentration P_t) with that of the dielectric probe, one of the variables in the previous fitting process can be fixed. Thus it should be possible to obtain a more accurate estimate of cell viability during the fitting process. The results of the fitting process, shown in Figure 9.11, bear this out: cell culture viabilities can be determined within 10% if the optical and dielectric signals are combined.
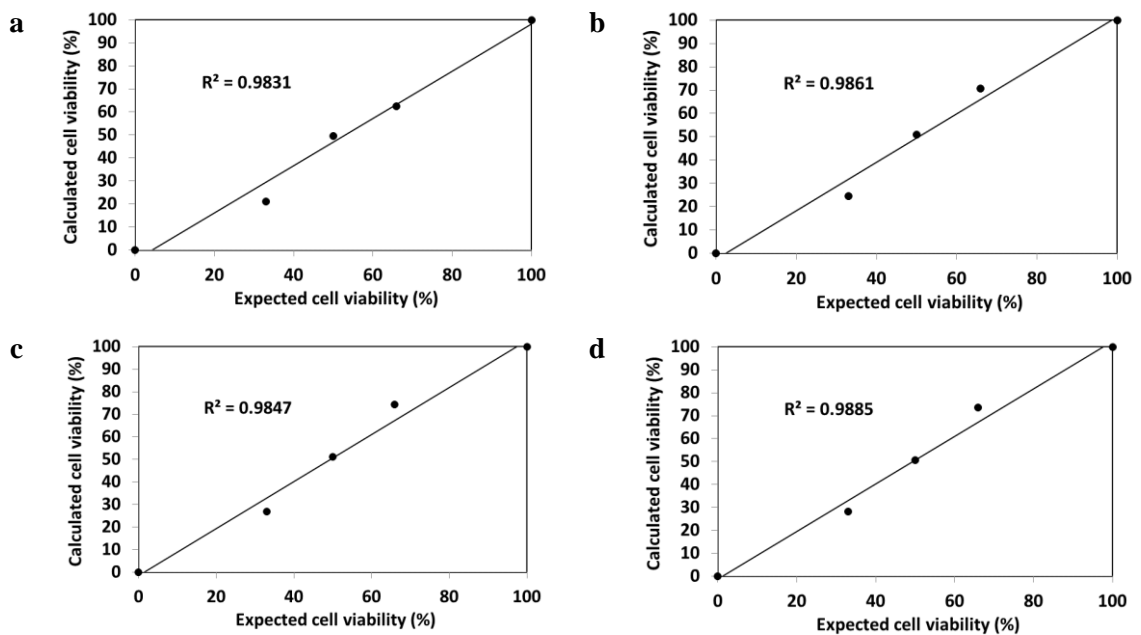
Figure 9.11 Expected and fitted (calculated) cell viabilities for different cell concentrations. Total cell concentrations were estimated using the NIR optical probe. Cell viability was estimated using permittivity data obtained 125 kHz, 374 kHz and 8 MHz. a) 0.4 b) 0.91 c) 1.35 d) 1.62×10^9 cell/ml.

9.4 Conclusions

Biomass level and viability of the cells are two of the most important variables during fermentation. Dielectric spectroscopy gives information on both, but to date separation of the information on viability and cell concentration has remained relatively unexplored.

The first method that was explored for the determination of cell viability was based on that fact that the characteristic frequency of the dispersion of non-viable cells occurred at a lower frequency than that of viable cells. This method used dielectric spectroscopy data only, and therefore has a smaller need for equipment as only one probe was needed. This method had some but limited success. This limited success could arguably be attributed to the fact that the signal of non-viable cell is quite small and occurs in a frequency range in which data are of a lesser quality. Although not available to us for these studies, higher resolution dielectric spectroscopy methods and/or electrodeless measurement methods in which no electrode polarisation occurs could potentially be used overcome this problem.

The second method involved the combined use of a dielectric and an optical probe for biomass measurement. The use of an optical sensor alongside a dielectric probe enabled us to obtain an independent measurement of the cell concentration, and obtain culture viability to within 10%. Further development and optimisation could improve this. Although more demanding on equipment (two sensors are needed rather than one), this method seems most promising.

Finally, only cell viability was investigated in these studies. Simultaneous use of optical and dielectric probes can significantly improve data (Dabros *et al*., 2009), and, if combined with multifrequency analysis of dielectric spectra, allow one to obtain improved estimates of changes in cell properties during cultivation, including their differentiation (Ansorge *et al*, 2010a&b; Opel *et al*., 2010; Bagnanchini and Drumman, 2011).

CHAPTER 10

CONCLUSIONS AND FUTURE WORK

Conclusions

The aim of the work described in the thesis was to investigate the effects of various interfering factors, and develop methods for overcoming these problems. Three different approaches were used. The first approach involved the measurement of dielectric spectra of both the biomass and the interferent. In many cases the frequency dependencies of the dielectric spectrum of biomass and interferent are large enough to decompose the spectra and obtain accurate estimates of the relative contributions of the biomass and the interferent to the spectra. The second approach involves the separation of the interferent from the sensor using a filter. The third approach involves the use of a second sensor in addition to the impedance biomass sensor which gave additional information through which the interferent can be compensated for. The three different approaches were used in a number of settings.

In the case of pre-treated hardwood, the signal from the wood was very small, and the presence of the wood had little effect on the dielectric readings. Measurement of the concentration of yeast in the presence of pretreated wood was therefore straightforward, the main issue being the low cell concentrations and sensitivity of the dielectric sensor probe. Dielectric spectroscopy therefore appears to be a good method for monitoring cellular biomass concentrations during simultaneous saccharification and fermentation of hardwood, and dielectric spectroscopy could potentially be used as a tool to optimize microbial growth during fermentations of lignocellulosic feedstock.

In contrast to wood, the addition of spent grain to a suspension gave a large increase in the (low frequency) permittivity. However, because the dielectric dispersion of the spent grain occurred mainly at low frequencies, and the dielectric dispersion of the yeast at higher frequencies, deconvolution of the relative contribution of spent grain and yeast to a spectrum was possible. It was therefore possible to obtain good estimates of yeast cell concentration despite the presence of spent grain.

170

At conductivity levels above 54 mS/cm the Aber Biomass Monitor model 220 stopped measuring. Below this conductivity the measurement of biomass levels was possible. There was little crosstalk between the conductance and capacitance, and changes in the conductivity had little effect on the baseline. Electrode polarisation however still is a problem, and its magnitude becomes larger with increasing conductivity. Fortunately, the dispersion caused by electrode polarisation also occurs at a lower frequency than that of cells, and deconvolution of the spectra can therefore also be used for compensating a permittivity spectrum for electrode polarisation. A mathematical model was developed to describe electrode polarisation, and used to correct spectra of baker's yeast and the microalga *Nannochloropsis oculata* for the effects of electrode polarisation. This made it possible to obtain estimates of the internal conductivity and membrane capacitance of the yeast and microalgae.

The characteristic frequency of the dispersion of non-viable cells also occurred at a lower frequency than that of viable cells. An attempt to use deconvolution to separate the relative contribution of viable and non-viable cells had some but limited success. The limited success could be attributed to the fact that the signal of non-viable cell is quite small compared to that of viable cells, and also occurs at a very low frequency range in which data are of a lesser quality.

In an attempt to monitor changes in the dielectric properties of suspensions interdigitated microelectrodes were fabricated from indium tin oxide (ITO) on glass with different widths and distances between the electrodes. It was shown that is was feasible to use these microelectrodes for monitoring (yeast) biomass levels in suspensions. Only interdigitated parallel electrodes were used; optimisation of the design is still needed. Electrode polarisation was observed with smaller electrode sizes, which also correlates well with previous findings that electrode polarisation decreases when the current density decreases when the electrode surface area is increased. Wider microelectrode widths and smaller electrode distances gave better signals.

The microelectrodes that were developed were used in a set of experiments in which cells but not medium was prevented from moving to the area near the electrode surface. To achieve this different membranes and agar gel were tested. The results indicated that it is possible to prevent cells from moving to the area near the electrode surface, allowing the measurement of the dielectric properties the suspending medium only.

However, the presence of a gel or membrane on the electrode surface does significantly increase the response time of the system. It could take up to 10 hours to sense changes in the suspending medium when working with membranes and 4 hours for gels. The application of ultrasound improved the response time of a membrane–based system to about 3 hours. This is only slightly better, and the signal was poor. Working with gels seems a simpler and more promising method, but optimisation of the electrodes and gel properties are still needed.

Finally, using an optical sensor alongside a dielectric probe made it possible to simultaneously obtain an independent measurement of the total cell concentration, as well as a signal that is mainly dependent on the concentration of viable cells. This in turn made it possible to not only to compensate biomass measurement based on dielectric spectroscopy for the concentration of non-viable cells, but also obtain culture viability to within 10%.

Overall, the project has been very successful. It has been shown that many interferents that occur during biomass measurement using dielectric spectroscopy can be compensated for using relatively simple mathematical relations, and it has also been shown that developments in sensor technology itself can also help in reducing the contribution of an interferent to the dielectric signal (by keeping the interferent away from the dielectric probe) or by measuring the contribution by the interferent to the signal (which can then be compensated for).

Future work

During the project a comparison was made between an optical probe and a dielectric probe. This provided not only useful data but was also useful by the fact that it pointed to the relative advantages and disadvantages of optical and dielectric approaches towards biomass measurements and the main future directions for the dielectric approach.

The optical approach measured biomass concentration based on the concentration of scattering particles. The technique was quite sensitive to changes in particle concentrations, and noise levels were considerably smaller than for dielectric

measurements. Measurement of small particles was straightforward. The method was quite insensitive to changes in the concentration of soluble compounds, including the concentration of salts. Where dielectric spectroscopy plays to its strength is where selectivity is important. The dielectric method is much more sensitive to the concentrations of particles surrounded by a membrane than particles without one. Therefore, dielectric spectroscopy is quite insensitive to the presence of non-cellular particles compared to optical techniques. The presence of any non-cellular particles immediate gave the optical sensor a high background signal. However, the sensitivity of the dielectric probe was less in comparison and data were noisy. The measurement of biomass levels of cells with a small size seems to be in particular one of the bigger challenges when working with dielectric spectroscopy. Improving the sensitivity of the dielectric technique therefore has to be the first suggestion for future work. Although not available for these studies, an allegedly higher resolution biomass monitor (the "Futura") has been developed by Aber Instruments, and it is hoped that some of the problems associated with instrument sensitivity have already been overcome by the development of this instrument. Additionally, more study should be done concerning the measurement of biomass levels of suspensions of mixed cell types. The development of electrodeless measurement methods in which no electrode polarisation occurs could potentially overcome some of the remaining problems associated with electrode polarisation. The development of specific dielectric sensors could be developed working with membranes or gels with different levels of permeability allowing measurement of the particle or chemical of interest only.

Dielectric spectroscopy as a technique for measuring biomass is solidly based on theory. Potentially dielectric spectroscopy can also be used to determine cell properties such as cell shape and size, lipid content, membrane permeability, membrane folding, membrane potential among others. Being able to determine these on-line and in real-time with greater accuracy would have many applications in the food and biofuel industry, chemical and pharmaceutical production, and medical and biological fields.

CHAPTER 11

REFERENCES

Ahmed, T., Tian, L., Zhang, Y., Ting, K.C. (2011). A review of remote sensing methods for biomass feedstock production. *Biomass and Bioenergy*, 35: 2455-2469.

Al-Muhtaseb, A.H., Hararah, M.A., Megahey, E.K., McMinn, W.A.M., Magee, T.R.A. (2010). Dielectric properties of microwave-baked cake and its constituents over a frequency range of 0.915-2.450 GHz. *Journal of Food Engineering*. 98: 84-92.

Ansorge S, Esteban G, Schmid G (2010a). On-line monitoring of response to nutrient feed additions by multi-frequency permittivity measurements in fed-batch cultivations of CHO cells. *Cytotechnology* 62(2): 121-132.

Ansorge S, Esteban G, Schmid G. (2010b). Multifrequency permittivity measurements enable on-line monitoring of changes in intracellular conductivity due to nutrient limitations during batch cultivations of CHO cells. *Biotechnology Progress*, 26(1): 272-283.

Arnold, W. M., Zimmermann, U., Pauli, W., Benzing, M., Niehrs, C., Ahlers, J. (1988). The comparative influence of substituted phenols (especially chlorophenols) on yeast cells assayed by electro-rotation and other methods. *Biochimica et Biophysica Acta - Biomembranes*, 942: 83-95.

Arnoux, A.S., Preziosi-Belloy, L., Esteban, G., Teissier, P., Ghommidh, C. (2005). Lactic acid bacteria biomass monitoring in highly conductive media by permittivity measurements. *Biotechnology Letters*, 27: 1551-1557.

Asami, K. (1994). The scanning dielectric microscope. *Measurement Science and Technology*, 5: 589-592.

Asami, K. (1999). Effect of cell shape on dielectric behaviour of fission yeast. *Biopchimica et Biophysica Acta-General Subjects*, 1472: 137-141.

Asami, K. (2002). Characterization of heterogeneous systems by dielectric spectroscopy. *Progress in Polymer science*. 27: 1617-1659.

Asami, K. (2006). Dielectric dispersion of erythrocyte ghosts. *Physics Review E.,* 73: 052903.

Asami, K. and Yonezawa, T. (1995b). Dielectric behavior of non-spherical cells in culture. *Biochimica et Biophysica Acta - General Subjects*, 1245: 317-324.

Asami, K., Gheorghiu, E., Yonezawa, T. (1998). Dielectric behavior of budding yeast in cell separation. *Biochimica et Biophysica Acta - General Subjects*, 1381: 234-240.

Asami, K., Gheorghiu, E., Yonezawa, T. (1999). Real-time monitoring of yeast cell division by dielectric spectroscopy. *Biophysical Journal*, 76: 3345-3348.

Asami, K., Hanai, T., Koizumi, N. (1980). Dielectric approach to suspensions of ellipsoidal particles covered with a shell in particular reference to biological cells. *Japanese Journal of Applied Physics*, 19: 359-365.

Bagnaninchi P.O. and Drummond N. (2011). Real-time label-free monitoring of adipose-derived stem cell differentiation with electric cell-substrate impedance sensing. *Proceeding of the Natural Academy of Sciences* USA 108(16): 6462-6467.

Ballesteros, M., Oliva, J.M., Negro, M.J., Manzanares, P., Ballesteros, I. (2004). Ethanol from lignocellulosic materials by a simultaneous saccharification and fermentation process (SFS) with *Kluyveromyces marxianus* CECT 10875. *Process Biochemistry*, 39: 1843-1848.

Barker, S.A., Craig, D.Q.M., Hill, R.M., Taylor, K.M.G. (1994). The low-frequency dielectric response of liposomes. *Journal of Colloid and Interface Science*, 166: 66-72.

Batton, J., Kadaksham, A.J., Nzihou, A., Singh, P., Aubry, N. (2007). Trapping heavy metals by using calcium hydroxyapatite and dielectrophoresis. *Journal of Hazardous Materials*, 139(3): 461-466.

Becker, F.F., Wang, X.B., Huang, Y., Pethig, R., Vykoukal, J., Gascoyne, P.R.C. (1994). The removal of human leukemia cells from blood using interdigitated micro-electrodes. *Journal of Physics D: Applied Physics*, 27: 2659-62.

Bellon-Maurel, V., Orliac, O., Christen, P. (2003). Sensors and measurements in solid state fermentation: a review. *Process Biochemistry*. 38: 881-896.

Bengtsson, N.E. and Risman, P.O. (1971). Dielectric properties of foods at 3 GHz as determined by a cavity perturbation technique. *Journal of Microwave Power EM Energy*, 6: 107-123.

Blanco, M., Iturriaga, H., Maspoch, S., Tarin, P. (1989). A simple method for spectrophotometric determination of two components with overlapped spectra. *Journal of Chemical Education*. 66: 178.

Bohigas, X., Amigo, R., Tejada, J. (2008). Characterisation of sugar content in yogurt by means of microwave spectroscopy. *Food Research International*. 41: 104-109.

Bone, S. and Pethig, R. (1979). Electronic and dielectric properties of protein-methylglyoxal complexes. *Submolecular Biology and Cancer*, 67: 83-98.

Bone, S. and Zaba, B. (1992). Bioelectronics, New York, Wiley.

Bonincontro, A. and Cametti, C. (2004). Interfacial characterization of mesoscopic particle suspensions by means of radiowave dielectric spectroscopy: a minireview. *Colloids and Surfaces A: Physicochemical Engineering Aspects*. 246: 115-120.

Bonincontro, A. and Risuleo, G. (2003). Dielectric spectroscopy as a probe for the investigation of conformational properties of proteins. *Spectrochimica Acta Part A: Molecular and Biomolecular Spectroscopy*, 59(12): 2677-2684.

Bordi, F., Cametti, C., Gili, T. (2001). Reduction of the contribution of electrode polarisation effects in the radiowave dielectric measurements of highly conductive biological cell suspensions. *Bioelectrochemistry*, 54: 53-61.

Brennan, L. and Owende, P. (2010). Biofuels from microalgae. A review of technologies for production, processing and extractions of biofuels and co-products. *Renewable and Sustainable Energy Review* 14: 557-577.

Bryant, D.N., Morris, S.M., Leemans, D., Fish, S.A., Taylor, S., Carvell, J., Todd, R.W., Logan, D., Lee, M., Garcia, N., Ellis, A., Gallagher, J.A. (2011). Modelling real-time simultaneous saccharification and fermentation of lignocellulosic biomass and organic acid accumulation using dielectric spectroscopy. *Bioresource Technology*. 102: 9675-9682.

Bunin, V.D., Ignatov, O.V., Guliy, O.I., Voloshin, A.G., Dykman, L.A., O'Neil, D., Ivnitski, D. (2004). Studies of *Listeria monocytogenes*-antibody binding using electro-orientation. *Biosensors and Bioelectronics*, 19(12): 1759-1761.

Bunin, V.D., Voloshin, A.G., Bunina, Z.F., Shmelev, A.V. (1996). Electrophysical monitoring of culture process of recombinant *Escherichia coli* strains. *Biotechnology and Bioengineering*, 51: 720-724.

Burmeister, J.J., Pomerleau, F., Huettl, P., Gash, C.R., Werner, C.E., Bruno, J.P., Gerhardt, G.A. (2008). Ceramic-based multisite microelectrode arrays for simultaneous measures of choline and acetylcholine in CNS. *Biosensors and Bioelectronics,* 23: 1382-1389.

Cametti, C., DeLuca, F., Macri, M.A., Maraviglia, B., Zimatore, G., Bordi, F., Misasi, R., Sorice, M., Lenti, L., Pavan, A. (1995). To what extent are the passive electrical parameters of lymphocyte membranes deduced from impedance spectrscopy altered by surface roughness and microvillosity? *Colloids Surface B: Biointerference*, 3: 309-316.

Carballo-Cardenas, E.C., Tuan, P.M., Janssen, M., Wijffels, R.H. (2003). Vitamin E (alphatocopherol) production by the marine microalgae *Dunaliella tertiolecta* and *Tetraselmis suecica* in batch cultivation. *Biomedical Engineering,* 20: 139–47.

Carrique, F., Zurita, L., Delgado, V. (1994). Correlation of the dielectric and conductivity properties of polystyrene suspensions with zeta potential and electrolyte concentration. *Journal of Colloid and Interface Science*. 166: 128-132.

Carstensen, E. L. (1967). Passive electrical properties of microorganisms II. Resistance of the bacterial membrane. *Biophysical Journal*, 7: 493-503.

Carstensen, E.L. and Marquis, R.E. (1968). Passive electrical properties of microosganisms III. Conductivity of isolated bacterial cell walls. *Biophysics Journal*, 8: 536-48.

Carstensen, E.L. and Marquis, R.E. (1975). Dielectric and electrochemical properties of bacterial cells. In: Gerhardt P, Costilow RN, Sadoff HL, editors. Spores VI. Sixth international spore conference. Washington, DC: American Chemical Society, 563-71

Carstensen, E.L., Cox, H.A., Mercer, W.B., Natale, L.A. (1965). Passive electrical properties of microorganisms I. Conductivity of *Escherichia coli* and *Micrococcus lysodeikticus*. *Biophysical Journal*, 5: 289-300.

Carvell, J.P and Dowd, J.E. (2006). On-line measurements and control of viable cell density in cell culture manufacturing processes using radio-frequency impedance. *Cytotechnology,* DOI 10.1007/s10616-005-3974-x

Castro-Giraldez, M., Dols, L., Toldra, F., Fito, P. (2011). Development of a dielectric spectroscopy technique for the determination of key biochemical markers of meat quality. *Food Chemistry,* 127(1): 228-233.

Castro-Giraldez, M., Fito, P.J., Chenoll, C., Fito, P. (2010). Development of a dielectric spectroscopy technique for the determination of apple (Granny Smith) maturity. *Innovative Food Science & Emerging Technologies*, 11(4): 749-754.

Castro-Giraldez, M., Fito, P.J., Fito, P. (2011). Application of microwaves dielectric spectroscopy for controlling long time osmotic dehydration of parenchymatic apple tissue. *Journal of Food Engineering*, 104(2): 227-233.

Castro-Giraldez, M., Fito, P.J., Rosa, M.D., Fito, P. (2011). Application of microwaves dielectric spectroscopy for controlling osmotic dehydration of kiwifruit (*Actinidia deliciosa cv Hayward*). *Innovative Food Science & Emerging Technologies*, 12(4): 623-627.

Cen, E., Dalton, C., Li, Y., Adamia, S., Pilarski, L.M., Kaler, K. (2004). A combined dielectrophoresis, travelling wave dielectrophoresis and electrorotation microchip for the manipulation and characterization of human malignant cells. *Journal of Microbiological Methods,* 58: 387-401.

Cevc, G. (1990). Membrane electrostatics. *Biochimica et Biophysica Acta*, 1031: 311-82.

Chan, K.L., Gascoyne, P.R.C., Becker, F.F., Pethig, R. (1997). Electrorotation of liposomes: verification of dielectric multi-shell model for cells. *Biochimica et Biophysica Acta (BBA) - Lipids and Lipid Metabolism*, 1349(2): 183-196.

Chen, H., Hassan, M.K., Peddini, S.K., Mauritz, K.A. (2011). Macromolecular dynamics of sulfonated poly(styrene-*b*-ethylene-*ran*-butylene-*b*-styrene) block copolymers by broadband dielectric spectroscopy. *European Polymer Journal,* 47(10): 1936-1948.

Chen, H., Liu, Y., Zhang, H., Yu, L., Zhu, Y., Li, D. (2010). Separation and manipulation of rare-earth oxide particles by dielectrophoresis. *Chinese Journal of Chemical Engineering*, 18(6): 1034-1037.

Chisti, Y. (2007). Biodiesel from microalgae. *Biotechnology Advances,* 25: 294-306.

Chiu, S.Y; Kao, C.Y; Tsai, M.T; Ong, S.C; Chen, C.H; Lin, C.S. (2009). Lipid accumulation and CO_2 utilization of *Nannochloropsis oculata* in response to CO_2 aeration. *Bioresource Technology*, 100: 833-838.

Christensen, P.V. and Keiding, K. (2008). The use of dielectric spectroscopy for the characterization of polymer-induced flocculation of polystyrene particles. *Journal of Colloid and Interface Science*. 327: 362-369.

Christensen, P.V., Christensen, M.L., Keiding, K. (2011). The use of dielectric spectroscopy for the characterisation of polymer-induced flocculation of core-shell particles. *Journal of Colloid and Interface Science*, 356(2): 681-689.

Cole, K.S. (1972). Membranes, ions and impulses. Berkeley: University of California Press.

Cole, K.S. and Cole, R.H. (1941). Dispersion and absorption in dielectrics. *Journal of Chemical Physics*, 9: 341-351.

Cole, R.H., Berberian, J.G., Mashimo, S., Chryssik, G., Burns, A., Tombari, E. (1989). Time domain reflection methods for dielectric measurements to 10 GHz. *Journal of Applied Physics*, 66: 793-802.

Colella, L., Beyer, C., Frohlich, J., Talary, M., Renaud, P. (2012). Microelectrode-based dielectric spectroscopy of glucose effect on erythrocytes. *Bioelectrochemistry*, 85: 14-20.

Converti, A; Casazza, A.A; Ortiz, E.Y; Perego, P; Del Borghi, M. (2009). Effect of temperature and nitrogen concentration on the growth and lipid content of *Nannochloropsis oculata* and *Chlorella vulgaris* for biodiesel production. *Chemical Engineering and Processing: Process Intensification*, 48: 1146-1151.

Costa, J.A.V. and de Morais, M.G. (2011). The role of biochemical engineering in the production of biofuels from microalgae. *Bioresource Technology*, 102: 2-9.

Costa, L.C. (2011). Double relaxation processes in the glass system xEu$_2$O$_3 \cdot$PbO$\cdot$2B$_2$O$_3$ studied by broadband dielectric spectroscopy. *Journal of Non-Crystalline Solids*, 357(10): 2178-2181.

Coster, H.G.L., Chilcott, T.C., Coster, A.C.F. (1996). Impedance spectroscopy of interfaces, membranes and ultrastructures. *Bioelectrochemistry and Bioenergetics*, 40: 79-98.

Dabros M, Amrhein M, Bonvin D, Marison IW, von Stockar U (2009). Data reconciliation of concentration estimates from mid-infrared and dielectric spectral measurements for improved on-line monitoring of bioprocesses. *Biotechnology Progress,* 25(2): 578-588.

Davey, C.L. and Kell, D.B. (1995). The low-frequency dielectric properties of biological cells. *Bioelectrochemistry of Cells and Tissues*, 159-207.

Davey, C.L. and Kell, D.B. (1998a). The influence of electrode polarisation on dielectric spectra, with special reference to capacitive biomass measurements: I. Quantifying the effects on electrode polarisation of factors likely to occur during fermentations. *Bioelectrochemistry and Bioenergetics*. 46: 91-103.

Davey, C.L. and Kell, D.B. (1998b). The influence of electrode polarisation on dielectric spectra, with special reference to capacitive biomass measurements: II. Reduction in the contribution of electrode polarisation to dielectric spectra using a two-frequency method. *Bioelectrochemistry and Bioenergetics*. 46: 105-114.

Davey, C.L., Davey, H.M., Kell, D.B. (1992). On the dielectric properties of cell suspensions at high volume fractions. *Bioelectrochemistry and Bioenergetics.* 28: 319-340

Davey, C.L., Davey, H.M., Kell, D.B. (1993a). Introduction to the dielectric estimation of cellular biomass in real time, with special emphasis on measurements at high volume fractions. *Analytica Chimica Acta,* 279: 155-161.

Davey, C.L., Markx, G.H., Kell, D.B. (1990). Substitution and spreadsheet methods for analysing dielectric spectra of biological systems. *European Biophysics Journal*, 18: 255-265.

Davey, C.L., Markx, G.H., Kell, D.B. (1993b). On the dielectric method of monitoring cellular viability. *Pure & Applied Chemistry*, 65: 1921-1926.

Davey, C.L., Peñaloza, W., Kell, D.B., Hedger, J.N. (1991). Real-time monitoring of the accretion of *Rhizopus oligosporus* biomass during the solid-substrate tempe fermentation. *World Journal of Microbiology and Biotechnology*, 7(2): 248-259.

Davey, H.M., Davey, C.L., Woodward, A.M., Edmonds, A.N., Lee A.W., Kell, D.B. (1996). Oscillatory, stochastic and chaotic growth rate fluctuations in permittistatically controlled yeast cultures. *Biosystems,* 39(1): 43-61.

Day, J.G., Thomas, N.J., Achilles-Day, U.E.M., Leakey, R.J.G. (2012). Early detection of protozoan grazers in algal biofuel cultures. *Bioresource Technology*, 114: 715-719.

Debye, P. (1929). Polar molecules. *New York, The Chemical Catalog Company, inc.*

Della Porta, G., Castaldo, F., Scognamiglio, M., Paciello, L., Parascandola, P., Reverchon, E. (2012). Bacteria microencapsulation in PLGA microdevices by supercritical emulsion extraction. *The Journal of Supercritical Fluids*, 63: 1-7.

Demirbas, A. (2010). Use of algae as biofuel sources. *Energy Conversion and Management*, 51: 2738-2749.

Di Basio, A. and Cametti, C. (2007). Effect of shape on the dielectric properties of biological cell suspensions. *Bioelectrochemistry*. 71: 149-156.

Di Basio, A., Ambrosone, L., Cametti, C. (2010). The dielectric behavior of nonspherical biological cell suspensions: An analytic approach. *Biophysical Journal*, 99: 163-174.

Dong, L., Huang, J.P., Yu, K.W. (2004). Theory of dielectrophoresis in colloidal suspensions. *Journal of Applied Physics*. 95: 8321-8326.

Du, H., Li, Y., Cao, C. (2010). Effect of temperature on dielectric properties of Si_3N_4/SiO_2 composite and silica ceramic. *Journal of Alloys and Compounds,* 503(1): L9-L13.

Duncan, L., Shermerdine, H., Hughes, M.P., Coley, H.M., Hubner, Y., Labeed, F.H. (2008). Dielectrophoretic analysis of changes in cytoplasmic ion levels due to ion channel blocker action reveals underlying differences between drug-sensitive and multidrug-resistant leukaemic cells. *Physics in Medicine and Biology*. 53: N1-N7.

Dziong, D., Kearney, R.E., Tabrizian, M., Bagnaninchi, P.A. (2005). A highly responsive system for online in vitro assessment of tissue growth within microporous polymer scaffolds. *Conference Proceedings - IEEE Engineering in Medicine and Biology Society*. 1: 1043-1046.

Ehret, R., Baumann, W., Brischwin, M., Schwinde, A., Stegbauer, K., Wolf, B. (1997). Monitoring of cellular behaviour by impedance measurements on interdigitated electrode structures. *Biosensors and Bioelectronics,* 12: 29-41.

Fairchild Semiconductor (2002). Section 6 - Noise, Cross-talk, Jitter, Skew, and EMI Backplane Designer's Guide. www.fairchildsemi.com/ms/MS/MS-566.pdf

Falokun, C.D. and Markx, G.H. (2007). Electrorotation of beads of immobilized cells. *Journal of Electrostatics*, 65(7): 475-482.

Feldman, Y., Kozlovich, N., Nir, I., Garti, N. (1997). Dielectric spectroscopy of microemulsions. *Colloids and Surfaces A: Physicochemical and Engineering Aspects*, 128(1-3): 47-61.

Feng, H., Tang, J., Cavalieri, R.P. (2002). Dielectric properties of dehydrated apples as affected by moisture and temperature. *Transactions of the American Society of Agricultural Engineers*, 45: 129-135.

Fernandez, D.P., Mulev, Y., Goodwin, A.R.H., Levelt Sengers, J.M.H. (1995) A database for the static dielectric constant of water and steam. *Journal of Physical and Chemical Reference Data*, 24(1): 33-69.

Ferreira, A.P., Vieira, L.M., Cardoso, J.P., Menezes, J.C. (2005) Evaluation of a new annular capacitance probe for biomass monitoring in industrial pilot-scale fermentations. *Journal of Biotechnology*, 116: 403-409.

Ferris, L.E., Davey, C.L., Kell, D.B. (1990). Evidence from its temperature dependence that the β-dielectric dispersion of cell suspensions is not due solely to the charging of a static membrane capacitance. *European Biophysics Journal*, 18: 267-276.

Foster, K.R. and Schwan, H.P. (1989). Dielectric properties of tissues and biological materials: a critical review. *Critical Reviews in Biomedical Engineering* 17: 25-104

Frangi, J.P., Richard, D.C., Chavanne, X., Bexi, I., Sagnard, F., Guilbert, V. (2009). New *in situ* techniques for the estimation of the dielectric properties and moisture content of soils. *Comptes Rendus Geoscience*, 341(10-11): 831-845.

Free, C. and Henry, M. (2007). Ceramics to 100 GHz: Including a novel free space dielectric measurement technique. *Journal of the European Ceramic Society*, 27(8-9): 2811-2815.

Fricke, H. (1923). The electric capacity of cell suspensions. *Physical Review*, xxi, 708.

Fricke, H. (1924). A mathematical treatment of the electrical conductivity and capacity of disperse systems. I. The electrical conductivity of a suspension of homogeneous spheroids. *Physical Review*, 24: 575-587.

Fricke, H. (1925). A mathematical treatment of the electrical conductivity and capacity of disperse systems. II. The capacity of a suspension of conducting spheroids surrounded by a non-conducting membrane for a current of low frequency. *Physical Review*, 26: 678-681.

Fricke, H. (1931). The electrical conductivity and capacity of disperse systems. *Physics*, 1: 106-115.

Fricke, H. (1953). The electric permittivity of a dilute suspension of membrane-covered ellipsoids. *Journal of Applied Physics*, 24: 644-646.

Fricke, H. (1955). The complex conductivity of a suspension of stratified particles of spherical or cylindrical form. *Journal of Physical Chemistry*, 59: 168-170.

Fröhlich, H. (1949) Theory of dielectrics. 2nd Ed. *The Clarendon Press*, 180p.

Fuhr, G., Schnelle, T., Hagedorn, R., Shirley, S.G. (1995). Dielectrophoretic field cages: Technique for cell, virus and macromolecule handling. *Cellular Engineering inc Molecular Engineering*, 1: 47-57.

Gabriel, C., Gabriel, S., Corthout, E. (1996a). The dielectric properties of biological tissues: I. Literature survey. *Physical Medical Biology*. 41: 2231-2249.

Gabriel, C., Lau, R.W., Gabriel, S. (1996b) The dielectric properties of biological tissues: II. Measurements in the frequency range 10Hz to 20GHz. *Physical Medical Biology*. 41: 2251-2269.

Gabriel, S., Lau, R.W., Gabriel, S. (1996c). The dielectric properties of biological tissues: III. Parametric models for the dielectric spectrum of tissues. *Physics in Medicine and Biology*. 41: 2271-2293.

Garcia-Casal, M.N., Ramirez, J., Leets, I., Pereira, A.C. Quiroga, M.F. (2009). Antioxidant capacity, polyphenol content and iron bioavailability from algae (*Ulva sp.,Sargassum sp. and Porphyra sp*.) in human subjects. *British Journal of Nutrition,* 101: 79–85.

Gascoyne, P.R.C., Wang, X.B., Huang, Y., Becker, F.F. (1997). Dielectrophoretic separation of cancer cells from blood. *IEEE Transactions on Industry Applications*, 33: 670-8.

Gellissen, G. and Hollenberg, C.P. (1997). Application of yeasts in gene expression studies: a comparison of *Saccharomyces cerevisiae, Hansenula polymorpha* and *Kluyveromyces lactis* – a review. *Gene*, 190: 87-97.

Gheorghiu, E. (1993). The resting potential in relation to the equivalent complex permittivity of a spherical cell suspension. *Physics in Medicine and Biology*, 38: 979-88.

Gheorghiu, E. (1999). On the limits of ellipsoidal models when analyzing dielectric behavior of living cells - Emphasis on red blood cells. *Electrical Bioimpedance Methods: Applications to Medicine and Biotechnology*. 873: 262-268.

Gheorghiu, E. (2011). Relating membrane potential to impedance spectroscopy. *Journal of Electrical Bioimpedance,* 2: 93-97.

Giaever, I. and Keese, C.R. (1992). Toxic? Cells can tell. *Chemtech,* Feb. 116-125.

Gimsa, J. (2001). A comprehensive approach to electro-orientation, electrodeformation, dielectrophoresis, and electrorotation of ellipsoidal particles and biological cells. *Bioelectrochemistry*, 54: 23-31.

Ginzburg, M., Lepkipfer, B., Porath, A., Ginzburgh, B.A. (1978). Passive electrical properties of halobacterium species I. Low-frequency range. *Biophysics,* 4: 237-249.

Gokcen, M. and Altuntas, H. (2009). On the profile of temperature dependent electrical and dielectric properties of $Au/SiO_2/n$-GaAs (MOS) structures at various frequencies. *Physica B: Condensed Matter*, 404(21): 4221-4224.

Gonchariva, L.V., Barinova, V.I., Egorov, U.M., Fedorov, V.M. (1991). Dielectric properties of disperse soils in microwave range. *Proceedings International Conference of Application of Microwave Energy in Technology and Science*, Saratov, Russia, pp. 104-105

Grant, E.H., Sheppard, R.J., South, G.P. (1978). Dielectric Behaviour of Biological Molecules in Solution, Oxford, UK, Oxford University Press.

Gray, S.A., Kusel, J.K., Shaffer, K.M., Shubin, Y.S., Stenger, D.A., Pancrazio, J.J. (2001). Design and demonstration of an automated cell-based biosensor. *Biosensors and Bioelectronics,* 16: 535–542.

Green, N.G., A. Ramos, H. Morgan. (2002). Numerical solution of the dielectrophoretic and travelling wave forces for interdigitated electrode arrays using the finite element method. *Journal of Electrostatics,* 56: 235–254.

Griffiths, M.J., Garcin, C., Van Hille, R.P., Harrison, S.T.L. (2011). Interference by pigment in the estimation of microalgal biomass concentration by optical density. *Journal of Microbiological Methods,* 85: 119-123.

Grosse, C., Delgado, A.V. (2010). Dielectric dispersion in aqueous colloidal systems. *Current Opinion in Colloid & Interface Science*, 15(3): 145-159.

Guan, L., Fen, X.L., Li, Z.C., Lin, G.M. (2009). Determination of octane numbers for clean gasoline using dielectric spectroscopy. *Fuel*, 88(8): 1453-1459.

Guan, L., Feng, X.L., Xiong, G., Xie, J.A. (2011). Application of dielectric spectroscopy for engine lubricating oil degradation monitoring. *Sensors and Actuators A: Physical*, 168(1): 22-29.

Guo, W., Liu, Y., Zhu, X., Wang, S. (2011). Dielectric properties of honey adulterated with sucrose syrup. *Journal of Food Engineering*. 107: 1-7.

Guo, W., Zhu, X., Liu, Y., Zhuang, H. (2010). Sugar and water contents of honey with dielectric property sensing. *Journal of Food Engineering*. 97: 275-281.

Gurr, L.M. (1965). The rational use of dyes in biology. p. 213-214. London

Gwo, J.C., Chiu, J.Y., Chow, C.C; Cheng, H.Y. (2005). Cryopreservation of a marine microalga, *Nannochloropsis oculata* (Eustigmatophyceae). *Cryobiology*, 50: 338-343.

Haggis, G.H., Hasted, J.B., Buchanan, T.J. (1952). The dielectric properties of water in solutions. *The Journal of Chemical Physics*, 20(9): 1452-1465.

Hamlin, M.G., Bowden A.L., Evans, N.G. (1995). Measurement and use of high temperature dielectric properties in ceramic processing, *Process International Conference in Microwave and High-Frequency Heating '95*, Cambridge, UK, pp 11-14.

Hanai, T., Doizumi, N., Gotoh, R. (1959). Dielectric properties of emulsions I. Dielectric constants of O/W emulsions. *Colloid & Polymer Science*, 167: 41-43.

Hanai, T., Haydon, D.A., Taylor, J. (1964). An investigation by electrical methods of lecithin-in-hydrocarbon films in aqueous solutions. *Proceedings of the Royal Society of London. Series A*, 281: 377-391.

Hanai, T., Koizumi, N., Gotoh, R. (1962). Dielectric constants of emulsions. *Bulletin of the Institute for Chemical Research Kyoto University*. 40: 240-270.

Hanumantharao, R. and Kalainathan, S. (2012). Growth, spectroscopy, dielectric and nonlinear optical studies of novel organic NLO crystal: L-Threonine formate. *Spectrochimica Acta Part A: Molecular and Biomolecular Spectroscopy*, 94: 78-83.

Harris, C.M. and Kell, D.B. (1985). The estimation of microbial biomass. *Biosensors*, 1: 17-84.

Harris, C.M., Todd, R.W., Bungard, S.J., Lovitt, R.W., Morris, J.G., Kell, D.B. (1987). Dielectric permittivity of microbial suspensions at radio frequencies: a novel method for the real-time estimation of microbial biomass. *Enzyme and Microbial Technology*, 9: 181-186.

Harris, D.C. (2007). Quantitative Chemical Analysis. 7th Ed., Freeman.

Harun, R; Singh, M; Forde, G.M; Danquah, M.K. (2010). Bioprocess engineering of microalgae to produce a variety of consumer products. *Renewable and Sustainable Energy Reviews*, 14: 1037-1047.

Hasted, J.B., Ritsom, D.M., Collie, C.H. (1948). Dielectric properties of aqueous ionic solutions. Parts I and II. *The Journal of Chemical Physics*, 16(1): 1-21.

Hause, L.L., Komorowski, R.A., Gayon, F. (1981). Electrode and electrolyte impedance in the detection of bacterial growth. *IEEE Transactions on Biomedical Engineering,* 28: 403-410.

Heer, F., Franks, W., Blau, A., Taschini, S., Ziegler, C., Hierlemann, A., Baltes, H. (2004). CMOS microelectrode array for the monitoring of electrogenic cells. *Biosensors and Bioelectronics*. 20: 358–366.

Hill, R.M. and Jonscher, A.K. (1983). The dielectric behaviour of condensed matter and its many-body interpretation. *Contemporary Physics*. 24: 75-110.

Hinman, N.D., Schell, D.J., Riley, C.J., Bergeron, P., Walter, P.J. (1992). Preliminary estimate of the costo of ethanol production for simultaneous saccharification and fermentation technology. *Applied Biochemistry and Biotechnology*. 34/35: 639-649.

Hipp, J.E. (1974). Soil electromagnetic parameters as a function of frequency, soil density and soil moisture. *Proceedings of the IEEE*, 62: 98-103.

Hober, R. (1910). Eine Methode, die Elektrische Leitfahigkeit im Innern von Zellen zu messen. *Arch Ges Psysiol*, 133: 237-59.

Hocalar, A., Turker, M., Karakuzu, U., Yuzgec, U. (2011). Comparison of different estimation techniques for biomass concentration in large scale yeast fermentation. *ISA transactions*, 50: 303-314.

Hoekstra, P. and Delaney, A. (1974). Dielectric properties of soils at UHF and microwave frequencies. *Journal of Geophysical Research*, 79: 1699-1708.

Huang, Y., Hölzel, R., Pethig, R., Wang, XB. (1992). Differences in the AC electrodynamics of viable and non-viable yeast cells determined through

combined dielectrophoresis and electrorotation studies. *Physics in Medicine and Biology*. 37: 1499-1517.

Iglesias, F.J., Lopez, M.C., Santamaria, C., Dominguez, A. (1985). Orientation of Schizosaccharomyces pombe nonliving cells under alternating uniform and nonuniform electric fields. *Biophysical Journal*, 48: 721-726.

Ikediala, J.N., Hansen, J., Tang, J., Drake, S.R., Wang, S. (2002). Development of saline-water-immersion technique with RF energy as a postharvest treatment against codling moth in cherries. *Postharvest Biology and Technology*, 24: 25-37.

Irimajiri, A., Hanai, T., Inouye, A. (1979). A dielectric theory of "multi-stratified shell" model with its application to a lymphoma cell. *Journal of Theoretical Biology*, 78(2): 251-269.

Ishikawa, A., Hanai, T., Koizumi, N. (1981). Evaluation of relative permittivity and electrical conductivity of ion-exchange beads by analysis of high-frequency dielectric relaxations. *Japanese Journal of Applied Physics*, 20: 79-86.

James, A.M. (1982). The electrical properties and topochemistry of bacterial cells. *Advances in Colloid and Interface Science*, 15: 171-221.

Jeong, H.J., Jung, Y.H., Lee, D.W. (2009). Attaching single carbon nanotube on tip's apex using dielectrophoresis of DC-pulse voltage. *Transactions of Nonferrous Metals Society of China*, 19(1): s280-s283.

Jones, T.B. (1990). Frequency-dependent orientation of isolated particle chains. *Journal of Electrostatics*, 25: 231-244.

Jones, T.B. (1995). Electromechanics of particles. Cambridge: Cambridge University Press.

Justice, C., Brix, A., Freimark, D., Kraume, M., Pfromm, P., Eichenmueller, B., Czermak, P. (2011). Process control in cell culture technology using dielectric spectroscopy. *Biotechnology Advances*, 29: 391-401.

Kakutani, T., Shibatani, S., Sugai, M. (1993). Electrorotation of non-spherical cells: Theory for ellipsoidal cells with an arbitrary number of shells. *Bioelectrochemistry and Bioenergy*, 31: 131-145.

Kalakkunnath S., Kalika, D.S., Lin, H., Raharjo, R.D., Freeman, B.D. (2007). Molecular relaxation in cross-linked poly(ethylene glycol) and poly(propylene glycol) diacrylate networks by dielectric spectroscopy. *Polymer*, 48(2): 579-589.

Kazarnovskiy, D.M. and Yamanov, S.A. (1972). Radio engineering materials. Vishaya Shkola Issue, Moscow.

Keim, C.R. and Venkatasubramanian, K. (1989). Economics of current biotechnological methods of producing ethanol. *Trends in Biotechnology*, 7: 22-29.

Kell, D.B., Markx, G.H., Davey, C.L., Todd, R.W. (1990). Real time monitoring of cellular biomass: methods and applications. *Trends in Analytical Chemistry*. 9: 190-194.

Kent, M. (1987). Electrical and dielectric properties of food materials. COST 90bis Production, Science and Technology Publishers, Hornchurch, Essex, UK.

Kivijarju K, Solaonen K, Moilanen U, Eerikäinen T (2008). Biomass measurement online: the performance of in situ measurements and software sensors *Journal of Industrial Microbiology and Biotechnology,* 53: 657-665.

Kolodiazhnyi, T., Annino, G., Younker, A., Malysz, P., Mascher, P., Haneda, H. (2006). Probing point defects in Ba($B'_{1/3}B''_{2/3}$)O$_3$ by ESR, PAS and dielectric spectroscopy. *Journal of the European Ceramic Society*, 26(10-11): 1921-1924.

Kremer, F. and Schonhals, A. (2002). Broadband Dielectric Spectroscopy. Springer, Berlin.

Krishna, S.H., Reddy, T.J., Chowdary, G.V. (2001). Simultaneous saccharification and fermentation of lignocellulosic wastes to ethanol using a thermotolerant yeast. *Bioresource Technology*, 77: 193-196.

Krupka, J. (2003). Developments in techniques to measure dielectric properties of low-loss materials at frequencies of 1-50 GHz. *Journal of the European Ceramic Society*, 23(14): 2607-2610.

Krupka, J., Gregory, A.P., Rochard, O.C., Clarke, R.N., Riddle, B., Baker-Jarvis, J. (2001). Uncertainty of complex permittivity measurements by split-post dielectric resonator technique. *Journal of the European Ceramic Society*, 21(15): 2673-2676.

Kua, C.H., Lam, Y.C., Yang, C., Youcef-Toumi, K., Rodriguez, I. (2008). Modeling of dielectrophoretic force for moving dielectrophoresis electrodes. *Journal of Electrostatics*, 66(9-10): 514-525.

Laczka, O., Ferraz, R.M., Ferrer-Miralles, N., Villaverde, A., Munoz, F.X., Campo, F.J. (2009). Fast electrochemical detection of anti-HIV antibodies: Coupling allosteric enzymes and disk microelectrode arrays. *Analytica Chimica Acta*. 641: 1–6.

Lee, R.E. (2008). Phycology. 4th ed. Cambridge University Press.

Li, J.K., Asali, E.C., Humphrey, A.E., (1991). Monitoring cell concentration and activity by multiple excitation fluorometry. *Biotechnology Progress,* 7: 21–27.

Liao, X., Raghavan, G.S.V., Dai, J., Yaylayan, V.A. (2003). Dielectric properties of α-D-glucose aqueous solutions at 2450 MHz. *Food Research International*. 36: 485-490.

Limayem, A. and Ricke, S.C. (2012). Lignocellulosic biomass for bioethanol production: Current perspectives, potential issues and future prospects. *Progress in Energy and Combustion Science*, 38(4): 449-467.

Liu, F., Turner, I., Siores, E., Groombridge, P. (1996). A numerical and experimental investigation of the microwave heating of polymer materials inside a ridge waveguide. *International Journal of Microwave Power EM Energy*, 31: 71-82.

Liu, J. and Li, G. (2000). Application of biosensors for diagnostic analysis and bioprocess monitoring. *Sensors and Actuators B,* 65: 26-31.

Lizhi, H., Toyoda, K., Ihara, I. (2008). Dielectric properties of edible oils and fatty acids as a function of frequency, temperature, moisture and composition. *Journal of Food Engineering,* 88(2): 151-158.

Markx, G.H. and Davey, C.L. (1999). The dielectric properties of biological cells at radiofrequencies: Applications in biotechnology. *Enzyme and Microbial Technology*, 25: 161-171.

Markx, G.H. and Kell, D.B. (1995). The use of dielectric permittivity for the control of the biomass level during biotransformations of toxic substrates in continuous culture. *Biotechnology Progress,* 11: 64-70.

Markx, G.H. and Pethig, R. (1995). Dielectrophoretic separation of cells: Continuous separation. *Biotechnology and Bioengineering*, 45: 337-343.

Markx, G.H., Alp, B., McGilchrist, A. (2002). Electro-orientation of *Schizosaccharomyces pombe* in high conductivity media. *Journal of Microbial Methods*, 50(1): 55-62.

Markx, G.H., Davey, C.L., Kell, D.B. (1991). To what extent is the magnitude of the Cole-Cole alpha of the beta-dielectric dispersion of cell suspension explicable in terms of the cell size distribution? *Bioelectrochemistry and Bioenergetics,* 25(2): 195-211.

Markx, G.H., Dyda, P.A., Pethig, R. (1996). Dielectrophoretic separation of bacteria using a conductivity gradient. *Journal of Biotechnology*, 51: 175-80.

Markx, G.H., Talary, M.S., Pethig, R. (1994). Separation of viable and non-viable yeast using dielectrophoresis. *Journal of Biotechnology*, 32: 29-37.

Marrakchi, M., Vidic, J., Jaffrezic-Renault, N., Martelet, C., Pajot-Augy, E. (2007). A new concept of olfactory biosensor based on interdigitated microelectrodes and

immobilized yeast expressing the human receptor OR17-40. *European Biophysics Journal,* 36: 1015-1018.

Maskow, T., Rollich, A., Fetzer, I., Ackermann, J., Harms, H. (2008). On-line monitoring of lipid storage in yeasts using impedance spectroscopy. *Journal of Biotechnology*, 135: 64-70.

Masoud, M.S., Ali, A.E., Mohamed, R.H., Mostafa, M.A.E.Z. (2005). Dielectric relaxation spectroscopy of heteronuclear cobalt(II)-copper(II) complex of 1-phenyl-3-methyl-5-pyrazolone. *Spectrochimica Acta Part A: Molecular and Biomolecular Spectroscopy,* 62(4-5): 1114-1119.

Maxwell, J. C. (1873). A Treatise on Electricity and Magnetism, Oxford, UK, Clarendon Press.

McCrystal, C.B., Ford, J.L., He, R., Craig, D.Q.M., Rajabi-Siahboomi, A.R. (2002). Characterisation of water behaviour in cellulose ether polymers using low frequency dielectric spectroscopy. International Journal of Pharmaceutics, 243(1-2): 57-69.

Miklavcic, D., Pavselj, N., Hart, F.X. (2006). Electric properties of tissues. *Wiley Encyclopedia of Biomedical Engineering*. 1-12.

Mopsik, F.I. and Martzloff, F.D. (1990). Time domain spectroscopy to monitor the condition of cable insulation. *Nuclear Engineering and Design*, 118(3): 505-512.

Morgan, H., Ginzburg, M., Ginzburg, B.Z. (1987). Dielectric properties of the halophilic bacteria *Halobacterium halobium* and *H. marismortui* with reference to the conductivities and permittivities of the cytoplasmic membrane and intracellular phases. *Biochimica et Biophysica Acta*, 924(1): 54-66.

Morgan, H., Izquierdo, A.G., Bakewell, D., Green, N.G., Ramos, A. (2001). The dielectrophoretic and travelling wave forces generated by interdigitated electrode arrays: analytical solution using Fourier series. *Journal of Physics D: Applied Physics,* 34: 1553–1561.

Morganti, D. and Morgan, H. (2011). Characterization of non-spherical polymer particles by combined electrorotation and electroorientation. *Colloids and Surfaces A: Physicochemical and Engineering Aspects*, 376(1-3): 67-71.

Morin, F.O., Takamura, Y., Tamiya, E. (2005). Investigating neuronal activity with planar microelectrode arrays: achievements and new perspectives. *Journal of Bioscience and Bioengineering,* 100: 131–143.

Moser, I., Jobst, G., Urban, G.A. (2002). Biosensor arrays for simultaneous measurement of glucose, lactate, glutamate, and glutamine. *Biosensors & Bioelectronics*, 17: 297-302.

Naik, S.N., Goud, V.V., Rout, P.K., Dalai, A.K. (2010). Production of first and second generation biofuels: A comprehensive review. *Renewable and Sustainable Energy Reviews*, 14: 578-597.

Natarajan, A., Molnar, P., Sieverdes, K., Jamshidi, A., Hickman, J.J. (2006). Microelectrode array recordings of cardiac action potentials as a high throughput method to evaluate pesticide toxicity. *Toxicology in Vitro,* 20: 375–381.

Neuman, E., Sowers, A.E., Jordan, C.A., (1989). Electroporation and electrofusion in cell biology. New York: Plenum Press.

Ng, S.K., Ainsworth, P., Plunkett, A., Haigh, A.D., Gibson, A.A.P., Parkinson, G., Stojceska, V., Jacobs, G. The characterisation of extruded brewer's spent grain and resistant starch using a microwave transmission line technique. *Journal of Food Engineering*, 83: 614-620.

Nguyen, Q.A. and Saddler, J.N. (1991). An integrated model for the technical and economic evaluation of an enzymatic biomass conversión process. *Bioresource Technology,* 35: 275-282.

Nicholson, D.J., Kell, D.B., Davey, C.L. (1996). Deconvolution of the dielectric spectra of microbial cell suspensions using multivariate calibration and artificial neural networks. *Bioelectrochemistry and Bioenergetics*, 39: 185-193.

Nigam, P.S. and Singh, A. (2011). Production of liquid biofuels from renewable resources. Review. *Progress in Energy and Combustion Science*, 37: 52-68.

Noll, T. and Biselli, M. (1998). Dielectric spectroscopy in the cultivation of suspended and immobilized hybridoma cells. *Journal of Biotechnology*. 63(3): 187-198.

Nurge, M.A. (2012). In situ dielectric spectroscopy for water detection on the lunar surface. *Planetary and Space Science*, 65(1): 76-82

O'Konski, C.T. (1960). Electric properties of macromolecules. V. Theory of ionic polarisation in polyelectrolytes. *The Journal of Physical Chemistry*. 64: 605-619.

Okiror, G.P. and Jones, C.L. (2012). Effect of temperature on the dielectric properties of low acylgellan gel. *Journal of Food Engineering*, 113(1): 151-155.

Olson, L. and Hahn-Hagerdal, B. (1996). Fermentation of lignocellulosic hydrolysates for ethanol production. *Enzyme and Microbial Technology*. 18: 312-331.

Opel CF, Li JC, Amanullah A (2010). Quantitative modelling of viable cells density, cell size, intracellular conductivity, and membrane capacitance in batch and fed-

batch CHO processes using dielectric spectroscopy. *Biotechnology Progress,* 26(4): 1187-1199.

Palmisano, F., Rizzi, R., Centonze, D., Zambonin, P.G. (2000). Simultaneous monitoring of glucose and lactate by an interference and cross-talk free dual electrode amperometric biosensor base don electropolymerized thin films. *Biosensors and Bioelectronics*, 15: 531-539.

Palmqvist, E., Hahn-Hagerdal, B. (2000). Fermentation of lignocellulosic hydrolysates II: inhibitors and mechanisms of inhibition. *Bioresource Technology*. 74: 25-33.

Panagopoulou, A., Kyritsis, A., Sabater, R., Serra, I., Gomez-Ribelles, J.L., Shinyashiki, N., Pissis, P. (2011). Glass transition and dynamics in BSA-water mixtures over wide ranges of composition studied by thermal and dielectric techniques. *Biochimica et Biophysica Acta (BBA)-Proteins and Proteomics*, 1814(12): 1984-1996.

Patel, P. (2009). Multi-frequency dielectric spectroscopy of fermentations. Thesis, The University of Manchester.

Patel, P.M. and Markx, G.H. (2008). Dielectric measurement of cell death. *Enzyme and Microbial Technology,* 43: 463-470.

Patel, P.M., Bhat, A., Markx, G.H. (2008). A comparative study of cell death using electrical capacitance measurements and dielectrophoresis. *Enzyme and Microbial Technology,* 43: 523-530.

Pauly, H. and Schwan, H.P. (1959). Über die impedanz einer suspension von Kugelformigen Teilchen mit einer Schale. *Zeiting der Naturforschung*, 14 B: 125-131.

Peñaloza, W., Davey, C.L., Hedger, J.N., Kell, D.B. (1992). Physiological studies on the solid-state quinoa tempe fermentation, using on-line measurements of fungal biomass production. *Journal of the Science of Food and Agriculture*, 59(2): 227-235.

Pethig, R. (1979). Dielectric and Electronic Properties of Biological Materials. Chichester, Wiley.

Pethig, R. (1990). Application of AC electrical fields to the manipulation and characterization of cells. In: Karube I, editor. Proceedings of the Fourth Toyota Conference. Amsterdam: Elsevier, 159-185.

Pethig, R. and Kell, D.B. (1987). The passive electrical properties of biological systems: Their significance in physiology, biophysics and biotechnology. *Physics in Medicine and Biology*, 32: 933-970.

Pethig, R., Burt, J.P.H., Parton, A., Rizvi, N., Talary, M.S., TAME, J.A. (1998). Development of biofactory-on-a-chip technology using excimer laser micromachining. *Journal of Micromechanics and Microengineering*, 8: 57-63.

Petiot, E., Bernard-Moulin, P., Magadous, T., Geny, C., Pinton, H., Marc, A. (2010). *In situ* quantification of microcarrier animal cell cultures using near-infrared spectroscopy. *Process Biochemistry,* 45: 1832-1836.

Peyman, A. (2011). Dielectric properties of tissues; variation with age and their relevance in exposure of children to electromagnetic fields; state of knowledge. *Progress in Biophysics and Molecular Biology*. 107: 434-438.

Pohl, H.A. (1978). Dielectrophoresis, Cambridge, UK, Cambridge University Press.

Prodan, C. and Bot, C. (2009). Correcting the polarisation effect in very low frequency dielectric spectroscopy. *Journal of Physics D: Applied Physics*, 42: 175505.

Richter, L., Stepper, C., Mak, A., Reinthaler, A., Heer, R., Kast, M., Bruckl, H., Ertl, P. (2007). Development of a microfluidic biochip for online monitoring of fungal biofilm dynamics. *Lab on a Chip*, 7: 1723-1731.

Rodgers, R.S. and Eggers, W.J. (1993). Correction for potentiostat response in impedance measurements. Paper #228, 183rd Meeting of the Electrochemistry Society, Honolulu, HI, May.

Rodrigues, A., Geraldo, M.D., Bento, M.F., Cassio, F. (2004). Assessment of *Candida utilis* growth by voltammetric reduction of acids using microelectrodes. *Journal of Electroanalytical Chemistry,* 566: 139- 145.

Roebuck, B.D. and Goldblith, S.A. (1972). Dielectric properties of carbohydrates-water mixtures at microwave frequencies. *Journal of Food Science*, 37: 199-204.

Ronnest, NP, Stocks, SM, Lantz, AE Gernaey, KV (2011). Introducing process analytical technology (PAT) in filamentous cultivation process development: comparison of advanced online sensors for biomass measurement *Journal of Industrial Microbiology and Biotechnology,* 38(10): 1679-1690.

Rourou, S., Gaumon, S., Kallel, H. (2010). On-line monitoring of Vero cells cultures during the growth and rabies virus process using biomass spectrometer. *Cell Culture*, 4: 829-832.

Rousselet, J., Markx, G.H., Pethig, R. (1998). Separation of erythrocytes and latex beads by dielectrophoretic levitation and hyperlayer field-flow fractionation. *Colloids and surfaces A: Physicochemical and Engineering Aspects.* 140: 209-216.

Salgado, A.M., Folly, R.O.M., Valdman, B. (2001). Biomass monitoring by use of a continuous on-line optical sensor. *Sensors and Actuators B,* 75: 24-28.

Salsman, J.B. (1991). Measurement of dielectric properties in the frequency range of 300 MHz to 3 GHz as a function of temperature and density. *Proceedings Symposium of Microwave Theory Applications Materials and Processes*, 34: 203-214.

Saltas, V., Vallianatos, F., Triantis, D. (2008). Dielectric properties of non-swelling bentonite: The effect of temperature and water saturation. *Journal of Non-Crystalline Solids*, 354(52-54): 5533-5541.

Salter, G.J., Kell, D.B., Ash, L.A., Adams, J.M., Brown, A.J. (1990). Hydrodynamic deposition: a novel method of cell immobilization. *Enzyme and Microbial Technology*, 12(6): 419-430.

Salton, M.R.J. and Horne, R.W. (1951). Studies Of the bacterial cell wall I. Electron microscopical observation on heated bacteria. *Biochimica et Biophysica Acta*, 7: 19-42.

Sanda, T., Hasunuma, T., Matsuda, F., Kondo, A. (2011). Repeated-batch fermentation of lignocellulosic hydrolysate to ethanol using a hybrid *Saccharomyces cerevisiae* strain metabolically engineered for tolerance to acetic and formic acids. *Bioresource Technology*, 102: 7917-7924.

Sandnes, J.M., Ringstad, T., Wenner, D., Heyerdahl, P.H., Kallqvist, T., Gislerod, H.R. (2006). Real-time monitoring and automatic density control of large-scale microalgal cultures using near infrared (NIR) optical density sensors. *Journal of Biotechnology,* 122: 209-215.

Sarra, M., Ison, A.P., Lilly, M.D., (1996). The relationships between biomass concentration, determined by a capacitance-based probe, rheology and morphology of *Saccharopolyspora erythraea* cultures. *Journal of Biotechnology,* 51: 157–165.

Schelder, W. (1975). Theory of the frequency dispersion of electrode polarisation. Topology of networks with fractional power frequency dependence. *Journal of Physical Chemistry*, 79: 2.

Schleifer, K.H. (2009). Classification of *Bacteria* and *Archaea:* Past, present and future. *Systematic and Applied Microbiology*, 32: 533-542.

Schwan, H.P. (1954). Electrical properties of muscle tissue at low frequencies. *Zeitschrift für Naturforschung* 9B: 245-251.

Schwan, H.P. (1957). Electrical properties of tissue and cell suspensions. *Advances in Biological and Medical Physics*, 5: 147-207.

Schwan, H.P. (1985). Analysis of dielectric data: Experience gained with biological materials. *IEEE Transactions on Electrical insulation*, EI-20: 913-922.

Schwan, H.P. and Ferris, C.D. (1968). Four-electrode null technique for impedance measurement with high resolution. *Review of Scientific Instruments*, 39: 481-485.

Schwan, H.P. and Morowitz, H.J. (1962). Electrical properties of the membranes of the pleuropneumonia-like organism A 5969. *Biophysical Journal*, 2: 395-407.

Schwan, H.P. and Pauly, H. (1959). The impedance of a suspension of spherical particles surrounded by a shell. *Zeitschrift für Naturforschung*, 14b: 125-131.

Schwan, H.P., Schwarz, G., Maczuk, J., Pauly, H. (1962). On the low-frequency dielectric dispersion of colloidal particles in electrolyte solution. *Journal of Physical Chemistry*, 66: 2626-2635.

Schwan, H.P., Takashima, S., Miyamoto, V.K. Stoeckenius, W. (1970). Electrical properties of phospholipid vesicles. *Biophysical Journal*, 10: 1102-1119.

Schwan, H.P. (1992). Linear and nonlinear electrode polarisation and biological materials. *Annals in Biomedical Engineering*. 20: 269-288.

Sekine, D. (1999). Finite-element calculations for dielectric relaxation of one-sphere systems in a parallel-electrode measuring cell. *Colloid and Polymer Science*, 277: 388-393.

Sekine, D. (2000). Application of boundary element method to calculation of the complex permittivity of suspensions of cells in shape of $D_{\infty h}$ symmetry. *Bioelectrochemistry*, 52: 1-7.

Sengun, I.Y. and Karabiyikli, S. (2011). Importance of acetic acid bacteria in food industry. *Food control*, 22: 647-656.

Sheen, J. (2005). Study of microwave dielectric properties measurements by various resonance techniques. *Measurement*, 37(2): 123-130.

Sheen, J. (2009). Measurements of microwave dielectric properties by an amended cavity perturbation technique. *Measurement*, 42(1): 57-61.

Shendruk, T.N., Hickey, O.A., Slater, G.W., Harden, J.L. (2012). *Current Opinion in Colloid and Interface Science*, 17(2): 74-82.

Shi, Y., Yu, Z., Shao, X. (2011). Combination of the direct-forcing fictitious domain method and the sharp interface method for the three-dimensional dielectrophoresis of particles. *Powder Technology*, 210(1): 52-59.

Siano, S.A. (1997). Biomass measurement by inductive permittivity. *Biotechnology and Bioengineering*, 55: 289-304.

Silva, P.S., Florencio, O., Botero, E.R., Eiras, J.A., Garcia, D. (2009). Phase transition study in PLZT ferroelectric ceramics by mechanical and dielectric spectroscopies. *Materials Science and Engineering: A,* 521-522: 224-227.

Singha, S. and Thomas, M.J. (2008). Dielectric properties of epoxy nanocomposites. *IEEE Transactions on Dielectrics and Electrical Insulation*. 15: 12-23.

Smith, J., Carr, A., Golding, M., Reid, D., Zhang, L. (2011). Assessing the use of dielectric spectroscopy to analyse calcium induced compositional and structural changes in a model cheese. *Procedia Food Science*. 1: 1833-1840.

Soley, A., Lecina, M., Gamez, X., Cairo, J.J., Riu, P., Rosell, X., Bragos, R., Godia, F. (2005). On-line monitoring of yeast cell growth by impedance spectroscopy. *Journal of Biotechnology*, 118: 398-405.

Song, B., Liu, D., Sun, L., Chen, L. (2011). Numerical study of a dielectrophoresis separation device at multiple frequencies. *Procedia Engineering*, 15: 341-345.

Sonnleitner, B., Locher, G., Fietcher, A. (1992). Biomass determination. *Journal of Biotechnology*, 25: 5-22.

Sorichetti, P.A. and Matteo, C.L. (2007). Low-frequency dielectric measurements of complex fluids using high-frequency coaxial sample cells. *Measurement*, 40(4): 437-449.

Spolaore, P., Joannis-Cassan, C., Duran, E., Isambert, A. (2006). Commercial applications of microalgae. *Journal of Bioscience and Bioengineering,* 101: 87–96.

Stephens, M., Talary, M.S., Pethig, R., Burnett, A.K., Mills, K.I. (1996). The dielectrophoresis enrichment of CD34(+) cells from peripheral-blood cell harvests. *Bone Marrow Transplantation*. 18: 777-82.

Stoicheva, N.G., Davey, C.L., Markx, G.H., Kell, D.B. (1989). Dielectric spectroscopy: a rapid method for the determination of solvent biocompatibility during biotransformations. *Biocatalysis* 2: 245-255.

Stoneman, M.R., Kosempa, M., Gregory, W.D., Gregory, C.W., Marx, J.J., Mikkelson, W., Tjoe, J., Raicu, V. (2007). Correction of electrode polarisation contributions to the dielectric properties of normal and cancerous breast tissues at audio/radiofrequencies. *Physics in Medicine and Biology*, 52: 6589-6604.

Sun, L.N., Liu, D.L., Chen, L.G. (2011). Improvement of microchannel geometry subject to lateral dielectrophoresis using numerical simulations. *Procedia Engineering*, 15: 336-340.

Sun, Y. and Cheng, J. (2002). Hydrolisis of lignocellulosic materials for ethanol production: a review. *Bioresource Technology*. 83: 1-11.

Sutton, S. (2011). Accuracy of plate counts. *Journal of Validation Technology*. 17(3): 42-46

Suzuki, M. and Akaguma, H. (2000). Chemical cross-talk in flow-type integrated enzyme sensors. *Sensors and Actuators B*, 64: 136-141.

Szoke, M., Sasvari-Szekely, M., Guttman, A. (1999). Ultra-thin-layer agarose gel electrophoresis: I. Effecto of the gel concentration and temperature on the separation of DNA fragments. *Journal of Chromatography A*, 830(2): 465-471.

Tang, J., Feng, H., Lau, M. (2002). Microwave heating in food processing, in X. Young and J. Tang, eds. *Advances in Bioprocessing Engineering*, World Scientific.

Tibayrenc P, Ghommidh C, Preziosi-Belloy L, (2011). Determination of yeast viability during a stress-modle alcoholic fermentation using reagent-free microscopy image analysis. *Biotechnology Progress,* 27: 539-546.

Torgovnikov, G.I. (1993). Dielectric properties of wood and wood based materials. Springer-Verlag, Berlin.

Tran, W.N., Stuchly, S.S., Kraszewski, A. (1984). Dielectric properties of selected vegetables and fruits 0.1-10.0 GHz. *Journal of Microwave Power*. 19(4): 251-258.

Ueda, K., Ochiai, H., Itaya, T., Yamaoka, K. (1992). Electric field orientation of sonicated κ-carrageenan in aqueous solution: ionic polarization of loosely bound counterions. *Polymer*. 33(2): 429-431

Wachner, D., Simeonova, M., Gimsa, J. (2002). Estimating the subcellular absorption of electric field energy: Equations for an ellipsoidal single shell model. *Bioelectrochemistry*, 56: 211-213.

Wagner, K.W. (1914). Erklarung der dielectrischen Nachwirkungsvorgange auf Grund Maxwellscher Vorstellungen. *Archiv der Elektrotechnik*, 2: 371-387.

Wakamatsu, H. (1997). A dielectric spectrometer for liquid using the electromagnetic induction method. *Hewlett-Packard Journal*, 48: 37-44.

Wakizaka, Y., Hakoda, M., Shiragami, N. (2004). Effect of electrode geometry on dielectrophoretic separation of cells. *Biochemical Engineering Journal,* 20: 13–19.

Van den Driesche, S., Rao, V., Puchberger-Enengl, D., Witarski, W., Vellekoop, M.J. (2012). Continuous cell from cell separation by travelling wave dielectrophoresis. *Sensors and Actuators B: Chemical*, 170: 207-214.

Wang, J.W., Wang, M.H., Jang, L.S. (2010). Effects of electrode geometry and cell location on single-cell impedance measurement. *Biosensors and Bioelectronics,* 25: 1271–1276.

Wang, S., Yu, H., Wickliffe, J.K. (2011). Limitation of the MTT and XTT assays for measuring cell viability due to superoxide formation induced by nano-scale TiO_2. *Toxicology in Vitro*, 25(8): 2147-2151.

Wang, W.Y., hang, D.F., Xu, T., Li, X.F., Zhou, T., Chen, X.L. (2002). Effect of temperature on nonlinear electric behaviour and dielectric properties of (Ca, Ta)-doped TiO_2 ceramics. *Materials Research Bulletin*, 37(6): 1197-1206.

Wang, X.B., Huang, Y., Burt, J.P.H., Markx, G.H., Pethig, R. (1993). Selective dielectrophoretic confinement of bioparticles in potential energy wells. *Journal of Physics D: Applied Physics*, 26: 1278-85.

Wang, X.B., Huang, Y., Hozel, R., Burt, J.P.H., Pethig, R. (1993). Theoretical and experimental investigations of the interdependence of the dielectric, dielectrophoretic and electrorotational behaviour of colloidal particles. *Journal of Physics D: Applied Physics*. 26: 312-322.

Varshney, M. and Li, Y. (2008). Double interdigitated array microelectrode-based impedance biosensor for detection of viable *Escherichia coli* O157:H7 in growth medium. *Talanta* 74: 518–525.

Wei, N; You, J; Friehs, K; Flaschel, E; Nattkemper, TW (2007). An in situ probe for on-line monitoring of cell density and viability on the basis of dark field microscopy in conjunction with image processing and supervised machine learning. *Biotechnology and Bioengineering*, 97: 1489-1500.

Von Hippel, A.R. (1954a). Dielectric materials and applications. New York: The Technology Press of M.I.T. and John Wiley & Sons.

Von Hippel, A.R. (1954b). Dielectrics and waves. New York: John Wiley & Sons.

Voyer, D., Frenea-Robin, M., Buret, F., Nicolas, L. (2010). Improvements in the extraction of cell electric properties from their electrorotation spectrum. *Bioelectrochemistry,* 79(1): 25-30.

Vrinceanu, D. and Gheorghiu, E. (1996). Shape effects on the dielectric behaviour of arbitrarily shaped particles with particular reference to biological cells. *Bioelectrochemistry and Bioenergy*, 40: 167-170.

Wu, Y., Huang, C., Wang, L., Miao, X., Xing, W., Cheng, J. (2005). Electrokinetic system to determine differences of electrorotation and travelling-wave electrophoresis between autotrophic and heterotrophic algal cells. *Colloids and Surfaces A: Physicochemical and Engineering Aspects*, 262(1-3): 57-64.

Wyman, C.E., Spindler, D.D., Grohmann, K. (1992). Simultaneous saccharification and fermentation of several lignocellulosic feedstocks to fuel ethanol. *Biomass and Bioenergy*. 3: 301-307.

Xi, W. and Tinga, W. (1991). Error analysis and permittivity measurements with re-entrant hig-temperature dielectrometer. *Journal of Microwave Power EM Energy*, 28: 104-112.

Yang, L. and Bashir, R. (2008). Electrical/electrochemical impedance for rapid detection of foodborne pathogenic bacteria. *Biotechnology Advances,* 26: 135–150.

Yardley, J. E., Todd, R., Nicholson, D. J., Barret, J., Kell, D. B., Davey, C. L. (2000). Correction of the influence of baseline artefacts and electrode polarisation on dielectric spectra. *Bioelectrochemistry,* 51: 53-65.

Zaengl, W.S. (2003). Dielectric spectroscopy in time and frequency domain for HV power equipment, part I: Theoretical considerations. *IEEE Electrical Insulation Magazine,* 19(5): 5-19.

Zewert, T.E. and Harrington, M.G. (1993). Protein electrophoresis. *Current Opinion in Biotechnology*, 4(1): 3-8.

Zhang, B., Guo, T., Zhang, T., Wang, J., Quan, Z. (2006). Effect of substrate temperature on microstructures and dielectric properties of compositionally graded BST thin films. *Transactions of Nonferrous Metals Society of China*, 16(1): 126-129.

Zhang, H.Z., Sekine, K., Hanai, T., Koizumi, N. (1983). Dielectric observations of polystyrene microcapsules and the theoretical analysis with reference to interfacial polarisation. *Colloid and Polymer Science*, 261: 381-389.

Zhou, X., Markx, G.H., Pethig, R., Eastwood, I.M. (1995). Differentiation of viable and non-viable bacterial biofilms using electrorotation. *Biochimica et Biophysica Acta* 1245: 85-93.

Zhou, X.F., Markx, G.H., Pethig, R. (1996). Effect of biocide concentration on electrorotation spectra of yeast cells. *Biochimica et Biophysica Acta,* 1281: 60-64.

Zimmerman, V. and Grosse, C. (2002). Contribution of electroosmosis to electrorotation spectra in the frequency range of the β dispersion. II. Application

to cells with a cell wall. *Colloids and Surfaces A: Physicochemical and Engineering Aspects*, 197(1-3): 69-77.

Zimmermann, U. (1982). Electric field-mediated fusion and related electrical phenomena. *Biochimica et Biophysica Acta*, 694: 227-77.